Author:
Marshall, Matthew G

Title:
Assessing the impact of glacier retreat on organic matter export and cycling in Chilean Patagonia

Assessing the impact of glacier retreat on organic matter export and cycling in Chilean Patagonia

Matthew Marshall

School of Geographical Sciences
University of Bristol

A dissertation submitted to the University of Bristol in accordance with the requirements for the degree of Doctor of Philosophy in the Faculty of Science.

January 2020

43,331 words

Abstract

Organic matter is an important component of global biogeochemical cycles, which are sensitive to processes of landscape change. The worldwide retreat of mountain glaciers is one of the most profound examples of such change. Chilean Patagonia represents a unique study region, which is both relatively untouched by direct human activity and undergoing significant rates of deglaciation. The biogeochemical role of glaciers in this region is relatively understudied and this thesis offers the first regional scale assessment of the sensitivity of organic matter in rivers and fjords to glacier retreat. This assessment comprises three complementary studies. The first adopts a space-for-time approach, in which the effects of spatial variations in landscape properties on organic matter flux and composition are used to infer the effects of ongoing glacier retreat over time. It was found that glaciers drive higher catchment yields for particulate organic matter and supply dissolved organic matter rich in protein-like and aliphatic substances. However, the influence of glaciers is dampened by non-glacial sources and sinks in the downstream landscape. The second study used incubation experiments to quantify the proportion of bioavailable dissolved organic carbon in river water from selected catchments. These incubations showed that bioavailability in these catchments is lower than that observed in glacial rivers of the northern hemisphere. This may be explained by prior processing and specific intrinsic compositional factors but is not systematically related to catchment glacier cover. The third study presents the first molecular level analysis of dissolved organic matter in a glaciated fjord. This analysis showed that riverine organic matter may comprise a significant proportion of the total organic carbon pool, which is sensitive to changes in glacier melt inputs. The relationships between organic matter cycling and landscape change in Chilean Patagonia established in this thesis highlight some potential implications of deglaciation for global biogeochemistry.

Acknowledgements

I would first like to thank Prof. Jemma Wadham for her enthusiastic supervision. It has been a privilege to work in such an interesting field and be supported in developing my own abilities by someone so positive and passionate about their work. Thanks also to Prof. Laura Robinson for keeping an eye on me when things looked a little bleak – your kindness was just enough to keep me going. Further thanks to Profs. Rachel Flecker, Alex Anesio and Martyn Tranter for helpful conversations along the way.

I am indebted to Dr Anne Kellerman for taking me under her wing and sharing her expertise in organic geochemistry. Without her support, getting to grips with molecular data would not have been so enjoyable. Thanks also to Prof. Rob Spencer for allowing Anne to get involved in Patagonian fieldwork and for providing lab support.

Much of my gratitude goes to Dr Jon Hawkings, whose dedication and diligence in field logistics and sample collection helped to make this thesis possible. Thanks also to the whole team at 'Camp Washout' (Alex Beaton, Ale Urra, Helena Pryer, Anne Kellerman and Rory Burford) for making great memories and Pisco hot chocolates. Especial thanks to Ale – I couldn't have wished for better company to see out the full 50 days! I extend thanks to Dr Giovanni Daneri and the team at CIEP for invaluable logistical support. I am also grateful to Dr Sebastien Bertrand, Loïc Piret and their team for field support and ensuring that we didn't starve! Thanks also to Don Rene, Rene Jr and Don Efrain for shipping us in and out of camp and topping us up with power from time to time.

I thank Dr Fotis Sgouridis, James Williams and Dr Chris Yates for their lab support. I also thank the team at the MAGLAB, Tallahassee, for granting me time to run my field samples, and especially to Lyssa for fixing the glitch and helping make up for lost time!

To all my office colleagues who made the tough times more bearable, especially Amy Sweet for boosting my confidence whenever it was needed and Helena Pryer for giving me a home when I was flooded out of my own. Thanks also to Ale (again!), Bea (and the dogs!), Sam, Miranda, Alex and the IcyBios team.

Finally, to Mom, Dad, Mary and Ed for your love and encouragement throughout. And especially to Nick for your understanding and for keeping me sane.

This thesis was funded through a studentship awarded by the NERC GW4+ DTP.

Author's declaration

I declare that the work in this dissertation was carried out in accordance with the requirements of the University's *Regulations and Code of Practice for Research Degree Programmes* and that it has not been submitted for any other academic award. Except where indicated by specific reference in the text, the work is the candidate's own work. Work done in collaboration with, or with the assistance of, others, is indicated as such. Any views expressed in the dissertation are those of the author.

Signed _____ Date _____

Table of contents

Table of figures

Table of tables

List of abbreviations

AI_{mod}	Aromaticity Index (modified)
BDOC	Bioavailable dissolved organic carbon
BEF	Broadleaf evergreen forest
BMF	Baker-Martinez Fjord
CA	Condensed aromatic
DOC	Dissolved organic carbon
DOM	Dissolved organic matter
DON	Dissolved organic nitrogen
EEM	Excitation-emission matrix
FT-ICR MS	Fourier transform ion cyclotron resonance mass spectrometry
GLOF	Glacial lake outburst flood
HUP	Highly unsaturated and phenolic
LoB/LoD/LoQ	Limit of blank/detection/quantitation
MANOVA	Multivariate analysis of variance
NHMFL	National High Magnetic Field Laboratory
NPI	Northern Patagonian Icefield
OC	Organic carbon
PARAFAC	Parallel factor analysis
PCA	Principal components analysis
PES	Polyethersulphone
POC	Particulate organic carbon
POM	Particulate organic matter
PP	Polyphenolic
RSD	Relative standard deviation
RMSE	Root mean square error
SPE	Solid phase extraction
SPI	Southern Patagonian Icefield
SSC	Suspended sediment concentration
TC	Total carbon

1. Introduction and background

1.1. Introduction

Aquatic organic matter consists of a complex mixture of substances derived from the decay of biological material. These substances serve many biogeochemical functions, such as regulating the pH of natural waters and controlling the availability of nutrients, metals and toxins to aquatic organisms (McKnight *et al.*, 1985, 1992; Breault *et al.*, 1996; Wymore *et al.*, 2016). Perhaps most critically, organic matter acts as a crucial food and energy source to aquatic bacteria (Battin *et al.*, 2009). If utilised for bacterial growth and incorporated into new biomass, it may be ingested by increasingly larger organisms and help to sustain complex foodwebs (Pace *et al.*, 2004). Ultimately, however, much of this material is converted back into its inorganic mineral constituents through respiration by bacteria and higher consumers (Welti *et al.*, 2017). For example, freshwater ecosystems are estimated to release 1.2 Pg (1 Pg = 10^{15} g) of carbon back into the atmosphere each year (approximately one quarter of the amount fixed by the terrestrial biosphere) via the respiration of organic matter (Battin *et al.*, 2009). Thus, organic matter comprises a significant phase within the global biogeochemical cycle of carbon as well as of other bioactive elements such as oxygen, nitrogen, phosphorus and sulphur (Burd *et al.*, 2016).

The production, transport and processing of organic matter within aquatic systems is sensitive to environmental change (Ward *et al.*, 2017; Zhuang and Yang, 2018). The biogeochemical function and fate of organic matter is determined by its composition, which is related to its source and the effects of biological and photochemical degradation (Kellerman *et al.*, 2015; Wagner and Jaffé, 2015; Riedel *et al.*, 2016). These factors are strongly influenced by perturbations to the hydrological system, including the reconfiguration of channel networks and changes to river flows and in-stream conditions (Aufdenkampe *et al.*, 2011; Asmala *et al.*, 2016). Therefore, changes in land-use and global climate are also driving changes in organic matter cycling along the aquatic continuum (Lambert *et al.*, 2017; Zhuang and Yang, 2018). Examining the influence of landscape conditions on organic matter composition therefore helps to understand the biogeochemical impacts of environmental change (Kellerman *et al.*, 2014; Osterholz *et al.*, 2016).

Organic matter cycling in glaciated regions may be particularly sensitive to climate change (Hood *et al.*, 2015). Although glacial ice is a relatively small global store of organics, glaciers are known to release highly reactive organic matter to downstream aquatic communities via melting (Hood *et al.*, 2009, 2015). Rising global temperatures and enhanced melt rates are likely to increase the size of these supplies, at least in the short term (Hood *et al.*, 2015; Milner *et al.*, 2017). The long-term worldwide decline in glacial ice cover will ultimately deprive highly specialised aquatic communities of a valuable and unique resource (Jacobsen *et al.*, 2012; Wilhelm *et al.*, 2013; Milner *et al.*, 2017) and also expose potentially vast organic matter reserves in subglacial sediments (Wadham *et al.*, 2019). Some of the world's most rapidly retreating glaciers are in Chilean Patagonia (Foresta *et al.*, 2018; Dussaillant *et al.*, 2019) but biogeochemical data for this region are scarce. Glaciers here contain the largest concentration of land ice in the southern hemisphere excluding Antarctica and over 40 times more ice than all glaciers in the European Alps (Millan *et al.*, 2019). Therefore, the analysis of organic matter in glacially fed rivers and fjords of Chilean Patagonia, as provided in this thesis, reflects a significant contribution towards a global assessment of the biogeochemical impacts of glacier retreat.

Understanding glaciers as highly sensitive organic matter stores has important biogeochemical implications, especially for their wider role in the global carbon cycle. Glaciers and ice sheets are known to affect atmospheric carbon concentrations via a suite of direct and indirect feedbacks (Wadham *et al.*, 2019). For example, photosynthesising algae in supraglacial environments sequester carbon dioxide at globally significant rates (Cook *et al.*, 2012; Stibal *et al.*, 2012c), whilst organic matter decay in subglacial environments may produce large methane reserves which are released via meltwaters and during glacier retreat (Wadham *et al.*, 2008, 2012; Boyd *et al.*, 2010; Stibal *et al.*, 2012a; Dieser *et al.*, 2014; Lamarche-Gagnon *et al.*, 2019). The release of ice-locked organic matter illustrates a further role for glaciers in the carbon cycle via the direct transfer of potentially reactive carbon into lakes, rivers and fjords (Hood *et al.*, 2015). Overall, these biogeochemical influences are part of a broader suite of ecosystem services which are sensitive to glacier retreat and could have profound global impacts for society (Milner *et al.*, 2017).

1.2. Research objectives

The overarching aim of this thesis is to provide the first regional scale assessment of the factors controlling the fluxes and composition of organic matter in aquatic systems of Chilean Patagonia, specifically in relation to changing glacier melt inputs. This helps contribute towards a global assessment of how glacier retreat affects downstream biogeochemistry. The thesis comprises three separate but complementary analytical chapters with distinct aims and objectives summarised below.

1.2.1. Research objective 1

To assess the impact of deglaciation-induced landscape change on organic matter yields and composition in Chilean Patagonian rivers (Chapter 3).

Aims:

- To quantify the yields of organic matter exported from river basins across Chilean Patagonia and relate trends to the degree of glacial influence.
- To use spatial and temporal data to assess the influence of glacial meltwaters on riverine dissolved organic matter (DOM) composition.
- To examine the relationships between landscape properties and riverine DOM composition to understand the effect of deglaciation on regional organic matter export.

This study combines organic matter concentration and composition data for samples collected from 29 rivers spanning a range of environmental gradients (glacier, lake and vegetation covers) between latitudes 42–48°S in Chilean Patagonia. Organic matter yields are calculated and compared for glacial and non-glacial catchments (where hydrological records are available) and also related to landscape properties. Time series observations from a heavily glaciated catchment provide additional insight into the impact of glacier melting on riverine organic matter composition on a seasonal basis. Glacial signatures in organic matter composition are compared to those identified in other glaciated regions and analysed within the context of other influences across the Chilean Patagonian landscape. The principles of space-for-time substitution are employed to infer the impact of deglaciation on riverine biogeochemistry from variations in organic matter composition that are linked to spatial gradients in landscape properties.

1.2.2. Research objective 2

To assess the controls on organic matter bioavailability in Chilean Patagonian rivers which are experiencing the effects of deglaciation (Chapter 4).

Aims:

- To measure the bioavailability of organic matter in a sample of Chilean Patagonian rivers and set the results in a global context for other glacially influenced regions.
- To relate patterns in bioavailability to regional scale trends in organic matter composition.
- To hypothesise on the constraints on bioavailability and the sensitivity of organic matter cycling to ongoing glacier retreat.

This study uses incubation experiments to measure the bioavailability of dissolved organic matter in Chilean Patagonian rivers for the first time (from a subsector of the study region in Chapter 3). Fluorescence scans are used to identify the reactive components in each incubation sample and these data are related to regional trends in organic matter composition, including at the molecular level, to aid interpretation of the factors controlling bioavailability. This study helps to inform an understanding of how aquatic organic matter cycling may be affected by changes in landscape properties.

1.2.3. Research objective 3

To assess the impact of changing glacier melt inputs on the composition of organic matter in a Chilean Patagonian fjord (Chapter 5).

Aims:

- To quantify the relative importance of dissolved and particulate organic matter in riverine fluxes to the Baker-Martinez Fjord.
- To assess the impact of glacier melt inputs on fjord organic matter composition by comparing summer (high discharge) and winter (low discharge) conditions.
- To examine variations in organic matter composition along the fjord salinity gradient to infer the impact of environmental controls over biogeochemical processes.

Spatial and seasonal variations in organic matter composition in a Chilean Patagonian fjord are analysed in relation to a range of marine and freshwater influences, including

glacial inputs. To my knowledge, this study is the first to use molecular level analytical techniques in a glacially influenced fjord to directly assess the impact of glacier melt inputs on organic matter composition. This assesses the impact of glacier melt inputs on organic matter cycling from within a marine setting and complements the findings from the previous chapters which explore the composition and reactivity of organic matter from an upstream perspective.

1.3. Scientific background

The purpose of this section is to establish the importance of glaciers in regulating the supply of organic matter to downstream ecosystems within the context of global climate change. Further scientific background related to specific research aims will be covered in the relevant analytical chapters. This literature review provides the basis for a critical commentary in Section 1.4, which identifies gaps in understanding and opportunities for future investigation that this thesis aims to facilitate.

1.3.1. Glaciers as sensitive stores of organic matter

1.3.1.1. Sources and cycling of organic matter in glaciers

Glaciers and ice sheets are collectively seen as a distinct global biome (Anesio and Laybourn-Parry, 2012) which supports the production and cycling of organic matter (Anesio *et al.*, 2009). This view reflects the culmination of approximately two decade's worth of research which has shown that glaciers are important drivers of geochemical weathering (Wadham *et al.*, 1997; Tranter *et al.*, 2002; Graly *et al.*, 2014; Tranter, 2014), nutrient cycling (Wynn *et al.*, 2007; Telling *et al.*, 2011; Hawkings *et al.*, 2016; Wadham *et al.*, 2016) and hosts to unique microbial ecosystems (Sharp *et al.*, 1999; Hodson *et al.*, 2008; Christner *et al.*, 2014). The discovery of specially adapted, cold-tolerant microorganisms throughout glacial systems wherever liquid water exists (Sharp *et al.*, 1999; Mader *et al.*, 2006; Christner *et al.*, 2014) has led to a paradigm shift, recognising that life not only exists in regions that were previously thought inhospitable but also plays an active role in regulating biogeochemical processes in icy environments (Wadham *et al.*, 2010; Tranter, 2014; Mikucki *et al.*, 2016). New biomass is created through primary production by photosynthetic algae on glacier surfaces (Cook *et al.*, 2012; Telling *et al.*, 2012) and by chemosynthetic microbes in dark, anoxic and relatively isolated subglacial environments (Boyd *et al.*, 2014). Combined with external inputs from atmospheric and wind-blown deposits on glacier surfaces (Stibal *et al.*,

2008; Stubbins *et al.*, 2012) and overridden soils, sediments and vegetation beneath the ice (Wadham *et al.*, 2008; Bhatia *et al.*, 2013), these organic substrates sustain extensive and diverse bacterial communities with an energy source (Sharp *et al.*, 1999; Tranter *et al.*, 2005; Stibal *et al.*, 2012b; Mikucki *et al.*, 2016; Nicholes *et al.*, 2019). Therefore, the resident biota may actively process glacial organic matter and regulate its overall composition.

1.3.1.2. Categorisation of glacial organic matter: dissolved and particulate

Organic matter is present in glacial (and indeed all aquatic) systems in a variety of forms but is principally divided into particulate and dissolved classes which are defined by filtration procedures (Thurman, 1985). Typically, dissolved organic matter (DOM) is distinguished by passing through filter pore sizes of 0.45 µm but pores ranging from 0.2–0.7 µm have been used to suit different methodological requirements (Nollet, 2013; Denis *et al.*, 2017a). Only the smallest polar molecules are likely to be truly dissolved, with most DOM existing as a colloidal suspension (Nebbioso and Piccolo, 2013). Particulate organic matter (POM) comprises the material too large to pass through the filter and can include living matter such as bacterial cells, phytoplankton and zooplankton (Figure 1.1). Over the wide range of fields in which POM is investigated, the term may refer to various and differing components of POM. For example, POM is frequently used in marine-based studies as a bulk measure of biomass in pelagic ecosystems (Andersson and Rudehall, 1993). In terrestrial systems, POM is used more routinely to refer to detrital material derived from soils, sediments, vegetation and leaf litter, and is often linked to erosional inputs (Galy *et al.*, 2015). Both POM and DOM are quantified using oxidation techniques (most commonly combustion) to measure its carbon content, which is the principal component of organic matter (Bolan *et al.*, 1996). As a result, particulate/dissolved organic carbon (POC/DOC) measurements provide a consistent means of estimating the size of POM/DOM pools in aquatic environments irrespective of compositional differences and the terms are often used interchangeably.

1.3.1.3. Quantifying glacial organic matter stores

The amount of organic matter held within glacial ice globally has been quantified in terms of its carbon (C) content and stands at ~6 Pg C (Hood *et al.*, 2015). The vast majority (93%) is held within the Antarctic Ice Sheet with the remainder contained in

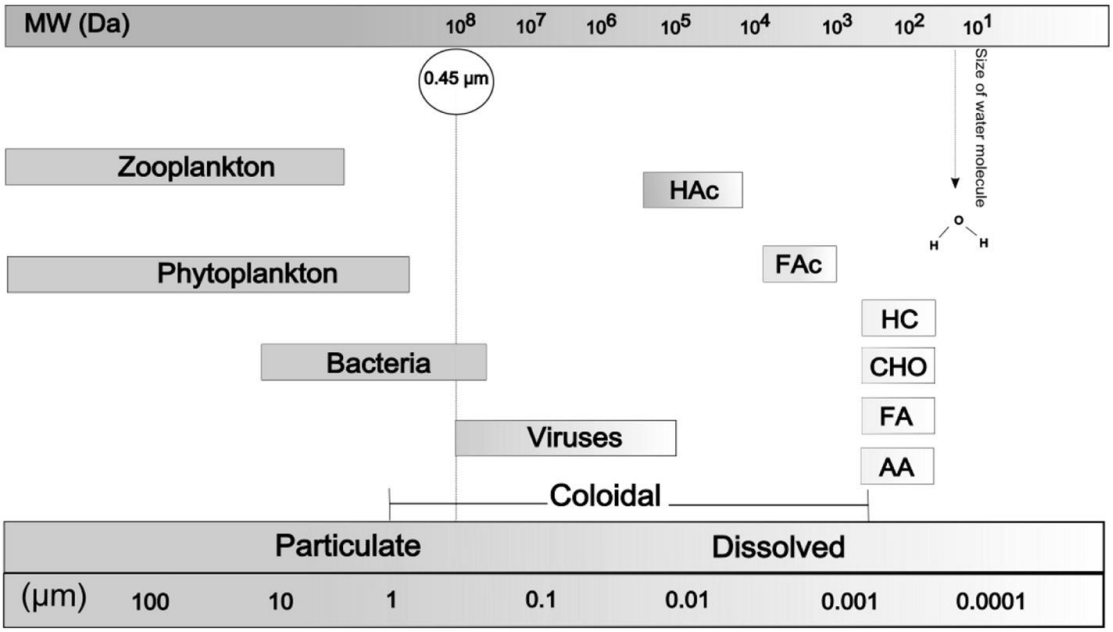

Figure 1.1. Size (µm) and molecular weight (Daltons, Da) ranges for particulate and dissolved organic matter in aquatic systems with reference to specific compound groups and classes of organism. The vertical line at 0.45 µm indicates the most commonly used filter pore size to distinguish DOM and POM. HAc: humic acid; FAc: fulvic acid; HC: hydrocarbons; CHO: carbohydrates; FA: fatty acids; AA: amino acid. Figure taken from Artifon *et al.* (2019).

the Greenland Ice Sheet (5%) and mountain glaciers (2%) globally (Hood *et al.*, 2015). These estimates are based on a compilation of all available concentration data (*c.* 2015) for DOC and POC in glacial ice from across five continents (Hood *et al.*, 2015). Due to access limitations, spatial coverage of glaciated regions is patchy and data are completely missing for some notable areas, such as for South American Andean glaciers. This leads to substantial uncertainties, especially for POC measurements which are particularly scarce (Hood *et al.*, 2015). Nevertheless, this first order calculation shows that glacial ice stores are modest in size compared to other global organic carbon reservoirs, such as 1600 Pg C in permafrost (Schuur *et al.*, 2008) or 2200 Pg C in the terrestrial biosphere (Carlson *et al.*, 2001). However, ice-locked organic matter may underestimate the true storage in glacial systems given that subglacial sediments in Antarctica and Greenland are hypothesised to contain between 6000–21000 Pg C and 0.5–27 Pg C, respectively (Wadham *et al.*, 2019). There are no global estimates of organic matter in sediments beneath mountain glaciers but they are likely to harbour any previously overridden soils, sediments and vegetation, with some material becoming incorporated into basal ice (O'Donnell *et al.*, 2016).

1.3.1.4. Sensitivity of glacial organic matter stores

The overall size of glacial organic matter stores is thought less important than their sensitivity to rising global temperatures. Annual meltwater fluxes from glaciers and ice sheets are estimated to export ~3 Tg C (1 Tg = 10^{12} g) of organic matter (Hood *et al.*, 2015), which is small compared to the ~900 Tg C exported annually by rivers (Battin *et al.*, 2009). Critically, however, glacial meltwaters are typically discharged into proglacial lakes, rivers and fjords (Hood *et al.*, 2015) without transiting through soils and therefore have a more direct impact on aquatic biogeochemistry. Mountain glaciers are the smallest but most dynamic glacial systems, accounting for 43% of the global annual export of organic matter from glaciers and ice sheets, and specifically account for 56% of the DOC flux (Figure 1.2) (Hood *et al.*, 2015).

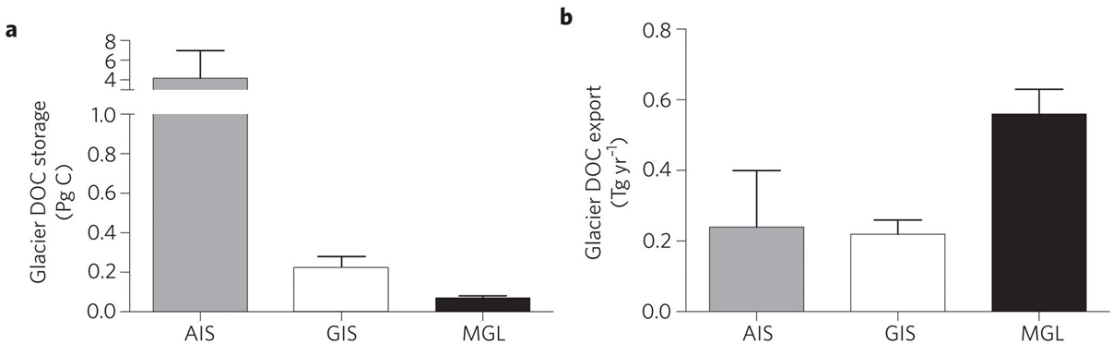

Figure 1.2. Total global (a) storage of DOC in glacial ice and (b) annual export in meltwaters for the Antarctic Ice Sheet (AIS), the Greenland Ice Sheet (GIS) and all mountain glaciers (MGL). Source: (Hood *et al.*, 2015).

Mountain glacier DOC fluxes are expected to increase as melt rates accelerate in response to rising global temperatures (Huss and Hock, 2018) and mountain glaciers worldwide have been retreating rapidly as a result (Zemp *et al.*, 2015). As glaciers waste away, an increasing proportion of annual organic matter flux will be derived from non-steady state melting that contributes to the long-term depletion of these organic matter stores (Hood *et al.*, 2015). Although in the short term, therefore, systems will experience increased input from glacial sources; in the long term the shrinkage of glaciers will mean that glacial inputs cease to be a significant source of aquatic DOM. The dramatic change outlined here should be seen in the context of the wider sensitivity of ecosystem services and societal impacts arising from the loss of glaciers (Milner *et al.*, 2017).

1.3.2. Accounting for the effect of glacial organic matter on aquatic systems

1.3.2.1. Significance of the effect

The impact of glacial organic matter on downstream aquatic ecosystems is of critical importance in understanding the biogeochemical effects of enhanced ice melting and glacier retreat. DOM in glacial meltwaters is typically more dilute than in non-glacial freshwaters but is disproportionately more labile (Fellman *et al.*, 2010a). Incubation studies have reported high percentages (up to ~90%) of bioavailable DOC (BDOC) being consumed by bacteria over a 28-day period in samples of glacial DOM collected from disparate locations: Alaska (Hood *et al.*, 2009; Fellman *et al.*, 2010a), European Alps (Singer *et al.*, 2012), Greenland (Lawson *et al.*, 2014a; Paulsen *et al.*, 2017), Himalayas (Spencer *et al.*, 2014b; Hemingway *et al.*, 2019). Positive correlation between BDOC and the partial pressure of CO_2 in Alpine glacial streams provides field evidence that glacial DOM is respired by aquatic heterotrophs (Singer *et al.*, 2012).

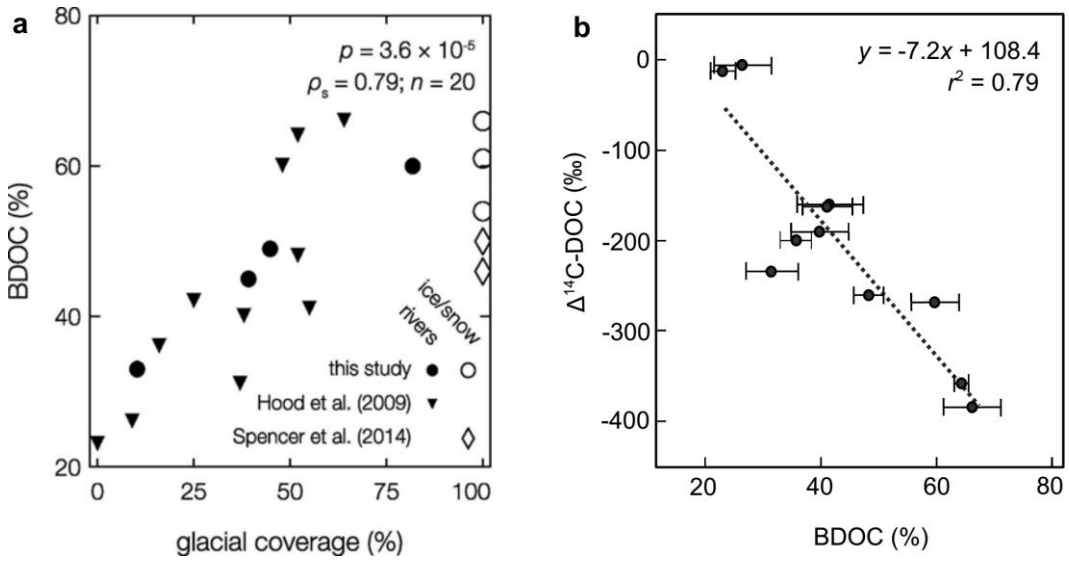

Figure 1.3. Bioavailability of dissolved organic carbon (BDOC) from example studies related to (a) catchment glacial cover as a percentage of total area (after: Hemingway *et al.*, 2019) and (b) radiocarbon content, with more negative Δ^{14}C-DOC values indicating more ancient material (after: Hood *et al.*, 2009).

Figure 1.3 shows that higher BDOC in glacial rivers is linked to greater catchment ice cover (Hood *et al.*, 2009; Fellman *et al.*, 2010a; Hemingway *et al.*, 2019) and ancient radiocarbon (^{14}C) signatures (Hood *et al.*, 2009; Singer *et al.*, 2012; Spencer *et al.*, 2014b). Therefore, glacial contributions to the aquatic DOM pool are unique in that their reactivity apparently increases with age. Conventional thinking implies that older

DOM is less bioavailable, reflecting an accumulation of recalcitrant material after fresh, reactive material has been preferentially consumed (Raymond and Bauer, 2001). The paradoxical properties of ancient yet labile glacial DOM have precipitated debate over the origin of this material.

1.3.2.2. Accounts linked to anthropogenic sources

Inputs of anthropogenic carbon via the deposition of atmospheric fossil fuel aerosols have been proposed as a possible source for the ancient labile organic matter previously identified in glacial systems (Hood *et al.*, 2009). This was suggested following the discovery of condensed aromatic formulae (via ultrahigh resolution molecular analysis), which are indicative of combustion products in snow and bulk discharge samples from the Mendenhall Glacier, Alaska (Stubbins *et al.*, 2012). Similar anthropogenic compounds have been found in glacial ice and meltwaters downwind of industrialised zones in Europe and Asia (Singer *et al.*, 2012; Spencer *et al.*, 2014b; Li *et al.*, 2016). This is also consistent with the detection of organic pollutants in industrial era glacial ice from across the globe (Legrand *et al.*, 2007; McConnell *et al.*, 2007; Wang *et al.*, 2008; Gabrieli *et al.*, 2010).

While such compounds could account for ancient ^{14}C signatures in DOM, the link with lability is predicated on the results of previous studies which identify relatively reactive compounds produced during combustion. Specifically, aliphatics and fatty acids have been associated with soot particles (Walker and Colwell, 1974; Yasuhara and Fuwa, 1982) and incomplete combustion may produce compounds that are proteinaceous or nitrogen- and sulphur-rich (Wozniak *et al.*, 2008; Mladenov *et al.*, 2011), which may offer a unique source of organic nutrients. Moreover, photodegradation of atmospheric aerosols might convert recalcitrant aromatic combustion products into smaller labile molecules (Stubbins *et al.*, 2010; Mostovaya *et al.*, 2017; Wagner *et al.*, 2018). However, this theory does not explain how such highly labile compounds might survive intense bacterial activity in supraglacial environments (Nicholes *et al.*, 2019) and be present in bulk runoff.

1.3.2.3. Accounts linked to natural sources

Microbial DOM is also a suggested source of labile material in glacial samples. Strong contributions to glacial DOM from microbial sources are characterised by:

- high protein-like fluorescence (Barker *et al.*, 2006, 2009; Dubnick *et al.*, 2010; Kellerman *et al.*, 2020; Lawson *et al.*, 2014a)
- low molecular weight compounds (Lawson *et al.*, 2014a; Musilova *et al.*, 2017)
- aliphatic material (Singer *et al.*, 2012; Stubbins *et al.*, 2012; Spencer *et al.*, 2014b; Hemingway *et al.*, 2019).

DOM with these properties is typically highly bioavailable (Fellman *et al.*, 2009, 2010a) but may not carry an ancient signature unless it has entered the system from an already ancient source, before further bacterial degradation within the system. It is the case that glacial DOM contains a high diversity of older allochthonous material from overridden plants, soils and sediments (Singer *et al.*, 2012). Given the right conditions and in the absence of more labile substrates, even ancient material is susceptible to some degree of biodegradation (Petsch *et al.*, 2005; Schillawski and Petsch, 2008). For example, during seasonal hydrological isolation in the subglacial environment, when external inputs are limited (Tranter *et al.*, 2005), buried ancient organic matter may be broken down by extensive bacterial communities (Boyd *et al.*, 2010, 2011; Stibal *et al.*, 2012b; Anesio *et al.*, 2017). Bacterial activity may simultaneously release labile exudates (O'Donnell *et al.*, 2016; Musilova *et al.*, 2017), which may have incorporated ancient carbon and be flushed from the glacier bed by seasonal meltwaters.

The seasonal progression in ^{14}C-POC signatures in bulk outflows from the Leverett Glacier, Greenland, shows that increasingly old sediments are mobilised from subglacial sources over the melt period (Kohler *et al.*, 2017). It is hypothesised that an expanding subglacial meltwater network accesses increasingly ancient POC and releases it into the outflows. It is possible that a corresponding dynamic might affect DOC export, which would establish a link with ancient subglacial sources. However, a seasonal time series for ^{14}C-DOC from this system is yet to be undertaken. An alternative link between DOC and ancient subglacial sources might be established through glacial erosion. Such erosion has recently been shown to liberate organic gases from rock minerals (Macdonald *et al.*, 2018) and trigger radical reactions which could release simpler compounds from buried organic material (Tranter, 2015). These

subglacial sources of re-worked (by erosion or biodegradation) organic matter could therefore account for both ancient and labile DOM.

1.3.2.4. Potential role of POM

Most bioavailability studies have focused on the analysis of DOM, which is arguably the more labile component of organic matter in aquatic systems (Brett *et al.*, 2017). Glacial POM is implicitly assumed to be largely recalcitrant and, to date, only one study has estimated its bioavailability through measurement of extractable carbohydrates (Lawson *et al.*, 2014a). These relatively labile compounds comprised <10% of total POC by weight in samples from the Leverett Glacier, Greenland (Lawson *et al.*, 2014a), but it is not known how well this reflects its bioavailability in natural waters. In general, the characterisation of glacial POM has been largely restricted to carbon isotope analyses at a handful of locations, mostly in Greenland (Bhatia *et al.*, 2013; Kohler *et al.*, 2017). This has helped to discriminate sources of POM and estimate its age but not to enhance understanding of its impact on downstream ecosystems.

1.3.3. Significance of the effect of glacial DOM on specifically marine systems

Glacial meltwaters have attracted great interest for their potential to impact nearshore marine ecosystems and nutrient cycling. The high bioavailability of glacial DOM is specifically thought to stimulate marine heterotrophs in regions where meltwaters reach the coast. This argument largely rests on evidence from incubations of glacial ice, snow and runoff following inoculation with a marine bacterial sample (Hood *et al.*, 2009; Fellman *et al.*, 2010a; Lawson *et al.*, 2014a). In the Gulf of Alaska, there is some suggestion that marine bacteria from highly saline waters are more efficient at respiring glacial DOM than those from brackish or relatively fresh waters (Fellman *et al.*, 2010a). In other regions, glacial bacteria are shown to survive in cold coastal waters and hypothesised to support the ongoing consumption of glacial DOM in offshore locations (Gutiérrez *et al.*, 2015; Paulsen *et al.*, 2017).

Whereas the studies mentioned above infer the effect on marine systems by inoculating a glacial sample with marine bacteria, two studies in Young Sound, northeast Greenland, have sought to explore the dynamics of glacial DOM where it enters the marine environment. Incubations of the input river waters, which are fed by glacial melt

to varying degrees, and samples from the fjord surface layer, show that measured BDOC declines with increasing distance from the land (Paulsen *et al.*, 2017). These changes coincide with a depletion in the nitrogen content of the DOM (Paulsen *et al.*, 2017). This is consistent with the removal of highly labile material from input waters as inferred by previous studies (e.g. Hood *et al.*, 2009). However, it is also consistent with the addition of less reactive organic matter from marine sources and more distant terrestrial inputs (Paulsen *et al.*, 2017).

The second study in Young Sound demonstrated that fjord bacteria and zooplankton grazing provide additional sources of protein-like material and therefore the supply of labile substances may not be limited to glacial inputs (Paulsen *et al.*, 2018). Some fjord bacterial species may also consume humic-like DOM (Paulsen *et al.*, 2018), which is classically assumed to derive from vegetation and soils and be less bioavailable than protein-like substances, due to complex aromatic and branched molecular structures (Grant, 1977; McKnight *et al.*, 2001; Nebbioso and Piccolo, 2013). The second Young Sound study demonstrated how fluorescence data can detect compositional changes associated with the biological processing of DOM that are not apparent in concentration changes measured over incubations (Paulsen *et al.*, 2018). Therefore, simple incubation studies may not capture the full complexity of DOM cycling in glaciated fjords.

1.4. Addressing key research opportunities

This section outlines how the analytical chapters of this thesis (Chapters 3–5) aim to address key gaps in our understanding and opportunities for future investigation identified from the literature review above. Specifically, this thesis targets gaps in the global coverage of studies to date, integrates terrestrial and marine perspectives on glacial organic matter export for a single region and deploys molecular level analyses in a glaciated fjord.

1.4.1. Global coverage

Organic matter research in glaciated environments has focused primarily on a few study regions in the northern hemisphere (Table 1.1; Figure 1.4a). The southern hemisphere has been less studied except for a small number of isolated locations in the McMurdo Dry Valleys and coasts of Antarctica (McKnight and Tate, 1997; Barker *et al.*, 2013;

Table 1.1. Summary of analytical methods employed to investigate glacial organic matter in terrestrial and nearshore marine settings.

	DOC	POC	$\delta^{13}C$	$\Delta^{14}C$	BDOC	Biomarkers	Fluorescence	FT-ICR MS
Terrestrial sites								
Gulf of Alaska	✓[1-8]		✓[1,4,6,8]	✓[1,4,5,8]	✓[1,7]	✓[1,5]	✓[1,4-8]	✓[5,6,8]
Greenland	✓[9-11]	✓[9,10,12]	✓[10]	✓[10]	✓[9]	✓[9,13]	✓[9]	✓[11,14]
Iceland	✓[15]	✓[15]					✓[15]	
Svalbard	✓[16]	✓[16]						
European Alps*	✓[17]			✓[17]	✓[17]		✓[17]	✓[17]
Himalayas/Tibet	✓[18,19]		✓[18,20]	✓[18,20]	✓[18,19]		✓[18]	✓[18,19]
Antarctica	✓[21,22]						✓[21,22]	✓[23]
Nearshore marine sites								
Greenland	✓[24]	✓[24]			✓[24]		✓[25]	
Svalbard	✓[26,27]	✓[26,27]	✓[26,27]				✓[28]	

Table notes

Analytical techniques

Concentration measurements (DOC, POC); natural stable isotope ($\delta^{13}C$) and radioisotope ($\Delta^{14}C$) analysis of organic carbon; bioavailability incubations (BDOC); analysis of specific biomarkers (including lipid extraction or ion chromatographic detection of low molecular weight organic acids and carbohydrates); fluorescence analysis; molecular characterisation of DOM by Fourier transform ion cyclotron resonance mass spectrometry (FT-ICR MS).

*denotes analysis of DOM from glacial ice only. Other studies include analysis of ice, snow and runoff.

Table references

1. (Hood *et al.*, 2009); 2.(Hood and Berner, 2009); 3. (Hood and Scott, 2008); 4. (Spencer *et al.*, 2014a); 5. (Stubbins *et al.*, 2012); 6. (Fellman *et al.*, 2014); 7. (Fellman *et al.*, 2010a); 8. (Fellman *et al.*, 2015b); 9. (Lawson *et al.*, 2014a); 10. (Bhatia *et al.*, 2013); 11. (Bhatia *et al.*, 2010); 12. (Kohler *et al.*, 2017); 13. (Musilova *et al.*, 2017); 14. (Lawson *et al.*, 2014b); 15. (Chifflard *et al.*, 2019); 16. (Zhu *et al.*, 2016); 17. (Singer *et al.*, 2012); 18. (Spencer *et al.*, 2014b); 19. (Hemingway *et al.*, 2019); 20. (Li *et al.*, 2016); 21. (Barker *et al.*, 2013); 22. (Smith *et al.*, 2017); 23. (Antony *et al.*, 2014); 24. (Paulsen *et al.*, 2017); 25. (Paulsen *et al.*, 2018); 26. (Holding *et al.*, 2017); 27. (Zhu *et al.*, 2016); 28. (Brogi *et al.*, 2019)

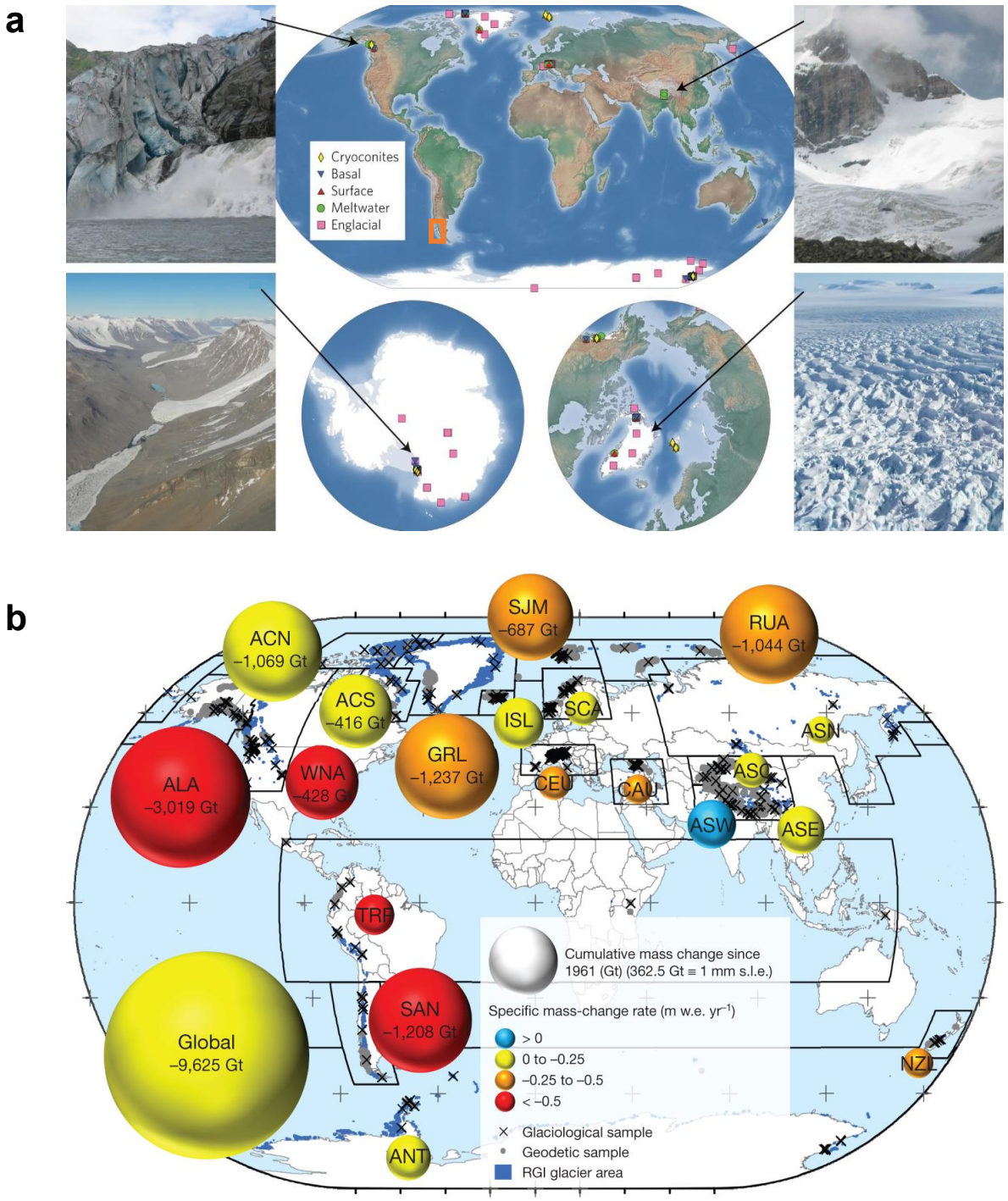

Figure 1.4. Distribution of samples collected for glacial organic matter analysis in comparison to rates of ice loss. (a) Location of samples (categorised by type) used to quantify global storage of organic carbon in glacial ice (after: Hood *et al.*, 2015). Chilean Patagonian region indicated on world map with orange box. (b) Size and rate of change in glacier ice mass between 1961 and 2016 by region: cumulative changes in total mass shown by size of bubbles; colour indicates rate of change; notable regions referred to in text include Alaska (ALA) and Southern Andes (SAN); full details given in original publication (Zemp *et al.*, 2019).

Antony *et al.*, 2014). Observations in the South American Andes have largely been restricted to isolated mountain top glaciers and focused on the contribution of black carbon from local anthropogenic to snowpack organic matter (Molina *et al.*, 2015; Rowe *et al.*, 2019). These studies have not contributed to a quantitative understanding of glacial organic matter export, nor have they provided a regional assessment of its composition. The general absence of data from Chilean Patagonia, in South America, highlights a significant gap in our understanding of how glaciated landscapes influence regional and global biogeochemistry, especially within the context of climate change.

Chilean Patagonia contains two major icefields (and many separate mountain glaciers) which comprise the greatest concentration of southern hemisphere land ice, excluding Antarctica (Lopez *et al.*, 2010; Davies and Glasser, 2012; Foresta *et al.*, 2018). The icefields dominate the supply of freshwater to the oceans in this region, with meltwaters entering the ocean via an extensive network of glacially carved fjords that receive inputs directly from marine-terminating glaciers and glacially fed rivers (Dávila *et al.*, 2002; Pantoja *et al.*, 2011; Dussaillant *et al.*, 2012; Moffat *et al.*, 2018). The glaciers of this region are undergoing some of the most intense rates of retreat in the world and, critically, those rates appear to be accelerating (Rignot *et al.*, 2003; Chen *et al.*, 2007; Ivins *et al.*, 2011; Willis *et al.*, 2012a, 2012b; Jaber, 2016; Dussaillant *et al.*, 2019). In global terms, glaciers in the South American Andes (which includes those in Chilean Patagonia) have lost the largest total amount of mass to the oceans, after the Gulf of Alaska region (Figure 1.4b; Zemp *et al.*, 2019). Enhanced meltwater fluxes may therefore drive an increasingly important, but so far overlooked, flux of organic matter into downstream aquatic systems.

Theories regarding the source and reactivity of glacial organic matter are derived from sites in the densely populated northern hemisphere. Although atmospheric pollutants may be globally dispersed (Antony *et al.*, 2014), looking toward southern hemisphere study sites provides opportunity to examine anthropogenic influences on glacial DOM in a different context. The Patagonian Icefields are primarily influenced by westerly winds which carry air masses from the South Pacific (Lopez *et al.*, 2010; Schaefer *et al.*, 2013; Foresta *et al.*, 2018) that will have been exposed to less concentrated direct anthropogenic inputs. Recent work on glaciers in northern Chile has identified black carbon deposits linked to local biomass burning and industrial activity (Molina *et al.*,

2015; Rowe *et al.*, 2019). However, these sources may be insignificant where population density is very low in the relatively pristine conditions of Chilean Patagonia (Pantoja *et al.*, 2011; Pérez *et al.*, 2018), which forms the study region for this thesis.

This thesis presents the first region-wide characterisation of the organic matter within terrestrial and marine aquatic systems of Chilean Patagonia with the aim of testing the impact of glacial meltwater contributions. Chapter 3 relates spatial trends in the size and character of riverine organic matter fluxes to a range of landscape gradients. The influence of glaciers on total organic matter export and DOM composition is identified from significant differences between the conditions in glacial and non-glacial rivers as well as through statistical relationships with catchment glacial cover. The effects of lakes and vegetation are also investigated as landscape factors that are affected by glacier retreat. Chapter 4 presents the first attempt to quantify the bioavailability of DOM in a subset of the rivers studied in Chapter 3 and identifies potential factors which may influence overall reactivity. Chapter 5 completes the suite of analytical studies by providing an assessment of the spatial and seasonal impact of glacial meltwaters on DOM composition in a Chilean Patagonian fjord.

1.4.2. Integration of terrestrial and marine perspectives

The most influential studies in this area adopt an approach that is focused on the characteristics of DOM near the point of release rather than at the point of entry into the receiving system under investigation (e.g. Hood *et al.*, 2009; Stubbins *et al.*, 2012; Lawson *et al.*, 2014b). In other words, the impact of glacial organic matter on downstream aquatic systems (including marine systems) is inferred from its composition and reactivity near the source. For example, high BDOC is measured in samples of glacial snow, ice and runoff in glacially fed rivers (Hood *et al.*, 2009; Singer *et al.*, 2012; Spencer *et al.*, 2014b; Hemingway *et al.*, 2019). The link with marine ecosystems is often established through use of a marine bacterial inoculum in BDOC incubations (Hood *et al.*, 2009). By contrast, studies which assess the impact of glacial DOM within a marine setting are comparatively rare (Paulsen *et al.*, 2017, 2018). Moreover, complementary marine-based studies of DOM are lacking for regions that have attracted considerable interest in understanding the impact of glacially exported DOM from a terrestrial perspective, such as in the Gulf of Alaska. Despite the strong

control of glacial meltwaters on marine ecosystem structures in this region of the North Pacific (Arimitsu *et al.*, 2016, 2018), no study has directly tested the impact of glacier melting on marine DOM composition in this region. The contribution of influential BDOC incubation studies is therefore limited by an inability to appreciate the potential for DOM transformation between upstream sampling sites and the ultimate receiving system and interactions with other components within a mixed marine DOM pool.

DOM may be transformed by a variety of processes, which might operate both between the sampling site and marine environment and within the marine environment itself. During riverine transport, glacial DOM may be subject to biological consumption, photodegradation and mixing with non-glacial DOM sources (Jones *et al.*, 2016). Upon entry to marine waters, DOM may also be removed by flocculation and adsorption to sediments (Eisma, 1986; Aufdenkampe *et al.*, 2001). Therefore, glacial DOM sampled from upstream locations may not be representative of that which enters the marine environment. Chapter 4 presents a test case for understanding how biological consumption of DOM may influence changes in its composition en route to and within the marine environment. For a DOM component identified as highly bioavailable, its absence from a system may imply prior consumption (although not necessarily). Absence of an unreactive component is unlikely to be due to consumption.

The mixing and interaction of different DOM sources within marine systems may also influence the reactivity and accessibility of individual DOM components. Marine waters along glaciated coasts may integrate DOM from multiple glaciers and rivers, diffuse contributions via overland flow and groundwaters and material produced by in situ ecosystems (Paulsen *et al.*, 2017, 2018). The significance of each source will be determined by the specific geography of the region. Research in Young Sound, Greenland, has shown that humic-like DOM from distant terrestrial sources may provide a reactive substrate for fjord bacteria (Paulsen *et al.*, 2018). Neglecting substrates from such distant sources or those produced in situ (as might result from the focus on individual river inputs) may not provide an accurate understanding of the reactivity of a mixed DOM pool. The consumption of glacial DOM during laboratory or field incubations, therefore, may not be representative of its reactivity when mixed with a larger heterogeneous DOM pool in coastal waters.

Unless the composition and reactivity of the DOM pool within the marine system is understood, it is difficult to test hypotheses concerning the impact of individual inputs such as from glacial meltwaters. Chapter 5 attempts to characterise DOM in a fjord fed by a variety of inputs, including from glaciers, to help inform a better appreciation of their impact on marine biogeochemistry. Complementary studies from terrestrial perspectives (Chapters 3, 4) mean that the thesis provides an integrated regional assessment of the impact of glacial meltwaters on fresh and marine waters in Chilean Patagonia. This kind of analysis is also a prerequisite to evaluating the representativeness of findings from the incubation of upstream samples. Chapter 4 provides a model of how composition data from the region might inform an understanding of which components of DOM may be the most reactive in the marine system. The findings from Chapter 4 support interpretation of direct analyses of DOM within a glaciated fjord in Chapter 5.

1.4.3. Potential of molecular level analyses

The composition of organic matter provides information about its source and reactivity but its heterogeneous nature defies complete characterisation by a single analytical technique (Derrien *et al.*, 2019). The development of ultrahigh resolution mass spectrometry (by Fourier transform ion cyclotron resonance mass spectrometry; FT-ICR MS) has provided unparalleled insight into organic matter compositions at the molecular level due to compound detection with high accuracy across a wide mass range (~100–1000 Da) and the availability of non-selective extraction procedures (Dittmar *et al.*, 2008; Nebbioso and Piccolo, 2013). Whilst unable to distinguish isomeric structures, this method has advanced insights into biological and photochemical degradation on molecular composition across a range of environments (Osterholz *et al.*, 2014; Spencer *et al.*, 2015; Riedel *et al.*, 2016; Seidel *et al.*, 2017; Kellerman *et al.*, 2018). The analysis generates semi-quantitative data which enables the use of a range of statistical methods (including multivariate techniques) to test for relationships with environmental factors (Kellerman *et al.*, 2015; Osterholz *et al.*, 2016).

Molecular characterisation of DOM by ultrahigh resolution mass spectrometry has greatly advanced understanding of the sources and reactivity of organic matter in glacial ice and meltwaters (Bhatia *et al.*, 2010; Singer *et al.*, 2012; Stubbins *et al.*, 2012).

However, to date, only one study in Svalbard has applied molecular level techniques to assess the composition of DOM in glacially influenced fjords (Osterholz *et al.*, 2014). This study demonstrated that fresh DOM produced during spring phytoplankton blooms is rapidly consumed and leaves little imprint on the molecular compositions preserved in deep marine waters (Osterholz *et al.*, 2014). No study has exploited molecular level techniques to explicitly examine the influence of glacial meltwater inputs on marine DOM composition.

Other work in Arctic fjords has used bulk isotopic ratios ($\delta^{13}C$, $\delta^{15}N$) in organic matter to differentiate marine and terrestrial contributions to POM (Holding *et al.*, 2017) but not specifically to test the transformation of DOM in the fjord. Whilst it is widely recognised that glaciated fjords are particularly affected by changes in meltwater runoff and the retreat of surrounding glaciers, most studies to date have focused on how changes in nutrient or light availability may impact on fjord ecosystem productivity (Aracena *et al.*, 2011; Arimitsu *et al.*, 2016; Van De Poll *et al.*, 2018; Halbach *et al.*, 2019). Focused molecular level investigations into the organic matter pools in glaciated fjords would seem to be a missing link in helping to advance our understanding in the role that glaciers play in controlling regional biogeochemical cycles via the supply of labile DOM.

Chapter 5 will demonstrate the potential for molecular level analysis by exploiting this technique to investigate the spatial and seasonal changes in DOM composition in a Chilean Patagonian fjord in relation to glacial meltwater inputs. It should also be noted that the wealth of molecular level analyses in Chilean Patagonian rivers enables an understanding of landscape level controls over organic matter biogeochemistry (Chapter 3) and provides an important tool to inform interpretation of BDOC incubations (Chapter 4).

2. Methodology

This chapter gives an overview of the study sites, sampling strategies and primary analytical techniques used in this thesis. Each analytical chapter (Chapters 3–5) contains additional methodological details relevant to the specific aims of that chapter.

2.1. Study region

The climate of Chilean Patagonia is defined by a temperate regime and a strong zonal precipitation gradient (Figure 2.1). Temperatures vary around an annual mean of 8°C, with seasonal means ranging between 4°C in austral winter and 13°C in austral summer (Sagredo and Lowell, 2012; Vandekerkhove *et al.*, 2016). However, temperatures rarely exceed 10°C south of 42°S (Aracena *et al.*, 2011). The orographic uplift of South Pacific air masses carried by prevailing south-westerly winds generates a hyper-humid climate on the western side of the Andes (Garreaud *et al.*, 2013). Here, rain may occur on more than 300 days a year (Kerr and Sugden, 1994), although it is heaviest in winter (Rebolledo *et al.*, 2019), and can lead to annual rainfall totals which regularly exceed 3 m a^{-1} (Figure 2.1b) and sometimes 7 m a^{-1} (Aracena *et al.*, 2011). These conditions contrast with a relatively arid climate to the east of the Andes, where annual rainfall is

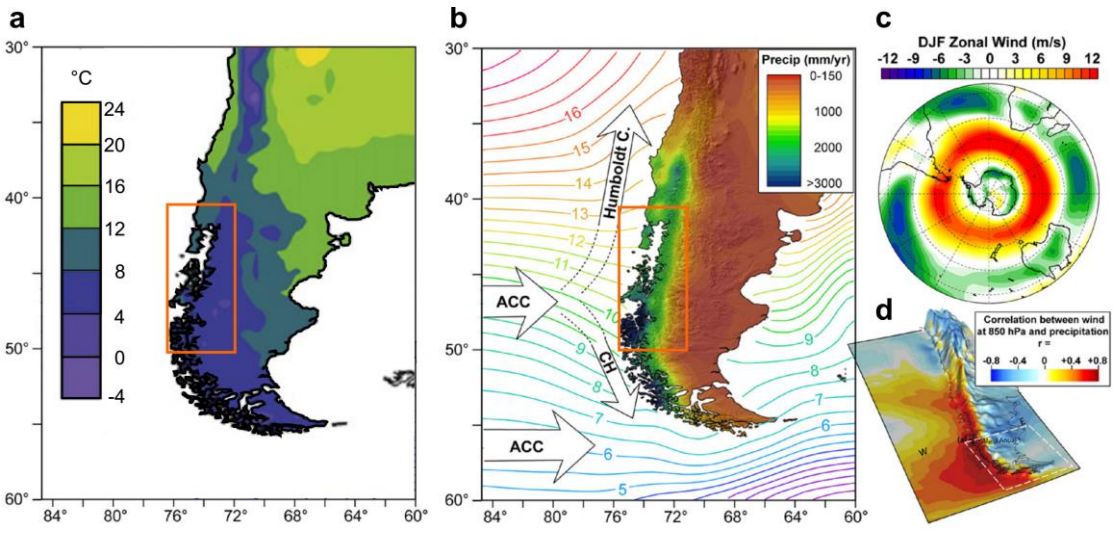

Figure 2.1. Climatic context for study region, showing (a) mean annual temperatures between 1961–1990 (data: New et al., 2002; plot adapted from: Sagredo and Lowell, 2012); (b) mean annual precipitation and sea surface temperature isotherms with respect to ocean circulation patterns: Antarctic Circumpolar Current (ACC), Humboldt and Cape Horn (CH) currents; (c) mean zonal wind speeds between December and February (1957–96) with positive and negative speeds indicating westerly and easterly winds, respectively; (d) correlation between windspeeds and precipitation with respect to continental elevation. Subplots b–d taken from Kilian and Lamy (2012). Orange boxes in subplots a–b show location of study region used in this thesis.

typically <0.25 m a^{-1} due to rain shadow effects (Vandekerkhove *et al.*, 2016). The correlation of windspeeds and rainfall in relation to continental relief (Figure 2.1d) shows the role of the Andes in controlling this zonal precipitation gradient.

The hyper-humid climate to the west of the Andes supports dense vegetation cover, with the distributions of individual species controlled by temperature and rainfall variations across latitudes and elevations (Abarzúa *et al.*, 2004). Ground cover in the northern part of the region (north of 46°S) is characterised primarily by dense broadleaf evergreen forest, which gives way to a more complex vegetation mosaic further south and at higher altitudes where there is greater deciduous and herbaceous shrub cover (Vandekerkhove *et al.*, 2016). Forests across the region are dominated by the *Nothofagus* genus (southern beech trees), with species-level compositions reflecting the postglacial succession of individual species competing in response to interannual climatic variations, such as the Pacific Decadal Oscillation and Southern Annular Mode (Srur *et al.*, 2018), and local disturbances, such as storms and floods (Armesto *et al.*, 1992).

The present-day hydrography of Chilean Patagonia reflects a landscape that has been largely shaped by glacial activity. The region contains a high density of freshwater lakes (Messager *et al.*, 2016), some of which occupy deep glacial basins and are among the largest in South America (e.g. Lake General Carrera; Figure 2.2). Large river systems drain through glacially eroded valleys on the western flanks of the Andes and provide a major freshwater flux to the ocean (Dávila *et al.*, 2002). Direct inputs to the ocean via overland runoff and groundwater discharge are not well constrained but are largely assumed to be relatively small components of the total freshwater flux (Dávila *et al.*, 2002; Pantoja *et al.*, 2011). The complex network of fjords and flooded glacial inlets along the Chilean coastline are testament to much more widespread ice cover during the last glacial period (Pantoja *et al.*, 2011).

The hydrology of Chilean Patagonia is influenced by a strong landscape-level gradient in ice cover. In the northern part of the study region (north of ~46°S), ice cover is largely restricted to individual valley glaciers and small ice caps on the highest peaks. Rivers here are more responsive to rainfall events and the melting of more extensive seasonal snow covers (Calvete and Sobarzo, 2011; Pérez *et al.*, 2018). River discharge patterns therefore exhibit a combination of 'nival' and 'pluvial' regimes, whereby peak annual

discharge coincides with spring snowmelt or winter rainfall, respectively. Ice cover south of 46°S is concentrated in the Northern and Southern Patagonian Icefields (NPI, SPI; Figure 2.2), which are ~4200 km^2 and ~13000 km^2, respectively (Lopez *et al.*, 2010). Rivers fed by meltwaters from the icefields follow a 'glacial' regime, whereby peak annual discharge is driven by summertime ice melt (Dussaillant *et al.*, 2012).

The icefields are sustained by low annual temperatures and orographic precipitation as a result of their high-altitude position (Lopez *et al.*, 2010; Lenaerts *et al.*, 2014). However, they are sensitive to rising global temperatures and are currently undergoing rapid rates of retreat (Glasser *et al.*, 2011; Willis *et al.*, 2012b, 2012a; Jaber, 2016; Foresta *et al.*, 2018). Warming ocean temperatures are further accelerating the loss of ice along marine-terminating margins of the SPI (Moffat *et al.*, 2018) and the San Rafael Glacier of the NPI (Willis *et al.*, 2012a). The formation of meltwater lakes along the margins of many land-terminating outlet glaciers of the NPI, combined with widespread glacial thinning, has triggered numerous glacial lake outburst floods (or GLOFs) and these may be occurring with increasing frequency (Dussaillant *et al.*, 2012; Carrivick and Tweed, 2016; Aniya, 2017). These GLOFs represent significant perturbations to the annual discharge regimes of even the largest rivers of the region, such as the Baker River (Dussaillant *et al.*, 2012). Continued melting of the icefields will control future landscape evolution, such as through proglacial lake formation (Wilson *et al.*, 2018).

2.1.1. Latitudinal river transect

A total of 29 rivers (42–48°S) were sampled for organic geochemical analysis between 7 January and 23 February 2017 (Figure 2.2). These catchments span large gradients in glacier cover, lake influence and vegetation cover (Table 2.1), which serve as spatial proxies for temporal landscape changes linked to deglaciation. Sites toward the south of the study region have generally higher glacier cover whereas northerly sites are in more densely forested deglacial valleys. There are also large variations in the number and sizes of freshwater lakes between catchments. Although spot sampling may limit the value of individual observations, since it is not clear how representative each sample may be, trends across the full dataset enable analysis of landscape level controls over DOM composition. This helps to assess the long-term impact of ongoing glacier retreat on the export of organic matter by Chilean Patagonian rivers.

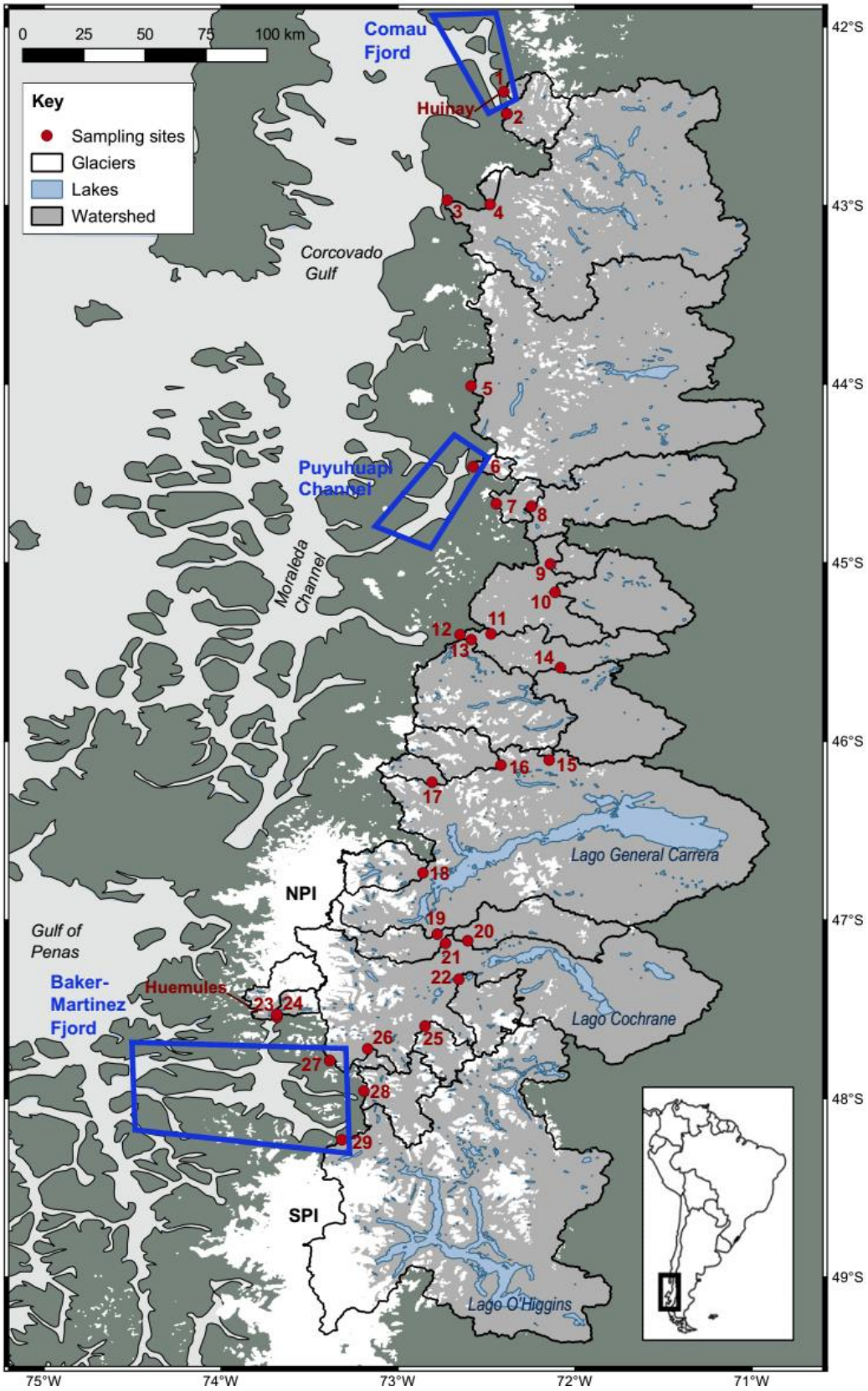

Figure 2.2. Location of terrestrial and fjord sampling locations across study region with respect to glacial cover and freshwater lake distribution. Northern and Southern Patagonian Icefields (NPI, SPI) and the three largest lakes are labelled. Terrestrial sampling site numbers correspond to those in Table 2.1; with Huinay and Huemules rivers additionally labelled. Blue boxes show fjord sampling regions referred to in text (Sections 2.1.3 and 2.1.4).

Table 2.1. Catchment properties for rivers sampled for organic geochemical analysis between 42–48°S in Chilean Patagonia. Numbers correspond to those in basemap (Figure 2.2).

No.	River	Catchment area (km^2)	Glacier cover (%)	Number of lakes	Total lake volume (x 10^6 m^3)	Forest cover (%)	Herbaceous/shrub cover (%)
1	Huinay	108	1.2	1	9	56	27
2	Vodudahue	911	7.8	5	39	45	43
3	Yelcho	11,354	2.2	64	33,695	50	27
4	Amarillo	133	19.8	0	0	15	60
5	Palena	12,506	2.6	81	17,580	52	30
6	Ventisqueros	176	32.7	3	43	43	4
7	Cisnes (I)	3,213	1.1	18	114	41	36
8	Cisnes (II)	3,607	1.1	20	130	43	35
9	Maniguales (I)	335	0.6	1	5	61	25
10	Nireguao	1,964	0.1	19	164	39	43
11	Maniguales (II)	4,333	0.2	24	176	54	32
12	Aysen	11,328	1.3	81	6,829	48	33
13	Blanco	2,987	4.4	32	6,358	59	26
14	Simpson	2,410	0.0	1	278	22	49
15	Estero del Bosque	33	14.2	1	2	28	47
16	Ibanez	899	12.4	8	20	42	38
17	Murta	345	12.6	5	23	53	26
18	Leones	821	31.1	16	2,267	25	26
19	Baker (I)	15,934	5.8	137	717,116	20	35
20	Chacabuco	1,495	1.6	7	58	15	62
21	Baker (I)	16,732	6.5	151	717,162	20	35
22	Salto	1,030	12.9	11	175	31	41
23	Huemules (I)	671	71.0	4	1,355	4	21
24	Huemules (II)	242	38.7	3	274	15	32
25	Nadis	575	17.0	9	17	36	39
26	Del Paso	129	14.8	2	4	25	45
27	Baker (III)	29,107	7.6	267	754,002	20	37
28	Bravo	1,062	14.8	13	67	23	50
29	Pascua	15,079	18.5	164	79,782	12	44

2.1.2. Steffen Glacier

Steffen Glacier is the third largest (~420 km^2) and southernmost outlet glacier of the NPI (Rivera *et al.*, 2007; Willis *et al.*, 2012a). It terminates in a ~20 km^2 freshwater lake (Glasser *et al.*, 2016) with an active calving front that has retreated >5 km since 1945 (Aniya, 2017). It has undergone 7 major periods of retreat since 1990, interspersed with dormant phases or minor re-advance (Aniya, 2017), and overall retreat has accelerated since 2000 (Rivera *et al.*, 2007; Dussaillant *et al.*, 2018). Satellite data show an area reduction of 11–12 km^2 over the last 70 years which accounts for ~8% of the loss from the whole NPI (Rivera *et al.*, 2007; Aniya, 2017). Estimates suggest that Steffen Glacier is losing mass at a rate of 0.43 ± 0.04 km^3 a^{-1} (Willis *et al.*, 2012a), which is the third fastest rate of loss amongst all NPI outlet glaciers (Aniya, 2017).

Meltwaters from Steffen Glacier supply a large proglacial lake, which provides the biggest input of water to the Huemules River. Other water sources include smaller outlet

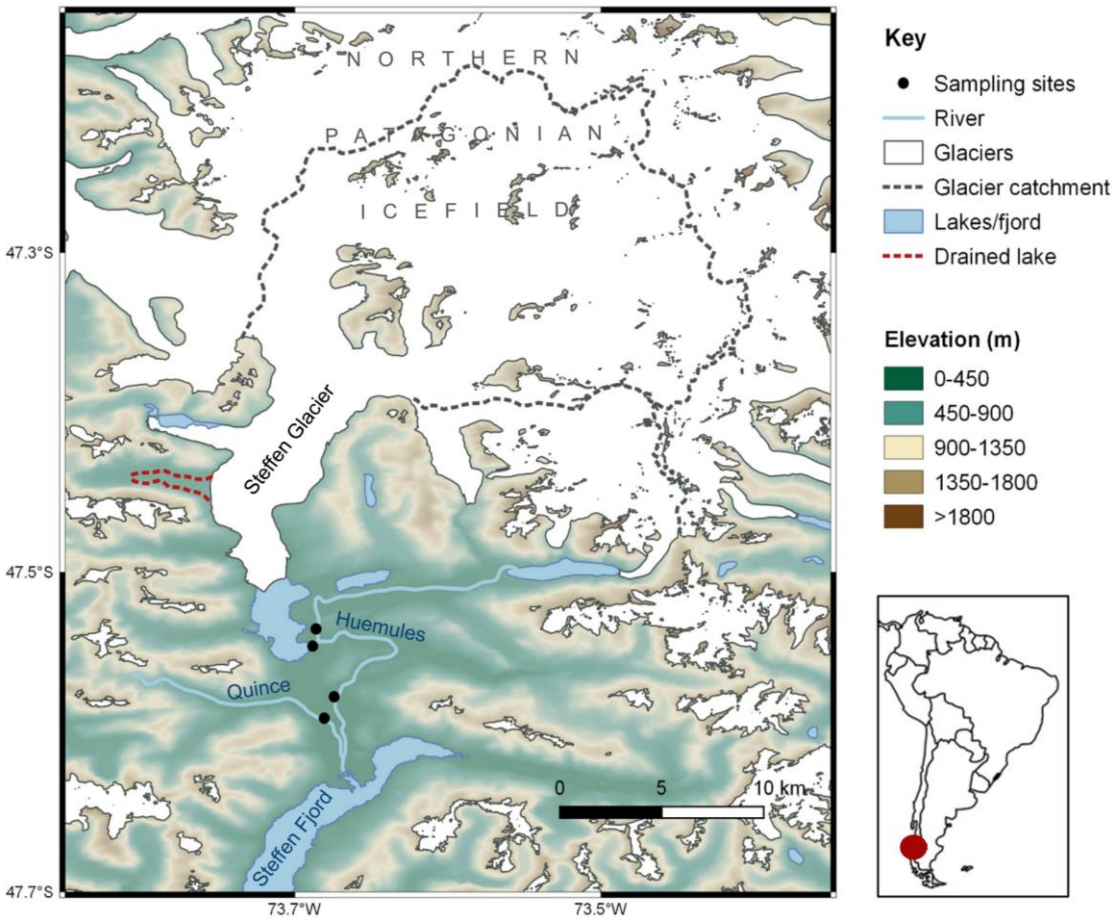

Figure 2.3. Map of sampling sites in Huemules catchment including Steffen Glacier.

glaciers of the NPI (Figure 2.3). River flow is thought to be sensitive to increased melting, glacier retreat and the failure of ice-dammed lakes. Since the 1980s, glacier thinning has triggered GLOFs from two ice-dammed lakes on the western side of Steffen Glacier (Anacona *et al.*, 2015; Aniya, 2017), usually taking place either side of the peak ablation season when thinning rates are high (Aniya, 2014, 2017). Satellite imagery showed that one of these lakes, which had an extent of >5 km^2 in 1987, drained completely in 2016 (Wilson *et al.*, 2018) — see location in Figure 2.3. Grounded icebergs were observed along the banks of the Huemules on arrival at the field site in January 2017, suggesting that discharge levels during GLOFs can flush icebergs out of the proglacial lake. Due to a lack of historical discharge data, it is not clear whether GLOFs from Steffen Glacier are becoming a more frequent hazard, as has been suggested for the NPI more generally (Dussaillant *et al.*, 2012).

Steffen Glacier is considered representative of other NPI outlet glaciers due to its scale, freshwater terminus and current rate of retreat. It may reflect future conditions for systems on the eastern margin of the NPI, where glacier retreat is driving the formation and expansion of proglacial lakes (Wilson *et al.*, 2018). Geochemical and discharge data for the Huemules River will provide critical insight into how glacier melt from the NPI affects river flow and composition.

2.1.2.1. Sample collection

Daily samples were collected between 11 January–26 February and 14–29 July 2017 at the outflow of the proglacial lake, where waters are considered well-mixed. Additional samples collected every 2–3 days from upstream and downstream locations on the Huemules River capture geochemical variations along its course. Samples were also collected every 2–3 days from the humic-rich Quince River, as a local non-glacial comparison site. Sampling locations are shown in Figure 2.3. Bulk samples were filtered immediately and stored according to the requirements for each geochemical analysis (Section 2.2).

Sensors were installed at the main sampling site near the outflow of the proglacial lake to obtain continuous data records, including for river stage and turbidity. Multi-year records of river stage (2016–2018) were also collected by a HOBO pressure transducer

mounted at a secure bedrock location ~200 m further downstream. Stage data were converted to a continuous discharge record using Rhodamine B dye injection traces to generate a rating curve; a method previously employed to measure meltwater discharge from Leverett Glacier, Greenland (Bartholomew *et al.*, 2011). The polynomial rating curve (R^2=0.97; RMSE=8.8%) was based on 14 separate dye traces spanning the full range of observed flow levels (excluding GLOFs) for both field seasons. This is the first ever discharge record for the Huemules River.

2.1.3. Baker-Martinez Fjord

The Baker-Martinez Fjord (BMF) is situated between the NPI and SPI at ~48°S and comprises two main west-east oriented sub-basins, the northerly Martinez Channel and southerly Baker Channel (Figure 2.4). Some exchange between the two channels occurs via north-south connections in the central and outer fjord. The Martinez Channel is on average shallower (typically <500 m), with the Baker Channel reaching maximum depths >1000 m in the central fjord region (Rebolledo *et al.*, 2019). The hydrographic

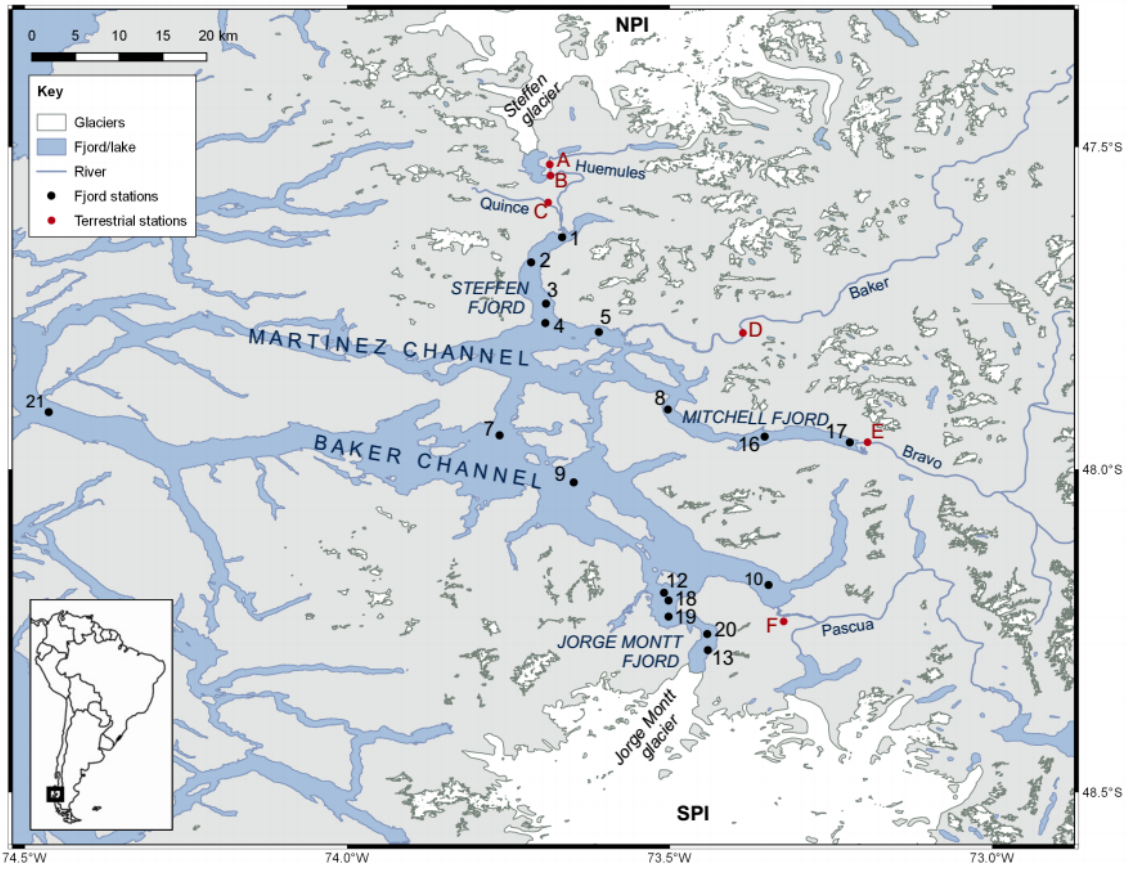

Figure 2.4. Geography of Baker-Martinez Fjord and location of sampling stations. Station numbers relate to those listed in Table 2.2. Terrestrial sampling sites (labelled A-E) along main input rivers also shown.

structure of BMF is typical of other fjords, comprising a thin freshwater surface layer above denser marine water (Bustamante, 2009; Ross *et al.*, 2014, 2015). Annual precipitation rates are high, peaking in the austral winter (May–August; Rebolledo *et al.*, 2019) but freshwater inputs are at a maximum during the austral summer (December–March) when glacier melting drives river discharge (Rebolledo *et al.*, 2019). The principal input rivers, the Baker and Pascua, receive meltwaters from the NPI and SPI respectively (Vargas *et al.*, 2011; Rebolledo *et al.*, 2019). Smaller but less well quantified meltwater inputs are derived from the Jorge Montt Glacier, SPI, and Steffen Glacier, NPI, via the Huemules River. The Bravo River at the head of Mitchell Fjord provides a further freshwater flux from a less glacially influenced catchment.

Tides follow a predominantly semidiurnal regime (Ross *et al.*, 2014) and the overall circulation pattern is controlled by the prevailing winds (Aiken, 2012). Wind forcing causes sub-surface warm water intrusions from the main Baker Channel into Jorge Montt Fjord over a shallow sill ~45 m deep (Moffat, 2014). This highlights a sensitivity of the Jorge Montt Glacier to ocean warming (Moffat *et al.*, 2018) and may contribute to its rapid recent retreat (Rivera *et al.*, 2012), leading to dynamic changes in circulation patterns in this sector of the fjord.

2.1.3.1. Sample collection

Sampling was conducted on the BMF on board the *RV Sur Austral* (University of Concepción) during the austral summer (16–23 February) and winter (4–9 July) of 2017. Sampling details for the fjord surface layer at each station are in Table 2.2, with station locations marked on Figure 2.4. A Seabird SBE model 25 CTD instrument was deployed at each station to measure vertical profiles in temperature, salinity, chlorophyll fluorescence and turbidity. Surface layer water was sampled with a Teflon diaphragm underway pump and passed through Whatman® Polycap GW 75 filter capsules (0.45 µm, PES membrane). Further underway samples were collected regularly during passage between the stations to provide better spatial coverage of variations in freshwater layer composition. At each station, Niskin bottles were used to collect water from selected depths. Samples were filtered for DOC, spectrofluorescence and dissolved nutrient analyses (protocols in Section 2.2). Where possible the same stations were revisited in winter to capture seasonal differences in water column structure and

Table 2.2. Surface layer sampling undertaken on the Baker-Martinez Fjord during austral summer (Feb) and winter (Jul) seasons 2017. Symbols denote measurements taken in summer only (†), winter only (§), or both seasons (✓).

Station location		Latitude (°S)	Longitude (°W)	Distance* (km)	CTD cast	DOC	FT-ICR MS	fluorescence	nutrients
MARTINEZ CHANNEL & INLETS									
Steffen Fjord	S1	47.640	73.667	1.4	✓	✓	✓	✓	✓
	S2	47.679	73.715	7.4	✓	✓		✓	✓
	S3	47.743	73.692	13.2	†				
	S4	47.773	73.693	16.4	✓	✓	✓	✓	✓
Rio Baker plume	S5	47.787	73.610	3.6	✓	✓	✓	✓	✓
Mitchell Fjord	S17	47.958	73.221	1.3	✓	✓	✓	✓	✓
	S16	47.949	73.353	11.2	✓	✓	✓	✓	✓
	S8	47.907	73.503	23.1	✓	✓	†	✓	✓
BAKER CHANNEL & INLETS									
Jorge Montt Fjord	S13	48.280	73.441	6.8	†	†	†	†	†
	S20	48.255	73.442	9.5	§	§	§	§	§
	S19	48.228	73.502	12.4	†	✓		✓	✓
	S18	48.203	73.502	15.2	†	✓		✓	✓
	S12	48.191	73.509	16.5	†	†	†	†	†
Rio Pascua plume	S10	48.179	73.347	3.9	✓	✓	✓	✓	✓
Central fjord	S7	47.947	73.764	24.4	✓	✓	§	✓	✓
	S9	48.020	73.649	27.0	✓	✓	§	✓	✓
Outer fjord	S21	47.911	74.463	79.4	§	§	§	§	§

* Distance refers to straight-line distance between sampling site and nearest river/glacier input

composition. Exceptions include Jorge Montt Fjord, where data from the ice-proximal summer station (S13) are compared to a winter station (S20) 2.7 km further down fjord due to access being limited by floating ice in winter. No data are available for the fjord sill station (S12) in winter. An additional station near the mouth of the Baker Channel (S21) was sampled in winter. Subsurface samples were collected at several stations in winter to examine DOM composition at depth across the fjord by FT-ICR MS (Table 2.3).

Table 2.3. Location of subsurface samples for FT-ICR MS analyses.

Station location		Latitude (°S)	Longitude (°W)	Depth (m)	Salinity (‰)
MARTINEZ CHANNEL & INLETS					
Steffen Fjord	S1	47.640	73.667	40	31.9
	S4	47.776	73.693	270	33.9
Rio Baker plume	S5	47.787	73.609	140	33.7
Mitchell Fjord	S17	47.958	73.221	130	33.7
BAKER CHANNEL & INLETS					
Jorge Montt Fjord	S20	48.255	73.442	30	30.7
	S20	48.255	73.442	180	31.5
Central fjord	S9	48.020	73.649	180	33.8

2.1.4. Other study sites

Additional data were collected during extended monitoring of the Huinay River (29 January–15 February 2018) surveys of Comau Fjord (5–8 February 2018) and Puyuhuapi Channel (12–16 February 2018); locations in Figure 2.2. These data are not a major focus of this thesis but were used to capture variations in freshwater and marine DOM and constrain the regional PARAFAC model (Section 2.3.2.3). Brief descriptions of these field sites are provided below.

2.1.4.1. Huinay River

The Huinay River drains a small, densely forested catchment with low glacier cover at the northern end of the study region (see Table 2.1) and is a relatively minor freshwater input to Comau fjord. Discharge is highly responsive to precipitation, which can exceed 5 m each year (Soto, 2009, cited by Mayr *et al.*, 2014).

2.1.4.2. Comau Fjord

Comau Fjord at ~42°S (Figure 2.2) is ~180 km^2 with a mean depth of 490 m (Pickard, 2011). It has a typical estuarine circulation with freshwater transported seaward in an upper layer and marine water ingress at depth (Mayr *et al.*, 2014). Inflowing rivers, including the Huinay and Vodudahue, drain densely forested relict glacial valleys.

2.1.4.3. Puyuhuapi Channel

Puyuhuapi Channel is a ~50km long, northeast-southwest oriented inlet ~44°S. Unlike other Patagonian fjords, subsurface marine waters overflow shallow sills at both ends of the channel via connections with the Jacaf Channel in the north and the Moraleda Channel to the south (Schneider *et al.*, 2014). The Cisnes River is the largest input of freshwater (Schneider *et al.*, 2014). In contrast to the relatively pristine BMF, salmon farming in Puyuhuapi Channel may have led to incidences of harmful algal blooms (Seguel *et al.*, 2005).

2.2. Sample filtration and storage

All samples were filtered and stored according to analytical requirements, summarised in Table 2.4. All equipment was purchased new and cleaned before use. All plasticware bottles and syringes were soaked in DECON® surfactant (5%) for 24 hours, soaked and rinsed thoroughly in MilliQ (MQ; 18 MΩ cm^{-1}) water, soaked for a further 24 hours in 10% HCl and then rinsed 6 times in MQ. In the field, all syringe filters were initially flushed through with ~10 ml of sample and this filtrate was discarded. Storage bottles were pre-rinsed 3 times with subsequent filtrate before collecting the final filtered sample. Field blanks of filtered MQ water were collected regularly for each analyte over the field seasons to monitor the cleanliness of sampling procedures.

Table 2.4. Filtration and storage methods for field samples.

Analysis	vol	Filter selection	Storage
DOC, fluorescence	30 ml	Whatman® Puradisc AQUA (0.45 µm) syringe filters. Specially designed for environmental DOM applications with cellulose acetate membrane pre-washed by manufacturer to remove organic contaminants.	• HDPE bottle • Pre-furnaced (450°C, 5 hrs) borosilicate vials for some fluorescence samples • All frozen (-20°C)
Incubation experiments	400 – 500 ml	Whatman® PES (0.2 µm) syringe filters; sufficiently small pore size to exclude most bacteria.	• Polycarbonate bottle • Frozen (-20°C)
FT-ICR MS	1 L	River samples filtered through pre-furnaced (450°C, 5 hrs) GF/Fs (0.7 µm). Furnacing removes organic contaminants. Fjord samples filtered through Whatman® Polycap GW 75 filter capsules with PES membrane or Whatman® PES filters (both 0.45 µm pore size) — multipurpose material suitable for trace level work.	• Polycarbonate bottle • Acidified to pH ~2 with 1 ml conc. HCl in 1L sample • At ambient temperature before extraction; see Section 2.3.3.2.
POC	> 2 L	Pre-furnaced (450°C, 5 hrs) GF/Fs (0.7 µm). Low carbon content of filter allows determination of sediment POC content to very low levels (~0.02%); see Section 0.	• Filter with sediment in clean zip-lock bag • Frozen (-20°C)
Dissolved nutrients	30 ml	Whatman® GD/XP (0.45 µm) syringe filters; suitable for trace level work.	• HDPE bottle • Frozen (-20°C)

2.3. Analytical methods

This section details the techniques used to analyse the concentration and composition of organic matter in Patagonian rivers and fjords, as this is the primary goal of the thesis. Complementary dissolved nutrient analyses of fjord waters are also briefly described.

2.3.1. Dissolved organic carbon (DOC) concentrations

DOC concentrations were determined on a Shimadzu TOC-L_{CHN} analyser equipped with a halogen scrubber to enable analysis of saline samples alongside freshwater samples. Briefly, inorganic carbon species were converted to CO_2 through automatic acidification with HCl to pH 2–3 and sparged from solution by bubbling carbon-free air through the sample. The sample was then transferred to the catalyst for high temperature combustion at 680°C. The resultant CO_2 was transferred by carrier gas to an electronic de-humidifier, for cooling and dehydration, and a halogen remover system. Carrier gas transfers the sample to a non-dispersive infrared detection cell to measure CO_2 absorbance as a proxy for the original DOC concentration. This method accurately measures non-purgeable organic carbon, with very few volatile aromatic structures (<5% total DOC; Shimadzu) likely to be lost during sparging. The method therefore provides a conservative measurement of total DOC.

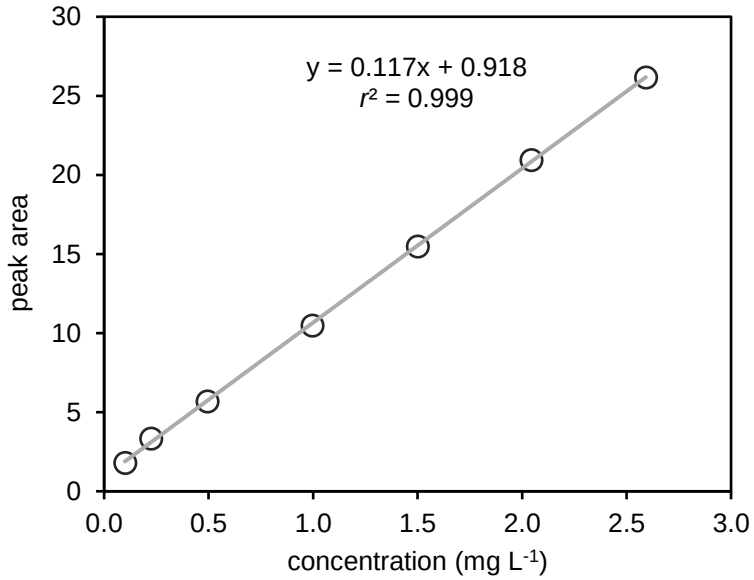

Figure 2.5. Typical calibration curve for DOC concentration determination on the Shimadzu TOC-L_{CHN} analyser.

Instrument calibration was based on measurement of a certified potassium hydrogen phthalate stock (1000 ± 10 mg L^{-1}; Sigma Aldrich) gravimetrically diluted to a range of concentrations (0.05–4.93 mg L^{-1}). Figure 2.5 shows an example calibration curve for the instrument. Calibrations were stable over multiple analytical runs and no significant drift in measurements was observed. Repeat measurement of intermediate concentration check standards (0.1, 0.5 and 1.0 mg L^{-1}) over each analytical run showed minimal variance (ranging between 2.0% and 6.9%, and typically <5%). Instrumental limits of detection (LoD) and quantitation (LoQ) were calculated as 0.033 mg L^{-1} and 0.044 mg L^{-1}, respectively, from repeat measurements of blanks and low concentration standards (Armbruster and Pry, 2008; Equation 2.1–Equation 2.3). Field blanks of filtered MQ water had an average DOC concentration of 0.034 ± 0.022 mg L^{-1} (n=14), which is very close to the LoD and confirms the cleanliness of sampling procedures.

Equation 2.1. Limit of blank (LoB)

$$\text{LoB} = \text{mean blank} + (1.645 \times \text{SD of blank})$$

Equation 2.2. Limit of detection (LoD)

$$\text{LoD} = \text{LoB} + (1.645 \times \text{SD of low concentration sample})$$

Equation 2.3. Limit of quantitation (LoQ)

$$\text{LoQ} = \text{LoB} + (5 \times \text{SD of low concentration sample})$$

2.3.2. Spectrofluorescence data

2.3.2.1. Scanning procedures

Samples were defrosted prior to analysis on an Agilent Cary Eclipse Fluorescence Spectrophotometer equipped with a xenon flash bulb. Excitation-emission matrices (EEMs) were collected over excitation wavelengths 240–450 nm (5 nm increments) and emission wavelengths 300–600 nm (2 nm increments) at a rate of 1200 nm min^{-1} and with 0.1 second integrations. Excitation and emission monochromator slit widths were 5 nm. All samples were scanned through 10 mm quartz cuvettes, which had been stored in 50% HNO_3 and thoroughly rinsed with MQ. In between scans, cuvettes were rinsed three times with both MQ and sample to avoid cross-contamination. Daily MQ scans were collected for blank corrections and to monitor both instrument performance and procedural cleanliness. Additional UV-absorbance measurements were collected on an Agilent Cary Eclipse 60 UV-vis spectrophotometer between 200–800 nm at a speed of 600 nm min^{-1}. Absorbance data accuracy was verified by measurement spectra for a certified holmium reference cell (holmium oxide in perchloric acid), which were consistent with the long-term average of the instrument.

2.3.2.2. Data processing

All fluorescence EEMs were corrected and processed in MATLAB using built-in functions from the drEEM Toolbox 0.2.0 (Murphy *et al.*, 2013).

First, all EEMs were corrected for instrumental biases. These relate to variable transmission efficiencies of different wavelengths through the monochromators and alignment discrepancies. An instrument-specific correction file was used to generate a matrix of correction factors for all wavelength pairs and applied to all sample EEMs.

Second, data were corrected for inner filter effects (IFEs). IFEs are most pronounced at shorter wavelengths and in more concentrated samples where chromophores, which absorb incident and re-emitted radiation, dampen fluorescence signals. Correction matrices were generated for each sample from UV-absorbance scans and applied to the corresponding EEM. Although not strictly necessary for low concentrations (DOC <1 mg l^{-1}) or absorbances <0.05 (Murphy *et al.*, 2013), the higher concentration samples in this dataset warranted correction. IFE corrections were performed for all samples to

ensure a consistent method, even though they had negligible effect for many samples. Correction accuracy is typically ±5% for absorbances <2.0 (Murphy *et al.*, 2013), which applies to most samples in this dataset.

Third, non-fluorescent signals relating to elastic Rayleigh and inelastic Raman scattering were removed from the dataset. These phenomena produce diagonal scatter bands in EEMs, cutting across true fluorescence signals, and do not conform to the assumptions of trilinear variation in PARAFAC modelling (Andersen and Bro, 2003; Ohno and Bro, 2006; Stedmon and Bro, 2008). Subtraction of the relevant daily MQ blank scan from each sample EEM reduced the intensity of Raman scatter peaks but it was necessary to excise all primary and secondary Rayleigh and Raman scatter peaks. Fluorescence signals were not interpolated across the excised scatter bands as this resulted in atypical component spectra in subsequent PARAFAC modelling.

2.3.2.3. PARAFAC Modelling

Parallel factor (PARAFAC) analysis is a multiway technique used to decompose a three-dimensional dataset into separate component factors which account for maximum signal variance across all samples (Figure 2.6). In the context of fluorescence data, components relate to excitation/emission spectra which vary only in intensity between samples. PARAFAC is a powerful statistical tool to analyse complex chemical signals but does not utilise any chemical information. PARAFAC components with chemically realistic spectra are assumed to represent actual chemical moieties in samples. Analysis is premised on the following critical assumptions (Murphy *et al.*, 2013):

- each model component must have distinct excitation/emission spectra which do not vary across the dataset;
- components must not perfectly covary in intensity with each other;
- a component's fluorescence intensity is proportional to its concentration;
- total sample fluorescence is the sum of all individual component intensities.

However, different fluorophores usually scale independently with concentration and so it is likely that there will be at least some covariation of components. Hence, there is a certain degree of subjectivity in the development and selection of the most appropriate

model for a specific dataset. Several key papers outline the principles of PARAFAC and highlight best practice when applying such models to real world data (Stedmon and Bro, 2008; Murphy *et al.*, 2013, 2014b).

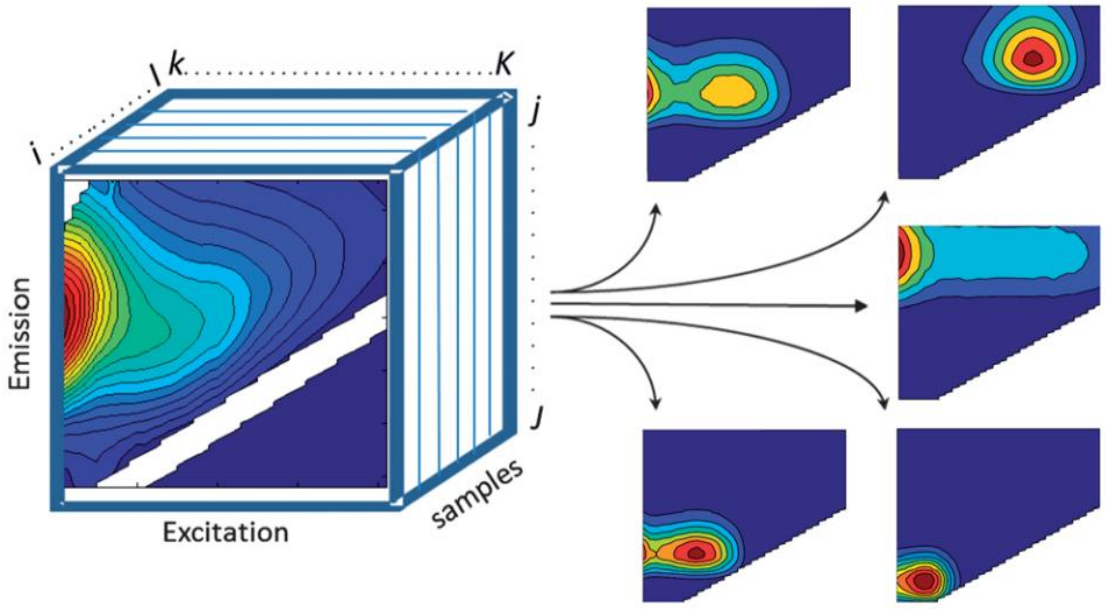

Figure 2.6. Conceptual diagram to illustrate PARAFAC methods. PARAFAC decomposes signals in a 3-dimensional fluorescence dataset (containing *i* samples, over *j* emission and *k* excitation wavelengths) into separate components that describe the majority of variance across the dataset. Source: Murphy *et al.* (2013).

Initial analysis involves an iterative process whereby a series of models with an increasing number of components are applied to the data and results compared between models and against performance criteria. An appropriate number of components are identified along with outlier samples/wavelengths which are excluded before model refinement. The final model is developed with stricter convergence criteria and random initializations. The PARAFAC model here was developed from 386 out of a total of 407 samples using 10 random initializations, non-negative spectral constraints and a convergence criterion of 10^{-8}. The excluded samples had atypical fluorescence profiles and high leverage (>0.3) scores. High leverage wavelengths (excitation <245 nm, emission >550 nm) were also excised from the dataset. Preliminary models confirmed the need to normalise fluorescence intensities to total fluorescence in each EEM, thus removing undue influence from variable DOC concentrations across the dataset on

model convergence. Overall, a 7-component model provided the best fit to the data based on the following assessments:

- All components exhibit realistic fluorescence signatures (Figure 2.7). Models with fewer components produced atypical spectral features that suggested underfitting.
- All component spectra were cross-referenced against published models in the OpenFluor database (Murphy *et al.*, 2014a) and had been identified previously. The similarity between components in this model and those in the database was assessed using the Tucker's Congruence Coefficient (TCC), where scores >0.9 reflect high similarity and those >0.95 are deemed to be identical. Descriptions of the matching fluorophores are in Table 2.5.

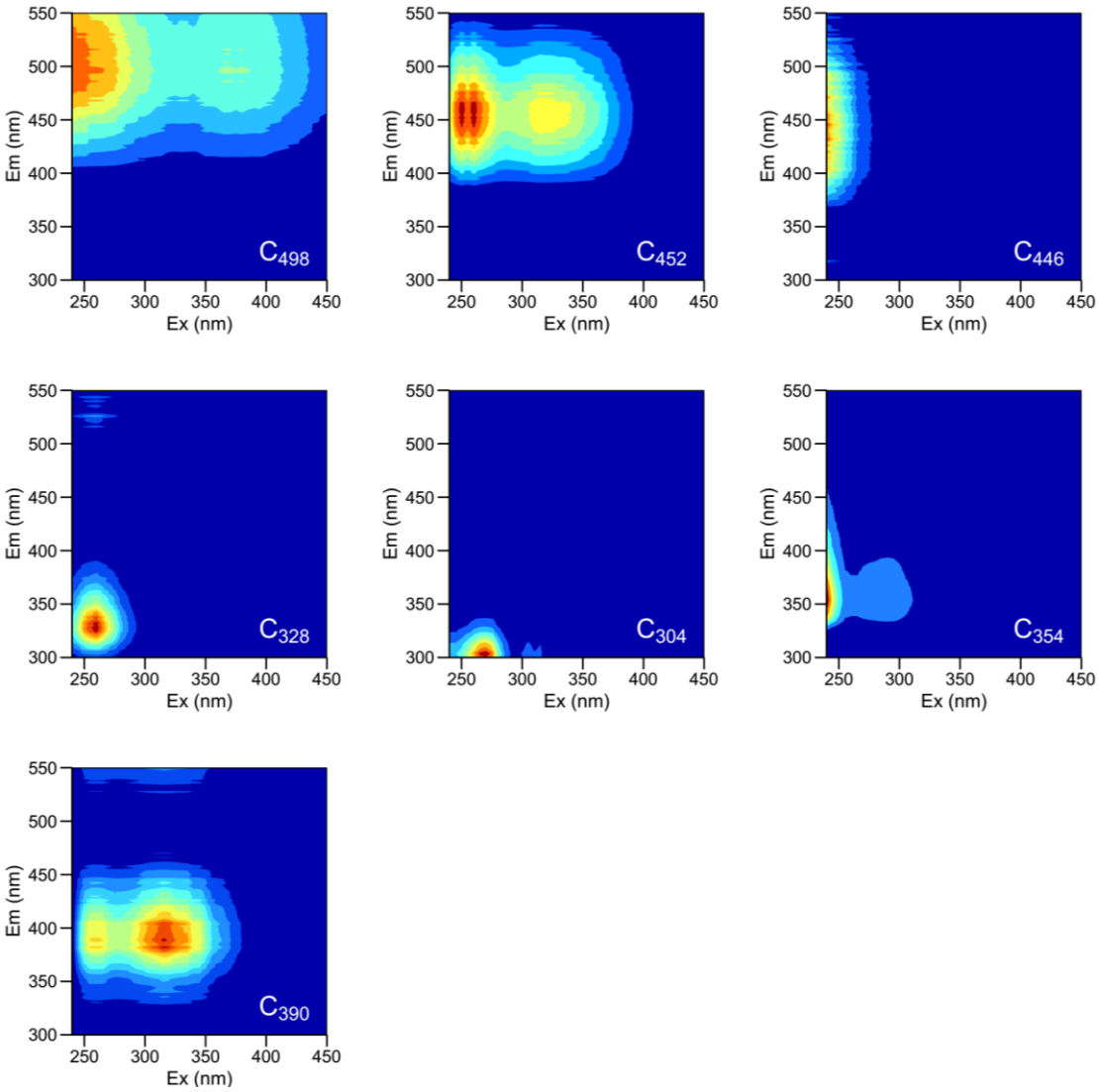

Figure 2.7. Results of 7-component PARAFAC model. Each plot shows the fingerprint of a separate component in excitation-emission space and is annotated with the component (C) name, where the subscripted number denotes the wavelength of maximum emission.

Table 2.5. Fluorophores identified in 7-component PARAFAC model and their description. Each component has been cross-referenced against other published PARAFAC models in the OpenFluor database (Murphy *et al.*, 2014a). Matches are subdivided into sample types and then ranked by the degree of similarity, as determined by the Tucker's Congruence Coefficient (TCC; where values >0.9 indicate high similarity and values >0.95 (and in bold) are regarded as identical matches).

		Matching fluorophores		
Component	**Type**	**Region**	**TCC**	**Reference**
C_{498} Ex. <240 (380) nm Em. 498 nm Terrestrial humic, with some aromatic character. Some similarity with classical peaks A and C.	Marine water	Baltic Sea	**0.980**	(Stedmon *et al.*, 2007b)
		Arctic	**0.977**	(Walker *et al.*, 2009)
		Baltic Sea	**0.972**	(Murphy *et al.*, 2014)
		Global	**0.967**	(Catalá *et al.*, 2015)
		North Atlantic & Beaufort Sea	**0.967**	(Dainard *et al.*, 2015)
		North Atlantic & North Pacific	**0.965**	(Murphy *et al.*, 2008)
	Coastal water	Canadian & Alaskan Arctic	**0.977**	(Walker *et al.*, 2009)
		North Atlantic & Gulf of Mexico	**0.974**	(Brym *et al.*, 2014)
		Arctic fjords	**0.964**	(Wünsch *et al.*, 2018)
	Sea ice	Baltic Sea	**0.970**	(Stedmon *et al.*, 2007)
	Freshwater	Otonabee River, Canada	**0.979**	(Peleato *et al.*, 2016)
		West Greenland lakes	**0.974**	(Osburn *et al.*, 2017)
		Congo rivers	**0.970**	(Lambert *et al.*, 2016)
		Great Lakes, USA	**0.962**	(Williams *et al.*, 2013)
	Terrestrial runoff	Denmark	**0.985**	(Søndergaard *et al.*, 2003)
		Europe	**0.971**	(Graeber *et al.*, 2012)
	Coastal lagoon	Southeast Atlantic	**0.968**	(Amaral *et al.*, 2016)
	Ballast water	Global	**0.980**	(Murphy *et al.*, 2006)
	Drinking water	Australia	**0.991**	(Shutova *et al.*, 2014)
C_{452} Ex. 260 (325) nm Em. 452 nm Terrestrial humic-like with some fulvic character. Some similarity to classical peaks A and C.	Marine water	Arctic	**0.971**	(Guéguen *et al.*, 2014)
		Global locations	0.935	(Jørgensen *et al.*, 2011)
		Arctic	0.918	(Gonçalves-Araujo *et al.*, 2016)
	Sea ice	Baltic Sea	**0.975**	(Stedmon *et al.*, 2007)
	Estuarine and coastal	South Atlantic Bight, USA	**0.958**	(Kowalczuk *et al.*, 2009)
		North America	**0.957**	(Osburn *et al.*, 2016)
	Freshwater lakes	Sweden	**0.959**	(Kothawala *et al.*, 2013)
		Great Plains, USA	**0.959**	(Osburn *et al.*, 2011)
		Argentinian Patagonia	0.939	(Cárdenas *et al.*, 2017)
	Subtropical wetlands	Florida, USA	**0.957**	(Yamashita *et al.*, 2010)

Table continued opposite

C_{446} Ex. <240 nm Em. 446 nm Terrestrial humic-like with some resistance to microbial and photo-degradation.	Terrestrial wetlands	Everglades, Florida, USA	0.947	(Yamashita *et al.*, 2010)
	Marine	Beaufort Sea	0.946	(Dainard *et al.*, 2015)
	Estuarine and coastal	Baltic Sea	0.946	(Murphy *et al.*, 2014)
		Yangtze Estuary, East China Sea	0.938	(Li *et al.*, 2015)
		North America	0.933	(Osburn *et al.*, 2016)
		Horsens Estuary, Denmark	0.924	(Stedmon *et al.*, 2003)
		Arctic fjords	0.920	(Wünsch *et al.*, 2018)
		Baltic Sea	0.918	(Stedmon *et al.*, 2007b)
C_{328} Ex. 260 nm Em. 328 nm Syringic acid/protein-like	Marine	Norwegian Sea	**0.951**	(Wünsch *et al.*, 2015)
C_{304} Ex. 270 nm Em. 304 nm Protein-like	Treated water supplies	Australia	**0.969**	(Murphy *et al.*, 2011)
	Ice core	Antarctica	0.947	(D'Andrilli *et al.*, 2017)
C_{354} Ex. <240 (295) nm Em. 354 nm Tryptophan-like. Similarity to classical peak T.	Sea ice brines	Antarctica	**0.980**	(Stedmon *et al.*, 2011)
	Estuarine and marine water	Arctic fjords	**0.971**	(Wünsch *et al.*, 2018)
		South Atlantic Bight, USA	**0.962**	(Kowalczuk *et al.*, 2009)
	Tidal saltmarsh	Georgia, USA	**0.956**	(Bittar *et al.*, 2016)
	Terrestrial	West Greenland lakes	**0.958**	(Osburn *et al.*, 2017)
	Treated water supplies	Australia	**0.961**	(Murphy *et al.*, 2011)
C_{390} Ex. 315 (265) nm Em. 390 nm Humic with marine-like character, indicating some microbial degradation. Similarity to classical peak M or degradation of classical peak C.	Estuarine and coastal	Baltic Sea	**0.984**	(Murphy *et al.*, 2014)
		North America	**0.972**	(Osburn *et al.*, 2016)
		South Atlantic Bight, USA	**0.970**	(Kowalczuk *et al.*, 2009)
		Yangtze Estuary, East China Sea	0.941	(Li *et al.*, 2015)
		Gulf of Maine	0.923	(Cawley *et al.*, 2012)
	Marine	Fram Strait, Davis Strait, Greenland Sea	**0.958**	(Gonçalves-Araujo *et al.*, 2016)
	Marine deepwater	Japan Sea, North Pacific	**0.980**	(Tanaka *et al.*, 2014)
	Freshwater lakes	Great Plains Lakes, USA	**0.968**	(Osburn *et al.*, 2011)
		Sweden	0.926	(Kothawala *et al.*, 2013)
			0.925	(Kothawala *et al.*, 2012)

- The 7-component model was validated using split-half analysis, whereby models developed from independent subsamples produced identical results. In this case, the dataset was randomly split into 4 equally sized groups that were recombined into 6 different data halves and modelled separately. Spectra from the separate models were compared in 3 tests of similarity (TCC) between corresponding data-halves. The split-half framework is summarised in Table 2.6 and the results shown in Figure 2.8. The model was validated with TCC scores >0.95 for all components across all tests.
- Split-half methods could not validate models with fewer than 7 components.
- Model residuals for 7 components contained mostly random noise; in contrast, 5- and 6-component models contained residuals with structural features.

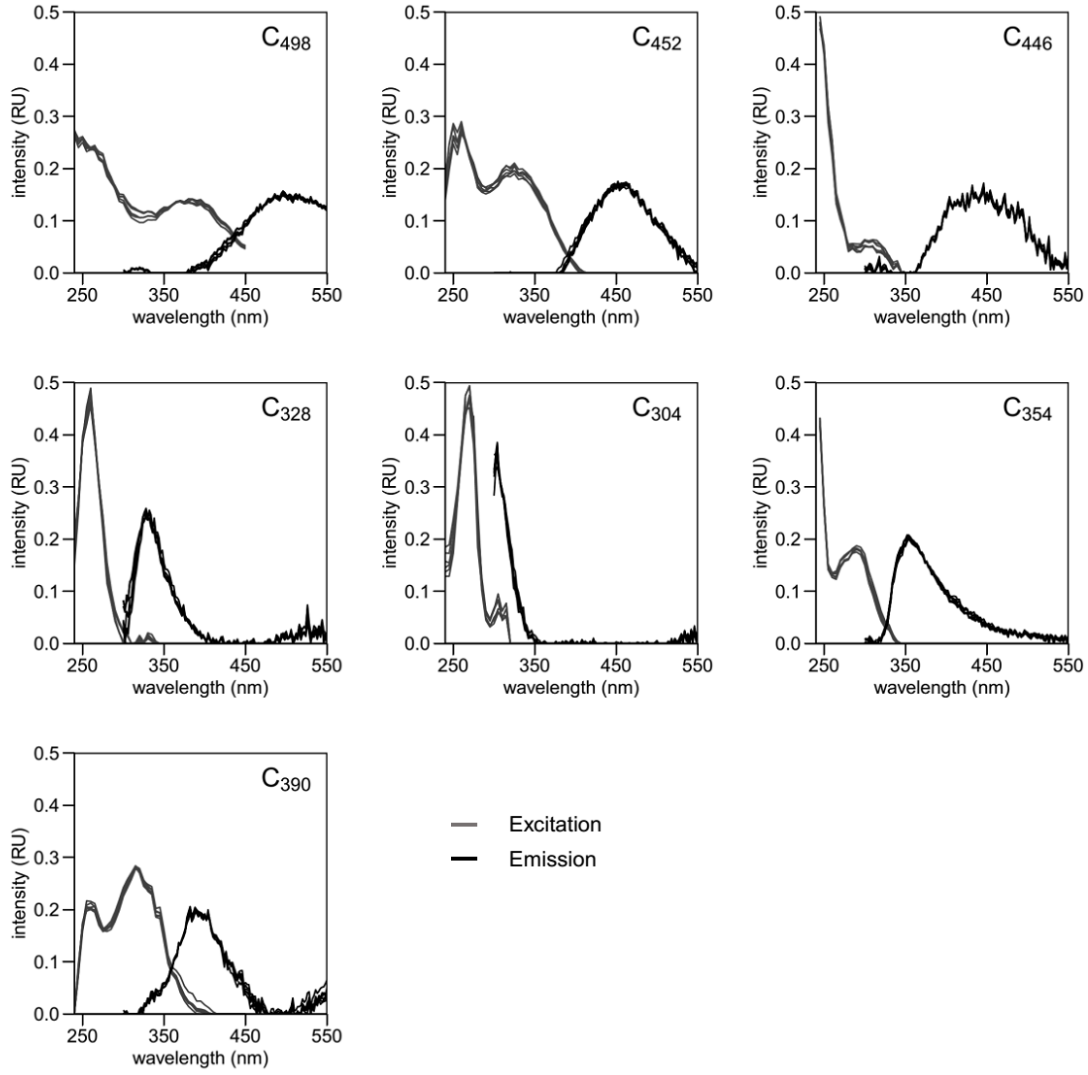

Figure 2.8. Split-half validation results for the 7-component PARAFAC model. Overlapping lines in excitation and emission spectra show the modelling results from separate data-halves.

- The 7-component model described >98.6% of the variance when re-projected onto the reverse-normalised dataset.
- A moderate core consistency (30.8%) in the final model is not dissimilar to that of 5- and 6-component models (<40%) and therefore does not imply a weakness in the model since performance against other criteria is strong (Murphy *et al.*, 2008, 2011, 2013). Model core consistency scores relate to the appropriateness of the model, and specifically its number of components, with higher percentages indicating a model better suited to the dataset (Bro and Kiers, 2003). However, in practice, modelling adjustments that improve core consistency are often offset by negative changes to other model features (A. Kellerman, *pers. comm.*).

Table 2.6. Split-half validation framework employed in development of PARAFAC model for DOM fluorescence in Chilean Patagonia.

Step	n	Groupings
Splits	4	A, B, C, D
Combinations	6	AB, CD, AC, BD, AD, BC
Tests	3	AB vs. CD, AC vs. BD, AD vs. BC

The full dataset here contains 407 samples from three fjords and multiple headwater rivers across Chilean Patagonia, including prolonged time series from the Huemules and Huinay rivers. The final validated model benefits from the large number of samples across a range of environments, whereas separate models for freshwater and marine samples were less robust and less reproducible. Moreover, the combined model helps to trace fluorescence signatures across environments and test the influence of rivers on fjord DOM composition.

2.3.3. Molecular determination of DOM

Ultrahigh resolution Fourier Transform ion cyclotron resonance mass spectrometry (FT-ICR MS) has advanced the study of environmental DOM by enabling molecular analysis (Nebbioso and Piccolo, 2013). It has been employed across varied freshwater and marine environments to investigate biogeochemical and photochemical processes (Kujawinski *et al.*, 2004; Singer *et al.*, 2012; Kellerman *et al.*, 2015; Riedel *et al.*, 2016; Seidel *et al.*, 2017). Despite the complexity of DOM, this technique generates highly accurate mass spectra to enable reliable formulae assignment and the determination of structural molecular properties (Koch and Dittmar, 2006). The data also lend themselves to multivariate and non-parametric statistical tests to determine relationships between DOM composition and environmental conditions (Kellerman *et al.*, 2015; Riedel *et al.*, 2016). Moreover, the availability of non-selective extraction matrices has made it possible to preconcentrate DOM to required analytical levels, without biasing against particular fractions (Dittmar *et al.*, 2008).

2.3.3.1. Principles of FT-ICR MS

The principles of FT-ICR MS are covered in detail elsewhere (Marshall *et al.*, 1998) and a brief summary is provided here along with a schematic for analysis in Figure 2.9. Individual molecules within a heterogeneous DOM sample are detected from the individual resonant frequencies of rotation of their ions following excitation in a magnetic field, which are linked to their mass to charge (*m/z*) ratio. To achieve this, a non-destructive ionization system is used to generate ions from a mixed DOM sample. The ion cloud is contained within a Penning trap (or ion trap) where it rotates under an imposed magnetic field. A variable radio frequency (RF) applied through excitation plates promotes individual ions to a higher orbit in the cloud at specific frequencies. Detector plates register these excited ions as an induced alternating current, with a frequency that matches the cyclotron frequency of the ions and a signal strength that scales with the number of excited ions. A Fourier Transform converts the registered signal into a frequency spectrum, which is then calibrated against theoretical *m/z* values for individual peaks. Formulae are assigned to peaks of sufficient size (defined by a pre-determined threshold above the baseline noise) using stoichiometrically constrained elemental combinations for each formula.

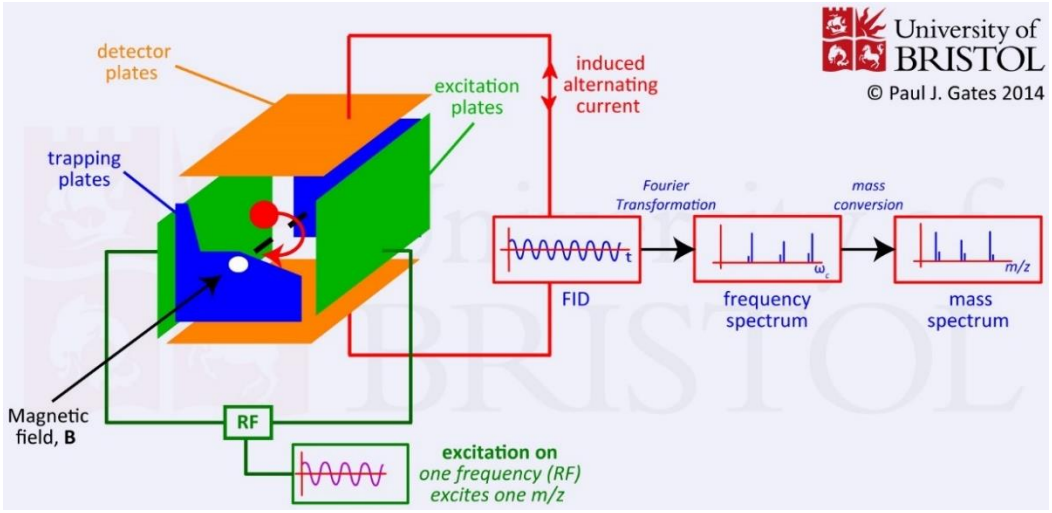

Figure 2.9. Schematic for FT-ICR MS analysis. Source: University of Bristol, School of Chemistry, Mass Spectrometry Facility http://www.chm.bris.ac.uk/ms/fticrms.xhtml.

2.3.3.2. Sample processing, analysis and formulae assignment

Filtered samples (see Section 2.2) underwent solid phase extraction (SPE) through Varian Bond Elut PPL (200 mg) cartridges, which contain a non-selective styrene divinyl benzene polymer with 15 nm pores, capable of extracting a diverse range of polar and non-polar compounds from heterogeneous mixtures (Dittmar *et al.*, 2008). Suggestions that these cartridges select against hydrophilic compounds (Hemingway *et al.*, 2019) are thought to have a minimal impact on mass spectra since the affected compounds form a relatively minor constituent of freshwater DOM (Raeke *et al.*, 2016),.

Cartridges were first soaked overnight with HPLC-grade methanol (MeOH) and rinsed with a further cartridge volume (3 ml) of MeOH, then subsequently rinsed in turn with 2 cartridge volumes of MQ, 1 of MeOH and then 2 of acidified (pH ~2) MQ. Since exact sample concentrations were not known *a priori*, and PPL cartridges may only have an extraction efficiency of 40% (Dittmar *et al.*, 2008), a conservative approach was used to estimate the sample volumes needed to extract 40 µg C onto each cartridge. Based on limited DOC concentration data for a few test samples from rivers across the region, we extracted 1 L volumes for more dilute glacial samples and 500 ml for more humic samples. Cartridges were then rinsed with 2 further volumes of acidified MQ to remove any salts and allowed to dry before storage at 4°C. Immediately prior to analysis, extracted DOM was eluted from each cartridge with 1 ml MeOH and collected

into pre-furnaced (450°C, 5 hours) 2 ml amber glass vials. Following measurement of DOC, the volume of eluent was adjusted with additional MeOH to achieve the target concentration of 40 µg C ml^{-1} for all samples. Consistent concentrations minimise the effects of differential selective ionization, which could otherwise limit inter-sample comparisons.

Extracted DOM samples were analysed on a 21 Tesla FT-ICR mass spectrometer fitted with a 22 cm ICR bore cylinder and operating in negative ion mode (National High Magnetic Field Laboratory (NHMFL), Tallahassee, FL, USA). Electro-spray ionization (600 nl min^{-1} flow rate and variable voltage of 2.6–3.2 kV) was used to deprotonate DOM molecules and produce a negatively charged ion cloud, which was drawn into the instrument. Sample signals were produced from a total of 100 coadded scans and then Fourier transformed into frequency spectra which were calibrated against known *m/z* values using Predator software (NHMFL). Calibrations were based on at least three identifiable and overlapping Kendrick series that spanned the full mass range (100–1000 Da), applying the same series to all samples where possible.

Formulae were assigned using PetroOrg software (Florida State University) for all peaks that were at least 6 times greater than the RMSE of baseline signal and had mass calibration errors <500 ppb. A unique formula from within the range of possible elemental combinations ($C_{1–45}H_{1–92}N_{0–4}O_{1–25}S_{0–2}$) was assigned to each peak. All assigned formulae were then allocated to specific compound categories based on elemental stoichiometries and values of a modified aromaticity index (AI_{mod}), which provides structural information and is calculated from molecular formulae (Equation 2.4). Threshold values for AI_{mod} provide strong evidence for the presence of aromatic (AI_{mod} > 0.5) and condensed aromatic (AI_{mod} > 0.66) structures (Koch and Dittmar, 2006). Compound category criteria were taken from Kellerman *et al.* (2018) and are summarised in Table 2.7. Relative peak intensities were calculated for each formula as a proportion of the total signal for each sample for use in all subsequent analyses.

Equation 2.4. Calculation of the modified aromaticity index (AI_{mod}) based on number of C, H, O, N and S atoms in a molecular formula.

$$AI_{mod} = \frac{1 + C - S - 0.5(O + H + N)}{C - 0.5(O) - N - S}$$

Table 2.7. Compound category assignments for FT-ICR MS peaks based on modified aromaticity index (AI_{mod}) values and elemental ratios of assigned formulae.

Compound category	Criteria
Condensed (or polycyclic) aromatic	$AI_{mod} > 0.66$
Polyphenolic	$0.66 \geq AI_{mod} > 0.5$
Highly unsaturated and phenolic	$AI_{mod} \leq 0.5$; $H/C < 1.5$
Aliphatic	$2 \geq H/C \geq 1.5$; $N = 0$
Peptide-like	$2 \geq H/C \geq 1.5$; $N > 0$
Sugar-like	$O/C > 0.9$

2.3.4. Particulate organic carbon (POC) concentrations

Due to practical constraints and low suspended sediment concentrations (SSCs), limited amounts of particulate material were available from some rivers to determine organic carbon content through standard methods of elemental analysis. This section outlines how POC concentrations were determined from small samples through direct analysis of particulates on filters. POC concentrations are calculated from SSCs and the percentage weight of organic carbon (OC%) in the sediment (Equation 2.5).

Equation 2.5. Calculation of particulate organic carbon (POC) concentrations.

POC	=	SSC	x	OC
mg C L^{-1}		*mg L^{-1}*		*% wt.*

2.3.4.1. Suspended sediment concentrations (SSCs)

SSCs were determined from the mass of sediment retained from filtered water samples of a known volume. In the field, ~300 ml of river water was passed through pre-weighed Whatman® cellulose nitrate filters (0.45 µm pore size; 47 mm diameter), which were left under a mild vacuum until air dry. In the laboratory, the filters were dried overnight at 60°C and re-weighed. The increase in weight was taken as the amount of sediment and this value was divided by the volume of the original water sample to obtain a concentration.

2.3.4.2. Elemental analysis of particulate organic carbon

River water particulates were retained on pre-furnaced (450°C,5 hours) GF/F filters and stored frozen. Large water samples (>2 L) were needed to obtain enough solid material for analysis. The filters were defrosted and dried thoroughly in the lab prior to analysis on a Thermo Electron Flash Elemental Analyser 1110, which uses high temperature (1000^{o}C) catalytic combustion to oxidise samples and collects the combustion products for measurement. The total amount of carbon (TC) liberated in each analysis is normalised by the sample weight to obtain elemental mass fractions (or percentages). Organic carbon (OC) is determined via the same process but after removal of inorganic carbonates by acidification (Hedges and Stern, 1984). A correction factor was applied to OC data to compensate for the increase in mass arising from the sorption of water vapour by hygroscopic salts following acidification (Hedges and Stern, 1984). These OC-specific corrections were of similar magnitude for field samples and blanks. Repeat measurements of a soil reference standard (CE Instruments part no: 338-400-25; TC = 2.29 ± 0.07%) were within <5% (RSD) variation and showed an absolute deviation of 0.026% from the true value.

Field samples were analysed directly on GF/F filters and corrected for the mass and C content of the filter. Overall, this approach was deemed preferable to methods which remove sediments from filters by washing or scraping as these may, respectively, bias against certain grain sizes or introduce unknown amounts of filter material into each analysis. A circular metal cutter (cleaned with acetone) was used to subsample each filter uniformly and ensure a consistent mass of filter material was analysed with each sample. This allowed reliable blank corrections (Equation 2.6) based on the composition of GF/F material (Table 2.8). Errors on individual terms in the blank corrections were also propagated (using rules for absolute and relative errors in Equation 2.6 and Equation 2.7, respectively) to calculate the total uncertainty on the corrected TC and OC sample values. The errors used were the standard deviations of mass (M_b) and elemental content (C_b) of blank filter material (Table 2.8), and instrument uncertainties for the mass (M_m) and elemental content (C_m) of samples.

Table 2.8. Mass and elemental content of blank filter material (GF/Fs) included in samples for POC determination on Elemental Analyser.

	mass (mg)	TC (%)	OC (%) [acidified filter]
mean	6.358	0.028	0.023
S.D.	0.037	0.008	0.010
n	10	10	8*

*OC measurements were 0% for two blanks, so blank OC content is taken as the mean of the remaining eight blanks which gave a positive reading, leading to more conservative blank corrections.

Blank corrections were performed for samples where the raw measurement was above the instrumental LoD (0.01% for TC and OC); values below this were not reliable and eliminated from the dataset. On this basis, sample rejection rates for TC and OC were 0% and 8%, respectively. Total nitrogen (TN) data were also generated by the elemental analyser but were deemed less reliable (due to 50% sample rejection rate, very low TN% content close to LoD in samples and poorly constrained blank values) and so were excluded from the final dataset. Reliable TC and OC measurements were, however, obtained for small particulate samples analysed directly on GF/F filters. The overall uncertainties on the final sample POC concentrations were <20%, which is considered acceptable for such small samples with low OC-content (down to 0.03%).

Equation 2.6. Blank correction in elemental analysis of suspended sediment samples.

$$C_s = ((C_m.M_m) - (C_b.M_b))/(M_m - M_b)$$

C_s = percentage weight of carbon in blank corrected sample
C_m = percentage weight of carbon in measured sample (filter + sediments)
M_m = measured mass of sample (filter + sediments)
C_b = percentage weight of carbon in blank filter
M_b = average mass of blank filter material included in each sample

Equation 2.7. Propagation of absolute errors for addition/subtraction terms in an equation.

$$\Delta Z = \sqrt{(k_1 \Delta A)^2 + (k_2 \Delta B)^2 + \ \ldots}$$

A, B, Z = terms in base equation
$\Delta A, \Delta B, \Delta Z$ = uncertainties on individual terms
k_n = any constants from base equation

Equation 2.8. Propagation of relative errors for multiplication/division terms in an equation.

$$\frac{\Delta Z}{Z} = \sqrt{\left(\frac{\Delta A}{A}\right)^2 + \left(\frac{\Delta B}{B}\right)^2 + \ldots}$$

A, *B*, *Z* = terms in base equation
ΔA, *ΔB*, *ΔZ* = uncertainties on individual terms
e.g. ΔZ/Z = relative uncertainty of *Z*

2.3.5. Dissolved nutrient analyses

Nutrient concentrations were determined by colorimetry for fjord water samples on a LaChat QuikChem® 8500 series 2 flow injection analyser. This approach is based on the Beer-Lambert law, whereby analyte concentration is proportional to the absorbance of light at a specified wavelength (Grasshoff *et al.*, 1999). Ammonium (NH_4^+) concentrations were calculated from absorbance readings at 640 nm following reaction with a phenol-hypochlorite reagent (Method 31-107-06-1-I). Nitrate (NO_3^-) and nitrite (NO_2^-) were measured combined from absorbance at 254 nm following photo-conversion by UV-light (Method 31-107-04-3-A). Total nitrogen (TN) was measured using the same method but following an additional alkaline persulphate/UV digestion at 100°C to convert all organic nitrogen to nitrate. The sum of inorganic nitrogen (NH_4^+ + NO_3^- + NO_2^-) was then deducted from TN concentrations to provide an estimate of dissolved organic nitrogen (DON; Fellman *et al.*, 2010). Soluble reactive phosphorus (SRP, or PO_4^{3-}) was determined following reaction with ammonium molybdate and antimony potassium tartate in acidic conditions and measurement of absorbance at 880 nm by the blue molybdate complex formed (Method 31-115-01-1-I). LoDs (µM) and precision (% RSD) have previously been reported by Hawkings (2015) as: 0.6 µM and ±15.7% (NH_4^+); 1.4 µM and ±11.3% (TN, NO_3^- and DON); 0.03 µM and ±2.9% (SRP).

3. Deglaciation-induced landscape change affects the composition and export of organic matter in Chilean Patagonian rivers

This chapter presents the first regional scale assessment of riverine organic matter in Chilean Patagonia with specific focus on its sensitivity to landscape changes driven by glacier retreat. It uses quantitative and high-resolution composition data to assess how freshwater fluxes of organic matter are influenced by landscape factors in contiguous river catchments across Chilean Patagonia (42–48°S). The principles of space-for-time substitution are used to infer how landscape changes arising from deglaciation might alter organic carbon cycling and freshwater biogeochemistry.

This chapter forms the basis of a manuscript in preparation for submission to *Biogeosciences Discussions* under the following reference:

Marshall, M., Kellerman, A., Wadham, J., Pryer, H., Hawkings, J., Beaton, A., Urra, A., Robinson, L., Spencer, R. (in prep.) Deglaciation-induced landscape change affects the composition and export of organic matter in Chilean Patagonian rivers. *Biogeosciences Discussions.*

Author contributions

I developed the specific aims of this study from those of a larger NERC/CONICYT-funded research project (Patagonian Icefield Shrinkage impacts on Coastal and fjord EcosystemS — PISCES) conceived by J. Wadham and L. Robinson. All authors (except R. Spencer) contributed to field sampling. I conducted all analyses, interpreted results and wrote the text. A. Kellerman assisted in the analysis of FT-ICR MS samples, with R. Spencer providing additional lab support. H. Pryer compiled regional river discharge records and led the calculation of catchment land cover properties. J. Hawkings produced the discharge record for the Huemules River. J. Wadham provided comments on analytical approaches and reviews of the text.

3.1. Abstract

Organic matter cycling in freshwater systems is sensitive to landscape change. The worldwide retreat of mountain glaciers represents one of the most profound examples of such change. Chilean Patagonia is a relatively pristine region and so offers a unique landscape to assess the impact of significant rates of glacier retreat on the composition and export of organic matter. Biogeochemical data for this region are scarce and this study offers the first regional scale assessment of its riverine organic matter. This study adopts a space-for-time approach, in which the effects of spatial variations in landscape properties on organic matter flux and composition are used to infer the effects of ongoing glacier retreat over time. We sampled river water and particulates from 29 river catchments spanning gradients in glacier, lake and vegetation cover (42–48°S) during the austral summer of 2017. We also sampled from a single highly glaciated site on the Huemules River daily for extended periods in summer and winter 2017. All samples were measured for organic carbon concentrations and analysed via spectrofluorescence and molecular level techniques. Where discharge data were available, catchment yields for particulate and dissolved organic carbon were estimated and related to catchment properties. Spatial variations in organic matter composition were also correlated with catchment properties and data for glacial and non-glacial regimes were compared. We found that glaciers drive higher catchment yields for particulate organic matter and supply dissolved organic matter rich in protein-like and aliphatic substances. However, other sources and sinks across the Chilean Patagonian landscape (e.g. lakes) dampen the influence of glaciers. This dampening effect is likely to increase as glaciers retreat, making organic matter export more sensitive to non-glacial controls.

3.2. Introduction

Rivers act as the primary conduit for organic carbon to flow from continents into the oceans and are hotspots of carbon cycling (Battin *et al.*, 2008, 2016; Aufdenkampe *et al.*, 2011). This flow of organic carbon is vulnerable to processes of landscape change which may alter both river discharge and the source of the carbon entering the system (Asmala *et al.*, 2016; Zhuang and Yang, 2018). Anthropogenic climate change is forcing the worldwide retreat of mountain glaciers (Zemp *et al.*, 2015), which has profound effects on the flow and composition of glacier fed rivers (Huss and Hock, 2018). Glacial systems have themselves been highlighted as sensitive components of

the global carbon cycle which exert direct and indirect feedbacks on atmospheric carbon concentrations (Hood *et al.*, 2015; Wadham *et al.*, 2019). The biodiversity and biogeochemical function of glacially fed rivers in the northern hemisphere have been attracting increasing academic interest (Hood *et al.*, 2009; Jacobsen *et al.*, 2012). However, a global assessment is needed to better understand how glacier retreat will affect the role of downstream rivers in the carbon cycle (Milner *et al.*, 2017).

Glaciers play a key role in the long-term storage of organic carbon through a combination of active biological processes and passive accumulation on the surface and at the bed (Wadham *et al.*, 2008; Cook *et al.*, 2012; Stibal *et al.*, 2012c; Stubbins *et al.*, 2012; Boyd *et al.*, 2014; Hood *et al.*, 2015). On a global scale, glacial stores of organic carbon are modest in size (~6 Pg) but highly sensitive to seasonal melt cycles and rising global temperatures (Hood *et al.*, 2015). Reductions in global ice cover could also expose significantly larger reactive reserves of organic carbon in subglacial sediments (Wadham *et al.*, 2019). Although mountain glaciers contain a small share (<5%) of total ice-locked carbon, they account for >40% of global export via meltwater runoff and hence have a disproportionate effect on downstream biogeochemistry (Hood *et al.*, 2015). Accelerated melting will drive larger fluxes of glacial carbon downstream in the short term but also result in the eventual depletion of supplies to which mountain river ecosystems are uniquely adapted (Milner *et al.*, 2017).

Glaciers are associated with the supply of dilute but highly labile dissolved organic matter (DOM), which stimulates aquatic bacterial respiration (Hood *et al.*, 2009; Fellman *et al.*, 2010a). The bioavailability of glacial DOM has been attributed to both microbial sources of proteinaceous material (Lawson *et al.*, 2014a) and combustion-derived compounds from atmospheric deposition (Stubbins *et al.*, 2012). In the short term, accelerated glacier melting may therefore support more intense microbial processing of organic matter in glacially fed rivers (Milner *et al.*, 2017). However, freshwater biota and their role in aquatic carbon cycling may be adversely affected by the simultaneous release of legacy pollutants, which have accumulated in glacial ice since the start of the industrial era (Legrand *et al.*, 2007; McConnell *et al.*, 2007; Wang *et al.*, 2008; Gabrieli *et al.*, 2010). The distribution of these chemicals within glaciers is not well constrained, which makes it difficult to predict whether ongoing melting will lead to a transient or sustained release of pollutants (Hodson, 2014). Since the increased

supply of materials released by enhanced glacier melting could either enhance or hinder microbial activity in rivers, it is difficult to predict the impact on downstream biodiversity and biogeochemistry (Milner *et al.*, 2017). Whilst particulate organic carbon (POC) comprises the bulk of organic matter export from glaciers, its biogeochemical reactivity has rarely been investigated (Lawson *et al.*, 2014a). As a result, the impact of changes in POC supply linked to dwindling glacier cover are less clear.

As glaciers retreat, new sources and sinks for organic matter in expanding proglacial zones will exert an increasing influence on organic matter in glacially fed rivers. The formation and growth of lakes in glacially eroded basins adds new regulation to catchment hydrology (Carrivick and Tweed, 2013, 2016; Loriaux and Casassa, 2013) and affects the size and composition of riverine organic matter fluxes (Tranvik *et al.*, 2009; Evans *et al.*, 2017). Turbid proglacial lakes may act as potential carbon sinks but as connectivity with the glacier declines, lakes may also become sites of carbon fixation as the freshwater ecosystem evolves in response to changing light and nutrient availability (Sommaruga, 2014). Moreover, as part of the long-term evolution of the proglacial landscape, new sources of carbon and nutrients become available through soil development and vegetation succession (Tscherko *et al.*, 2003; Raffl *et al.*, 2006; Cannone *et al.*, 2008). The increased relative importance of soils and vegetation will likely lead to more humic, aromatic and higher molecular weight DOM entering rivers. These qualities are classically associated with lower bioavailability (Fellman *et al.*, 2010a) and contrast with the low molecular weight, protein- and aliphatic-rich DOM associated with glacial ecosystems (Dubnick *et al.*, 2010; Fellman *et al.*, 2010a; Musilova *et al.*, 2017).

Current hypotheses for the biogeochemical impact of glacier retreat in mountain regions are focused upon northern hemisphere study sites. Several Greenland outlet glaciers (Bhatia *et al.*, 2010, 2013; Lawson *et al.*, 2014a), the Gulf of Alaska (Hood *et al.*, 2009; Fellman *et al.*, 2010a) and the European Alps (Singer *et al.*, 2012) have attracted most attention in the literature, with an increasing effort afforded to the study of Asian glaciers and their meltwater streams (Spencer *et al.*, 2014b; Hemingway *et al.*, 2019). Chilean Patagonia is a relatively pristine region that contains the greatest concentration of glaciers in the southern hemisphere excluding Antarctica (Millan *et al.*, 2019). It

therefore serves as a unique landscape in which to test the effects of variable glacier cover on riverine biogeochemistry. The region is experiencing rapid rates of glacier retreat and associated landscape change (Foresta *et al.*, 2018; Wilson *et al.*, 2018) but there are very little available data from which to assess the biogeochemical impacts.

Here, we present the first regional scale geochemical assessment of particulate and dissolved organic matter in Chilean Patagonian rivers. We use space-for-time substitution to relate trends in organic matter export and composition to spatial variations in landscape properties as a proxy for the effects of ongoing glacier retreat. Specifically, we focus our analysis on the variable influences of glaciers, lakes and vegetation cover as three principal aspects of landscape change linked to deglaciation. We supplement this with time series observations in a heavily glaciated catchment to infer the effects of enhanced meltwater generation from seasonal cycles in discharge and organic matter fluxes. Whilst we consider only a broad sweep of variables linked to landscape change, this study serves as a baseline for future investigations into the long-term biogeochemical impacts of glacier retreat in this region.

The specific aims of the study are to:

1. Quantify the export and yields of organic matter (dissolved and particulate) from Chilean Patagonian river basins and relate these to the degree of glacial influence (as measured by glacier cover as a percentage of total basin area and, discretely, by existence of a ‘glacial’ hydrological regime where peak discharge coincides with summertime ice melt).
2. Use spatial and temporal data to assess the influence of glacial meltwaters on riverine DOM composition.
3. Examine the relationships between river basin properties and DOM composition to understand the effect of deglaciation on regional organic matter export.

3.3. Methods

3.3.1. Study region

Chilean Patagonia is a relatively pristine environment, with limited industry and a sparse human population, and it is sensitive to the effects of climate change. Its landscape was largely shaped by glacial activity and its regional hydrology is strongly

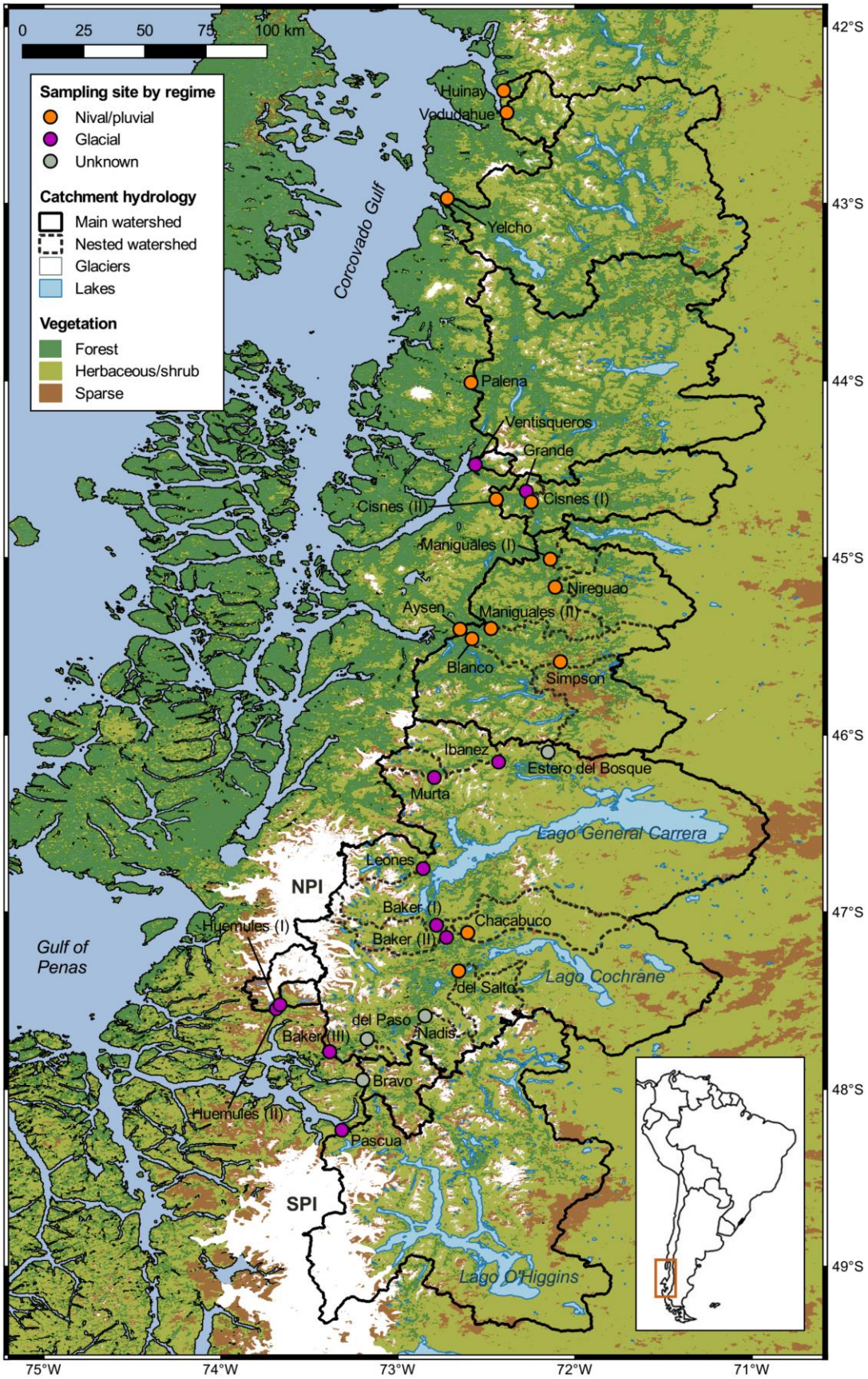

Figure 3.1. Basemap showing location of study river catchments with respect to glacial cover, freshwater lakes and vegetation cover. Catchment watersheds drawn for areas upstream of sampling points (colour denotes hydrological regime).

influenced by present day latitudinal variations in ice cover (Figure 3.1). South of ~46°S, rivers predominantly follow 'glacial' regimes whereby peak discharge is driven by ice melt in summer. The Northern and Southern Patagonian Icefields (NPI, SPI) dominate the landscape here and accelerated melting (Glasser *et al.*, 2011; Willis *et al.*, 2012b, 2012a; Jaber, 2016; Foresta *et al.*, 2018) may be increasing river flows in summer (Dussaillant *et al.*, 2012). East-west oriented basins south of 46°S, such as the Chacabuco River (a tributary of the Baker), have lower glacier cover and river discharge responds more strongly to rainfall events (Dussaillant *et al.*, 2012). North of 46°S, peak river discharge is mostly driven by a combination of springtime snowmelt (nival regime) and winter rainfall (pluvial regime). However, river flows in the Aysen basin (45–46°S) are sensitive to a long-term decline in seasonal snow cover (Calvete and Sobarzo, 2011; Pérez *et al.*, 2018). And more generally, river discharges may be falling in response to a shift in the westerly winds and a decline in overall rainfall (Garreaud *et al.*, 2013; Garreaud, 2018; Aguayo *et al.*, 2019).

Freshwater lakes are a key feature of the landscape, occupying numerous over-deepened glacial basins across the region. These lakes vary in size by several orders of magnitude (10^5–10^{11} m^3), with the biggest, Lake General Carrera, among the largest freshwater bodies in South America (Messager *et al.*, 2016). They extend catchment water residence times and regulate river flows across the region. New lakes that are forming through glacier retreat exert an increasing influence over river hydrology in rapidly deglaciating catchments (Loriaux and Casassa, 2013; Wilson *et al.*, 2018).

Patterns in vegetation cover follow a zonal precipitation gradient as well as changes in temperature and growing season length across latitudes and altitudes (Abarzúa *et al.*, 2004). Dense forest cover along the coast and in more northerly catchments is sustained by a hyper-humid climate (rainfall 1–7 m a^{-1}) driven by intense orographic uplift of Pacific air masses over the Andes (Kerr and Sugden, 1994; Pantoja *et al.*, 2011; Lenaerts *et al.*, 2014). These conditions favour broadleaf evergreen species of the *Nothofagus* genus (Armesto *et al.*, 1992; Srur *et al.*, 2018), which dominates the forest cover across the entire study region. Smaller shrubs and herbaceous plants are favoured further east by the drier conditions in the lee of the Andes and further south by the reduced growing season length (Vandekerkhove *et al.*, 2016). Very sparse vegetation cover exists on the highest ground and near the icefields (Figure 3.1).

Most of the region west of 72°W is underlain by granitic batholith which runs along the spine of the Patagonian Andes (Pankhurst *et al.*, 1999). East of 72°W, Mesozoic and Cenozoic volcanic rocks are the dominant lithology (Vandekerkhove *et al.*, 2016). In between these two major rock types, Palaeozoic metamorphic complexes underly much of the terrain south of 46°S in the Baker, del Salto, Nadis, del Paso and Bravo catchments (Vandekerkhove *et al.*, 2016). Several volcanoes punctuate the Andean peaks north of 46°S but most lie outside the study catchments (Vandekerkhove *et al.*, 2016). Eruptions from the Hudson volcano near the head of the Ibanez river account for a high proportion of quaternary volcanic and pyrogenic deposits (31% of total area, versus 9% average for all basins) in this catchment (Weller *et al.*, 2014).

3.3.2. Sampling

During the austral summer (7 Jan–23 Feb 2017), we sampled river water and particulates from 29 catchments spanning gradients in glacier, lake and vegetation cover, which characterise the Chilean Patagonian landscape between 42–48°S (Figure 3.1). Data from spot samples are limited to single points in space and time but, collectively, the dataset enables spatial variations in riverine organic matter to be related to landscape level controls. Moreover, summertime sampling helps to assess conditions in the rivers when glacial meltwater contributions are at their strongest. We argue that the overall trends across our study catchments provide insight into the impact of deglaciation-induced landscape change on organic matter in regional rivers.

Additional time series data from the Huemules River capture seasonal variations in river discharge and organic matter in a highly glaciated catchment. These observations help to constrain the impact of changing meltwater inputs in a glacial end-member system and provide context for data from other glacial rivers along the latitudinal transect. Time series data were collected during extended field campaigns over the austral summer (11 Jan–26 Feb) and winter (14–29 Jul) of 2017. A continuous annual discharge record was derived from sensor data (see Section 3.3.4.2). Manual sampling of water/particulates took place at a site ~100 m downstream of the proglacial lake where the waters were considered well mixed. Samples were collected daily for dissolved organic carbon (DOC) and fluorescence determination, and every 2–3 days for POC measurement. No glacial lake outburst floods (GLOFs) occurred during the 2017 field seasons.

3.3.3. Sample analysis

3.3.3.1. Organic matter concentrations

Samples for DOC determination were filtered in the field to 0.45 µm (Whatman® Puradisc AQUA) and stored frozen prior to analysis. DOC concentrations were measured as non-purgeable organic carbon through high temperature combustion (680°C) on a Shimadzu TOC-L_{CHN} analyser. Instrument calibration (r^2 >0.999) was based on measurement of a certified potassium hydrogen phthalate stock (1000 ± 10 mg L^{-1}; Sigma Aldrich) gravimetrically diluted to a range of concentrations (0.05–4.93 mg L^{-1}). All sample measurements were significantly higher (>0.105 mg L^{-1}) than the limit of quantitation (0.044 mg L^{-1}) calculated as the mean blank concentration plus 5 times the standard deviation on the lowest concentration standard (Armbruster and Pry, 2008). Repeat measurement of intermediate concentration standards (0.10, 0.50 and 1.00 mg L^{-1}) typically varied by <5% and standard deviation on triplicate measurements was typically <2%.

POC concentrations were determined for sediments retained from large volume samples (1–3 L) on pre-combusted (450°C, 5 hours) GF/Fs which had been frozen. Sediments were analysed directly on filters through high temperature (1000°C) catalytic combustion on a Thermo Electron Flash Elemental Analyser 1110. Samples were first acidified with HCl to remove any inorganic carbon content (Hedges and Stern, 1984) and measurements were blank-corrected for the mass and organic carbon content of the filter material (mass = 6.36 ± 0.04 mg, OC = 0.02 ± 0.01%, n=10). Repeat measurement of a reference standard (total carbon = 2.29 ± 0.07%) showed that instrument precision was <±5%. Final POC concentrations were calculated by multiplying the measured percentage OC content with suspended sediment concentrations (SSCs), which were measured separately as the mass of dry sediment retained on pre-weighed filters from a known volume of water (~300 ml). Overall uncertainties on final POC values were quantified through propagation of experimental/measurement errors and were typically <20%, which is considered acceptable for the low %OC content of these sediments.

3.3.3.2. Dissolved organic matter composition

DOM composition is assessed via spectrofluorescence and ultrahigh resolution mass spectrometry (FT-ICR MS).

Spectrofluorescence scans were conducted for filtered samples (0.45 µm; Whatman® Puradisc AQUA) on an Agilent Cary Eclipse Fluorescence Spectrophotometer with a xenon flash bulb. Excitation-emission matrices (EEMs) were collected through a 10 mm quartz cuvette over excitation wavelengths 240–450 nm (5 nm increments) and emission wavelengths 300–600 nm (2 nm increments) using 5 nm monochromator slit widths and 0.1 second integrations. Instrumental biases, Raman/Rayleigh scatter and blank signals were removed from all sample EEMs following established procedures before further analysis (Stedmon and Bro, 2008; Murphy *et al.*, 2013).

Molecular level analysis was performed for large volume samples (1 L) from 28 rivers (we were unable to collect such a sample from the Rio Grande) filtered through pre-combusted GF/Fs (450°C for 5 hours; 0.7 µm pore size) and acidified to pH ~2 with HCl. DOM was solid phase extracted (SPE) through non-selective 200 mg Varian Bond Elut PPL cartridges (Dittmar *et al.*, 2008) and reconstituted in methanol to obtain a consistent target concentration (~40 µg C ml^{-1}) for all samples. SPE-DOM was ionized via an electro-spray rig (2.6–3.2 kV; flow rate 600 nl min^{-1}) and analysed on a 21 Tesla FT-ICR mass spectrometer with 22 cm ICR bore cylinder at the National High Magnetic Field Laboratory (NHMFL), USA (Smith *et al.*, 2018). Mass spectra were generated from 100 coadded scans and calibrated against known m/z values for 3 overlapping Kendrick series which spanned the full mass range (Predator software, NHMFL).

Formulae were assigned within the combination range $C_{1–45}H_{1–92}N_{0–4}O_{1–25}S_{0–2}$ for all peaks with mass calibration errors <500 ppb and intensities at least 6 times greater than the RMSE of the baseline signal (PetroOrg software, Florida State University). Molecular formulae were categorised into compound classes following the approach of Kellerman *et al.* (2018) based on values of the modified aromaticity index (AI_{mod}; Koch and Dittmar, 2006) and elemental stoichiometries. The compound categories are as follows: condensed aromatics (CA; $AI_{mod} > 0.66$); polyphenolics (PP; $0.66 \geq AI_{mod} > 0.5$); highly unsaturated and phenolic (HUP; $AI_{mod} \leq 0.5$; $H/C < 1.5$); aliphatic ($2 \geq H/C \geq 1.5$; $N = 0$); peptide-like ($2 \geq H/C \geq 1.5$; $N > 0$) and sugar-like ($O/C > 0.9$).

Further subdivisions include O-poor and O-rich categories (O/C <0.5 and O/C >0.5 respectively) for CAs, PPs, HUPs and aliphatics.

3.3.4. Catchment properties

3.3.4.1. Catchment boundaries and landscape cover

River catchment areas and landscape covers were calculated in QGIS software (QGIS Development Team, 2019). Catchment boundaries upstream of sampling locations were defined from a high resolution digital elevation model (DEM) developed from the Shuttle Radar Topography Mission database (Farr *et al.*, 2007). The Whitebox-GAT geospatial processing package (Lindsay, 2016) was used to simulate river networks, which accurately mapped onto actual channel configurations thus validating the DEM-defined catchments. Mean catchment slope was then calculated from the DEM.

Landscape covers were extracted from superimposed datasets. Glacial cover, as a percentage of total catchment area, was measured from glacier areas reported in the Randolph Glacier Inventory (RGI Consortium, 2017). Total lake area and volume were calculated for each catchment from the HydroLAKES database (Messager *et al.*, 2016) and wetland cover was extracted from the SWAMP raster (Gumbricht *et al.*, 2019). The percentage area of each river basin covered by different vegetation types (falling into broad categories including 5 different types of forest, 5 different combinations of shrubland, herbaceous and sparsely vegetated areas, and 3 agricultural categories) was calculated from the National Mapping Organization's Global Land Cover raster (Tateishi *et al.*, 2011, 2014). The underlying catchment geology was determined from a high resolution lithological map (Hartmann and Moosdorf, 2012).

3.3.4.2. Catchment hydrology

Hydrological data were used to define river regimes and calculate organic matter fluxes and yields. These data were compiled from the following:

- The first continuous annual discharge record for the Huemules (I) catchment derived from field data and a stage-discharge rating curve, following established methods (Bartholomew *et al.*, 2011; Hawkings *et al.*, 2015). River stage was recorded every 15 minutes between 27 Jul 2016 and 28 Jul 2017 using an automated

pressure transducer mounted on bedrock at a fixed location on the bank. Stage data were calibrated against manual discharge measurements from 14 Rhodamine B dye injection traces performed over a range of river levels during the 2017 field seasons. A polynomial regression provided a strong calibration (r^2=0.97) with an overall uncertainty of ± 8.8% (RMSE) on discharge data. Meteorological data from the nearest weather station in Tortel (30 km away) were obtained from the Chilean Water Authority (Dirección General de Aguas, 2019) to provide context for discharge variations in the Huemules River.

- Multiannual discharge records from the Chilean Water Authority (Dirección General de Aguas, 2019). These records were of varying length (up to 25 years) and completeness and available only for 18 gauged rivers of the study region. We used only those records which contained at least one complete annual discharge cycle since 2010 to ensure that our analyses were based on relatively recent conditions within each river system.

- Where complete annual hydrographs were unavailable, mean annual discharge values were obtained from the literature for the Yelcho and Bravo (Aracena *et al.*, 2011) and Chacabuco and del Salto (Dussaillant *et al.*, 2012) rivers.

3.3.4.2.1. River regime classification

To aid interpretation of trends in organic matter export and composition across study catchments, river regimes were classified based on the timing of peak annual discharge through inspection of annual hydrographs (where available). In 'glacial' rivers peak discharge occurs in summer (Dec–Mar) due to maximum ice melt, in 'nival' rivers it is driven by snowmelt in spring (Sep–Nov) and in 'pluvial' rivers it coincides with winter rainfall (May–Aug). Some rivers reflect multiple regimes and very few could be defined as exclusively nival or pluvial. Hence, these two regimes were combined into a single category (nival/pluvial) for analytical purposes, allowing more robust comparison of a larger group of non-glacial rivers with glacial systems. The Blanco River was one system which displayed a combination of nival, pluvial and glacial influences, consistent with previous reports (Pérez *et al.*, 2018). We classified the Blanco as a nival/pluvial system for all subsequent analyses given its highly stochastic annual

hydrograph, usual timing of peak discharge outside of summer and low catchment glacier cover (4%). Where annual hydrographs were unavailable, regimes were classified based on descriptions in the literature for the Yelcho (Di Prinzio and Pascual, 2008), Chacabuco and del Salto (Dussaillant *et al.*, 2012), Huinay and Vodudahue rivers (Rebolledo *et al.*, 2011). The regimes of the Bravo, del Paso, Nadis and Estero del Bosque rivers could not be classified due to a lack of information.

3.3.4.2.2. Flux and yield calculations

We estimated the annual fluxes and yields of sediment and organic matter from summer concentrations for rivers with available discharge data (Equation 3.1–Equation 3.3). Yields based on summer conditions in glacial rivers are considered good approximations of annual yields since summer meltwaters (Dec–Mar) drive a major share (e.g. >50% in Baker River near Tortel) of total annual discharge. We acknowledge that summer sampling may underestimate yields for nival/pluvial catchments but argue that they help to constrain baseline conditions in neighbouring glacial catchments if meltwater inputs were hypothetically cut off. Whilst single point data offer limited insight into each river system, our calculations provide useful first order estimates of organic matter export across a range of remote study catchments for which biogeochemical data are scarce.

Equation 3.1. Annual DOC flux

DOC flux	=	Cumulative annual discharge	x	Mean DOC concentration
$Gg\ a^{-1}$		$km^3\ a^{-1}$		$mg\ L^{-1}$

Equation 3.2. Annual POC flux

POC flux	=	Cumulative annual discharge	x	Mean SSC	x	OC content
$Gg\ a^{-1}$		$km^3\ a^{-1}$		$mg\ L^{-1}$		%

Equation 3.3. Annual catchment yields

Annual yield	=	Annual flux	÷	Catchment area	x	1000
$Mg\ km^{-2}\ a^{-1}$		$Gg\ a^{-1}$		km^2		*unit conversion*

We quantified uncertainties on our estimates through the propagation of relative errors (according to the rules in Equation 2.8, p50), using measurement errors on concentration

data and measures of variability on annual discharge. In most cases we used the mean (± SE) cumulative annual discharge from multiannual records in our calculations. For the Huemules River, we integrated the area under the 2017 annual hydrograph as a more reliable measure of the total annual freshwater flux, taking the RMSE on discharge values (8.8%) as the overall uncertainty. We were unable to quantify the specific uncertainties for rivers where only single reported values of mean annual discharge were available in the literature. However, we still calculate fluxes and yields for these rivers and treat them as first order estimates. We were unable to calculate annual fluxes and yields for five rivers (Huinay, Vodudahue, Estero del Bosque, Nadis and del Paso) due to a lack of discharge data.

Alongside annual estimates for the Huemules River, we also calculated instantaneous organic matter fluxes for the 2017 field seasons. The average daily DOC flux was calculated using DOC concentrations in daily samples and the mean daily discharge. POC fluxes were calculated as the product of individual SSCs, mean %OC content (which did not vary significantly over the year; 0.09 ± 0.01%) and mean daily discharge for days when particulates were collected. We were unable to generate continuous POC flux records from continuous turbidity sensor (Campbell Scientific) records due to poor calibration against SSCs (r^2=0.2), which displayed little variability within each field season (summer: 85 ± 12 mg L^{-1}, winter: 53 ± 3 mg L^{-1}). Propagation of errors produces an overall uncertainty of <10% on instantaneous DOC fluxes and <20% on POC fluxes.

3.3.4.3. Statistical analyses

Here we provide details of the main statistical methods used to identify the controls over organic matter fluxes and composition. Other supporting statistical tests which aid overall interpretation of the dataset are referred to in the Results section. Unless otherwise stated, all tests were conducted in R (R Core Team, 2015) and a significant result is defined as one with a *p*-value <0.05.

Mann Whitney tests were used to assess differences in organic matter concentrations, yields and bulk FT-ICR MS compound category intensities between rivers of differing hydrological regime. These non-parametric tests are suited to the unpaired, non-normally distributed data.

Parallel factor (PARAFAC) analysis was performed through the drEEM Toolbox for MATLAB (Murphy *et al.*, 2013) to deconvolve variance in DOM fluorescence into separate component factors. A 7-component model was developed from 386 EEMs using random initializations and non-negative spectral constraints. The dataset included all terrestrial samples (from latitudinal transect and time series stations) and additional EEMs for Patagonian fjord samples (collected over 2017 and 2018), which helped to constrain regional variance in fluorescence signatures. The 7-component model was validated using split-half methods, whereby separately modelled combinations of randomly split subsets of the larger dataset produced identical results. The model explained 98.6% of the total variance and residuals displayed random noise. All components had realistic fluorescence spectra and matched other PARAFAC components in published models held on the OpenFluor database (Murphy *et al.*, 2014a). Based on this cross-referencing, three components were defined as terrestrial humic-like (C_{498}, C_{452}, C_{446}), another as marine humic-like (C_{390}) and the remaining three as protein-like (C_{304}, C_{328}, C_{354}). The model was re-projected onto all sample EEMs to obtain component intensity scores and loadings (raw intensity as a percentage of the sample total) for use in subsequent analyses.

Spearman correlations between PARAFAC loadings and FT-ICR MS relative intensities were used to define molecular fingerprints for each PARAFAC component. Similar approaches have been used previously (Herzsprung *et al.*, 2012; Stubbins *et al.*, 2014). FT-ICR MS data were first subset to include only those 5833 formulae common to all 28 river SPE-DOM samples, reducing data volume and the influence of many very low intensity peaks. A false discovery rate correction (Benjamini and Hochberg, 1995) was applied to minimise the number of Type I errors (false positives) generated by 40,831 individual correlation tests (7 components x 5833 formulae) and a *p*-value <0.0074 was thus deemed significant at the 95% confidence level. Formulae that were significantly and positively correlated with more than one component were assigned to the component with which they had a stronger correlation. This mostly affected formulae related to humic components and some that were shared between C_{304} and C_{328}. All formulae correlated with C_{354} were unique.

The same correlative approach was used to identify relationships between FT-ICR MS formulae and environmental variables. Significant relationships were identified for

DOC concentrations, broadleaf evergreen forest (BEF) cover, glacial cover, and lake volume normalised to the catchment area. Molecular fingerprints of positively and negatively correlated formulae were defined following false discovery rate correction of 23,332 individual test results (4 variables x 5833 formulae), where a *p*-value <0.011 was considered significant with 95% confidence.

Principal Components Analysis (PCA) was used to reduce the complexity of multivariate patterns in DOM composition across the study region. The PCA was based on PARAFAC loadings and FT-ICR MS compound category and formula class relative intensities. All data were standardised to zero mean and unit variance using the *decostand* function (Oksanen *et al.*, 2016). The first two principal components accounted for 62.2% of the total variance. A range of environmental variables were correlated with the PCA and a significance value computed by permutation using the *envfit* function (Oksanen *et al.*, 2016). These variables included glacial cover, lake volume normalised to catchment area, vegetation covers (comprising forests, herbaceous plants, shrubs, sparse vegetation), wetland cover and also concentrations of DOC and total dissolved solids (TDS) as indicators of bulk riverine chemistry. TDS was calculated as the sum of major ions (in river water samples filtered to 0.45 µm; Whatman® GD/XP) determined through capillary ion chromatography (Thermo Scientific Dionex ICS-5000). It was not possible to test relationships with POC concentrations as these were not determined for all 28 samples.

3.4. Results

3.4.1. Quantifying organic carbon export

We examine the differences in organic matter concentrations and yields between hydrological regimes (Mann Whitney; *p*-values reported in parentheses) and present relationships with key catchment parameters of glacial cover and mean slope (Figure 3.2). We include suspended sediments (SS) in our analysis for context.

Rivers with glacial regimes have significantly higher SS (p=0.017) and POC (p=0.019) concentrations than nival/pluvial rivers but show no overall correlation with catchment glacial cover (Figure 3.2a–b). In contrast, DOC concentrations show a significant but moderate negative correlation with glacial cover (Figure 3.2c), with DOC significantly

lower in glacial rivers (p=0.001). Sediment and POC yields are significantly higher in catchments with glacial regimes (p=0.001) and both are significantly correlated with catchment glacial cover (Figure 3.2d–e). Three glacial rivers (Ibanez, Murta, Baker (II)) deviate from a simple linear trend between POC yield and glacial cover, which may indicate catchment specific controls. The moderate correlation of sediment yields with catchment slope does not extend to POC yields (Figure 3.2g–h). DOC yields are unrelated to catchment glacial cover (Figure 3.2f) but show a positive correlation with slope (Figure 3.2i), which does not differ significantly between regimes (p=0.352).

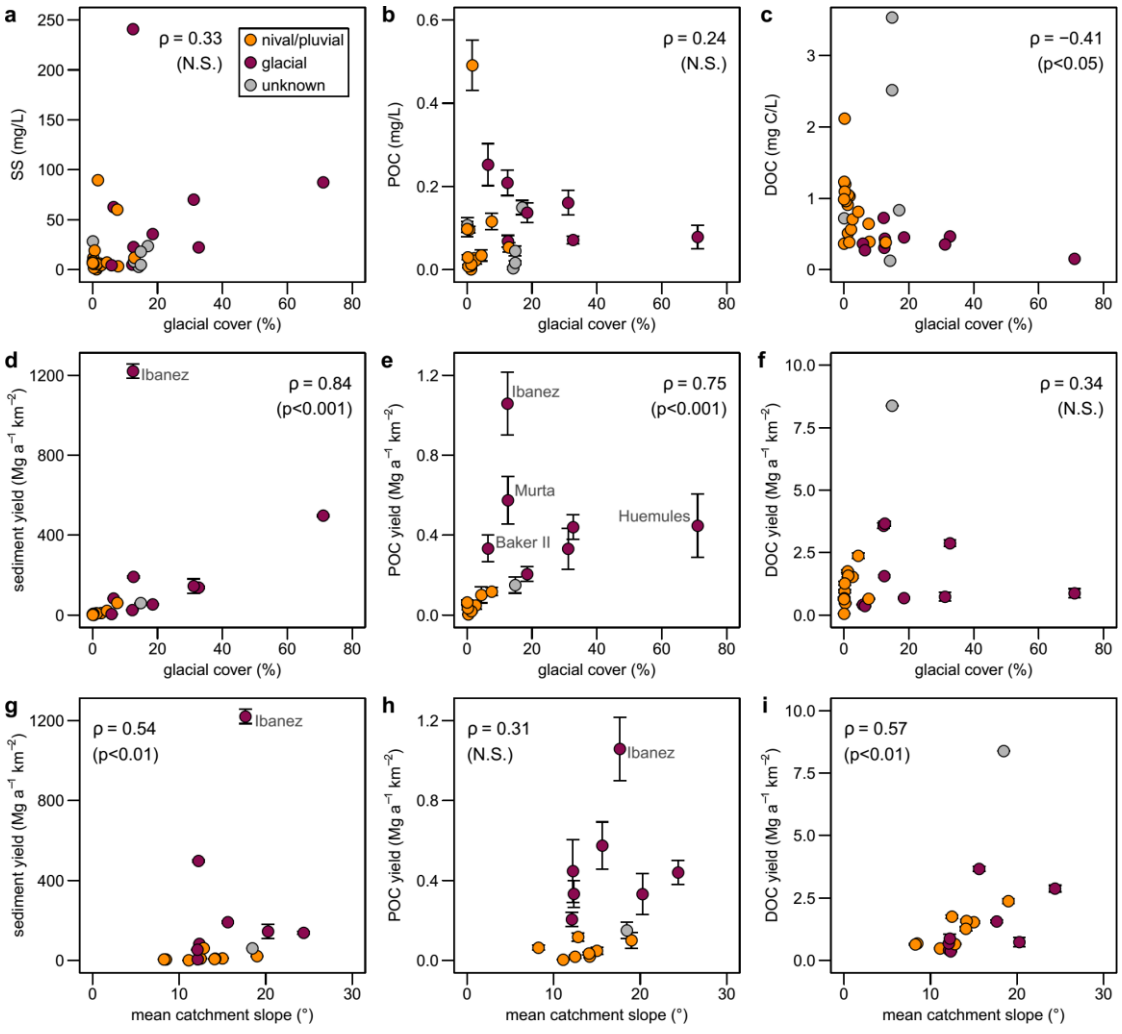

Figure 3.2. Export of suspended sediments (SS) and organic matter (POC and DOC) by rivers in Chilean Patagonia. Top row (a-c) shows concentrations versus catchment glacial cover; middle row (d-f) shows yields versus annual catchment glacial cover; bottom row (g-i) shows yields versus mean catchment slope. Each subplot is annotated with Spearman correlation coefficient (ρ) and *p*-value (or 'N.S.' where not significant; *p*>0.05) for relationship shown. Error bars reflect concentration measurement error (± 1 SD) or propagated errors (95% confidence) for fluxes and yields; where not visible, errors are smaller than symbols. Fill colour denotes river regime; key in subplot (a). Note different vertical scales for each subplot. Sites referred to in text are labelled on some subplots.

At the regional scale, organic matter yields from glacial rivers are directly associated with total lake volume in the catchment. POC and DOC yields show significant logarithmic declines with increasing lake volume relative to catchment area, with the strongest relationships for POC yields (Figure 3.3). The site with the greatest influence from lakes (Baker (II)) has a higher POC yield than the overall trend would suggest. There are no discernible relationships with lakes for the corresponding yields in nival/pluvial catchments.

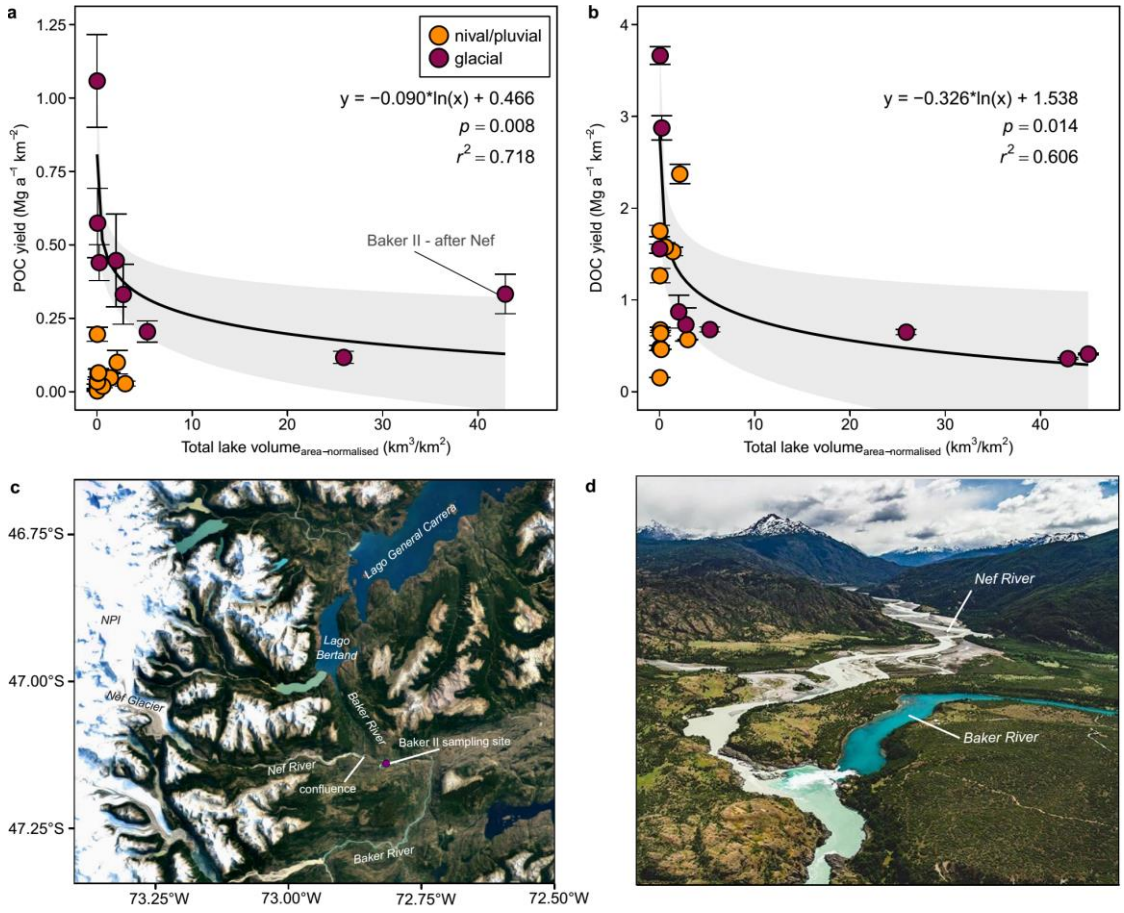

Figure 3.3. Changes in (a) POC and (b) DOC yields in Chilean Patagonian river catchments with respect to total lake volume (normalised to catchment area). Symbol colour denotes river regime; key in subplot (a). Error bars reflect 95% confidence intervals for yield estimates; where not visible, errors are smaller than symbols. Black curves and grey shading indicate logarithmic relationship and 95% confidence range for glacial catchments only; curve equation, r^2 and *p*-value annotated on each subplot. Subplot (c) shows location of Baker (II) sampling site (satellite image source: Google Maps), downstream of (d) the confluence with the Nef River (photo source: National Geographic).

Overall, dissolved phases dominate the export of organic matter by Chilean Patagonian rivers (Table 3.1). Although glacial regimes are linked with higher particulate loadings, none of the region's rivers show a dominance of POC that is typical of glacial systems

Table 3.1. Summary of riverine particulate and dissolved organic matter export in Chilean Patagonian rivers compared to glacial systems, Arctic rivers and other major world rivers.

Catchment	Area (10^3 km^2)	Annual discharge (km^3 a^{-1})	Concentration (mg L^{-1})		Annual flux (Gg a^{-1})		Annual yield (Mg km^{-2} a^{-1})		Total export (%)	
			POC	*DOC*	*POC*	*DOC*	*POC*	*DOC*	*POC*	*DOC*
CHILEAN PATAGONIA										
Northern Patagonian basins										
Yelcho (NP)	11.4	11.5	0.03	0.56	0.3	6.5	0.03	0.57	5	95
Palena (NP)	12.5	27.0	0.02	0.71	0.6	19.1	0.05	1.53	3	97
Ventisqueros (G)	0.2	1.1	0.07	0.47	0.1	0.5	0.44	2.87	13	87
Cisnes (NP)	3.2	1.3	0.01	1.20	<0.1	1.5	<0.01	0.48	1	99
Aysen basin										
Maniguales (NP)	4.3	5.0	0.03	1.10	0.1	5.5	0.03	1.27	3	97
Simpson (NP)	2.4	1.6	0.10	0.99	0.2	1.5	0.06	0.64	9	91
Blanco (G)	3.0	8.7	0.03	0.81	0.3	7.1	0.10	2.37	4	96
Aysen (NP)	11.3	17.0	0.01	1.05	0.2	17.9	0.02	1.58	1	99
Baker basin										
Ibanez (G)	0.9	4.6	0.21	0.31	1.0	1.4	1.06	1.56	40	60
Murta (G)	0.3	2.9	0.07	0.44	0.2	1.3	0.57	3.66	14	86
Leones (G)	0.8	1.7	0.16	0.35	0.3	0.6	0.33	0.73	31	69
Baker – after Nef (G)	16.7	22.1	0.25	0.27	5.6	6.1	0.33	0.36	48	52
Chacabuco (NP)	1.5	0.6	0.49	0.39	0.3	0.2	0.20	0.15	56	44
Del Salto (NP)	1.0	1.2	0.05	0.38	<0.1	0.5	0.06	0.46	12	88
Baker – nr. Tortel (G)	29.1	29.4	0.11	0.64	3.4	18.9	0.12	0.65	15	85
Southern Patagonian basins										
Huemules (G)	0.7	3.8	0.08	0.17	0.3	0.7	0.45	0.97	32	68
Bravo (U)	1.1	3.5	0.05	2.26	0.2	8.0	0.15	7.51	2	98
Pascua (G)	15.1	22.5	0.14	0.36	3.1	8.2	0.20	0.54	27	73
GLACIATED REGIONS										
Gulf of Alaska [a]	75.3	410.0	–	0.32	–	130	–	1.65	–	–
All mountain glaciers [b]	726.8	1,500	0.50	0.37	700	580	0.96	0.80	55	45
Greenland Ice Sheet [c]										
(1)	1,700	251	3.70	0.32	900	80	0.53	0.05	92	8
(2)	1,700	348	0.52	0.93	360	130	0.21	0.08	72	28
(3)	1,700	559	4.15	1.45	1,520	170	0.89	0.10	90	10
(4)	1,700	385	3.50	0.51	1,190	220	0.70	0.13	84	16
ARCTIC RIVERS [d]										
Kolyma	650	136	0.90	6.01	123	818	0.19	1.26	13	87
Lena	2,460	588	1.38	9.66	814	5,681	0.33	2.31	13	87
MacKenzie	1,780	316	2.40	4.36	758	1,377	0.43	0.77	36	64
Ob	2,990	427	1.34	9.65	572	4,119	0.19	1.38	12	88
Yenisey	2,540	673	0.37	6.90	249	4,645	0.10	1.83	5	95
Yukon	830	208	2.59	7.08	539	1,472	0.65	1.77	27	73
WORLD RIVERS [e]										
Brahmaputra	580	671	2.54	3.14	1,705	2,105	2.94	3.63	45	55
Ganges	1,100	380	4.58	4.60	1,738	1,747	1.58	1.59	50	50
Yangtze	1,800	905	4.87	1.92	4,410	1,738	2.45	0.97	72	28
Mississippi	3,200	537	1.73	4.20	928	2,257	0.29	0.71	29	71
Congo	3,700	1,270	1.57	9.36	1,998	11,889	0.54	3.21	14	86
Amazon	6,100	5,390	2.12	5.70	11,407	30,720	1.87	5.04	27	73

Table notes overleaf…

Table 3.1. notes

Label in parentheses after name of each Patagonian river name denotes regime designation as either nival/pluvial (NP), glacial (G) or unknown (U). Data are compiled from multiple sources and any missing variables (whether concentrations, fluxes or yields) are calculated from available data as described below.

a. DOC concentration and yield calculated from reported flux, area and discharge estimates (Hood *et al.*, 2009).
b. Mean annual discharge calculated from reported DOC and POC concentrations and fluxes (Hood *et al.*, 2015); yields based on estimate of total area of all mountain glaciers globally (Pfeffer *et al.*, 2014).
c. Range of yield estimates calculated for Greenland Ice Sheet using total area given by Huybrechts *et al.* (1991) and:
   (1) Upscaled discharge, concentrations and fluxes from small outlet 'N' glacier in 2008 (Bhatia *et al.*, 2013);
   (2) Upscaled discharge (Fettweis *et al.*, 2011) and concentrations/fluxes (Lawson *et al.*, 2014a) from Leverett Glacier 2009;
   (3) As above but for Leverett Glacier 2010 data from same sources;
   (4) Mean concentrations and total fluxes for whole ice sheet (Hood *et al.*, 2015).
d. Concentrations and yields calculated from flux data for POC (McClelland *et al.*, 2016) and DOC (Holmes *et al.*, 2012), using reported catchment areas and discharges (Stubbins *et al.*, 2015).
e. Reported catchment areas and POC yields (Galy *et al.*, 2015) and discharge, DOC concentrations/fluxes data (Dai *et al.*, 2012) used to calculate POC concentrations and fluxes and DOC yields.

(Table 3.1). A relatively high POC export loading (40%) from the Ibanez catchment is associated with the highest sediment yield (~1200 Mg a^{-1} km^{-2}), which is more than double the next largest sediment yield from the heavily glaciated Huemules catchment (~500 Mg a^{-1} km^{-2}). The largest total POC flux in the region, however, is in the glacial Baker River after its confluence with highly turbid discharge from the Nef Glacier, NPI (Table 3.1). Approximately 150 km downstream at Tortel, discharge of the Baker increases by 33% due to contributions from multiple tributaries but POC fluxes decline by 40% and DOC fluxes increase threefold (Table 3.1).

3.4.2. Trends in DOM composition and environmental controls

A total of 19,208 individual formulae were identified from 28 SPE-DOM samples, with 5833 (or ~30%) being common to all rivers and accounting for 91.8 ± 2.1% (mean ± SD) of total sample intensity. The composition of all samples is dominated by HUPs, which on average account for 81.9 ± 2.9% of sample relative intensity, with glacial rivers encompassing the highest and lowest percentages (78–87%). Polyphenolics are the next most dominant group at 11.1 ± 2.5%. Smaller contributions from aliphatics and peptides (3.6 ± 1.0% combined), condensed aromatic compounds (2.8 ± 0.9%) and sugars (0.6 ± 0.2%) make up the remainder of sample intensities. However, small differences in sample composition show that glacial rivers are significantly enriched in aliphatics and peptides with respect to nival/pluvial systems and are relatively depleted in polyphenolics and condensed aromatics (Figure 3.4a, c–d). In contrast, HUPs do not vary significantly between different hydrological regimes (Figure 3.4b).

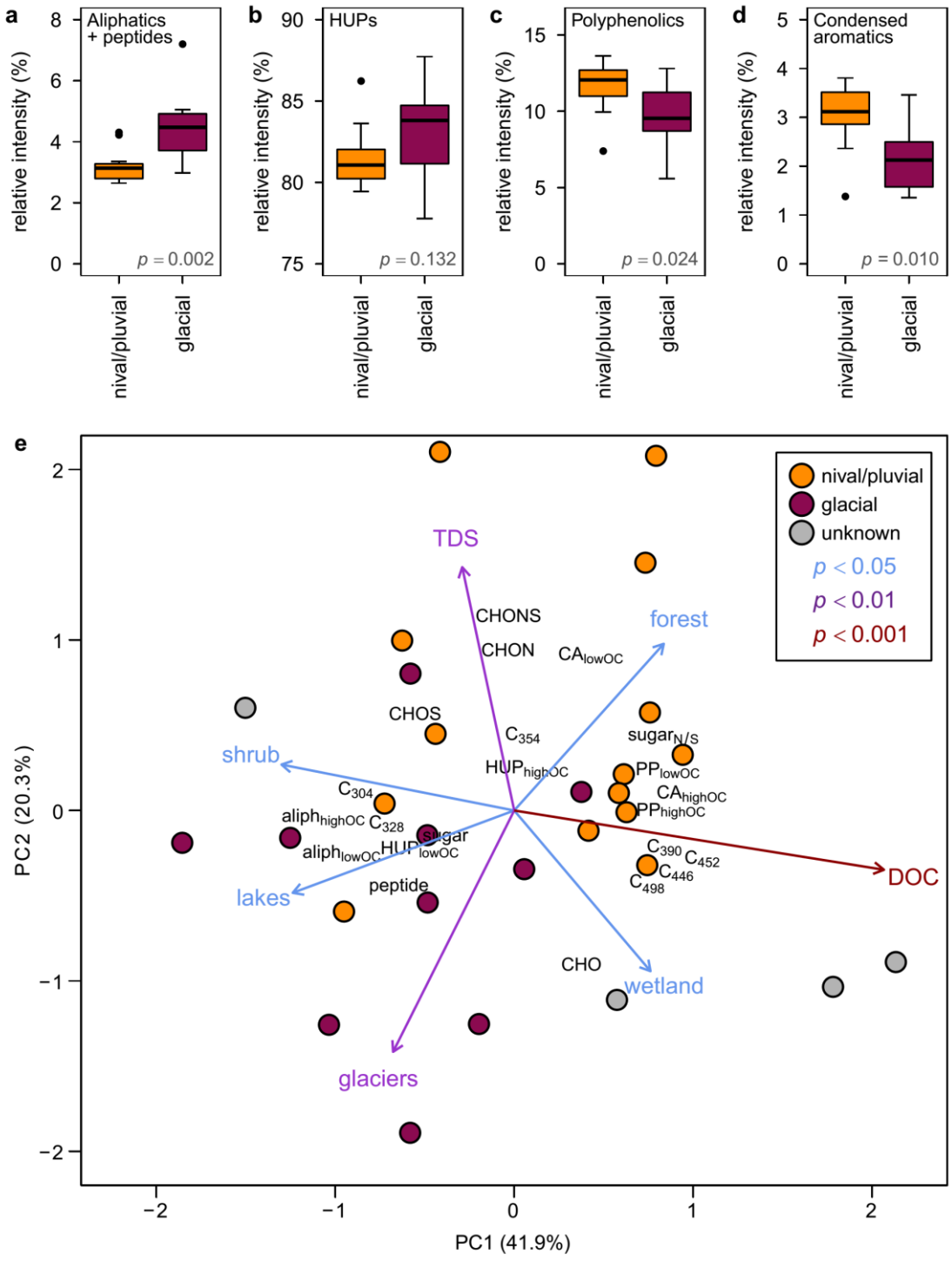

Figure 3.4. Compositional differences between DOM in glacial and nival/pluvial rivers. Subplots include boxplots of relative intensities for (a) aliphatic and peptide formulae combined, (b) HUPs, (c) polyphenolics and (d) condensed aromatic formulae, all annotated with *p*-values for Mann Whitney tests of difference between regimes. Subplot (e) shows the results of principal components analysis of DOM composition based on FT-ICR MS relative intensities for compound categories (see Section 3.3.3.2 for notation), formula class (CHO, CHON, CHONS, CHOS) and PARAFAC fluorescence loadings (also see Section 3.3.3.2). Environmental variables (glacier cover, lake influence, vegetation covers, DOC and TDS concentrations) fit to the ordination by permutation are colour coded according to the significance level of the correlation (see key).

The PCA biplot illustrates differences in DOM composition with respect to correlated environmental variables (Figure 3.4e). Overall, the PCA reaffirms that glacial regimes are generally associated with higher aliphatic and peptide signatures but also with O-poor HUPs and protein-like fluorophores C_{304} and C_{328}. These patterns are also significantly correlated with total lake volume relative to catchment size and glacier cover. Many nival/pluvial regimes show positive association with condensed aromatic and polyphenolic signatures alongside humic-like fluorescence. These characteristics are most strongly correlated with higher DOC concentrations and show weaker independent correlations with forest cover and wetland area. Other nival/pluvial rivers with high PC2 values are distinguished by higher heteroatom (N/S) content and correlated with total dissolved solids (Figure 3.4e). However, some catchments with different regimes have overlapping traits. For example, the Vodudahue and del Salto are nival/pluvial catchments with moderate glacial cover for the region (8% and 13% respectively) for which negative PC1 scores denote protein-like, unsaturated and aliphatic content (Figure 3.4e). Three rivers of unclassified regime — the Bravo, Nadis and del Paso; all of which are neighbouring catchments at ~48°S with similar (~15%) glacier cover (Figure 3.1) — are characterised by high DOC concentrations, humic fluorescence and correlated with higher wetland covers.

Despite several significant correlations with the ordinations of bulk compositional data, only 4 environmental variables are significantly correlated with any individual formulae (Figure 3.5; Table 3.2). The largest molecular cluster is correlated with DOC concentrations (n=2053; or 35% of all 5833 common formulae). Forest cover itself is not significantly correlated with any formulae, but broadleaf evergreen forest (BEF) cover, as the dominant forest type across the entire region (88.8 ± 4.4% of total forested area), is significantly correlated with 713 formulae (12% of common formulae). Glacial cover and lake storage are correlated with 835 (14%) and 568 (10%) formulae, respectively. Wetlands, shrub cover and total dissolved solids did not show any significant relationships with individual formulae. In total, 3816 (65.4%) of all common formulae are not correlated with any environmental variable tested.

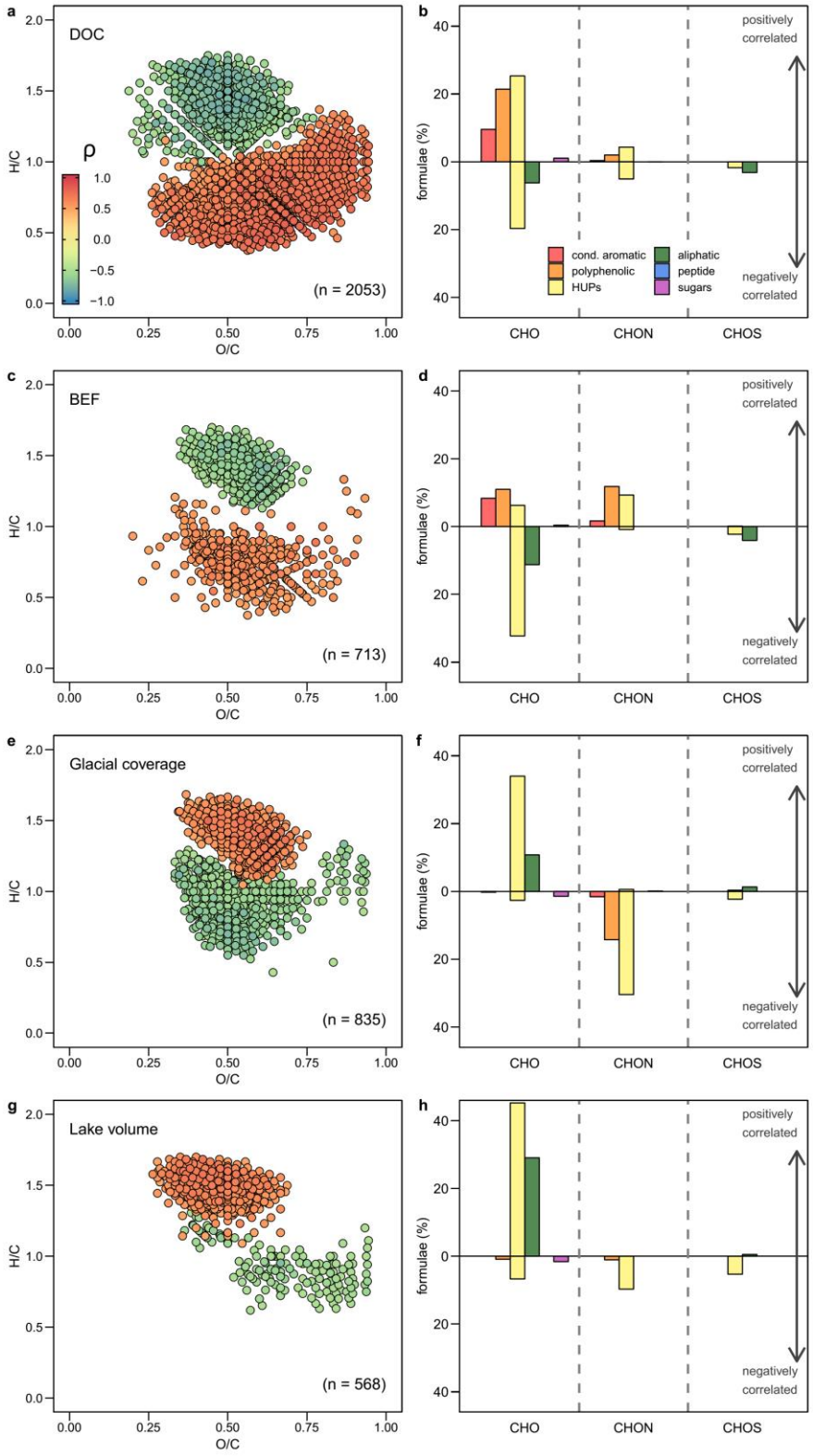

Figure 3.5. Molecular formulae in DOM from study rivers in Chilean Patagonia that are significantly correlated with DOC concentration (a-b), the percentage area of the catchment covered by broadleaf evergreen forest (c-d) and glaciers (e-f), and total lake volume normalised to the size of the catchment area (g-h). Left-hand column shows formulae in Van Krevelen space, where each symbol represents a single formula and the fill colour shows the strength and direction of the correlation (Spearman; *p*-value <0.011 accounts for false discovery rate correction). Right-hand column shows compound and class (CHO, CHON, CHOS) composition of these molecular families. Legends in subplots (a) and (b) apply to all plots of the same type.

Table 3.2. FT-ICR MS formulae correlated with environmental variables.

		DOC		BEF		glaciers		lakes	
		pos	neg	pos	neg	pos	neg	pos	neg
Total formulae		1,315	738	352	361	392	415	425	143
Unique formulae		1,065	452	98	34	51	192	92	33
(as % of group total)		81%	61%	28%	9%	13%	46%	22%	23%
(as % of group intensity)		77.7 ± 2.9%	66.6 ± 2.7%	40.6 ± 3.0%	2.7 ± 0.2%	8.8 ± 1.0%	50.4 ± 2.9%	12.8 ± 1.2%	7.9 ± 1.7%
Intensity-weighted averages									
mass	total	501.9 ± 8.8	409.4 ± 5.9	380.2 ± 5.0	479.8 ± 5.3	507.5 ± 5.2	431.4 ± 3.1	421.1 ± 9.0	471.9 ± 1.8
	unique	523.4 ± 7.2	407.0 ± 5.0	341.9 ± 7.0	570.6 ± 4.2	590.4 ± 2.1	429.7 ± 2.6	427.2 ± 11.3	478.3 ± 1.9
H/C	total	0.790 ± 0.011	1.286 ± 0.007	0.767 ± 0.014	1.375 ± 0.006	1.360 ± 0.008	0.947 ± 0.009	1.409 ± 0.003	0.866 ± 0.010
	unique	0.797 ± 0.010	1.233 ± 0.004	0.831 ± 0.008	1.339 ± 0.009	1.203 ± 0.006	1.014 ± 0.005	1.408 ± 0.007	1.107 ± 0.008
O/C	total	0.639 ± 0.009	0.495 ± 0.005	0.596 ± 0.008	0.508 ± 0.004	0.516 ± 0.004	0.610 ± 0.014	0.462 ± 0.005	0.754 ± 0.011
	unique	0.622 ± 0.008	0.500 ± 0.006	0.567 ± 0.008	0.539 ± 0.004	0.577 ± 0.005	0.603 ± 0.014	0.386 ± 0.007	0.524 ± 0.010
Percentage of shared formulae by group									
DOC	pos			36%	0%	0%	19%	0%	64%
	neg			0%	43%	37%	0%	53%	0%
BEF	pos	10%	0%			0%	38%	0%	5%
	neg	0%	21%			71%	0%	44%	0%
glaciers	pos	0%	20%	0%	77%			49%	0%
	neg	6%	0%	45%	0%			0%	23%
lakes	pos	0%	30%	0%	52%	53%	0%		
	neg	7%	0%	2%	0%	0%	8%		

Some formulae correlated with environmental variables are unique but many are shared (either positively or negatively; Table 3.2) and reflect consistent landscape-level influences on DOM at the molecular level. For example, glaciers and BEF cover have broadly inverse influences. High glacier cover and low forest cover are linked with aliphatic and unsaturated DOM, whilst low glacier cover and high forest cover are both linked with aromatic and polyphenolic formulae (Figure 3.5c–f). The overlap between those formulae that are correlated positively with glacier cover and negatively with DOC concentrations (Figure 3.5a–b, e–f) corroborates the observation that glacial rivers contain dilute DOM (Figure 3.2c). However, molecular signatures also indicate distinct environmental influences over DOM composition. For example, those formulae positively correlated with BEF cover contain many low mass (<400 Da) polyphenolics

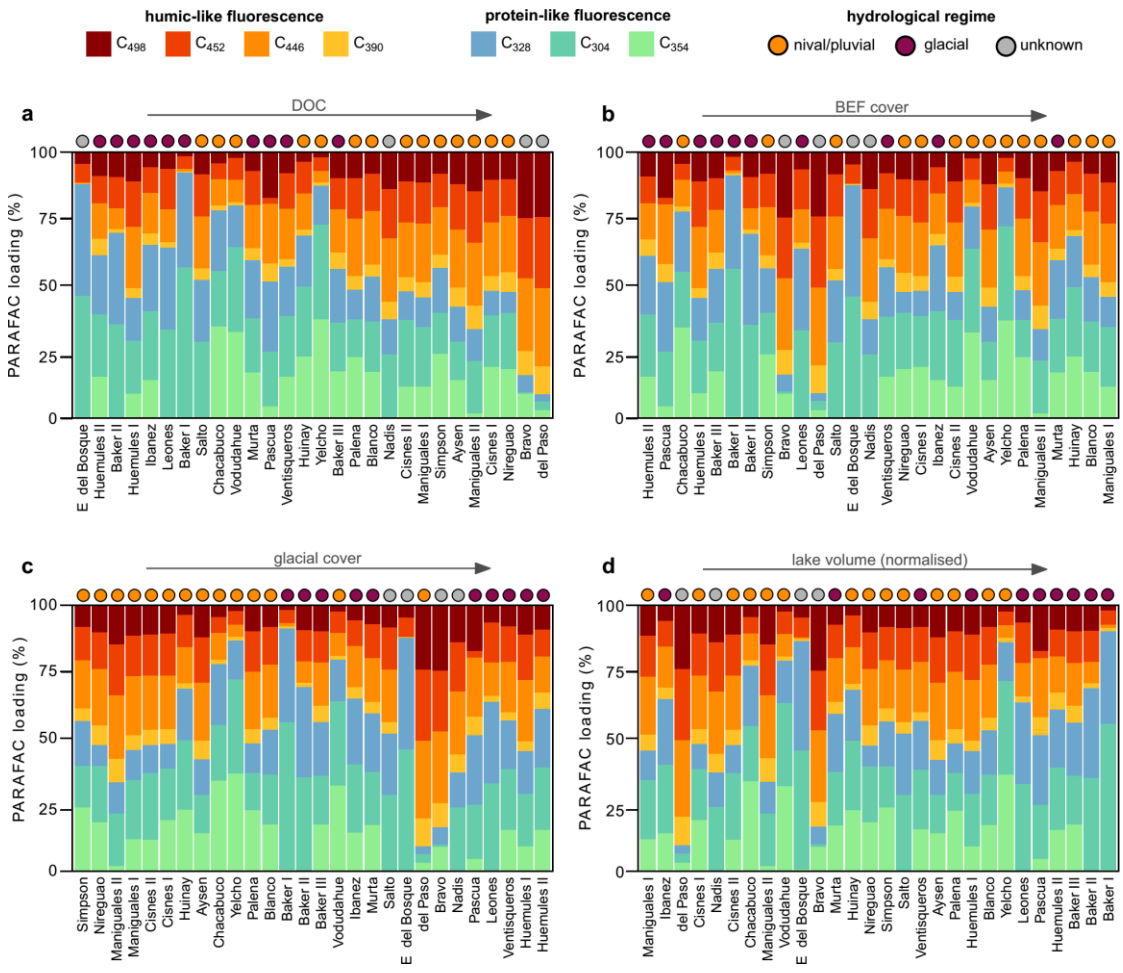

Figure 3.6. PARAFAC component loadings for all rivers ranked in ascending order from left to right for (a) DOC concentration, (b) broadleaf evergreen forest (BEF) cover, (c) glacial cover and (d) total lake volume normalised to catchment area. Humic-like and protein-like fluorescence components shown in warm and cool colours, respectively. Coloured circles above each stacked fluorescence bar denotes hydrological regime of the river.

and are largely distinct from the higher mass (>500 Da) and many HUP formulae associated with higher DOC concentrations (Figure 3.5a–d; Table 3.2). Despite similar influences of glaciers and lakes on DOM composition, lakes are linked with a higher proportion of aliphatic formulae and lower O/C ratios (Figure 3.5e–h; Table 3.2). We note a lack of systematic relationships between these same environmental variables and spectrofluorescence signatures, except for DOC concentrations which are positively correlated with higher humic-like fluorescence (Spearman >0.74; p<0.001; Figure 3.6).

3.4.3. Molecular characterisation of PARAFAC components

To enhance the utility of PARAFAC components we present correlations with FT-ICR MS data which allow molecular level interpretation of fluorescence signals. We do not propose that correlated formulae necessarily contribute to fluorescence but, rather, reflect pools of covarying DOM (Herzsprung *et al.*, 2012; Stubbins *et al.*, 2014; Wagner *et al.*, 2015). We identify distinct molecular families for 5 of the 7 PARAFAC components (Figure 3.7; Table 3.3). Combined, PARAFAC-correlated formulae comprise 32.6 ± 5.2% (mean ± SD) of the total FT-ICR MS sample intensity, suggesting fluorescence signatures convey information about a substantial portion of total DOM.

Humic-like C_{498} and C_{452} are correlated with higher molecular masses, O/C ratios and double bond equivalents. The former is associated exclusively with O-rich (O/C >0.5) highly unsaturated and phenolic compounds (HUPs), whilst the latter also includes a broader pool of compounds comprising O-poor (O/C <0.5) HUPs, polyphenolics and condensed aromatics. Formulae correlated with the two other humic-like components (not shown), C_{446} (n=797) and C_{390} (n=89), were not unique to those groups and were more strongly related to C_{452}. As the largest molecular group, the C_{452} family (n=1454) may therefore represent DOM that is associated with humic material more generally.

Protein-like fluorescence is linked with more N- and S-containing formulae and, although HUPs are the dominant compound, aliphatic formulae also covary with components C_{328} and C_{304}. The C_{304} family is dominated by O-poor compounds, which distinguishes it from all other groups. In contrast to other protein signals, tryptophan-like C354 is strongly linked to N-containing polyphenolics and low H/C ratios. The characteristics and origin of this component are discussed more fully in Chapter 4.

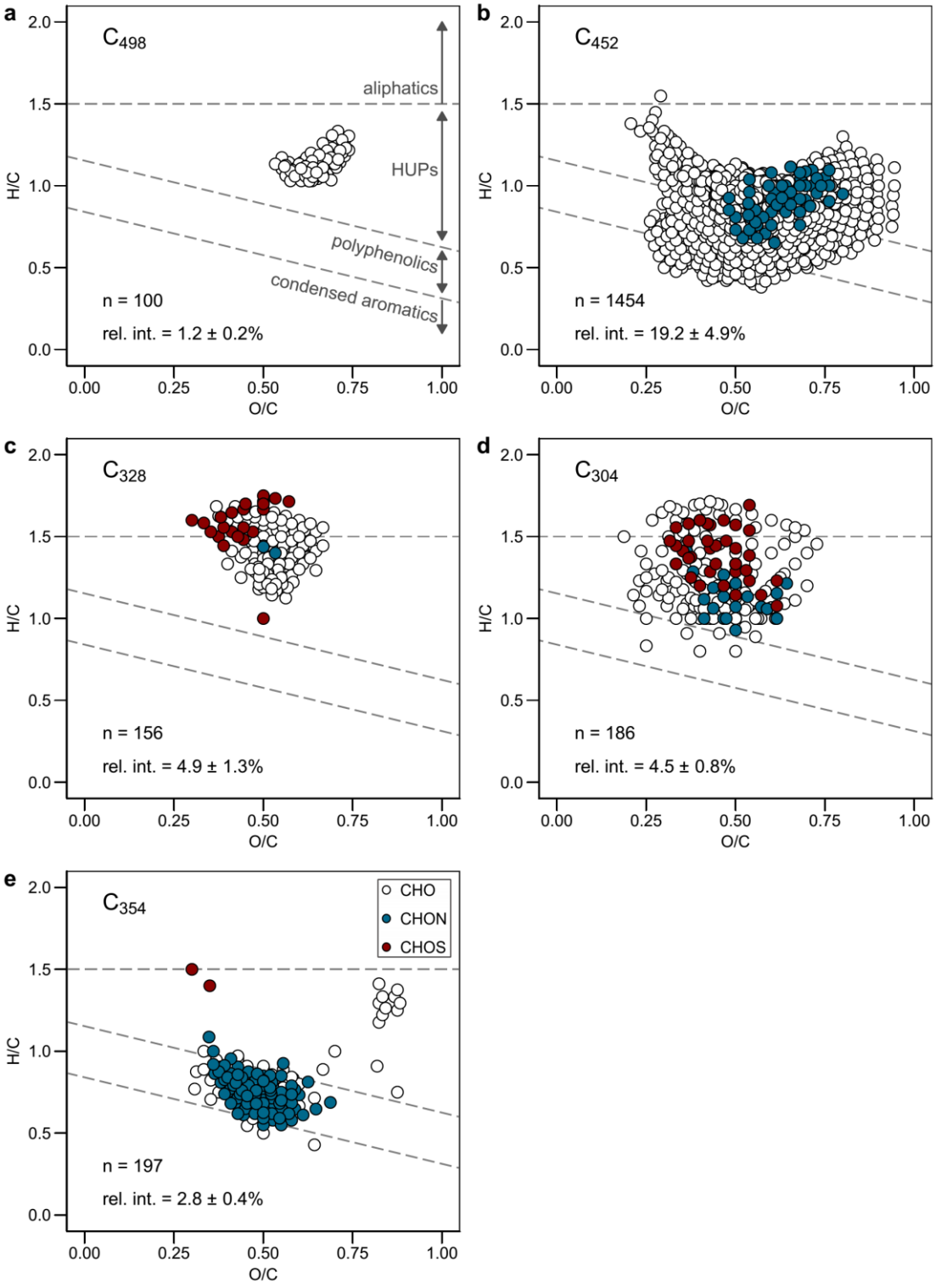

Figure 3.7. Van Krevelen diagrams showing FT-ICR MS formulae linked to individual PARAFAC components of fluorescent DOM in Chilean Patagonian rivers. Symbol fill colour denotes formula class plotted in the order of the legend in subplot (e). Dashed lines, which are annotated in subplot (a), indicate approximate distinctions between compound categories. All subplots are annotated with the number of formulae significantly and positively correlated (Spearman; adjusted *p*-value <0.0074) with the PARAFAC component and their mean ± SD total intensity across samples.

Table 3.3. Molecular properties of FT-ICR MS formulae positively correlated with PARAFAC components of fluorescent DOM in Chilean Patagonian rivers.†

		Humic-like						Protein-like								
		C_{498}			C_{452}			C_{328}			C_{304}			C_{354}		
PARAFAC loading (%)		9.74	±	4.58	12.39	±	4.67	16.06	±	7.74	25.32	±	15.53	14.00	±	12.17
FT-ICR MS intensity (%)		1.17	±	0.23	19.18	±	4.88	4.89	±	1.32	4.45	±	0.80	2.81	±	0.42
Number of formulae		100			1,454			156			186			197		
FT-ICR MS intensity-weighted averages	**mass**	602.33	±	4.00	554.08	±	5.12	386.91	±	4.36	341.94	±	5.29	382.76	±	3.92
	C	25.80	±	0.18	24.83	±	0.30	17.77	±	0.20	16.48	±	0.22	18.24	±	0.19
	H	28.77	±	0.17	21.19	±	0.49	24.19	±	0.27	19.30	±	0.19	14.74	±	0.24
	O	16.55	±	0.11	14.73	±	0.19	9.36	±	0.12	7.74	±	0.17	9.22	±	0.09
	N	0.000	±	0.000	0.010	±	0.002	0.001	±	0.000	0.023	±	0.004	0.17	±	0.02
	S	0.000	±	0.000	0.000	±	0.000	0.016	±	0.003	0.051	±	0.005	0.00	±	0.00
	H/C	1.117	±	0.002	0.847	±	0.013	1.363	±	0.006	1.174	±	0.010	0.804	±	0.006
	O/C	0.645	±	0.001	0.604	±	0.010	0.528	±	0.003	0.471	±	0.006	0.510	±	0.004
	N/C	0.000	±	0.000	0.000	±	0.000	0.000	±	0.000	0.001	±	0.000	0.008	±	0.001
	AI_{mod}	0.233	±	0.001	0.449	±	0.008	0.152	±	0.003	0.311	±	0.004	0.535	±	0.004
	DBE	12.414	±	0.096	15.239	±	0.192	6.671	±	0.084	7.844	±	0.155	11.956	±	0.094
Contribution to intensity of molecular family	**CHO**	100	±	0.0	99.03	±	0.16	98.25	±	0.27	92.71	±	0.71	83.28	±	2.17
	CHON	0.0	±	0.0	0.97	±	0.16	0.14	±	0.02	2.18	±	0.39	16.43	±	2.18
	CHOS	0.0	±	0.0	0.00	±	0.00	1.62	±	0.27	5.11	±	0.46	0.30	±	0.06
	Aliph. O-rich	0.00	±	0.00	0.00	±	0.00	5.65	±	0.65	1.17	±	0.25	0.00	±	0.00
	Aliph. O-poor	0.00	±	0.00	0.00	±	0.00	6.04	±	0.85	4.33	±	1.20	0.00	±	0.00
	HUP O-rich	100	±	0.00	57.59	±	2.26	68.60	±	2.07	42.36	±	2.72	22.79	±	1.21
	HUP O-poor	0.00	±	0.00	10.39	±	1.71	19.72	±	1.26	51.22	±	2.35	12.50	±	1.23
	PP O-rich	0.00	±	0.00	21.71	±	2.12	0.00	±	0.00	0.33	±	0.08	37.08	±	1.76
	PP O-poor	0.00	±	0.00	5.86	±	0.63	0.00	±	0.00	0.59	±	0.13	22.69	±	0.87
	CA O-rich	0.00	±	0.00	0.00	±	0.00	0.00	±	0.00	0.00	±	0.00	1.42	±	0.23
	CA O-poor	0.00	±	0.00	4.29	±	0.69	0.00	±	0.00	0.00	±	0.00	3.41	±	0.56
	Sugars	0.00	±	0.00	0.16	±	0.05	0.00	±	0.00	0.00	±	0.00	0.00	±	0.00

† Values are means ± SD across 28 rivers for which there were paired fluorescence and molecular-level FT-ICR MS data. Compound category abbreviations: aliphatic (Aliph.), highly unsaturated and phenolic (HUP), polyphenolic (PP) and condensed aromatic (CA), all subdivided into O-rich (O/C>0.5) and O-poor (O/C<0.5) formulae.

3.4.4. Time series observations in a glaciated catchment

Time series data from the glacial Huemules River show how seasonal shifts in organic matter export may be linked to hydrological dynamics and the varying strength of glacial inputs. River discharge is higher in summer (60–383 $m^3 s^{-1}$) than winter (48–70 $m^3 s^{-1}$) and related to seasonal differences in air temperature as a trigger for ice melt (Figure 3.8a–b). Cross-correlations of time series differentials show that fluctuations in discharge lag precipitation (coefficient=0.453, p<0.001) and air temperature (coefficient=0.306, p=0.018) by a day. However, the preceding day's air temperature

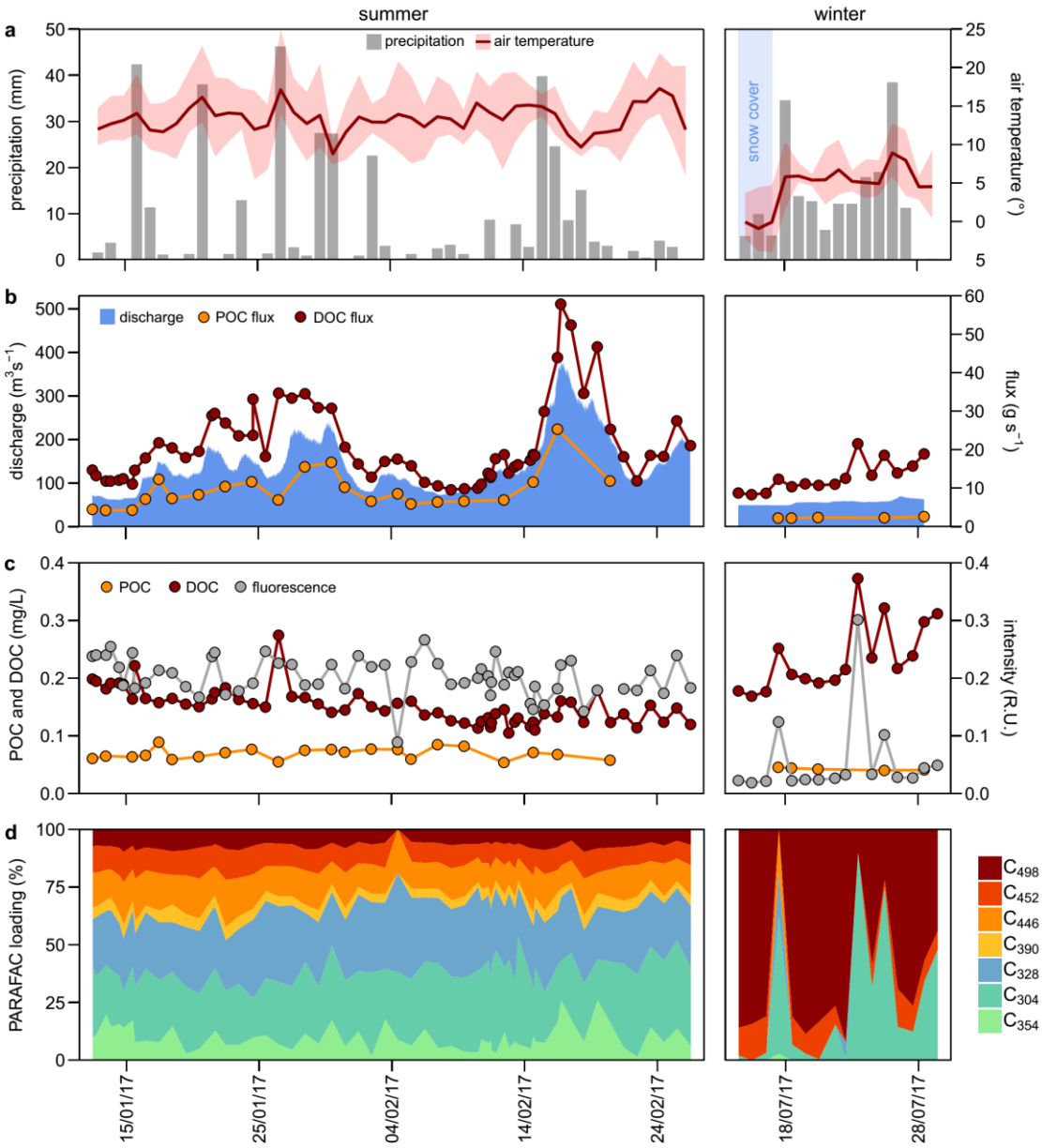

Figure 3.8. Time series observations for the Huemules River below the outflow of Steffen proglacial lake in summer and winter 2017 showing: (a) air temperature and rainfall data retrieved from nearest DGA meteorological station in Tortel; (b) discharge and organic matter fluxes; (c) POC and DOC concentrations and total fluorescence intensity; (d) variations in fluorescent DOM composition as measured by PARAFAC model component loadings.

and precipitation explain only a third of total discharge variability (multiple linear regression, adjusted R^2=0.33, p<0.001). Larger discharge fluctuations in summer suggest greater sensitivity when the overall flow is higher (Figure 3.8b). Although meteorological data from Tortel (~30 km away) may not fully capture local conditions, sub-zero temperatures coincide with a period of observed snow cover in the Huemules valley and, more generally, the timing of discharge fluctuations is consistent with broad scale weather patterns.

During high flow conditions in summer, daily organic carbon fluxes correlate with discharge levels (Pearson 0.91, $p<0.001$; Figure 3.8b) but not with concentrations, which show slight dilution over the season (Figure 3.8c). POC fluxes are relatively stable at low flow in winter but DOC flux variations are more strongly correlated with concentration (Pearson 0.96, $p<0.001$) than with discharge (Pearson 0.66, $p=0.007$). DOC is the larger component of organic matter export over the time series but its relative contribution to total flux increases from 62 ± 3% in summer to 79 ± 3% in winter. This is partly due to lower discharge and POC concentrations in winter. Higher DOC concentrations in winter produce daily fluxes that are comparable with those in summer for periods when discharge is <200 $m^3 s^{-1}$ (Figure 3.8b).

Fluorescence data show that DOM composition is relatively stable in summer and characterised by high protein-like fluorescence across a wide range of flow conditions (Figure 3.8d). Variations in PARAFAC component loadings over this period are not correlated with discharge fluctuations and deemed random, indicating increased flushing of a constant DOM source during high flows. When average discharge drops to <60 $m^3 s^{-1}$ in winter, DOM is generally characterised by higher concentrations and lower total fluorescence dominated by humic-like C_{498} (Figure 3.8d). Spikes in protein-like C_{304} fluorescence are coincident with those in DOC. The first of these spikes coincides with rising temperatures and loss of snow cover whilst the second and third occur during a period of rising rainfall. There are no corresponding changes in POC concentrations, although lower resolution sampling for POC may hinder detection of trends.

3.5. Discussion

This study begins to address how future landscape changes linked to glacier retreat will affect the riverine export of organic matter in a region for which biogeochemical data are presently scarce. The samples collected for this study cover a large geographic area and provide insight into trends in organic matter composition with respect to different river regimes and multiple environmental gradients over several degrees of latitude. The highly variable glacier cover across this region enables testing of differences between glacial and non-glacial regimes, with samples collected in summer when melt rates are higher and the contrasts between these regimes are likely to be greater. Thus, the study helps to assess the sensitivity of aquatic biogeochemical processes to changing glacial influences across this region. We acknowledge that summertime sampling might lead to an overestimation of glacial influences on an annual basis but, in the absence of any previous comparable data, this dataset provides a useful baseline for any future studies of these river systems.

The spot sampling strategy helps to cover a large number of rivers but it is difficult to determine how representative samples are of conditions at each site without longer term monitoring. We supplement the latitudinal transect data with time series data from one site on the Huemules River, our high glacial end-member catchment, to help constrain the daily and seasonal variability in organic matter fluxes at that site and provide context for other glacially fed rivers. Nevertheless, rivers are considered good integrators of upstream catchment processes and therefore samples from each site along the latitudinal transect will carry signals relating to multiple organic matter sources and landscape controls. Moreover, sampling upstream of settlements and isolated plots of farmland helps to minimise any local anthropogenic influences. Thus, our dataset allows us to test the influence of multiple environmental gradients on a larger number of rivers without risking extrapolation of findings from any one sample which has an uncertain representativity.

Overall, the results presented here are consistent with the prevailing view that glaciers supply particulate and proteinaceous organic matter to downstream rivers (Dubnick *et al.*, 2010; Hood *et al.*, 2015). However, some properties of riverine organic matter in Chilean Patagonia differ from those that define glacial influences elsewhere and may

reflect influences from additional sources and sinks of DOM and POM in the proglacial landscape. We focus our discussion on the degree to which the yields and composition of riverine organic matter in Chilean Patagonia (42–48°S) are regulated by glaciers and then modulated by two principal features of the proglacial environment which expand in response to glacier retreat — lakes and vegetation cover. We also argue that there is very limited direct impact from anthropogenic activity in this region, but highlight local catchment lithology and subsurface water sources as possible secondary influences on riverine organic matter. From the available evidence, we hypothesise the overall effect of deglaciation on regional organic matter export and carbon cycling.

3.5.1. Glaciers as regulators of organic matter export

The enhanced POC yields of rivers under glacial regimes in Chilean Patagonia suggest that glacial erosion is a strong influence on POM export. This is consistent with observations from Greenland and mountain glaciers of the northern hemisphere (Lawson *et al.*, 2014b; Hood *et al.*, 2015). The intensity of glacial erosion may be a more powerful driver of POM export from the relatively barren ice-covered regions of Chilean Patagonia than other non-glacial processes of erosion in vegetated regions (Galy *et al.*, 2015). However, overall lower POC concentrations and yields in this region compared to other glacial systems suggest that there are large sinks for POM in proglacial zones (see Section 3.5.2.).

It is not possible to determine the origin of POC in glacial rivers from concentration data alone. However, we hypothesise that relict vegetation and paleosols overridden during past glacial advances (Wadham *et al.*, 2008; Chu, 2014; Kohler *et al.*, 2017), such as during the neoglacial re-expansion of the icefields (Rabassa and Clapperton, 1990), are major sources for this material. The underlying granitic batholith (Pankhurst *et al.*, 1999) precludes the erosion of petrogenic carbon as a significant source (Hilton *et al.*, 2014). Moreover, particulates flushed from the supraglacial environment (Anesio *et al.*, 2010; Cook *et al.*, 2016), and the adsorption of DOC to glacial flour (Saidy *et al.*, 2013; Sommaruga and Kandolf, 2014) are likely to make only very minor contributions to total POC fluxes. Compositional analyses of larger particulate samples would provide further insight into POM sources and should be a focus of future studies.

DOC yields, in contrast, are unrelated to catchment glacier cover and glacial regimes (Figure 3.2f). However, the negative correlation between DOC concentrations and glacier cover (Figure 3.2c) and association of glacial regimes with higher protein-like (C_{304}, C_{328}), aliphatic and peptide content (Figure 3.4), are consistent with glaciers as a source of dilute, microbially-derived proteinaceous DOM (Hodson *et al.*, 2008; Anesio *et al.*, 2009; Dubnick *et al.*, 2010; Fellman *et al.*, 2010a; Singer *et al.*, 2012; Bhatia *et al.*, 2013; Lawson *et al.*, 2014a). Time series data from the Huemules River clearly illustrate a link between high protein-like fluorescence and increased melt inputs (Figure 3.8), which may reflect conditions in other glacial rivers of the region.

However, the lack of relationship between protein-like loadings and glacier cover on a regional basis (Figure 3.6) suggests that multiple sources of proteinaceous material across the Chilean Patagonian landscape confound detection of exclusively glacial fluorescence signatures. Local sources of humic DOM in glacial catchments may also skew regional patterns in fluorescence composition (Figure 3.6). Whilst fluorescing compounds might comprise as little as 1% of the total DOM pool in freshwater systems (Cory *et al.*, 2011), PARAFAC components are correlated with a much larger fraction (32.6 ± 5.2%; mean ± SD) of the molecular intensity of FT-ICR MS spectra in samples from this region (Figure 3.7). This is consistent with the findings of previous studies, demonstrating that fluorescence signals can provide valuable insight into the sources of a much broader pool of covarying and non-fluorescing DOM (Herzsprung *et al.*, 2012; Stubbins *et al.*, 2014; Kellerman *et al.*, 2015; Wagner *et al.*, 2015).

A key inference from our dataset is that glaciers may not be a major source of atmospherically deposited organic pollutants to Chilean Patagonian rivers. Sulphur-containing aliphatics have been cited as possible products of incomplete combustion (Wozniak *et al.*, 2008), but the positive correlation of such compounds with protein-like fluorescence (C_{304}, C_{328}; Figure 3.7) in our study suggests a stronger link with microbial sources. Moreover, these sources may not have an exclusive link to glaciers (Figure 3.4 and Figure 3.6) but instead reflect more widespread biological activity across all freshwater systems. The presence of condensed aromatic formulae in glacial snow, ice and runoff samples from the northern hemisphere has also been argued to indicate the storage and release of anthropogenic combustion products derived from atmospheric deposition (Singer *et al.*, 2012; Stubbins *et al.*, 2012; Spencer *et al.*,

2014b). Whilst these compounds are detected in all Patagonian river samples, they are more abundant in nival/pluvial systems (Figure 3.4) and hence do not appear linked to glacial sources. We note that our correlative approach contextualises the influence of glaciers on DOM composition within a suite of environmental controls and, whilst this cannot preclude glaciers as a possible source of condensed aromatics, suggests that they are not a major source. The lack of association between condensed aromatic formulae and glacial influences may be due to the following:

- Anthropogenic (or black) carbon may not be a quantitatively significant source of organic matter to Chilean Patagonian glaciers south of 42°S. This sparsely populated region is impacted far less from local sources of airborne pollution, such as industry or biomass burning, which have been linked to black carbon deposits on glaciers in more developed regions of northern (18–41°S) Chile (Rowe *et al.*, 2019). In addition, the long-range transport of atmospheric pollutants has a limited impact on air quality in southern Chilean Patagonia (Pozo *et al.*, 2004; Bogdal *et al.*, 2013), especially when compared to northern hemisphere locations where atmospheric deposition is a significant source of black carbon to glaciers (Stubbins *et al.*, 2012; Li *et al.*, 2016).

- Possible preferential removal of condensed aromatics from glacial DOM via photodegradation (Stubbins *et al.*, 2010) and biological consumption (Mostovaya *et al.*, 2017) on glacier surfaces and within proglacial lakes.

- Non-pyrogenic condensed aromatics may be more significant sources, especially in less heavily glaciated catchments. DOM leached from soils could be a major source of condensed aromatics especially where there is dense vegetation cover (Ohno *et al.*, 2010). Greater light penetration in less turbid (non-glacial) rivers may also produce condensed aromatics via the photodegradation of plant-derived lignins (Chen *et al.*, 2014; Waggoner *et al.*, 2015).

We cannot rule out the storage and release of anthropogenic carbon from glaciers in Chilean Patagonia (42–48°S) but our data suggest that this is not a major source of the condensed aromatic compounds in riverine DOM. This region is unlikely to completely escape the long-range transport of atmospheric pollution (Grannas *et al.*, 2006; Antony *et al.*, 2014; Arienzo *et al.*, 2017), as indicated by the detection of certain anthropogenic

aerosols at a remote location of the wider Aysen catchment (Scipioni *et al.*, 2012). Whilst the prevailing south-westerlies (Lenaerts *et al.*, 2014) are likely to be rich in organic aerosols from marine sources (blue carbon), even South Pacific air masses may be contaminated with anthropogenic black carbon (Shank *et al.*, 2012). However, it is not clear how far Patagonian glaciers preserve any carbon deposits derived from long-range atmospheric transport (natural or anthropogenic, black or blue) and, less still, how far black carbon deposits might enhance glacial melting and carbon export (Hodson, 2014; Molina *et al.*, 2015). Future studies should assess the composition of atmospheric organic matter (aerosols) in this region via the direct analysis of rain and snow samples. This could help to confirm the presence/absence of condensed aromatic compounds in glacial ice, alongside other black and blue carbon sources, and allow for more accurate tracing through the downstream hydrological network using detailed molecular and isotopic techniques.

3.5.2. Proglacial modulators of organic matter export

As glaciers retreat, expanding proglacial zones and lakes will have an increased influence over riverine organic matter. Here we consider the effects of lakes and vegetation, as two critical landscape variables which respond to long-term deglaciation, on regional organic matter export.

3.5.2.1. Lakes

Lakes are becoming increasingly important sources and sinks of organic matter in Chilean Patagonia as they grow in number and size as glaciers retreat (Loriaux and Casassa, 2013; Wilson *et al.*, 2018). The negative relationship between POC yields and lake volume in glacial catchments (Figure 3.3) is consistent with lakes being physical and biogeochemical traps for POM (Grossart and Simon, 1998; Tranvik *et al.*, 2009; Liermann *et al.*, 2012; Carrivick and Tweed, 2013). The estimated POC yield at the Baker (II) site is higher than would be expected from the general trend as a result of the turbid Nef River (fed by the Nef Glacier) bringing a new supply of glacial sediments downstream of Lake General Carrera (Figure 3.3). The 40% decline in the POC flux along the fast-flowing Baker River between the Nef confluence and Tortel (Table 3.1) suggests that these particulates are rapidly removed. Therefore, long water residence times in lakes would allow more significant POC losses through physical settling or

biological consumption (Tranvik *et al.*, 2009). Removal within lakes may explain why POC yields in all but one of the Chilean Patagonian glacial catchments are lower than the average for all mountain glaciers globally (Table 3.1). The absence of lakes from other prominent glacial study sites, such as in Greenland (Bhatia *et al.*, 2013; Lawson *et al.*, 2014a), means that these are high end members for glacial POC yields (Hood *et al.*, 2015). The lack of relationship between POC yields and lake size in nival/pluvial catchments in Chilean Patagonia (Figure 3.3) reflects lower rates of erosion and the limited capacity of smaller lakes to act as POC sinks.

The decline in DOC yields with increasing lake volume in glacial catchments (Figure 3.3) suggests that lakes are also important DOM sinks. The lack of a corresponding pattern for nival/pluvial catchments implies that the conditions in glacial lakes favour net DOM consumption. High turbidity in glacial lakes limits primary production as a source of autochthonous DOM and therefore the consumption of in-washed DOM by freshwater bacteria may drive carbon cycling in these lakes (Singer *et al.*, 2012; Sommaruga, 2014). Glacial DOM may be a favourable substrate if its link with high protein-like fluorescence is indicative of a high lability found elsewhere (Hood *et al.*, 2009; Dubnick *et al.*, 2010; Fellman *et al.*, 2010a; Lawson *et al.*, 2014a). In contrast, any DOM removed in non-glacial lakes may be offset by new production (Sommaruga, 2014), albeit limited by oligotrophic conditions in freshwater bodies across the region (Garcia *et al.*, 2015). Overall, lakes act as biogeochemical sinks for organic matter, and effective physical traps for POM, which is consistent with the global role for inland water bodies as carbon sinks (Battin *et al.*, 2009; Tranvik *et al.*, 2009; Catalán *et al.*, 2016; Evans *et al.*, 2017). Moreover, lakes along glacial rivers effectively modulate the size and character of organic matter export fluxes from glaciers.

The common geographical distribution of glaciers and lakes (Figure 3.1) makes it difficult to disentangle their effects on DOM composition. Both are linked with protein-like fluorescence, peptide-like, aliphatic and unsaturated compounds (Figure 3.4), which are indicative of microbially processed DOM and consistent with the character of glacial and lake ecosystems (Hodson *et al.*, 2008; Arora-Williams *et al.*, 2018). The higher proportion of aliphatic formulae and lower O/C ratios of formulae uniquely associated with lakes could be molecular signatures of fresh autochthonous DOM in non-glacial lakes (Sleighter and Hatcher, 2008; Kujawinski *et al.*, 2009; Landa *et al.*,

2014). However, such autochthonous DOM may form only a small fraction of the total DOM pool, especially if rapidly cycled, given the accumulation of allochthonous DOM (humic-like, aromatic-rich) from vegetated terrain in nival/pluvial systems (Kellerman *et al.*, 2015). It was not possible to differentiate the DOM associated with lakes between glacial and nival/pluvial catchments, in part due to the reduced statistical power of these smaller size subgroups.

Proglacial lakes may also help to stabilise the composition of DOM in glacial rivers at times of high melt inputs. This is inferred from the relatively constant fluorescent profile of the Huemules River in summer, despite significant variations in discharge linked to rainfall patterns (Figure 3.8). When the level of Steffen Glacier's proglacial lake is higher due to strong meltwater inputs, rain events may lead to increased flushing of the well-mixed lake waters which are dominated by glacial signals. Reduced outflow from the lake in winter leaves riverine DOM composition more sensitive to direct inputs from the surrounding land, such as during snowmelt or rainfall events. In other glacial systems without proglacial lakes, such as Leverett Glacier in Greenland, a seasonal evolution in the composition of exported DOM and POM reflects a growing meltwater network accessing different organic matter sources (Kellerman *et al.*, in prep.; Kohler *et al.*, 2017). The lake at Steffen Glacier may buffer any seasonal patterns in DOM/POM export, although we cannot rule out an established seasonal meltwater network (or a permanent one) at the time of sampling. These buffering effects may be broadly applicable to most outlet glaciers of the NPI which drain into freshwater lakes (Lopez *et al.*, 2010; Loriaux and Casassa, 2013).

3.5.2.2. Vegetation

As glaciers retreat, soil development and the establishment of increasingly complex vegetation covers creates new sources of organic matter over the long term (Tscherko *et al.*, 2003; Raffl *et al.*, 2006; Cannone *et al.*, 2008). The association of nival/pluvial regimes with higher DOC concentrations (Figure 3.2), humic-like fluorescence, polyphenolic and aromatic compounds (Figure 3.4) is consistent with strong inputs from vegetated terrain in catchments with low glacier cover. Such sources may also be relatively important in the lower reaches of glacial catchments, especially when glacier melt inputs are low in winter. The relationship between DOM composition and

vegetation covers across Chilean Patagonia, and especially in nival/pluvial catchments, provides valuable insight into the evolution of riverine DOM in response to deglaciation.

The dominance of HUP formulae in all samples, many of which are correlated with humic-like fluorescence (Figure 3.7), suggests a ubiquitous influence of vegetation on DOM composition irrespective of river regime. In glacial catchments, HUPs comprise >80% of total FT-ICR MS sample intensity, suggesting that non-glacial sources of DOM can have a significant influence on glacial rivers even in summer when meltwaters dominate overall discharge. HUP compounds are not strongly linked to a specific vegetation type and reflect the accumulation of a complex mixture of substances from numerous vegetation sources (Mostovaya *et al.*, 2017). The structural ambiguity of HUPs encompasses a diverse array of plant-derived degradation products (Riedel *et al.*, 2016; Mostovaya *et al.*, 2017), including lignins (Lu *et al.*, 2017), tannins (Porter, 1992) and phenolic structures which may fluoresce (Weiss, 1943). The O-rich HUPs (O/C>0.5) associated with high DOC concentrations and humic-like fluorescence (Figure 3.5 and Figure 3.7; Table 3.2) could reflect a source of plant-derived tannins which differentiate vegetation inputs from the O-poor HUPs (O/C<0.5) thought linked to recent biological activity in aquatic systems (Sleighter and Hatcher, 2008; Kujawinski *et al.*, 2009; Landa *et al.*, 2014). These widespread vegetation influences may overprint glacial signatures in riverine DOM further downstream, especially as glacial inputs decline in the long term.

The dominant vegetation cover in Chilean Patagonia, broadleaf evergreen forest (BEF), provides a distinct supply of nitrogen-rich polyphenolics to riverine DOM (Figure 3.5c–d). All vascular plants are a source of polyphenolic compounds (Riedel *et al.*, 2016; Mostovaya *et al.*, 2017) but other forest types, sparse tree cover, herbaceous cover and shrublands across this region are not correlated with these or any other formulae. This suggests that DOM derived from BEF, as the most abundant forest type, carries a unique molecular signature which can be distinguished from the broader range of phenolic and aromatic substances that are more generally associated with a range of vegetation types from diffuse sources. BEF cover is greatest in catchments north of 46°S (18–56% by area) and likely provides a rich source of DOM to the rivers here. Limited BEF cover in heavily glaciated catchments (e.g. 3% BEF and 71% glacier cover in Huemules

valley), may provide a small but critical source of N-rich polyphenolics, given that glaciers are an unlikely source (Figure 3.5e–f).

The striking similarity between molecular signatures associated with BEF cover and tryptophan-like (C_{354}) fluorescence (Figure 3.5 and Figure 3.7) suggests that the availability of an ostensibly reactive protein may be influenced to some extent by the dominant regional vegetation cover. These congruent molecular signatures might reflect a common source for tryptophan and polyphenolics via the bacterial decay of leaf litter (Maie *et al.*, 2007; Wickland *et al.*, 2007). Alternatively, they might show a propensity for phenolic and polyphenolic structures to bind to proteins (Maie *et al.*, 2006; Aiken, 2014; Cuss and Guéguen, 2015; Bai *et al.*, 2017). However, the lack of direct correlation between BEF cover and C_{354} fluorescence itself (Figure 3.6) suggests that there could be multiple tryptophan sources (and sinks) across the region. For example, the summertime-only presence of C_{354} in the Huemules River could be accounted for by the degradation of proteinaceous DOM (Mopper and Schultz, 1993; Stedmon and Markager, 2005b, 2005a; Murphy *et al.*, 2008) from glacial ecosystems (Dubnick *et al.*, 2010). This may be likely given the dominance of glacial meltwater in summer discharge and the low BEF cover within the catchment. We cannot entirely discount the possibility that tryptophan is also sourced from the vegetated slopes. Longer water residence times in Steffen proglacial lake in the winter, due to reduced meltwater throughput, could favour tryptophan removal through bacterial consumption. The relationship between BEF cover and tryptophan is explored more fully in Chapter 4.

3.5.3. Other influences on organic matter export

Our dataset highlights catchment lithology as a possible secondary influence over POC concentrations and organic matter export. This is consistent with the view that POC export from terrestrial systems is controlled by erosion rates and underlying geology (Galy *et al.*, 2015; Hilton, 2017; Tan *et al.*, 2017). The Chacabuco River, an east-west draining tributary of the Baker River with <1% catchment glacier cover, has the highest relative loading of POC in all sampled rivers (56% of total organic carbon export; Table 3.1). This could be accounted for by high rates of non-glacial erosion of a susceptible lithology, with pyroclastic and unconsolidated sediments comprising 46% and 15% of the catchment area, respectively (versus 9% average for both rock types across all 29 catchments). The largest absolute yields of sediment and POC (>1 Mg C km^{-2} a^{-1}; Table

3.1) in the Ibanez catchment could be accounted for by a combination of glacial erosion and a large area (31% of catchment) of pyroclastic material in Quaternary volcanic deposits (Weller *et al.*, 2014).

Subsurface water sources (soils, groundwater) may also be important controls on riverine DOM composition in our study catchments. The most concentrated and humic-rich rivers are associated with a wide range of HUPs, polyphenolic and condensed aromatic compounds that are not correlated with the dominant vegetation cover, BEF (Figure 3.5 and Figure 3.7; Table 3.2 and Table 3.3). This suggests inputs from other widespread organic-rich sources, such as soils (Ohno *et al.*, 2010). Soil DOM may enter rivers via gradual seepage and macropore flushing during storms (Jeanneau *et al.*, 2015; Denis *et al.*, 2017b), or discharge from wetlands and peat bogs (Junk, 2013). Three neighbouring catchments at ~48°S — Nadis, del Paso and Bravo (Figure 3.1) — provide evidence that modest wetland cover (4-10% catchment area) may be a significant local source of concentrated humic-rich DOM (Figure 3.4), consistent with conventional understanding of wetland DOM (Chin *et al.*, 1998; Fellman *et al.*, 2008, 2010a). Such inputs could account for humic-like fluorescence loadings being higher than in other catchments with comparable glacier cover (14-17%; Figure 3.6c). Chilean Patagonian wetlands have not been extensively studied (Clausen *et al.*, 2006; Iturraspe, 2018), but their biogeochemical function may be sensitive to hydrological changes linked to changes in precipitation (Chimner *et al.*, 2011) and glacier retreat (Polk *et al.*, 2017). Wetlands also provide routes for groundwater to resurface (Chimner *et al.*, 2011) but the overall contribution of groundwater to the riverine DOM pool is impossible to assess due to a lack of data for this region (Valdés-Pineda *et al.*, 2014). Direct sampling of soils, wetlands and groundwater is needed to help constrain the relative contributions of these subsurface water sources, which may exert an increasing influence over riverine DOM as glaciers recede.

However, anthropogenic influences related to agriculture and aquaculture, which have severely affected freshwater systems elsewhere in Chilean Patagonia (León-Muñoz *et al.*, 2013), have only a limited direct impact on our study region. In northern Chilean Patagonia (38–41°S), agricultural runoff and effluent from freshwater salmon farms have loaded local rivers with excess nutrients and raised POC and DOC concentrations (Tello *et al.*, 2010; León-Muñoz *et al.*, 2013; Graeber *et al.*, 2015; Nimptsch *et al.*,

2015; Kamjunke *et al.*, 2017). These same anthropogenic sources also release highly reactive microbial-like DOM (rich in nitrogen, peptides, lipids), which could stimulate bacterial heterotrophy and lead to greater CO_2 outgassing from inland waters (Graeber *et al.*, 2012, 2015). In some of these catchments, intensive farming has degraded >50% of the land area (León-Muñoz *et al.*, 2013) and freshwater bodies are being increasingly exploited for an expanding aquaculture industry (Quiñones *et al.*, 2019).

In contrast, our study catchments (42–48°S) span a sparsely populated (<1 person per km^2) and near-pristine landscape (Delgado *et al.*, 2013) where towns and villages occupy <0.01% of the land area and <0.4% is used for agriculture (Tateishi *et al.*, 2011, 2014). Despite its regional economic importance, most farmland is fragmented in small (<100 ha) plots of cropland and pasture (Delgado *et al.*, 2013). Moreover, there is no active freshwater aquaculture in any of our study catchments, with historical operations in the Yelcho basin having ceased by 2007 (León-Muñoz *et al.*, 2007) and no new licences granted as of 2016 (Quiñones *et al.*, 2019). Thus, organic matter concentrations in our study rivers are low in global terms (Table 3.1), and more in line with unpolluted rivers (DOC: 0.2–0.4 mg L^{-1}) rather than the developed catchments (DOC: 1.5–10.8 mg L^{-1}) of northern (38–41°S) Chilean Patagonia (Nimptsch *et al.*, 2015; Kamjunke *et al.*, 2017). Sampling upstream of settlements and farmland (where possible) should have minimised any local anthropogenic influences on our dataset and these would therefore be unlikely to significantly affect the latitudinal-scale trends analysed in this study.

3.5.4. Impact of deglaciation on organic matter export and carbon cycling

Having examined relationships between riverine organic matter and different landscape components, we may infer a range of implications for organic matter export and carbon cycling as a result of deglaciation-induced landscape change in Chilean Patagonia.

In the short term, enhanced glacier melting might intensify summertime conditions in glacial rivers, subject to any modification in the proglacial environment. Stronger inputs of POM and dilute, proteinaceous DOM would be typical of glacial systems elsewhere but effective sinks and additional sources of organic matter across the Patagonian landscape may dampen the magnitude of any changes. Nevertheless, stronger meltwater inputs to river systems would favour carbon cycling by freshwater foodwebs that are

specifically adapted to cold temperatures, high turbidity and low DOC concentrations (Brown *et al.*, 2007; Jacobsen and Dangles, 2012; Wilhelm *et al.*, 2013). An abundance of protein-like and aliphatic compounds might also stimulate heterotrophic activity (Singer *et al.*, 2012; Lawson *et al.*, 2014a; Hemingway *et al.*, 2019). We are unable to infer any enhanced release of stored anthropogenic carbon which is thought to subsidise reactive organic matter supplies downstream of other glacial systems (Stubbins *et al.*, 2012; Spencer *et al.*, 2014b). This might reflect a limitation of our correlative approach which direct sampling of snow/ice samples would help to address.

In the long term, glacier retreat may lead to less POM and proteinaceous DOM entering Patagonian river systems. Catchments with small, isolated mountain-top glaciers may be especially vulnerable (Davies and Glasser, 2012), whereas basins fed by the icefields may continue to receive seasonal meltwater inputs far into the future given the time (>400 years) it would take for them to disappear completely even at present, accelerated melt rates (Carrivick *et al.*, 2016; Dussaillant *et al.*, 2018, 2019). Sediment and POC yields may be particularly sensitive to the reduced erosive power of diminished glaciers (Hallet *et al.*, 1996). Non-glacial drivers of POC erosion may also be mitigated by the stabilising effect of low level vegetation growth on deglaciating slopes (Rogers and Schumm, 1991). However, lithological controls may support relatively high POC yields in some catchments despite dwindling glacier cover. DOC yields will be less directly affected by glacier retreat but may be influenced by the legacy of glacial erosion where it creates steeper catchments as suggested by the positive correlation between DOC yields and mean catchment slope (Figure 3.2). Steeper catchments are thought to encourage more rapid transit of waters, allowing more DOM to escape biological removal and thus lead to higher DOC yields (Aufdenkampe *et al.*, 2011).

Lakes would exert an increasing influence over organic matter export as they increase in number and size across deglaciating catchments (Loriaux and Casassa, 2013; Wilson *et al.*, 2018). In the short term, lakes may act as important sinks for glacial organic matter, especially POM, thereby dampening some of the effects of enhanced glacier melting on riverine organic matter composition (Tranvik *et al.*, 2009; Catalán *et al.*, 2016; Evans *et al.*, 2017). Microbial ecosystems in these lakes may also be sustained by the influx of organic carbon from glaciers (Hood *et al.*, 2015). In the long term, declining connectivity with glaciers may support greater primary production and lead

to a new role for lakes as sources of autochthonous DOM (Carrivick and Tweed, 2013; Sommaruga, 2014). Moreover, reduced meltwater discharge would extend lake flushing times which could promote the preferential removal of allochthonous aromatic DOM and the persistence of more tightly cycled aliphatic compounds (Kellerman *et al.*, 2015). The overall evolution of proglacial lakes may create new sources of protein-like and aliphatic compounds to downstream rivers, negating the decline in glacial DOM. Future studies should focus on comparing DOM in lakes that are downstream of different glaciers at varying stages of retreat to help assess how lake biogeochemical function responds to deglaciation.

Long-term declines in glacial runoff would lead to a rise in river DOC concentrations, consistent with conventional theory (Milner *et al.*, 2017). DOM in deglaciating catchments would drift towards compositions more typical of nival and pluvial systems, where residual glacial cover has limited impact on summertime conditions and vegetation/soils exert greater control. However, the exact evolution of DOM composition would be susceptible to local landscape covers (i.e. wetlands, forests) in expanding proglacial zones. Widespread vascular plant cover would maintain an overall dominance of HUPs, including lignins and tannins, and humic-like fluorescence. BEF cover may enrich river DOM with nitrogen-containing polyphenolics and tryptophan-like fluorescence but forest expansion in response to glacier retreat, as has been observed in the tropical Andes, may be limited across Chilean Patagonia due to a regional decline in rainfall linked to a shift in the prevailing westerly winds. Therefore, existing vegetation cover in deglaciating catchments may become increasingly influential over riverine DOM composition.

Finally, as retreating glaciers exert less control over catchment hydrology, organic matter export will be increasingly influenced by stochastic snowmelt and rainfall events (Milner *et al.*, 2017). Winter conditions in the Huemules catchment, when glacial melt inputs are much reduced, provide evidence for the episodic activation of alternative organic matter sources (Figure 3.8). Whilst we cannot ascribe all wintertime spikes in DOC concentration and protein-like fluorescence to specific weather events, they are suggestive of microbial DOM released via snowmelt (Antony *et al.*, 2017) or mobilised from soils during storm events (Maie *et al.*, 2007). Direct sampling and analysis of snow, rainwater and soil porewaters would help to constrain potential contributions

from these sources. Critically, these wintertime spikes are dominated by a single protein-like fluorophore (C_{304}) and decoupled from changes in the POC flux (though less frequent sampling in winter limits the resolution of POC data) and therefore distinct from glacial meltwater inputs in summer. The association of the C_{304} component with many S-containing formulae suggests that these wintertime events in the Huemules valley, could provide ephemeral nutrient subsidies to downstream ecosystems.

3.6. Conclusions

This is the first regional scale study to quantify and characterise riverine organic matter export in Chilean Patagonia and highlight its sensitivity to deglaciation. Consistent with observations elsewhere, we find that glaciers drive higher catchment POC yields and are significant sources of proteinaceous DOM to downstream rivers in summer. In contrast to evidence from northern hemisphere glaciers, we do not detect a significant supply of anthropogenic carbon entering glacial rivers. This could suggest either preferential removal of such compounds or proglacial sources of DOM which overprint these signals. Proglacial lakes act as effective sediment traps and carbon sinks in this region and continued lake expansion may mitigate any effects of enhanced glacier melting on organic matter export. Ongoing deglaciation may drive the long-term evolution of proglacial lakes from net sinks for glacial organic matter towards more productive ecosystems which could supply fresh organic carbon to downstream ecosystems. Significantly depleted glacier cover would ultimately generate less meltwater to dilute riverine DOM and concentrations would likely rise — though catchment DOC yields may be unaffected due to a corresponding decline in discharge. Richer sources of organic matter, such as vegetation and soils in the proglacial landscape, would increasingly control the composition of riverine DOM, which will be sensitive to local variations in landscape cover. Overall, the composition and export patterns of riverine organic matter in rapidly deglaciating catchments would become more like those in nival and pluvial catchments, affecting the delivery and character of organic carbon sources supplied to downstream ecosystems.

4. Potential vegetation controls on the bioavailability of dissolved organic matter in deglaciating catchments of Chilean Patagonia

This chapter presents the first assessment of the bioavailability of DOM in rivers in Chilean Patagonia (42–45°S). Molecular data from the broader region (42–48°S) inform the interpretation of both concentration and fluorescence composition changes over the course of 28-day incubations of riverine DOM. Following the investigation of the effects of deglaciation in Chapter 3, this chapter proceeds to examine the bioavailability of DOM in catchments at a late stage of deglaciation, i.e. where downstream carbon cycling may be more heavily influenced by supplies of labile material from non-glacial sources. This chapter focuses on a selected sample of river catchments within Chilean Patagonia and thereby complements findings from the broader study region examined in Chapter 3, albeit with a specific focus on bioavailability.

Results from this chapter may supplement those from Chapter 3 prior to publication and were presented in a poster at Goldschmidt 2019 conference under the reference:

Marshall, M., Kellerman, A., Wadham, J., Pryer, H., Hawkings, J., Robinson, L., Spencer, R. (2019) Variations in composition and bioavailability of dissolved organic matter in glacially-fed river catchments in Chilean Patagonia. *Goldschmidt Abstracts*, 2019, 2162.

Author contributions

I conceived the study with J. Hawkings and A. Kellerman to complement the larger NERC/CONICYT-funded PISCES project, led by J. Wadham with support from L. Robinson. I conducted all incubation experiments and associated analyses, interpreted the data and wrote the text. J. Hawkings collected the field samples and inoculum used in the incubations. H. Pryer assisted in calculating catchment properties in QGIS. R. Spencer provided additional lab support. A. Kellerman and J. Wadham provided reviews of the analyses and text.

4.1. Abstract

The Chilean Patagonian landscape is undergoing extensive and rapid deglaciation but understanding of the effects on regional biogeochemistry is hampered by a lack of data. There are no previous assessments of the bioavailability of riverine dissolved organic matter (DOM) for this region despite growing interest in glaciers as a source of highly reactive DOM elsewhere. The forecast reduction in glacier cover across Chilean Patagonia necessitates a better understanding of the environmental factors controlling DOM bioavailability in catchments with relatively low glacier cover. We use incubation experiments to quantify the proportion of bioavailable dissolved organic carbon (BDOC) in river water (sampled in February 2018) from seven catchments, spanning a range of low to intermediate glacier cover (0–33%), in northern Chilean Patagonia (42–45°S). We show that BDOC values here (7–23%) are lower than those observed in glacial rivers of the northern hemisphere (31–69%) and that variations in BDOC and residual glacier cover in our study catchments are not systematically related. We argue that lower overall DOM bioavailability in Chilean Patagonia may be related to intrinsic molecular properties, which reflect a degree of prior degradation upstream of sampling sites and inputs of less reactive material from across the wider catchment. We also use spectrofluorescence data to show that bacterial consumption of DOC is associated with a decline in tryptophan-like fluorescence over the incubations and that this pattern is consistent for all river samples. We infer from the relationship between fluorescence and ultrahigh resolution molecular level data (Fourier-transform ion cyclotron resonance mass spectrometry) for the broader study region (42–48°S) that tryptophan-like material is associated with a small pool of formulae (n=197) that is rich in nitrogen-containing polyphenolics. We argue that this relationship suggests a common source via the bacterial decay of vegetation, which may be linked to dense broadleaf evergreen forest cover. Overall, this highlights the potential for vegetation to exert a greater influence over riverine DOM bioavailability following the long-term retreat of glaciers across Chilean Patagonia.

4.2. Introduction

Dissolved organic matter (DOM) is an important component of the global carbon cycle due to its role as a substrate for bacterial respiration and growth in aquatic systems (Battin *et al.*, 2009). Globally, inland waters may release 1.2 Pg C into the atmosphere

each year via respiration, which equates to roughly one quarter of total annual carbon fixation by the terrestrial biosphere (Battin *et al.*, 2009). Exact rates of remineralization, however, vary between locations and are controlled by differences in DOM composition and intrinsic molecular factors which affect its overall reactivity (Kellerman *et al.*, 2015, 2018; Mostovaya *et al.*, 2017). DOM contains substances from a variety of sources, some of which may be relatively reactive and rapidly cycled whilst others may be more recalcitrant and persist for longer in natural waters (Kellerman *et al.*, 2015). Tracing the exact provenance of DOM is complicated by the compositional diversity of individual sources, multiple shared sources for particular compounds and the effects of biological and photochemical degradation (Battin *et al.*, 2008; Nebbioso and Piccolo, 2013; Jones *et al.*, 2016; Hawkes *et al.*, 2018). Nevertheless, riverine DOM composition and reactivity is sensitive to changes in supply which may be triggered by changes in climate and landscape properties (Battin *et al.*, 2008; Asmala *et al.*, 2016; Lambert *et al.*, 2017; Ward *et al.*, 2017).

Long-term glacier retreat is considered a critical aspect of global environmental change (alongside anthropogenic land-use and shifting rainfall patterns), which may have profound consequences for the carbon cycle (Zhuang and Yang, 2018). Glaciers have attracted much academic interest as a source of highly reactive DOM, and it is thought that enhanced melting due to rising global temperatures may stimulate bacterial carbon cycling in downstream aquatic systems (Hood *et al.*, 2009; Fellman *et al.*, 2010a; Singer *et al.*, 2012; Lawson *et al.*, 2014a). This biogeochemical effect may be particularly important where meltwaters reach coastal zones (Hood *et al.*, 2009; Lawson *et al.*, 2014a), given the potential for bacterial activity to influence overall ecosystem productivity in marine environments (Azam *et al.*, 1994). However, processing of glacial DOM within mountain river systems may contribute to the net heterotrophy of fluvial networks (Battin *et al.*, 2008; Singer *et al.*, 2012), and remove the most reactive material before export further downstream (Hemingway *et al.*, 2019). Indeed, the assimilation of glacial organic carbon by freshwater foodwebs has been demonstrated through isotopic analysis of cell tissues from apex predators in glacial rivers (Fellman *et al.*, 2015a). However, the character and bioavailability of DOM from terrestrial sources downstream of glaciers, which will have an increasing influence over freshwater carbon cycling following long-term glacier retreat (Milner *et al.*, 2017; Hemingway *et al.*, 2019), has received less attention in the literature. An understanding

of DOM bioavailability in catchments with relatively low glacier cover could serve as a model for future conditions in nearby catchments undergoing deglaciation.

Conceptual models for the biogeochemical impact of glacier retreat have developed mostly from studies carried out in the northern hemisphere (Hood *et al.*, 2015; Milner *et al.*, 2017). Therefore, the lack of published estimates of DOM bioavailability from glaciated regions in the southern hemisphere, for example, limits any global assessment of how glacier retreat will affect biogeochemical processes. Chilean Patagonia contains the largest concentrations of ice in the southern hemisphere excluding Antarctica (Foresta *et al.*, 2018; Millan *et al.*, 2019) and its glaciers are undergoing the most globally intense (per unit area) rates of retreat (Jacob *et al.*, 2012; Willis *et al.*, 2012a; Willis *et al.*, 2012b; Gardner *et al.*, 2013; Carrivick *et al.*, 2016). Deglaciation is driving simultaneous changes in regional hydrology, where the formation and growth of proglacial lakes (Wilson *et al.*, 2018) is increasing catchment water residence times and providing new sites for freshwater carbon cycling (Tranvik *et al.*, 2009; Catalán *et al.*, 2016). Moreover, the importance of Patagonian fjords as biological hotspots (Iriarte *et al.*, 2014), carbon sinks (Aracena *et al.*, 2011; Smith *et al.*, 2015) and sites of commercial fisheries (Niklitschek *et al.*, 2013) necessitates a baseline assessment of DOM bioavailability for rivers of the region and potential sensitivities to landscape change.

Here we present the first assessment of DOM bioavailability for seven river catchments in northern Chilean Patagonia (42–45°S) with a range of low to intermediate glacier cover (0–33% by area). We present the results of incubation experiments to determine the proportion of bioavailable dissolved organic carbon (BDOC) and compare our BDOC measurements to those from other published studies, which offer global context. Additionally, we utilise spectrofluorescence data to monitor changes in DOM composition over the incubations and identify bioavailable components. The relationship between spectrofluorescence and high-resolution molecular level data across the broader study region (42–48°S), comprising 28 catchments (as reported on in Chapter 3), provides enhanced interpretation of these bioavailable components and helps to identify potential sources. We also compare molecular data from our study region to those from published studies of glacial DOM to help explain the regional differences in bioavailability that were observed.

The aims of this study are to:

1. Measure BDOC in Chilean Patagonian rivers and set values in a global context.
2. Relate patterns of bioavailability to regional trends in DOM composition.
3. Hypothesise the constraints on DOM bioavailability and the sensitivity of carbon cycling to ongoing glacier retreat across Chilean Patagonia.

4.3. Methods

4.3.1. BDOC incubation experiments

We used incubation experiments to determine the proportion of bioavailable DOC (BDOC) in river water samples, defined as the percentage decrease in DOC concentrations following the addition of a bacterial inoculum (Hood *et al.*, 2009; Fellman *et al.*, 2010; Spencer *et al.*, 2014; Hemingway *et al.*, 2019). For consistency with previous studies we adopted the protocol outlined by Fellman *et al.* (2010). In February 2018, river water was sampled from seven catchments (Figure 4.1), filtered in the field through 0.2 µm PES filters to remove bacteria and particulates, and frozen immediately. Samples were defrosted in the laboratory and incubations were started within 1 month of collection, thus minimising the effects of degradation in storage. All samples (18 ml) were filtered (0.2 µm PES) into pre-furnaced (450 °C for 5 hours) amber glass vials and treated with 2 ml of a regional marine inoculum which was filtered to 2.7 µm (GF/D filters) to remove grazers. The inoculum was prepared from Comau Fjord water (42.17°S and 72.72°W, 10 m depth, salinity 31.6‰, 05/02/18). The vials were sealed with PTFE-lined caps (acid soaked, MQ rinsed) and then incubated in the dark at 15°C in triplicate. After 3, 7 and 28 days, a subset of the incubations was terminated and re-filtered to 0.2 µm for analysis. Control incubations were conducted for each river in triplicate using MQ water in place of an inoculum.

4.3.1.1. Sample analysis

DOC concentrations were measured as non-purgeable organic carbon through high temperature combustion (680°C) using a Shimadzu TOC-L_{CHN} analyser fitted with a halogen scrubber. Concentrations were determined from a linear calibration ($r^2 > 0.999$) based on standards (0.05–3.00 mg L^{-1}) prepared from a certified potassium hydrogen

phthalate solution (1000 ± 10 mg L^{-1}; Sigma Aldrich) through gravimetric dilution. The limits of instrumental detection and quantitation were calculated as 0.033 mg L^{-1} and 0.044 mg L^{-1}, respectively, following the approach of Armbruster and Pry (2008). Monitoring of repeat standard measurements of intermediate concentrations (0.10, 0.50 and 1.00 mg L^{-1}) showed minimal variance over the analytical run (typically <5%).

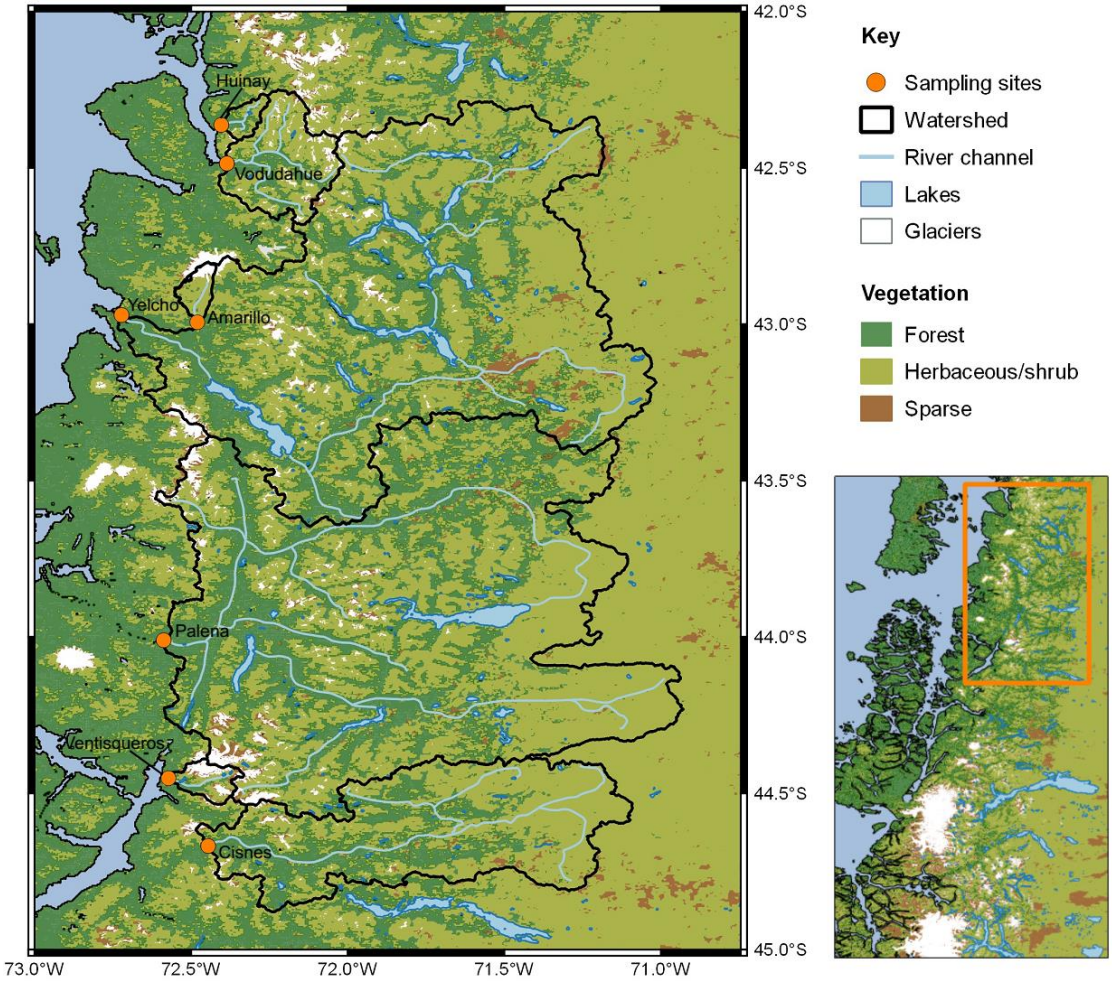

Figure 4.1. Sampling locations for seven rivers in northern Chilean Patagonia used in BDOC incubations alongside hydrological networks, glacial cover and vegetation covers. Inset map shows location of these catchments (orange box) within the broader study region used in Chapter 3.

4.3.1.2. Spectrofluorescence scans

All spectrofluorescence scans were conducted on an Agilent Cary Eclipse Fluorescence Spectrophotometer equipped with a xenon flash bulb. Excitation-emission matrices (EEMs) were collected between excitation wavelengths 240–450 nm (5 nm increments) and emission wavelengths 300–600 nm (2 nm increments) at a rate of 1200 nm min^{-1} with 0.1 second integrations and 5 nm monochromator slit widths. All samples were

analysed through 10 mm quartz cuvettes, which were stored in 50% HNO_3 and thoroughly rinsed with MQ and sample water between scans. Daily MQ scans were run to monitor instrument performance and procedural cleanliness. Corrections were applied to the EEMs using established procedures to remove instrumental bias, Raman and Rayleigh scatter and blank signals (Stedmon and Bro, 2008; Murphy *et al.*, 2013). We then projected a validated PARAFAC model for DOM composition across the broader study region to quantify changes in the intensity of fluorophore components (Section 4.3.2.1).

4.3.1.3. Representativeness of incubation experiments

Despite the limitations associated with this relatively small-scale study, the data obtained may still provide a representative and reliable basis for discussion, given the following considerations:

- The low number of samples has a limited statistical power to examine the relationship between bioavailability and catchment properties. Nevertheless, the scale of our study is in line with other published works with similar aims (Hood *et al.*, 2009; Fellman *et al.*, 2010a; Lawson *et al.*, 2014a).

- The low range of glacier cover in our study catchments (0–33%) may limit the extent to which these incubations reflect the influence of glaciers on DOM bioavailability. Nevertheless, variations in BDOC have been observed over similarly low ranges of glacier cover in other regions (Hood *et al.*, 2009; Hemingway *et al.*, 2019). Moreover, the low range of glacier cover is representative of most study catchments in the broader study region across Chilean Patagonia (all are <40% except for the Huemules (II) catchment at 71%). Despite low catchment glacier cover, river regimes such as that of the Ventisqueros are strongly influenced by glacial meltwater inputs.

- The study catchments in northern Chilean Patagonia are characterised by low glacier cover and relatively high forest cover. This selection enables us to identify controls over BDOC in catchments at relatively late stage of deglaciation, which may serve as a model for future conditions in other deglaciating catchments.

4.3.2. Contextual DOM data

The interpretation of BDOC incubation results was informed by the PARAFAC model and molecular level data for the broader geographical region (42–48°S) presented in Chapter 3.

4.3.2.1. Regional PARAFAC model

The 7-component PARAFAC model developed for the broader region was projected onto the incubation EEMs to quantify changes in fluorescence. The model was built from 386 EEMs generated from samples collected in summer and winter from a range of terrestrial and marine locations across Chilean Patagonia (Section 2.3.2.3). The model was developed from 10 random initializations using the drEEM Toolbox for MATLAB (Murphy *et al.*, 2013), specifying non-negative spectral constraints and a convergence criterion of 1×10^{-8}. The model explained 98.6% of the variance across all samples, with model residuals comprising mostly random noise. The model was validated through split-half analysis, whereby the full dataset was broken down into 4 random subsets, which were recombined into 6 data-halves that when modelled separately produced identical results (defined by a Tucker's congruence coefficient > 0.95). All components had been identified previously in other published PARAFAC models available on the OpenFluor database (Murphy *et al.*, 2014a) and were deemed to reflect realistic chemical fluorescence spectra.

4.3.2.2. Molecular level data

Fourier-transform ion cyclotron resonance mass spectrometry (FT-ICR MS) data from the broader region (Section 2.3.3) were used to identify molecular signatures for components of the PARAFAC model. This analysis offers additional insight into the potential changes in DOM composition over each incubation than can be obtained through spectrofluorescence data alone (which only detects actively fluorescing components). Molecular signatures for each PARAFAC component were identified as those formulae whose variations in relative intensity were positively and significantly correlated with variations in PARAFAC component loadings (% of total sample fluorescence) across all samples. The FT-ICR MS data were selected to include only those peaks common to all 28 river samples (n=5833) from the broader region. Non-normally distributed data necessitated the use of non-parametric Spearman correlations.

A false discovery rate correction (Benjamini and Hochberg, 1995) was applied to minimise the number of Type I (false positive) errors arising from the large number of correlations (7 PARAFAC components x 5833 individual formulae = 40831 tests). Following correction, a *p*-value <0.0074 was deemed significant at the 95% confidence interval. All statistical analyses were carried out using R (R Core Team, 2015).

4.3.3. Secondary data

We compared bulk molecular properties in our riverine DOM samples from Chilean Patagonia (n=28) to comparable FT-ICR MS data that are available from other regions where glaciers control freshwater DOM. Specifically, we make use of data obtained from runoff samples (n=12) collected over the 2010 melt season from the outflow of Leverett Glacier, Greenland, as a high glacial end-member comparison site (Lawson *et al.*, 2014b). We also use data from glacial river samples (n=55) collected during the 2014 monsoon season from the Upper Ganges basin, Western Himalayas (Hemingway *et al.*, 2019), as a dataset reflecting a range of catchment glacier covers (1–82%), similar to that of Chilean Patagonia (0–71%). We acknowledge that the reliability of such inter-study comparisons may be limited by methodological differences (e.g. in DOM extraction efficiency, ionization technique, instrument sensitivity, formulae assignment methods). However, the Himalayan data were generated using the same methods as this study and should provide reliable comparisons.

4.4. Results

4.4.1. BDOC rates

Measured rates of BDOC range from ~7% for the Yelcho River to ~23% for the Cisnes River, which reflect decreases in DOC concentration of 0.038 and 0.165 mg C L^{-1}, respectively (Table 4.1). In comparison, all control incubations displayed <2% change in DOC over 28 days. The pattern of DOC consumption follows a similar trend across all river sample incubations (Figure 4.2a). The greatest reduction in DOC concentration is observed over the first timestep (3 days) of the incubation, stabilising thereafter (Figure 4.2a). Three rivers with BDOC rates in the upper half of the observed range (Huinay, Vodudahue, Cisnes) showed continued declines in DOC concentrations between day 3 and day 28, albeit at a reduced rate (Figure 4.2a; Table 4.1).

Table 4.1. Summary of riverine DOC concentrations, BDOC rates and catchment properties for river samples used in incubation experiments.

	Huinay	**Vodudahue**	**Yelcho**	**Amarillo**	**Palena**	**Ventisqueros**	**Cisnes**
Sample data							
Riverine DOC (mg C/L)	0.350	0.569	0.554	0.382	0.581	0.330	0.731
BDOC (%)	18.8	16.0	6.8	17.4	14.2	10.8	22.5
(± 1 S.E.)	*(4.7)*	*(1.4)*	*(2.7)*	*(2.2)*	*(1.4)*	*(4.6)*	*(0.3)*
Catchment properties							
Total area (km^2)	108	911	11,354	133	12,506	176	3,213
Number of lakes	1	5	64	0	81	3	18
Total lake volume (x 10^6 m^3)	9	39	33,695	0	17,580	43	114
Vol. weighted lake residence time (days)	219	998	795	0	2,772	85	166
Glacier cover (%)	1.2	7.8	2.2	19.8	2.6	32.7	1.1
Forest cover (%)	56.8	49.2	51.2	15.2	52.9	63.7	43.7
Broadleaf evergreen forest cover (%)	52.0	41.9	44.1	14.5	46.0	34.4	39.9
Wetland cover (%)	0.6	3.3	4.6	5.7	4.6	1.1	2.5

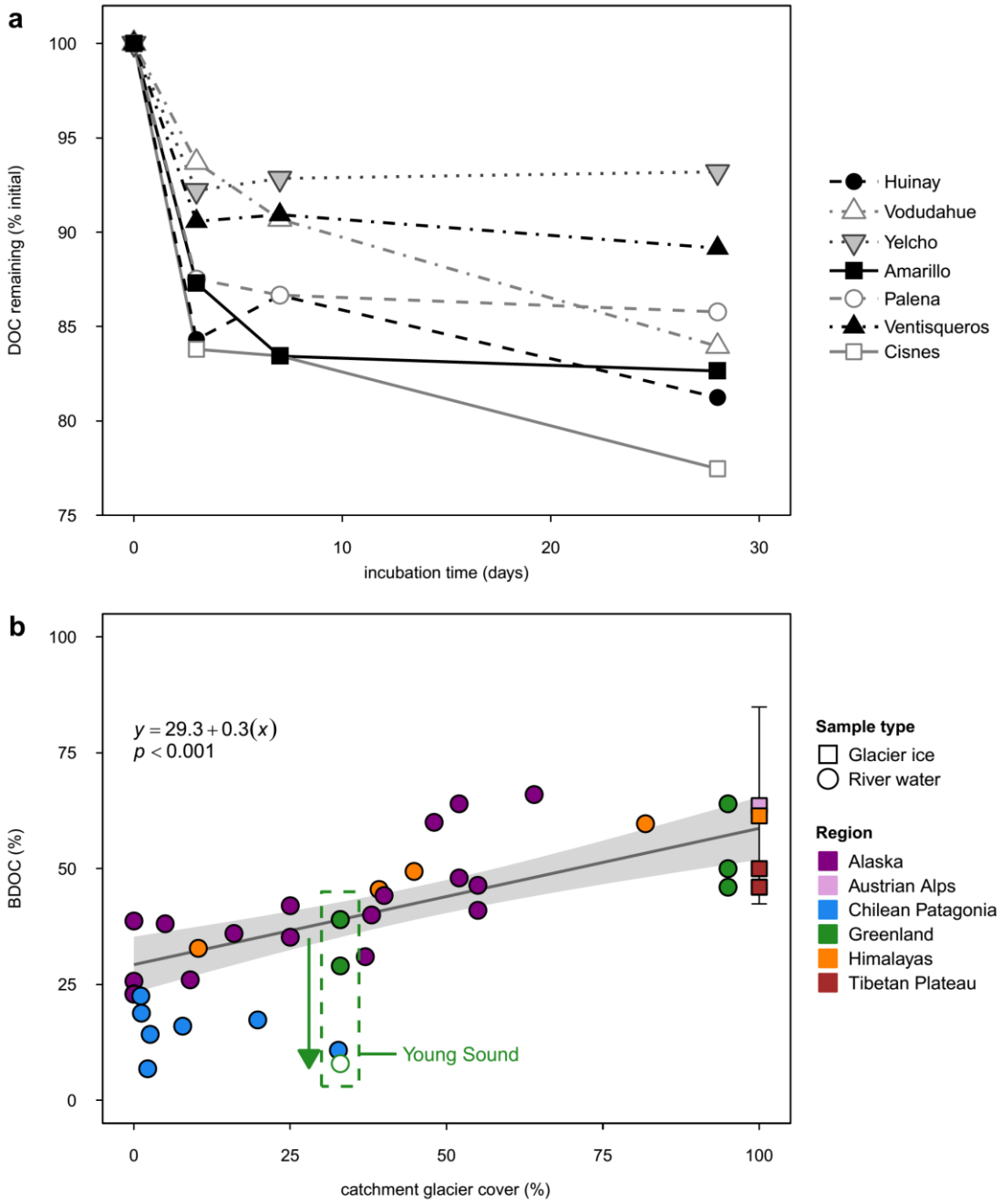

Figure 4.2. DOM incubation results showing (a) the consumption of DOC in Chilean Patagonian river samples over 28 days following addition of bacterial inoculum; and (b) measured rates of bioavailable dissolved organic carbon (BDOC) from this study compared with those from other glaciated regions — Alaska (Hood *et al.*, 2009), Austrian Alps (Singer *et al.*, 2012), Greenland (Lawson *et al.*, 2014a; Paulsen *et al.*, 2017), Himalayas (Hemingway *et al.*, 2019) and Tibetan Plateau (Spencer *et al.*, 2014). Results of linear regression for all data excluding Chilean Patagonian samples are shown by annotated equation, *p*-value, by solid line (grey shading shows 95% confidence envelope). Dashed green box identifies data from Young Sound, Greenland (Paulsen *et al.*, 2017), with arrow showing decline in BDOC between samples collected from rivers (filled symbols) and fjord freshwater lens (open symbol). Catchment glacier cover for Leverett Glacier, Greenland, nominally set at 95% for sampling site approx. 1 km downstream of meltwater portal. Austrian Alps data reflect average BDOC for ice samples, with error bars showing range of ± 1 SD (n=27).

BDOC rates in this study are near the minimum values reported for other regions where rivers are influenced by glacial meltwaters (Figure 4.2b). Within the small sample size of this study (n=7), BDOC rates do not vary systematically with catchment glacier cover (Figure 4.2b), or with other catchment properties summarised in Table 4.1. Indeed, we observed the greatest range in measured BDOC values for catchments with <5% glacier cover.

4.4.2. Fluorescence changes

Total fluorescence intensity declined between 14–60% for all incubations (Table 4.2). The pattern of these changes across EEM space is broadly consistent for all sample incubations, regardless of differences in the starting compositions of initial river water (Figure 4.3). Projected PARAFAC model component scores show that the changes in total fluorescence were primarily driven by a reduction in the intensity of the C_{354} fluorophore (Table 4.2), which is thought to reflect tryptophan-like fluorescence (Table 2.5, Section 2.3.2.3). The intensity of protein-like C_{304} decreased slightly in five of the incubations and shows little change in the remaining two (Amarillo, Cisnes). The average reduction in absolute intensity of C_{304} (-0.021 ± 0.018 R.U.) was smaller than that for the C_{354} component (-0.180 ± 0.069 R.U.) by an order of magnitude. Overall, the most significant changes occur in the C_{354} component, with marginal declines in C_{304} and the humic-like C_{498} (-0.015 ± 0.003 R.U.) components and negligible changes for other fluorophores (Table 4.2).

In the initial river water samples, DOC concentrations show a strong positive correlation with total fluorescence intensities (Pearson 0.83; p=0.02). However, the changes in DOC concentration and fluorescence over the incubations are not significantly correlated (Pearson 0.26; p=0.80). The fluorescence intensity of C_{354} (which displayed the greatest reduction in intensity over the incubations) is not correlated with DOC concentrations in the initial river waters (Pearson 0.43; p=0.33). Neither is the change in C_{354} fluorescence significantly correlated with the change in DOC concentration (Pearson -0.64; p=0.12).

Table 4.2. Summary of changes in sample fluorescence over the incubation study. Reported for each river is the total fluorescence in Raman units of the initial river water (F_{tot}), the change in fluorescence in Raman units and as a percentage of initial fluorescence (ΔF_{tot}), and the change in intensity for all components of the regional PARAFAC subdivided into broadly humic ($\Delta F_{humic\text{-}like}$) and proteinaceous ($\Delta F_{protein\text{-}like}$) fluorophores. Numerical subscript in name for each PARAFAC component (C) denotes the emission wavelength at which there is maximum fluorescence. The mean and standard deviation of all measurements across all incubation experiments are also provided.

	F_{tot}	ΔF_{tot}		$\Delta F_{humic\text{-}like}$ (R.U.)				$\Delta F_{protein\text{-}like}$ (R.U.)		
River	**(R.U.)**	**(R.U.)**	**(%)**	**C_{498}**	**C_{452}**	**C_{446}**	**C_{390}**	**C_{328}**	**C_{304}**	**C_{354}**
Huinay	0.544	-0.284	-52.2	-0.018	0.006	-0.013	-0.012	0.004	-0.025	-0.226
Vodudahue	0.620	-0.115	-18.5	-0.017	0.011	0.019	-0.005	0.000	-0.034	-0.089
Yelcho	0.706	-0.424	-60.0	-0.020	0.000	-0.084	-0.020	0.009	-0.030	-0.278
Amarillo	0.682	-0.096	-14.0	-0.011	0.008	0.002	0.006	0.021	0.003	-0.124
Palena	0.698	-0.272	-39.0	-0.014	-0.002	-0.006	-0.015	0.005	-0.043	-0.198
Ventisqueros	0.587	-0.256	-43.6	-0.015	0.003	0.003	-0.005	0.000	-0.023	-0.220
Cisnes	0.862	-0.381	-44.2	-0.013	0.005	0.002	0.006	0.021	0.003	-0.124
Mean	0.671	-0.261	-38.8	-0.015	0.004	-0.011	-0.006	-0.009	-0.021	-0.180
(± SD)	± 0.104	± 0.123	± 16.9	± 0.003	± 0.005	± 0.034	± 0.010	± 0.009	± 0.018	± 0.069

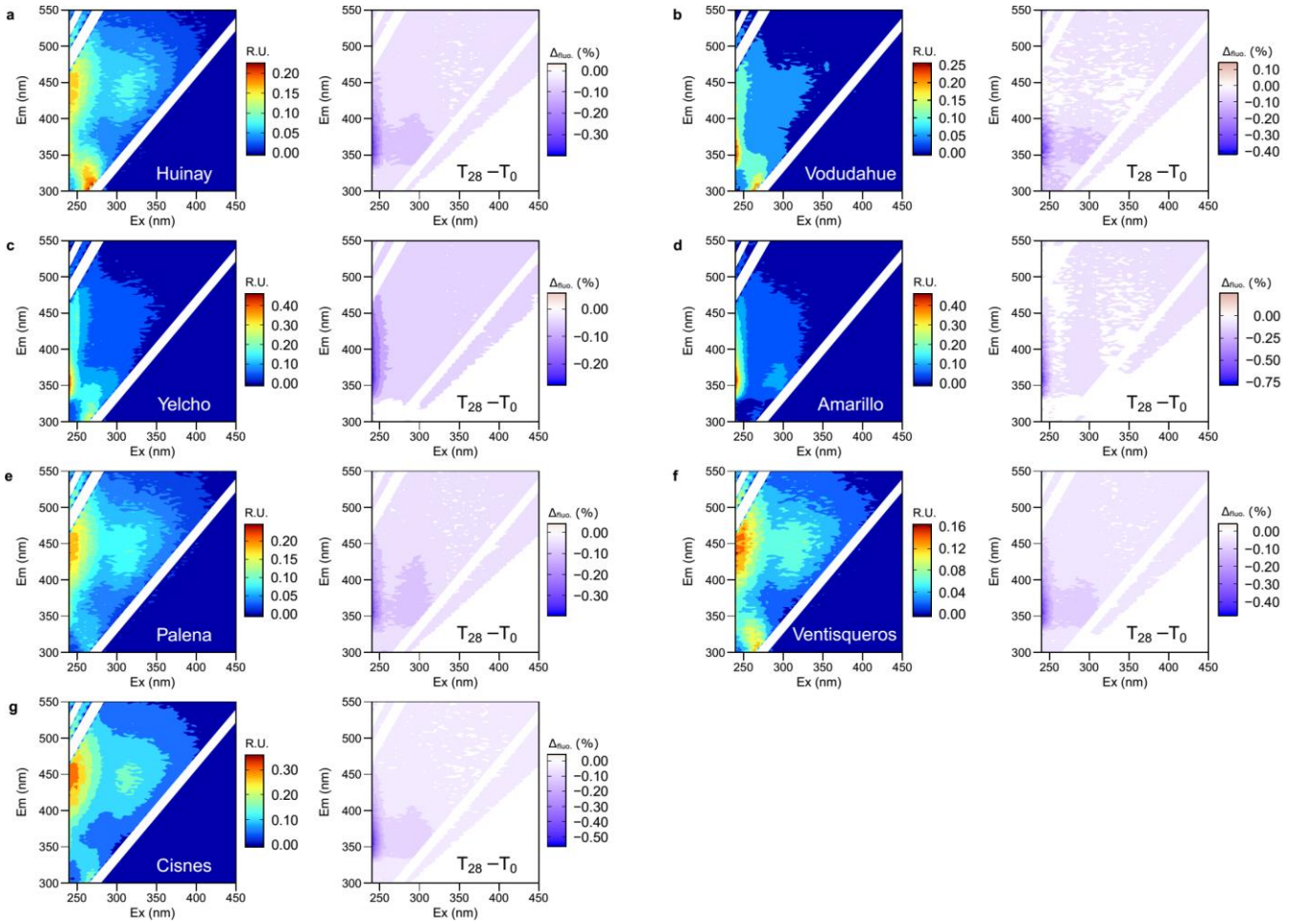

Figure 4.3. Spectrofluorescence EEMs showing the patterns of intensity in initial river waters and the net changes over 28-day incubations for the seven study catchments. In all subplots (a-g), left-hand panel shows the absolute fluorescence signal in Raman Units (R.U.) at day 0 and the right-hand panel shows the changes in intensity (expressed as a percentage of total fluorescence change) by day 28 (T_{28}–T_0), where deeper colours reflect a greater proportion of the total change. Note individual colour scales for each plot. See Table 4.2 for values of total fluorescence intensity change.

4.4.3. Molecular signatures of fluorescence changes

Since C_{354} was shown to be the most important fluorophore driving the decrease in fluorescence intensity during our incubations, we focus analysis upon this component and its relationship with the detailed molecular composition of DOM as indicated by FT-ICR MS. We identified 197 FT-ICR MS molecular formulae that were significantly and positively correlated with C_{354} fluorescence loadings (Figure 4.4b). These formulae are a small fraction of the 5833 individual formulae that are common to all river samples (n=28) used in the correlations. These formulae do not exhibit a statistically significant

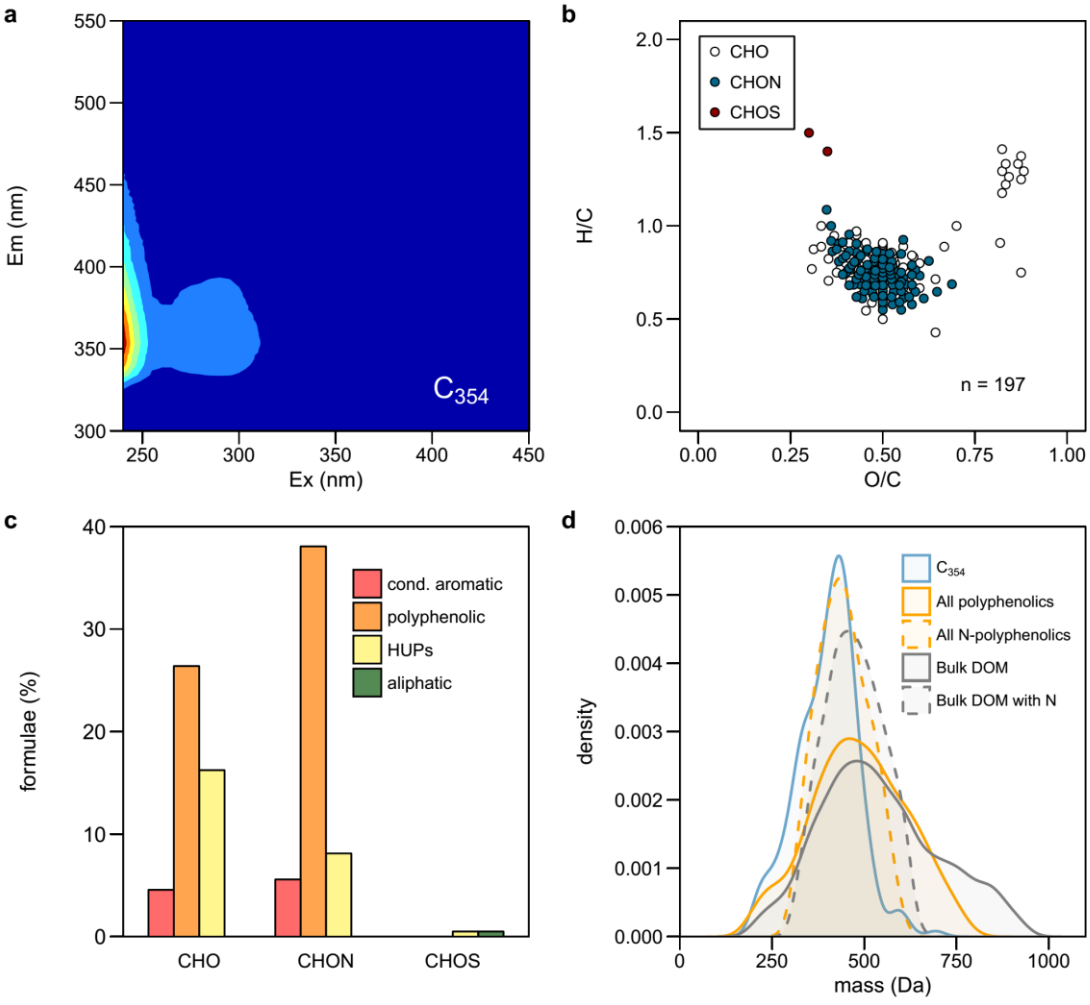

Figure 4.4. Molecular composition of DOM associated with C_{354} (tryptophan-like) fluorophore. (a) Fluorescence EEM of C_{354} component; (b) Van Krevelen diagram of FT-ICR MS-derived formulae that are significantly and positively correlated (Spearman; p <0.0074) with C_{354} loadings. Symbols show elemental classifications (CHO, CHON, CHOS) plotted in order of legend; (c) Compound category classification of molecular formulae associated with C_{354} fluorescence; (d) Molecular mass distributions of formulae correlated with C_{354} fluorescence with respect to polyphenolic formulae and all formulae common to 28 rivers of broader study region (dashed distribution curves reflect subcategories which only include formulae that contain nitrogen atoms).

relationship with any other PARAFAC component and so are uniquely associated with C_{354} fluorescence. These formulae have an average mass of 401.3 ± 81.7 Da and average H/C ratios of 0.80 ± 0.17 and O/C ratios of 0.50 ± 0.11. The average modified aromaticity index (AI_{mod}) is 0.54 ± 0.15 and the nominal oxidation state of carbon (NOSC) is 0.292 ± 0.259.

The molecular signature of C_{354} is dominated by polyphenolic, and specifically N-containing polyphenolic, formulae (Figure 4.4c). Of the polyphenolic formulae common to all rivers (n=727), 17.5% are significantly correlated with C_{354}. Moreover, 59% of the N-containing polyphenolic formulae found in all rivers (n=145) are significantly correlated with C_{354}. Highly unsaturated and phenolic formulae (HUPs) make up the bulk of the remainder of the C_{354} pool, with a modest proportion (~10%) being condensed aromatics (Figure 4.4c). Only one formula is aliphatic, which is one of two sulphur-containing formulae (Figure 4.4b). The average mass of formulae correlated with C_{354} (442.4 ± 67.8 Da) is lower than that of the bulk DOM (540.7 ± 161.0 Da) common to all rivers across the broader region (Figure 4.4d). This gives C_{354} a similar mass profile to the N-containing polyphenolic molecules common to all rivers (Figure 4.4d).

4.4.4. Inter-regional comparisons of molecular level DOM data

The inter-regional molecular level comparisons show that in samples from Chilean Patagonian rivers, a lower proportion of the detected molecular formulae contain nitrogen (Figure 4.5a). Moreover, these formulae comprise an even lower proportion of total FT-ICR MS sample intensity than is observed in samples from Greenland and the Himalayas (Figure 4.5b). Molecular formulae in samples from Chilean Patagonia and the Himalayas on average have a higher mass and aromaticity than those from Greenland (Figure 4.5c–d). On both measures, Chilean Patagonia exhibits the highest averages. For all measures of DOM composition compared here, the differences between samples taken from the three regions are statistically significant (Welch's t-test, which assumes unequal variance; $p<0.001$).

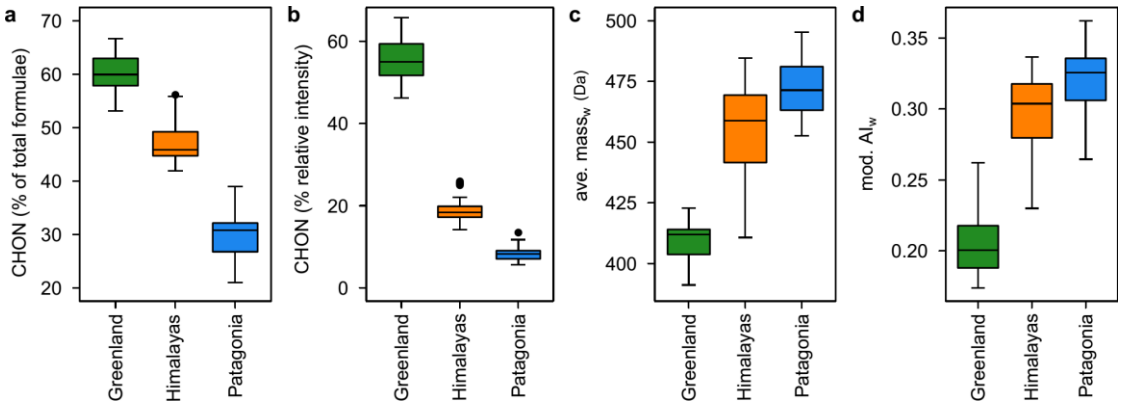

Figure 4.5. Boxplots comparing molecular DOM composition (FT-ICR MS) data from Greenland (green; Lawson *et al.*, 2014a), the Himalayas (orange; Hemingway *et al.*, 2019) and Chilean Patagonia (blue; this study). Plots show (a) number of N-containing formulae (CHON) expressed as a percentage of total formulae and (b) relative sample intensity, alongside intensity-weighted measures of (c) average molecular mass and (d) the modified aromaticity index.

4.5. Discussion

4.5.1. Setting BDOC rates in global context

The overall range of measured BDOC in Chilean Patagonia is lower than that observed in studies of glacial DOC (Figure 4.2b). Much of the pioneering work on glacial DOC bioavailability was conducted for Alaskan rivers which have a much higher mean average (± SD) BDOC of 43.4 ± 14.8% (Hood *et al.*, 2009; Fellman *et al.*, 2010) than Patagonian rivers at 15.2 ± 5.2%. The maximum BDOC observed in Chilean Patagonia (~23%) from the Cisnes catchment, which has minimal glacial cover (~1%), is in line the lowest BDOC in Alaskan non-glacial catchments — the Montana, Peterson and St. James rivers (Hood *et al.*, 2009; Fellman *et al.*, 2010). Other BDOC values from this study are lower than those from catchments elsewhere with corresponding low to intermediate glacier cover (<40%).

Although the DOC concentrations in Chilean Patagonian rivers are more in line with those in glacial systems (Hood *et al.*, 2009; Fellman *et al.*, 2010; Bhatia *et al.*, 2013; Lawson *et al.*, 2014; Spencer *et al.*, 2014), BDOC values are similar to those observed in temperate North American catchments (0–24%), from a relatively pristine and densely forested region (Coble *et al.*, 2019). For context, BDOC is typically higher (26–31%) in temperate catchments that are more heavily influenced by agriculture (Williams *et al.*, 2010; Cory and Kaplan, 2012). However, DOC concentrations in Chilean Patagonia (0.3–0.7 mg C L^{-1}) are one to two orders of magnitude lower than those in

the North American catchments (2–30 mg C L^{-1}) in which comparable BDOC rates would represent a higher absolute turnover of carbon (Coble *et al.*, 2019).

The lack of a clear systematic relationship between BDOC and catchment glacier cover in Chilean Patagonia (Figure 4.2b) suggests that residual glaciers do not exert a significant control over the bioavailability of riverine DOM. This is in stark contrast to the results of multiple studies, which have demonstrated a consistently positive association between BDOC and catchment glacier cover (Figure 4.2b). This applies in regions with a similarly low range of catchment glacier cover (<40%) to Chilean Patagonia. This positive relationship elsewhere has led to the hypothesis that accelerated glacier melting increases the supply of labile DOM to downstream ecosystems (Hood *et al.*, 2009; Singer *et al.*, 2012; Lawson *et al.*, 2014; Hemingway *et al.*, 2019). It also suggests the remarkable possibility that glaciers in disparate locations store and release similar types of organic matter, which are highly reactive and distinct from non-glacial material that dominates bulk DOM in freshwater systems (Hemingway *et al.*, 2019). The lack of any significant relationship between BDOC and selected key catchment properties (Table 4.1) in our dataset means that we cannot ascribe patterns in bioavailability to a single explanatory environmental variable.

We argue that prior degradation upstream of sampling sites in Chilean Patagonia is likely to be the most important control over BDOC and its relationship with glacial coverage. In support of this hypothesis, we note that BDOC values in Young Sound, northeast Greenland decline (from 39% to 8% BDOC) with distance from glacial sources and continue to do so even within the fjord freshwater lens (Paulsen *et al.*, 2017). This decline is illustrated by the direction of the arrow on Figure 4.2b. Such downstream reductions in BDOC are consistent with the consumption of reactive components and increased non-glacial inputs of more recalcitrant and aromatic compounds (Hood *et al.*, 2009; Paulsen *et al.*, 2017; Hemingway *et al.*, 2019). Whilst we did not sample DOM directly from glacial ice or outflows, the data presented in Chapter 3 suggest that Chilean Patagonian glaciers export protein-rich and aliphatic material, which is consistent with prevailing understanding of glacial DOM (Lafrenière and Sharp, 2006; Barker *et al.*, 2009; Hood *et al.*, 2009; Dubnick *et al.*, 2010; Stubbins *et al.*, 2012; Bhatia *et al.*, 2013; Fellman *et al.*, 2014; Lawson *et al.*, 2014a; Spencer *et al.*, 2014a; Hemingway *et al.*, 2019). Consequently, the extent to which glacial

influences on BDOC can be observed will be affected by the distance of sampling sites from glaciers. This is a limitation of the current study, where for practical reasons our sampling locations were either distant from upstream glacial sources or downstream of lakes with long residence times. Nevertheless, the samples collected reflect how glacial DOM is integrated with material from the wider catchment before export towards the marine environment, which has been the major focus of previous glacial BDOC studies (Hood *et al.*, 2009).

We consider other factors less likely to account for the lack of an observed relationship between BDOC and catchment glacier cover in Chilean Patagonia:

- The spot sampling strategy is vulnerable to random variabilities within individual river systems (Mann *et al.*, 2012; Spencer *et al.*, 2015; Coble *et al.*, 2019). This is an almost inevitable consequence of practical constraints and the relative inaccessibility of study regions, which affects all the above-mentioned studies, including this one. However, all studies have focused BDOC analyses in the peak melt season when the influence of glaciers on DOM composition will be strongest. Therefore, random variability is unlikely to explain the difference in BDOC values observed in Chilean Patagonia compared to other regions.

- The comparability of the studies presented in Figure 4.2b may be compromised by experimental differences, such as the use of different bacterial inocula. It is possible that marine bacteria may be more efficient than freshwater bacteria at degrading riverine DOM (Fellman *et al.*, 2010) and so studies utilising a marine inocula (Hood *et al.*, 2009) may exhibit higher levels of biodegradation than those using a freshwater inocula (Hemingway *et al.*, 2019). However, individual studies show broad internal consistency linking higher BDOC with glacier cover; inoculum composition may account for differences in BDOC between studies but not the overall relationship with glacier cover. Inter-regional cross-fertilization could be used to compare the efficiency of different inocula in a given sample.

4.5.2. Compositional insights into low BDOC

Intrinsic molecular properties have a major influence over DOM reactivity (Kellerman *et al.*, 2015, 2018; Mostovaya *et al.*, 2017) so the relatively low BDOC rates in Chilean Patagonia may be explained by inter-regional differences in DOM composition. Molecular indicators of bulk DOM from the broader study region in Chilean Patagonia suggest that, compared to other regions, it has low nitrogen content, high average mass and high aromaticity (Figure 4.5). These qualities are classically thought to hinder biological reactivity (Sun *et al.*, 1997; Hopkinson *et al.*, 1998; Fellman *et al.*, 2008). In this context, DOM which is relatively enriched in nitrogen, lower in mass and less aromatic may offer more favourable substrates to aquatic bacteria, so we would expect to see greater consumption of compounds with these relative properties. This is consistent with our data which suggest that bioavailability is linked to a relatively small component of the DOM pool associated with N-containing compounds (Figure 4.4) but not those moieties, like amino acids, that are typically considered labile (Coffin, 1989).

Placing these observations into a wider geochemical context, we note that glacial rivers are thought to supply organic and inorganic nitrogen to downstream ecosystems (Hood and Scott, 2008; Lawson *et al.*, 2014; Hawkings *et al.*, 2015; Wadham *et al.*, 2016). Indeed, the FT-ICR MS data for Leverett Glacier, Greenland, demonstrated how glacial meltwaters could provide an important seasonal supply of nitrogen to N-limited fjords in the form of N-enriched DOM (Lawson *et al.*, 2014). In contrast, dissolved inorganic nitrogen concentrations in Chilean Patagonian rivers are mostly below analytical detection (*pers. comm.*, J. Hawkings), consistent with oligotrophic conditions observed in freshwater systems in nearby Argentinian Patagonia (Garcia *et al.*, 2015b). This may reflect low rates of atmospheric nitrogen deposition across the region (Weathers and Likens, 1997; Galloway *et al.*, 2004). The higher nitrogen content of Himalayan DOM may be accounted for by high rates of atmospheric deposition (Galloway *et al.*, 2004; Li *et al.*, 2016), provided there is a mechanism for its incorporation into organic matter (Brookshire *et al.*, 2007). However, N-rich DOM in Greenland is more likely derived from microbial sources given that local rates of nitrogen deposition are low in global terms (Galloway *et al.*, 2004; Lawson *et al.*, 2014b).

Given the scarcity of nitrogen in Chilean Patagonian rivers, any dissolved nitrogen source may be a valuable resource for freshwater ecosystems. Moreover, microbial

communities may become specially adapted to local DOM compositions (Judd *et al.*, 2006; Hoostal and Bouzat, 2008; Smith *et al.*, 2018b; D'Andrilli *et al.*, 2019) and support a biological mechanism for the release of organic N (Brookshire *et al.*, 2005). The analysis presented here is compatible with a role for DOM in aquatic nitrogen cycling in both forested river catchments (Brookshire *et al.*, 2005; Fellman *et al.*, 2009) and estuarine settings (Kerner and Spitzy, 2001; Badr *et al.*, 2008; Knudsen-Leerbeck *et al.*, 2017).

The overall difference in DOM composition may be linked to the influence of upstream lakes. As noted in Chapter 3, lakes in Chilean Patagonia may act as important sinks for DOM. By contrast, this cannot be a significant influence on DOM in Greenland (Lawson *et al.*, 2014) and the Himalayas (Hemingway *et al.*, 2019), with which we compare our molecular data, since none of these study catchments contains any freshwater lake. We suggest that the presence of lakes creates greater opportunity for the removal of reactive DOM components, such as those containing nitrogen, leading to the export of less bioavailable DOM. Our incubation data offer some qualitative support for this from three sites where lakes have a relatively small influence (Huinay, Vodudahue, Cisnes). Whereas samples from these sites lost an additional 5–10% DOC between day 7 and day 28, other sites did not show any further decrease in DOC after the first week of incubation (Figure 4.2a). For example, DOC loss ceases after the first 3 days for samples from the Palena and Yelcho catchments, which have similar forest and glacial cover to the Huinay, Vodudahue and Cisnes catchments but contain lakes that are larger by 2–4 orders of magnitude (Table 4.1). A greater sample size is needed to test if this assertion is statistically valid but the overall picture suggests that low BDOC might be explained by compositional factors relating to prior processing in upstream lakes.

4.5.3. Character and origin of bioavailable DOM components

Here we consider the specific components of DOM that are consumed during our incubations, as inferred from fluorescence scans and molecular-level data for the broader region. We discuss how this sheds light on the overall bioavailability of DOM in Chilean Patagonia. The reduction in total fluorescence intensity for all incubations is consistent with net DOC consumption but the relative changes in fluorescence (%) are

greater than corresponding rate of DOC consumption and not correlated with changes in concentration (Table 4.1 and Table 4.2). This suggests the preferential consumption of optically active DOM, and especially protein-like fluorophores. Such compounds are known to comprise a very minor (<1%) but disproportionately reactive fraction of the total DOM pool in freshwater systems (Cory *et al.*, 2011; Cory and Kaplan, 2012).

Protein-like fluorophores (characterised by shorter emission wavelengths) underwent the greatest reduction in intensity, which is consistent with the prevailing view that such compounds are highly labile (Fellman *et al.*, 2010) even in humic-dominated systems (Wickland *et al.*, 2007; Fellman *et al.*, 2009). The limited changes in tyrosine-like (component C_{304}) fluorescence in some samples might be explained by simultaneous consumption and production processes. The largest reduction in intensity across all incubations is for component C_{354}, which is representative of tryptophan-like fluorescence, previously observed in a variety of aquatic environments including freshwater lakes (Osburn *et al.*, 2017), estuarine and marine waters (Wünsch *et al.*, 2015; Bittar *et al.*, 2016), sea ice and brines (Stedmon *et al.*, 2011; Granskog *et al.*, 2015) and municipal supplies (Murphy *et al.*, 2011) and attributed to bacterial activity (Determann *et al.*, 1998; Cammack *et al.*, 2004).

Our molecular level FT-ICR MS data for the wider region establishes that in Chilean Patagonia tryptophan-like (C_{354}) fluorescence is linked with a relatively small pool of low molecular weight compounds rich in N-containing polyphenolics. Although this molecular family includes some condensed aromatics and HUPs, its overall composition is more like the N-containing polyphenolics that are common to all rivers. This is illustrated by the mass distributions in Figure 4.4d, which also show a discrepancy between the C_{354} family and both total polyphenolics and bulk DOM. The statistical correlations between FT-ICR MS and PARAFAC data do not prove that any of the molecules identified contribute directly to C_{354} fluorescence or its apparent bioavailability. However, as observed in other studies (Herzsprung *et al.*, 2012; Stubbins *et al.*, 2014; Wagner *et al.*, 2015), fluorescence signatures provide insight into a broader and more diverse molecular pool that includes non-fluorescing DOM.

The link we establish between tryptophan and polyphenolic substances is consistent with their derivation from a common source, such as leachates from microbially

degraded vegetation (Maie *et al.*, 2007; Wickland *et al.*, 2007). There are three possible justifications for this link.

1. Although the C_{354} component in our samples is consistent with fluorescence signatures commonly ascribed to tryptophan, it may also derive (simultaneously) from phenolic groups in lignin or polyphenolic compounds (which are reflective of vegetation inputs). The overlap in fluorescence signals may be due to the structural similarity of amino acids in proteins and propyl-monomers in lignin phenols (Hernes *et al.*, 2009). However, polyphenolics have generally been found to quench tryptophan fluorescence elsewhere (Min *et al.*, 2004; Mishra *et al.*, 2005; Labieniec and Gabryelak, 2006).

2. Given the propensity for proteins to bind to phenolic and polyphenolic structures (Maie *et al.*, 2007; Aiken, 2014; Cuss and Guéguen, 2015), the C_{354} fluorescence signal may be related to tryptophan bound in such supramolecular assemblies. Other studies have connected such binding in humic-rich freshwaters with a red-shift in fluorescence (Aiken, 2014), which could explain our emission maximum of 354 nm that falls at the upper limit of wavelengths observed for tryptophan-like fluorescence. Binding might also reduce the accessibility of tryptophan to heterotrophic bacteria and thus limit overall bioavailability (Maie *et al.*, 2006; Cory and Kaplan, 2012; Bai *et al.*, 2017). Indeed, this has been cited elsewhere to account for a greater recalcitrance in bound tryptophan than in other free proteins, such as tyrosine (Cory and Kaplan, 2012). Nevertheless, in our Chilean Patagonian samples bound tryptophan may still be the most viable carbon source in the absence of more reactive substrates. We note that in other humic-rich systems, such as Alaskan soil porewaters, bioavailability has been linked to tryptophan fluorescence (Fellman *et al.*, 2008). Therefore, the bioavailability of tryptophan in Chilean Patagonian rivers may be influenced by a dominant supply of DOM from vegetation sources.

3. The broader pool of N-rich polyphenolic compounds associated with C_{354} fluorescence may act as bioavailable substrates. Elsewhere, polyphenolics are negatively associated with BDOC (Hemingway *et al.*, 2019) and labile material is thought to be rich in aliphatics, peptides and proteins (Dubnick *et al.*, 2010; Singer *et al.*, 2012; Lawson *et al.*, 2014a; Musilova *et al.*, 2017). However, recent evidence

shows that compound reactivity is not linearly related to aromaticity and so plant-derived polyphenolics may be a viable substrate for heterotrophic respiration in aquatic ecosystems (Mostovaya *et al.*, 2017). In environments where aliphatic compounds are quickly depleted, such as humic freshwater lakes (Kellerman *et al.*, 2015), there is greater opportunity for polyphenolics to provide an important source of BDOC. Moreover, ongoing degradation processes (e.g. photochemical) might break down larger polyphenolic structures and thereby enhance their reactivity (Sulzberger and Durisch-Kaiser, 2009). The breakdown of supramolecular assemblies is thought to explain the enhanced reactivity of polyphenolics following the treatment of natural lake DOM with UV radiation (Mostovaya *et al.*, 2017). However, direct testing is needed to assess the susceptibility of DOM in Chilean Patagonian rivers to photochemical breakdown and its impact on bioavailability. In addition, the bioavailability of phenolic and polyphenolic groups may be facilitated by the adaptation of microbial communities to local DOM compositions, e.g. by resisting the suppression of enzyme production imposed by some polyphenolic substances (Hoostal and Bouzat, 2008).

On balance, our findings are consistent with a common source for bacterial tryptophan and plant-derived polyphenolics in decaying leaf litter (Maie *et al.*, 2007). This supports the link we established in Chapter 3 between broadleaf evergreen forest (BEF) cover and a greater dominance of nitrogen-containing polyphenolics in riverine DOM. This is also consistent with the findings of previous studies which show that leaf decay in forests across central and southern Chile is an important regional source of dissolved organic nitrogen (Perakis and Hedin, 2002; Pérez *et al.*, 2003). Figure 4.6 shows the compound category classifications of 128 formulae that are positively correlated with both C_{354} fluorescence and BEF cover across the broader region. These formulae overall comprise a low proportion of relative intensity in FT-ICR MS spectra (1.90 ± 0.21% in the 7 incubation sample rivers and 1.72 ± 0.28% across the 28 rivers from the broader study region). We also show in Chapter 3 that these types of compounds are negatively associated with catchment glacier cover, which is consistent with the idea that vegetation cover exerts a stronger control over the composition of riverine DOM where glacial influences are reduced (Hood and Scott, 2008; Hood and Berner, 2009; Fellman *et al.*, 2010a). It is not, however, possible to determine from our data whether DOM bioavailability is limited to tryptophan (which may be free or bound in supramolecular

assemblies) or a combination of protein and polyphenolic substrates. Moreover, these interpretations do not preclude contributions of tryptophan from alternative microbial sources (e.g. glaciers), which may interact with a broader pool of plant-derived DOM.

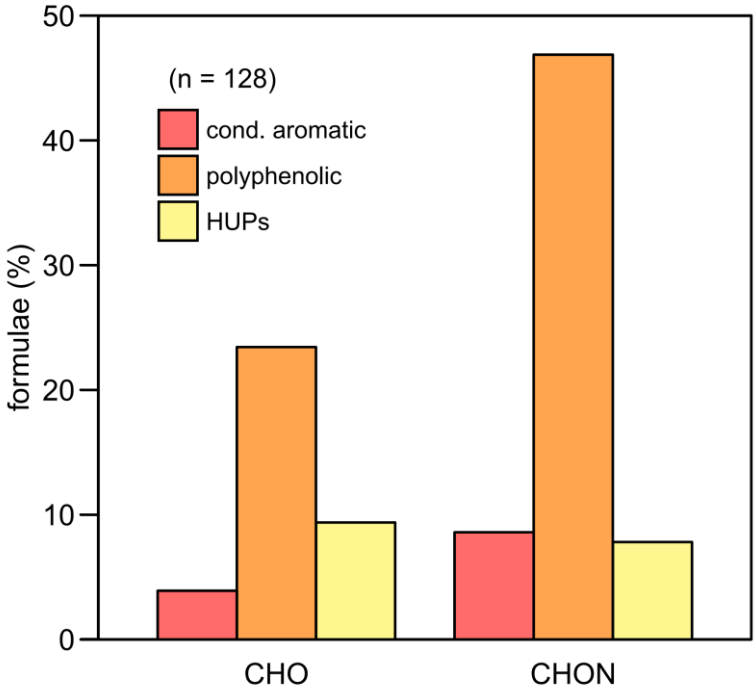

Figure 4.6. Compound and class (CHO, CHON) composition of molecular formulae shared between C_{354} and broadleaf evergreen forest families. Molecular families defined as those formulae with variations in relative intensity that are significantly and positively correlated with the respective variables (i.e. the relative fluorescence loading of C_{354} fluorophore and the percentage of the catchment covered by broadleaf evergreen forest).

4.5.4. Insights into carbon cycling processes in Chilean Patagonia

The potential role of vegetation in controlling the bioavailability of DOM in our incubations may be relevant for other catchments in Chilean Patagonia undergoing deglaciation (Jacob *et al.*, 2012; Willis *et al.*, 2012a, 2012b; Gardner *et al.*, 2013; Carrivick *et al.*, 2016). Our evidence is consistent with the presence of bioavailable tryptophan derived from the bacterial decay of vegetation (Maie *et al.*, 2007), and specifically material from broadleaf evergreen forest. Moreover, such decay may also release phenolic and polyphenolic compounds that either could bind to and control the accessibility of tryptophan to bacteria (Maie *et al.*, 2007; Aiken, 2014; Cuss and Guéguen, 2015), or might provide a viable substrate for direct consumption (Mostovaya *et al.*, 2017). As the influence of glaciers in Chilean Patagonia declines, the relative

influence of catchment vegetation cover on riverine DOM will increase, even if forest expansion is limited by climatic factors (Abarzúa *et al.*, 2004; Garreaud *et al.*, 2013; Garreaud, 2018; Aguayo *et al.*, 2019). Low levels of forest cover in highly glaciated catchments, which may currently provide a key source of polyphenolics, could become relatively more important as glaciers retreat.

Since our incubation waters were sampled from a region with relatively low glacier cover, it is not surprising that we have detected a possible link between DOM bioavailability and vegetation controls, which may override any influence from glacial sources. In Chilean Patagonia, glacier retreat is driving to the production and expansion of freshwater lakes (Loriaux and Casassa, 2013; Wilson *et al.*, 2018), which act as important sites for organic carbon cycling (Tranvik *et al.*, 2009; Evans *et al.*, 2017), controlling organic carbon fluxes downstream. If indeed, lakes provide significant sinks for organic carbon (Chapter 3), then any highly labile material in glacial meltwaters may be preferentially consumed within lakes upstream of sampling sites and before it can be exported to the marine environment. The aliphatic molecular signatures associated with glacier cover reported in Chapter 3, may reflect a comparatively recalcitrant fraction of the aliphatic pool which has escaped processing within rivers and lakes. In order to test whether the bioavailability of glacial DOM in Chilean Patagonia is more in line with that from other glaciated regions, we would need to sample meltwaters directly from glaciers before entering lakes. At our sampling sites, decaying vegetation may be the most significant factor in controlling DOM bioavailability, overriding other upstream controls (e.g. glaciers).

4.6. Conclusions

We have shown through incubation experiments that riverine DOM from catchments with limited glacier cover (0–33%) in northern Chilean Patagonia is proportionately less bioavailable (BDOC 7–23%) than DOM sampled from rivers in glaciated regions of the northern hemisphere (BDOC 31–69%). Moreover, BDOC does not increase with catchment glacier cover in Chilean Patagonia, contrasting with the results of previous studies in other regions which have observed such a relationship across catchments with similar glacier cover. It is possible that this lack of relationship and overall low BDOC in Chilean Patagonia reflects compositional constraints on DOM bioavailability,

specifically relating to its low nitrogen content, higher average mass and higher aromaticity than DOM from other regions. These compositional traits might reflect prior removal of the most labile components of DOM upstream of our sampling sites. Such prior processing may be facilitated by the presence of lakes, which act as carbon sinks and will have an increasing influence on riverine DOM as they grow in number and size. We observed consistent patterns of fluorescence change over each incubation which suggested that DOM bioavailability in all study rivers was linked to tryptophan-like material. In turn, tryptophan-like fluorescence was statistically associated with a significant proportion of the N-containing polyphenolic formulae found in all rivers across the broader region. This association may be explained by a common source, such as the bacterial decay of vegetation, which may be closely related to the dominant broadleaf evergreen forest cover. These potential influences of vegetation on DOM bioavailability will be stronger in the more densely forested catchments of northern Chilean Patagonia (42–45°S) but may become increasingly important downstream of glaciers, especially as glaciers retreat in the long term, in catchments further south. The extent to which N-containing polyphenolics provide viable substrates to aquatic bacteria or potentially bind to tryptophan and constrain overall bioavailability is uncertain and necessitates further investigation.

5. Organic matter composition in a Patagonian fjord linked to changing glacier melt inputs

This chapter provides the first molecular-level analysis of DOM in a glaciated fjord. Seasonal variations in fjord DOM composition are analysed within the context of different extents of glacial meltwater influence and related changes in fjord hydrographic structure. The annual balance between riverine inputs of organic matter and primary production is also quantified. The seasonal patterns identified are used to infer the likely impact of increased glacier melting on DOM composition and biogeochemical cycling in the fjord.

This chapter forms the basis of a manuscript in preparation for submission to *Frontiers in Marine Science* under the following reference:

Marshall, M., Kellerman, A., Wadham, J., Hawkings, J., Pryer, H., Beaton, A., Spencer, R. (in prep.) Organic matter composition in a Patagonian fjord linked to changing glacier melt inputs. *Frontiers in Marine Science.*

Author contributions

I conceived the study in collaboration with A. Kellerman and J. Wadham. I collected samples from terrestrial field sites, conducted all laboratory and data analysis, prepared all figures and wrote the text. A. Kellerman also assisted in sample collection and the analysis of samples by FT-ICR MS. J. Hawkings, H. Pryer and A. Beaton helped collect fjord samples. H. Pryer also assisted in the collation and interpretation of river discharge records. R. Spencer provided additional lab support. A. Kellerman and J. Wadham provided comments on analytical methods and reviews of the text.

5.1. Abstract

Biogeochemical processes in glaciated fjords are sensitive to changes in glacier melt inputs and surrounding ice cover. Glacial meltwater is often rich in highly labile dissolved organic matter (DOM) which is hypothesised to stimulate heterotrophic activity of marine bacteria, but it is not clear how far this contributes to DOM composition and cycling in downstream fjords. To date, DOM dynamics in glaciated fjords have been assessed using a range of geochemical and microbiological techniques in a small number of northern hemisphere locations, but no study has employed the in-depth molecular techniques that have been applied in estuarine systems. Here we present the first dataset of its kind both for a glaciated fjord and for the Chilean Patagonian region. We combine dissolved organic carbon (DOC) concentration data, together with spectrofluorescence and ultrahigh resolution mass spectrometry to characterise seasonal variations in DOM composition in the Baker-Martinez Fjord (~48°S) and relate these to different states of glacial meltwater input. We quantify the fluxes of organic matter from four major glacially fed rivers entering the fjord and show that DOM drives most (68–98%) organic matter export, in contrast to other world glaciated regions where particulate organic matter (POM) is the larger component of export (up to 90%). Riverine DOM may comprise up to 57% of the total organic carbon pool in the fjord and exert a strong control over biogeochemical processes. The overall patterns in fjord surface DOM composition are consistent with typical estuarine systems, showing the preferential removal of terrestrially sourced aromatic and humic material and the addition of unsaturated and heteroatom-rich marine DOM. The effects of strong glacial meltwater discharge in summer include direct inputs of protein-like fluorescence, weaker autochthonous DOM production and weaker conservative vertical mixing which dampens marine DOM signatures in the surface layer. We highlight a difficulty in tracing glacier melt inputs via protein-like fluorescence due to other possible sources within the fjord. We also suggest that the shifting seasonal balance between marine and riverine peptide supplies may regulate organic nitrogen cycling in the fjord. The findings here highlight biogeochemical sensitivities in coastal waters relating to increasing glacier melt inputs which may have relevance for other glaciated fjords.

5.2. Introduction

Dissolved organic matter (DOM) plays a key role in the biogeochemical cycling of carbon and other nutrients in coastal waters (Bauer and Bianchi, 2012). Inputs to these waters include primary production and fluxes of terrestrial material by rivers, overland flow and groundwaters (Bauer and Bianchi, 2012). Atmospheric deposition can also play a minor role (Liu *et al.*, 2005). Removal processes include flocculation (Sholkovitz, 1976; Eisma, 1986), adsorption to sediments (Keil *et al.*, 1994; Aufdenkampe *et al.*, 2001), biological processing and photodegradation (Hernes and Benner, 2003; Spencer *et al.*, 2009; Benner and Kaiser, 2011; Seidel *et al.*, 2017). The combined effects of these processes are difficult to disentangle and most attempts draw upon known differences in terrestrial and marine DOM (Bauer and Bianchi, 2012). This is complicated by uncertainties in end-member compositions and the particular sensitivity of rivers to environmental change (Asmala *et al.*, 2016). Furthermore, changes to the upstream landscape which affect riverine DOM composition also impact upon biogeochemical cycling in coastal waters (Osterholz *et al.*, 2016).

In regions where climate change is driving reductions in glacier cover, downstream marine waters may be sensitive to changes in the supply of reactive DOM linked to meltwater inputs (Zhuang and Yang, 2018). This hypothesis has developed from land-based investigations which suggest that DOM from glaciers is highly bioavailable and easily respired by marine heterotrophs (Hood *et al.*, 2009; Fellman *et al.*, 2010a; Singer *et al.*, 2012; Lawson *et al.*, 2014a). The relative lability of these inputs is thought to decline as glacial sources retreat further inland and are superseded by less labile terrestrial inputs (Paulsen *et al.*, 2017; Hemingway *et al.*, 2019). Additional observations in a Greenland fjord further imply that the competitive advantage of glacier-sourced bacteria in colder waters favours their continued processing of terrestrial DOM in surface coastal waters (Paulsen *et al.*, 2017, 2018). The degree to which glacial DOM is assimilated into new biomass is not well known but data from a high Arctic fjord suggest that marine microbes preferentially assimilate marine DOM over glacial sources (Holding *et al.*, 2017). However, the formation of new DOM (autochthonous supplies) in fjords with marine terminating glaciers may also be negatively impacted by glacier retreat (Hopwood *et al.*, 2018). As glaciers retreat onto land, submarine meltwater discharge is redirected to the surface, which simultaneously shuts down nutrient-rich upwellings from deeper fjord waters (Meire *et al.*, 2017;

Hopwood *et al.*, 2018) and increases turbidity in the surface layer (Aracena *et al.*, 2011; Landaeta *et al.*, 2012), which together limit primary productivity. This may offset any potential benefits of nutrient subsidies delivered by enhanced meltwater fluxes in nearshore areas (Hawkings *et al.*, 2014, 2015, 2016, 2018; Lawson *et al.*, 2014b; Wadham *et al.*, 2016). Therefore, in-washed DOM (allochthonous supplies) may comprise an increasingly important component of the organic matter pool as in situ primary production becomes limited.

The role of fjords as an important global sink for terrestrial carbon is well established (Smith *et al.*, 2015; Cui *et al.*, 2017). Numerous studies have quantified the contributions from autochthonous production via stable isotope signals and molecular biomarkers in sediments (Silva *et al.*, 2011; Kuliński *et al.*, 2014; Kumar *et al.*, 2016; Rebolledo *et al.*, 2019). The impact of glacier discharge on phytoplankton blooms and the burial of autochthonous particulate organic matter (POM) has attracted some attention (Calleja *et al.*, 2017) but influences over DOM dynamics and biogeochemical cycling within fjords are not well constrained. Spectrofluorescence and microbiological techniques have been applied in a Greenland fjord to understand how glacial and riverine DOM is processed in surface waters (Paulsen *et al.*, 2017, 2018). However, focused molecular-level investigations that have been applied in temperate estuaries (Osterholz *et al.*, 2016; Seidel *et al.*, 2017) are so far lacking for glacially-influenced fjords. Addressing this gap will help to improve understanding of how glacier meltwaters impact organic matter composition in coastal waters, with implications for biogeochemical cycling and productivity in these sensitive ecosystems.

Chilean Patagonia contains an extensive network of glacially carved fjords (Pantoja *et al.*, 2011) and is undergoing significant landscape change as a result of rapid retreat of its two major icefields (Glasser *et al.*, 2011; Willis *et al.*, 2012a, 2012b; Jaber, 2016; Foresta *et al.*, 2018). Primary productivity in central Patagonian fjords (48–51°S) is light-limited in summer due to significant inputs of turbid glacial meltwaters (Aracena *et al.*, 2011). This leads to terrestrial material dominating (up to 100%) organic matter burial in sediments (Rebolledo *et al.*, 2019). Most carbon burial studies distinguish marine and terrestrial signatures using the composition of POM, but it is unclear how far the assimilation of riverine and glacial DOM contributes to these signatures in fjord biomass (Meerhoff *et al.*, 2019) and bulk sediments (Rebolledo *et al.*, 2019). This is

despite evidence of relatively constant rates of secondary bacterial production across these fjords (González *et al.*, 2013), which suggests that the microbial food web may be a more important driver of carbon cycling at the heads of the fjords where primary productivity is suppressed in turbid river plumes. Moreover, increased glacier melt inputs in summer may support a zooplankton community structure which selectively consumes terrestrial POM (Meerhoff *et al.*, 2014) and a bacterial community which is dominated by glacial biota (Gutiérrez *et al.*, 2015; Paulsen *et al.*, 2018). This highlights the potential for labile riverine and glacial DOM to also shape fjord food webs, especially under high river discharge conditions. The importance of the microbial loop to ecosystem function and carbon cycling therefore warrants a better understanding of DOM composition in Patagonian fjords and its sensitivity to changing glacier melt inputs.

Here we present the first dataset of its kind on DOM composition for both a glaciated fjord and the Baker-Martinez Fjord (BMF) in Chilean Patagonia. Data include DOM concentration and composition as determined from spectrofluorescence scans and ultrahigh resolution mass spectrometry for the summer and winter seasons in a single year. We examine the broad seasonal shift in DOM composition across the fjord within the context of changing glacier melt inputs and relate trends to changes in sources and possible processes within the fjord. The specific aims of this study are to:

1. Quantify the relative importance of DOM and POM fluxes in the tributary rivers of the BMF.
2. Assess the impact of glacier melt inputs on fjord DOM composition by comparing summer (high discharge) and winter (low discharge) conditions.
3. Examine variations in DOM along the salinity gradient to elucidate environmental controls over molecular composition and infer the impact on biogeochemical processes.

5.3. Methods

5.3.1. Study region

The BMF is situated between the Northern and Southern Patagonian Icefields (NPI, SPI) at ~48°S (Figure 5.1). It consists of two largely disconnected sub-basins lying along west-east axes; the northerly Martinez Channel is typically <500 m deep whereas the southerly Baker Channel reaches maximum depths >1000 m in the central fjord (Rebolledo *et al.,* 2019). Tides are semidiurnal (Ross *et al.,* 2014) and circulation is largely driven by the prevailing winds (Aiken, 2012), including subsurface warm water intrusions into Jorge Montt Fjord over a shallow sill (~45 m deep) at its junction with Baker Channel (Moffat, 2014). The hydrographic structure of the BMF is typical of fjords with a thin surface lens of freshwater overlying marine water (Bustamante, 2009; Ross *et al.,* 2014, 2015). High annual precipitation rates peak during the austral winter (May–August) but maximum freshwater input occurs during the austral summer (December–March) when glacier melt drives up river levels (Rebolledo *et al.,* 2019). Seasonal melting of the NPI and SPI dominates the regimes of the Baker and Pascua rivers, respectively (Dirección General de Aguas, 2019; Rebolledo *et al.*, 2019). Meltwater fluxes from Steffen Glacier (via the Huemules River) and Jorge Montt Glacier are not well quantified but sensitivity to warming air and ocean temperatures, respectively, will make these increasingly important freshwater sources to the fjord in future (Rivera *et al.*, 2012; Willis *et al.*, 2012b, 2012a; Aniya, 2017; Dussaillant *et al.*, 2018; Moffat *et al.*, 2018). Discharge from the Bravo River at the head of Mitchell Fjord is influenced by glacier melt to a lesser degree. The locations of all fjord and terrestrial sampling locations are shown in Figure 5.1.

5.3.2. Sampling

Fjord water samples were collected during the austral summer (16–23 Feb) and winter (4–9 Jul) of 2017. A Seabird SBE model 25 CTD instrument was deployed from the *RV Sur Austral* to obtain vertical profiles in temperature, salinity, turbidity and chlorophyll fluorescence at each station. Water was sampled from selected depths in rosette-mounted Niskin bottles. Where possible the same stations were revisited in winter to capture seasonal differences. Key exceptions are the stations in Jorge Montt Fjord, where floating ice restricted accessibility in winter, and an additional station sampled

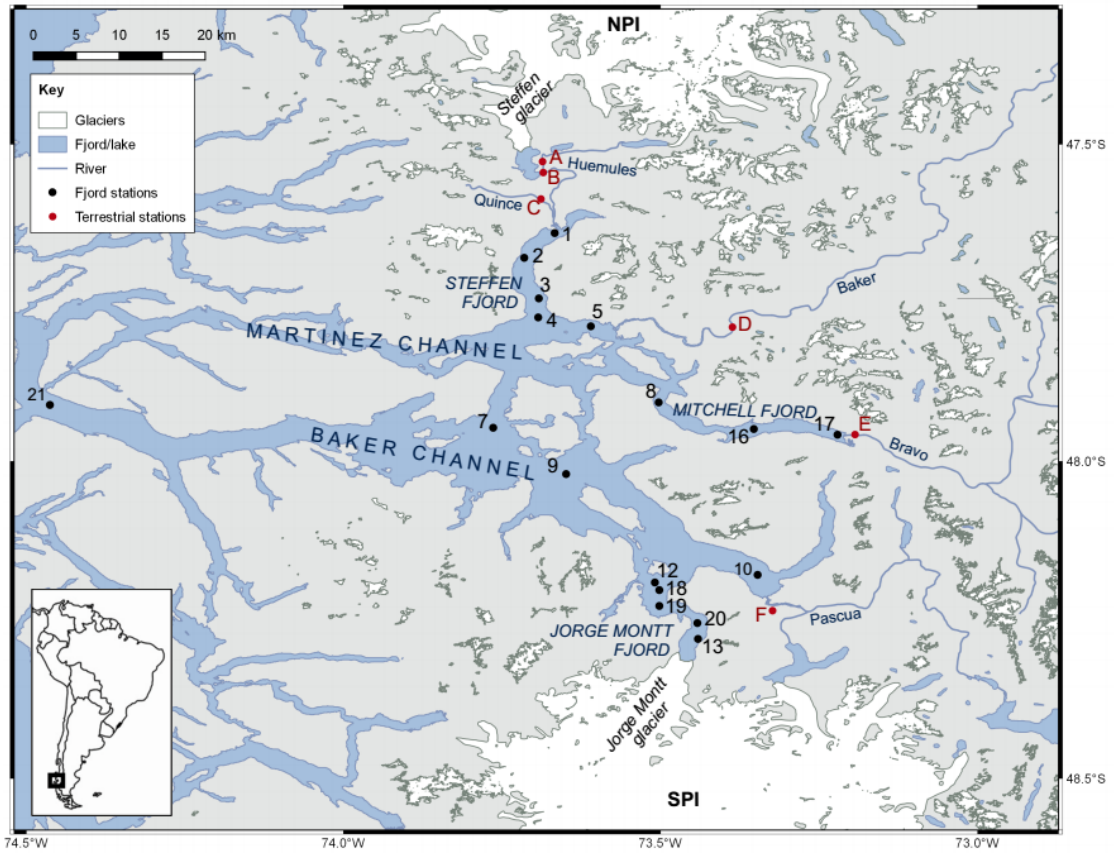

Figure 5.1. Geography of Baker-Martinez Fjord and location of sampling stations in the fjord (1–21) and on the tributary rivers (A–F).

near the mouth of the Baker Channel (S21) in winter. Regular surface sampling with a Teflon diaphragm underway pumping system during passage between the stations captured a better spatial coverage of variations in freshwater layer composition.

River samples from the Steffen and Baker (in summer) valleys were collected during complementary terrestrial campaigns. Samples from the Bravo, Pascua and Baker (in winter) rivers were collected from a RIB boat during the fjord surveys. Although the Baker, Bravo and Pascua rivers were sampled only once per season, collectively these samples establish the range of conditions in riverine DOM inputs. The composition of rivers in the Steffen valley (Huemules and Quince) are well constrained due to extended monitoring over the study periods.

5.3.3. Analytical methods

5.3.3.1. Dissolved organic carbon (DOC) and nutrient concentrations

Samples for DOC measurement were filtered to 0.45 µm using either PES membranes (fjord samples) or Whatman® Puradisc AQUA syringe filters (river samples) and stored frozen prior to analysis. DOC concentrations were determined on a Shimadzu TOC-L_{CHN} analyser equipped with halogen scrubber to process saline samples. Using the approach of Armbruster and Pry (2008), limits of detection (LoD) and quantitation (LoQ) were calculated as 2.7 µM and 3.7 µM, respectively. Repeat measurement of a 40 µM standard varied by < ±5%.

Samples for dissolved nutrient analysis were filtered using Whatman® GD/XP PES syringe filters (0.45 µm) and stored frozen. Nutrient concentrations were measured on a LaChat QuikChem® 8500 series 2 flow injection analyser using established colorimetric methods. Dissolved organic nitrogen (DON) concentrations were taken as the difference between total nitrogen (TN), measured following an alkaline persulphate/ UV digestion at 100°C to convert all organic nitrogen to nitrate, and the sum of inorganic nitrogen forms ($NH_4^+ + NO_3^- + NO_2^-$) measured prior to digestion. LoDs are reported as 0.10 µM, 0.07 µM and 0.03 µM for DON, NO_3 and soluble reactive phosphorus (SRP), respectively, with a precision < ±5%.

5.3.3.2. Spectrofluorescence

Samples for spectrofluorescence analysis were obtained in the same way as for DOC measurement. Excitation-emission matrices (EEMs) were collected on an Agilent Cary Eclipse Fluorescence Spectrophotometer with xenon flash bulb. Scans were conducted through 10 mm quartz cuvettes over excitation wavelengths 240–450 nm at 5 nm intervals and emission wavelengths 300–600 nm at 2 nm intervals, using 5 nm monochromator slit widths and 0.1 second integrations. All EEMs were corrected for instrumental biases and Raman/Rayleigh scatter prior to subsequent analysis (Stedmon and Bro, 2008; Murphy *et al.*, 2013).

5.3.3.3. Ultrahigh resolution mass spectrometry

Large volume samples (1 L) were filtered through either PES filters (0.45 µm; fjord samples) or pre-combusted (450°C, 5 hours) GF/Fs (0.7 µm; all Steffen and summer

Baker river samples) into clean polycarbonate bottles and acidified to pH ~2 with HCl. Filtered samples underwent solid phase extraction (SPE) through 200 mg Varian Bond Elut PPL cartridges following established procedures (Dittmar *et al.*, 2008). Based on DOC measurements for each sample and an extraction efficiency of 40%, the SPE-DOM was reconstituted in methanol to obtain a target concentration of ~40 µg C ml^{-1} to ensure analytical consistency and allow reliable comparisons between samples.

Analyses were conducted on a 21 Tesla Fourier transform ion cyclotron resonance mass spectrometer (FT-ICR MS) at the National High Magnetic Field Laboratory (NHMFL), Tallahassee, FL, USA (Smith *et al.*, 2018a). Samples were introduced via electro-spray ionization (2.6–3.2 kV) at a rate of 600 nl min^{-1} and analysed in negative ion mode. Mass spectra for each sample were derived from 100 coadded scans and calibrated against known *m/z* values using Predator software (NHMFL). Formulae assignments within the stoichiometric combination ranges of $C_{1–45}H_{1–92}N_{0–4}O_{1–25}S_{0–2}$ were applied to all peaks that were 6 times greater than the RMSE of the baseline signal and with mass calibration errors <500 ppb (PetroOrg software, Florida State University). Each formula was allocated to a specific compound category based on elemental ratios and modified aromaticity index values (AI_{mod}; Koch and Dittmar, 2006). We used the compound classification scheme of Kellerman *et al.* (2018): condensed aromatics (CA; $AI_{mod} > 0.66$); polyphenolics (PP; $0.66 \geq AI_{mod} > 0.5$); highly unsaturated and phenolic (HUP; $AI_{mod} \leq 0.5$; $H/C < 1.5$); aliphatic ($2 \geq H/C \geq 1.5$; $N = 0$); peptide-like ($2 \geq H/C \geq 1.5$; $N > 0$) and sugar-like ($H/C > 1.5$; $O/C > 0.9$). Further subdivisions include low and high O/C ratios (<0.5 or >0.5) for CAs, PPs, HUPs and aliphatics, and sugars with and without heteroatoms (N or S).

5.3.3.4. Particulate organic carbon concentrations

Particulate organic carbon (POC) concentrations were measured for the four main tributary rivers in order to calculate fluxes. Particulates from large volume samples (1–3 L) were retained on pre-combusted GF/Fs (450°C, 5 hours). Filters and sediments were subsampled and analysed directly through high temperature (1000°C) catalytic combustion on a Thermo Electron Flash Elemental Analyser 1110. Organic carbon (OC) content was determined following removal of inorganic carbonates by acidification (Hedges and Stern, 1984). Acidification was deemed effective as OC was

lower than the total carbon (TC) content of the unmodified sample in all cases. All samples were corrected for the mass and carbon content of the filter material, assessed as 0.03 ± 0.01% for TC and 0.02 ± 0.01% for OC (n=10). The % OC content was converted to POC concentrations by multiplication with suspended sediment concentrations (SSCs), which were measured separately as the mass of dry sediment retained on pre-weighed filters from a known volume of water (~300 ml).

5.3.4. Flux calculations

We estimate the magnitudes of dissolved and particulate organic carbon fluxes from the four principal rivers using Equation 5.1 and Equation 5.2. Annual discharge for the Baker and Pascua rivers is well constrained by long-term records from the Chilean Water Authority (Dirección General de Aguas, 2019). We also make use of the first ever discharge data for the Huemules River, derived from a stage-discharge rating curve (r^2=0.97; RMSE < ± 9%) based on pressure sensor readings from a stable bedrock position within the river and 14 separate Rhodamine B dye injection traces over the austral summer and winter in 2017. This method has been successfully deployed at Leverett Glacier, Greenland (Bartholomew *et al.*, 2011). Only one estimate of the average annual discharge of the Bravo River was available (Aracena *et al.*, 2011). However, calculations based on averaged conditions are useful in establishing order of magnitude differences in the fluxes from each river and the relative importance of dissolved and particulate organic phases.

Equation 5.1. DOC flux calculation

DOC flux	=	Cumulative annual discharge	x	Mean DOC concentration	x	10^{-9}
Mg a^{-1}		*m^3 a^{-1}*		*mg m^{-3}*		*unit conversion*

Equation 5.2. POC flux calculation

POC flux	=	Cumulative annual discharge	x	Mean SSC	x	OC content	x	10^{-6}
Mg a^{-1}		*m^3 a^{-1}*		*g m^{-3}*		*(%)*		*unit conversion*

5.3.5. Statistical tests

Parallel factor (PARAFAC) analysis was deployed using the drEEM Toolbox for MATLAB (Murphy *et al.*, 2013) and identified seven separate components of DOM fluorescence from intensity variations across EEMs from the BMF (n=129), its tributary

rivers (n=102) and additional freshwater and marine samples (n=176) from the broader region (42–48°S). These extra samples were included to better characterise regional DOM fluxes and help constrain the model. The model was validated by split-half methods and all component spectra had been identified previously in models held on the OpenFluor database (Murphy *et al.*, 2014a).

All other statistical tests were performed in R (R Core Team, 2015) with multivariate tools deployed from the vegan package (Oksanen *et al.*, 2016). The significance of seasonal differences in fjord water column structure and geochemistry is assessed using non-parametric Mann Whitney tests, which are appropriate for non-normally distributed data and unpaired observations (some data are unpaired due to differences in sampling stations between seasons).

Relationships between environmental variables and the intensities of individual molecular formulae are assessed using Spearman rank correlations. A false discovery rate correction (Benjamini and Hochberg, 1995) was applied to all *p*-values to minimise the number of Type I (false positive) errors arising from the large number of correlations for ~18,000 individual formulae. Raw *p*-values <0.028 were deemed significant at the 95% confidence interval.

Principal Components Analysis (PCA) was applied to a dataset of DOM composition, comprising FT-ICR MS compound category relative intensities and PARAFAC fluorescence loadings for each fjord sample. To reduce the influence of many very low intensity formulae common to all samples (i.e. HUPs) and without removing any data, total intensities for each compound category were first normalised by the number of formulae. All variables were then standardised between 0–1 using the *decostand* function (Oksanen *et al.*, 2016). We fitted environmental variables to the ordination results by permutation (n=999) using the *envfit* function (Oksanen *et al.*, 2016).

Details of additional statistical tests are included in the Results and Discussion sections.

5.4. Results

5.4.1. River fluxes into the Baker-Martinez Fjord

Annual freshwater, DOC and POC flux estimates for the four principal rivers entering the BMF are summarised in Table 5.1. The largest fluxes in DOC, suspended sediments and POC are from the Baker River which provides the biggest single input of freshwater, ~50% of the annual total from rivers. The Pascua provides a further ~40% of the annual total freshwater flux, with contributions from the Huemules and Bravo making up the remainder in similar proportions (~5% each). Total OC fluxes are largely driven by discharge, with the Baker and Pascua supplying >75% of all terrestrial OC to the fjord. The Bravo River has a disproportionately high DOC flux (due to high concentrations), which on an annual basis is comparable to that of the much larger Pascua River. Low OC content (<0.4%) in sediments leads to small POC fluxes despite high SSCs in the Baker, Pascua and Huemules Rivers and, overall, dissolved phases dominate terrestrial OC fluxes (68–98%). As a discharge-weighted average, DOC comprises 81% of the annual flux of organic matter from the four rivers.

5.4.2. Fjord water column

The physical properties of the water column display marked seasonality (Table 5.2). Mann Whitney tests show that the freshwater lens is significantly deeper (p=0.006), less saline (p<0.001) and more turbid (p=0.011) in summer, reflecting increased glacier melt inputs. Surface temperatures are higher in summer (p=0.003) despite strong meltwater inputs, except at the head of Steffen Fjord (S1, S2) where there is warming in winter. This sub-fjord also sees the largest rise in salinity in winter, suggesting that circulation patterns here may differ from those downstream of the other rivers. Chlorophyll concentrations are higher across the fjord in winter (p=0.006).

5.4.3. Dissolved organic matter and nutrients in the fjord

DOC concentrations are highly variable in the fjord surface layer (~20–200 µM) and seasonal differences (summer = 85.7 ± 41.1 µM; winter = 72.1 ± 33.1 µM; mean ± SD) are not statistically significant (Figure 5.2a). Subsurface DOC is less variable across the fjord in both seasons (summer = 53.3 ± 8.8 µM; winter = 41.7 ± 4.3 µM).

Table 5.1. Annual fluxes of dissolved and particulate organic carbon into Baker-Martinez Fjord from its four main tributary rivers. Concentrations are expressed in units of mass per litre rather than molar units (used elsewhere) as is more appropriate for flux calculations.

	Baker	Pascua	Huemules	Bravo
Catchment properties				
Total area (km^2)	29,107	15,079	671	1,062
Glacial cover (%)	8	19	71	15
Forest cover (%)	20	12	4	23
Wetland cover excl. lakes (%)	4	4	4	4
Total lake volume ($x10^6$ m^3)	754,002	79,782	1,355	67
Lake residence time (vol. weighted; days)	51,627	4,879	130	292
Discharge				
Mean annual (m^3 s^{-1})	932	714	121	112
Mean summer (m^3 s^{-1})	1,268	835	218	-
Mean winter (m^3 s^{-1})	754	617	51	-
Cumulative annual (km^3 a^{-1})	29.4	22.5	3.8	3.5
Specific annual discharge (m a^{-1})	1.01	1.49	5.66	3.30
DOC				
Mean concentration (mg C L^{-1})	0.644	0.364	0.171	2.258
Summer conc. (mg C L^{-1})	0.644	0.454	0.153	2.518
Winter conc. (mg C L^{-1})	0.643	0.273	0.236	1.997
Annual flux (Mg C a^{-1})	18,920	8,201	653	7,975
Suspended sediments				
Mean concentration (mg L^{-1})	60.2	35.7	87.5	18.1
Annual flux (Gg a^{-1})	1,769	804	334	64
POC				
Sediment OC content (%)	0.19	0.38	0.09	0.25
Mean concentration (mg C L^{-1})	0.114	0.136	0.079	0.045
Annual flux (Mg C a^{-1})	3,360	3,056	301	160
TOTAL OC flux (Mg C a^{-1})	22,280	11,257	954	8,135
DOC (%)	85	73	68	98
POC (%)	15	27	32	2
Share of all river inputs (%)	52	26	2	19

Table 5.2. Physical and chemical properties of surface lens and selected subsurface depths at fjord surface stations in austral summer (Feb) and austral winter (Jul) 2017. Some concentrations were not detectable (n.d.). Subsurface data only provided for winter depths from which samples were taken for FT-ICR MS analysis.

Station		Depth (m)	Freshwater lens depth (m)		Salinity (‰)		Temperature (°C)		Turbidity (NTU)		Chlorophyll (µg/L)		DOC (µM)		DON (µM)		N/C (molar ratio)		NO_3 (µM)		SRP (µM)	
			Feb	*Jul*	*Feb*	*Jul*	*Feb*	*Jul*	*Feb*	*Jul*	*Feb*	*Jul*	*Feb*	*Jul*	*Feb*	*Jul*	*Feb*	*Jul*	*Feb*	*Jul*	*Feb*	*Jul*
SURFACE LENS																						
MARTINEZ CHANNEL & INLETS																						
Steffen Fjord	S1	1	4.2	0.7	1.6	16.4	4.9	6.8	60.0	9.7	0.192	0.975	36.6	21.2	1.1	3.4	0.030	0.161	0.34	3.04	n.d.	0.39
	S2	1	6.5	4.7	1.3	13.1	4.7	6.2	63.7	11.2	0.235	0.683	49.0	64.8	1.1	5.1	0.023	0.079	0.33	0.57	n.d.	0.37
	S3	1	7.7	-	1.2	-	7.4	-	59.5	-	0.215	-										
	S4	1	7.6	3.4	1.2	5.6	10.4	5.8	29.1	15.6	0.312	1.066	39.3	64.8	2.4	3.5	0.061	0.054	0.08	1.18	n.d.	0.12
Baker plume	S5	1	5.0	3.0	0.5	0.7	11.6	5.9	93.5	32.9	0.226	0.484	44.1	61.9	1.9	1.7	0.043	0.028	n.d.	0.50	n.d.	0.27
Mitchell Fjord	S17	1	6.0	5.3	0.4	1.9	9.3	3.7	32.0	9.9	0.500	1.005	199.7	188.3	2.9	3.7	0.014	0.020	0.21	0.89	n.d.	0.03
	S16	1	8.6	5.7	0.6	3.3	12.4	4.0	15.7	12.9	0.567	1.144	130.8	110.1	2.0	3.2	0.015	0.029	n.d.	1.18	n.d.	0.26
	S8	1	7.7	4.4	0.9	4.7	13.0	4.4	20.1	10.3	0.394	1.032	128.3	166.8	3.6	5.1	0.028	0.030	n.d.	0.84	n.d.	0.10
BAKER CHANNEL & INLETS																						
Jorge Montt Fjord	S13	1	8.2	-	2.1	-	4.9	-	3.0	-	0.966	-	60.0	-	3.6	-	0.063	-	n.d.	-	n.d.	-
	S20	1	-	8.6	-	6.7	-	2.1	-	4.2	-	1.140	-	52.7	-	2.4	-	0.046	-	1.18	-	0.10
	S12	1	8.2	-	2.0	-	7.1	-	4.4	-	0.963	-	60.6	-	3.8	-	0.060	-	n.d.	-	n.d.	-
Pascua plume	S10	1	5.0	5.5	1.1	5.9	8.8	4.9	30.4	7.4	0.296	0.892	46.0	58.0	2.3	2.2	0.049	0.038	0.53	1.30	0.04	0.20
Central fjord	S7	1	6.8	3.8	0.8	7.2	11.6	5.8	51.2	12.1	0.385	0.795	60.9	95.6	1.9	3.2	0.031	0.033	0.07	1.96	n.d.	0.30
	S9	1	7.8	6.2	2.5	13.2	11.0	6.3	8.8	2.3	0.652	0.897	77.3	65.3	2.0	2.7	0.026	0.041	n.d.	2.91	n.d.	0.28
Outer fjord	S21	1	-	3.1	-	16.0	-	6.4	-	1.1	-	0.972	-	67.2	-	6.9	-	0.103	-	0.83	-	0.44
SUBSURFACE																						
Steffen Fjord	S1	40	-	-	-	31.9	-	11.4	-	0.4	-	0.053	-	41.9	-	7.6	-	0.182	-	8.78	-	1.06
	S4	270	-	-	-	33.9	-	8.2	-	0.5	-	0.035	-	36.7	-	7.5	-	0.204	-	19.06	-	1.92
Baker plume	S5	140	-	-	-	33.7	-	8.9	-	0.7	-	0.044	-	45.9	-	1.6	-	0.036	-	21.13	-	1.72
Mitchell Fjord	S17	130	-	-	-	33.7	-	8.8	-	0.4	-	0.087	-	74.9	-	7.4	-	0.098	-	17.78	-	1.35
Jorge Montt Fjord	S20	30	-	-	-	30.7	-	8.9	-	49.9	-	0.073	-	43.1	-	5.3	-	0.123	-	8.28	-	0.90
	S20	180	-	-	-	31.5	-	10.8	-	0.9	-	0.048	-	47.5	-	7.0	-	0.147	-	5.35	-	0.96
Baker Channel	S9	180	-	-	-	33.8	-	8.4	-	0.2	-	0.021	-	38.8	-	9.0	-	0.233	-	20.56	-	1.76

Spatial patterns in surface DOC are largely set by the composition of input rivers (Figure 5.3a–b). The highest concentrations occur in Mitchell Fjord in both seasons due to inflow from the Bravo River; the lowest concentrations are near the mouth of the Huemules River in Steffen Fjord.

Surface DON concentrations are generally low in summer and increase in winter (Figure 5.2b). The difference is only statistically significant (p=0.035; Mann Whitney) when samples from the Baker and Pascua river plumes (S5 and S10, respectively) are excluded. DON at these stations shows little seasonal change (Table 5.2), suggesting that the general increase in fjord DON in winter is not due to river inputs. Another deviation from the general trend is lower wintertime DON in Jorge Montt Fjord (2.4 µM; S20), versus values that are among the highest observed in summer (3.6–3.8 µM; S12–13) and comparable with winter concentrations elsewhere (Table 5.2). In general, DON is highest in the subsurface but there is considerable variability at high salinities (Figure 5.2b). Variations in DON control the range of N/C molar ratios, which are typically higher in more saline waters, but the highest values are at intermediate salinities ~16‰ found towards the marine end of the fjord in the winter surface layer (Figure 5.2c–d; Figure 5.3f).

Inorganic nutrients (NO_3, SRP) in the surface layer mostly fall below the analytical LoD in summer but reach detectable concentrations in winter (Table 5.2). Nutrient concentrations increase gradually with salinity in the surface layer but display a rapid increase in the subsurface at salinities >25‰. Although the highest NO_3 and SRP concentrations of ~25 µM and ~2 µM, respectively, are found in the most saline samples, concentrations are highly variable in the subsurface (Figure 5.2e–f).

5.4.4. DOM composition

5.4.4.1. Spectrofluorescence data

The PARAFAC model identified seven components of DOM fluorescence, three of which are classed as terrestrial humic-like (C_{498}, C_{452}, C_{446}), one as marine humic-like (C_{390}) and the remaining three as protein-like (C_{304}, C_{328}, C_{354}), with the latter exhibiting a tryptophan-like spectra. Fjord surface DOM adopts broadly the same fluorescence properties as riverine inputs in both seasons (Figure 5.4) and spatial patterns are largely

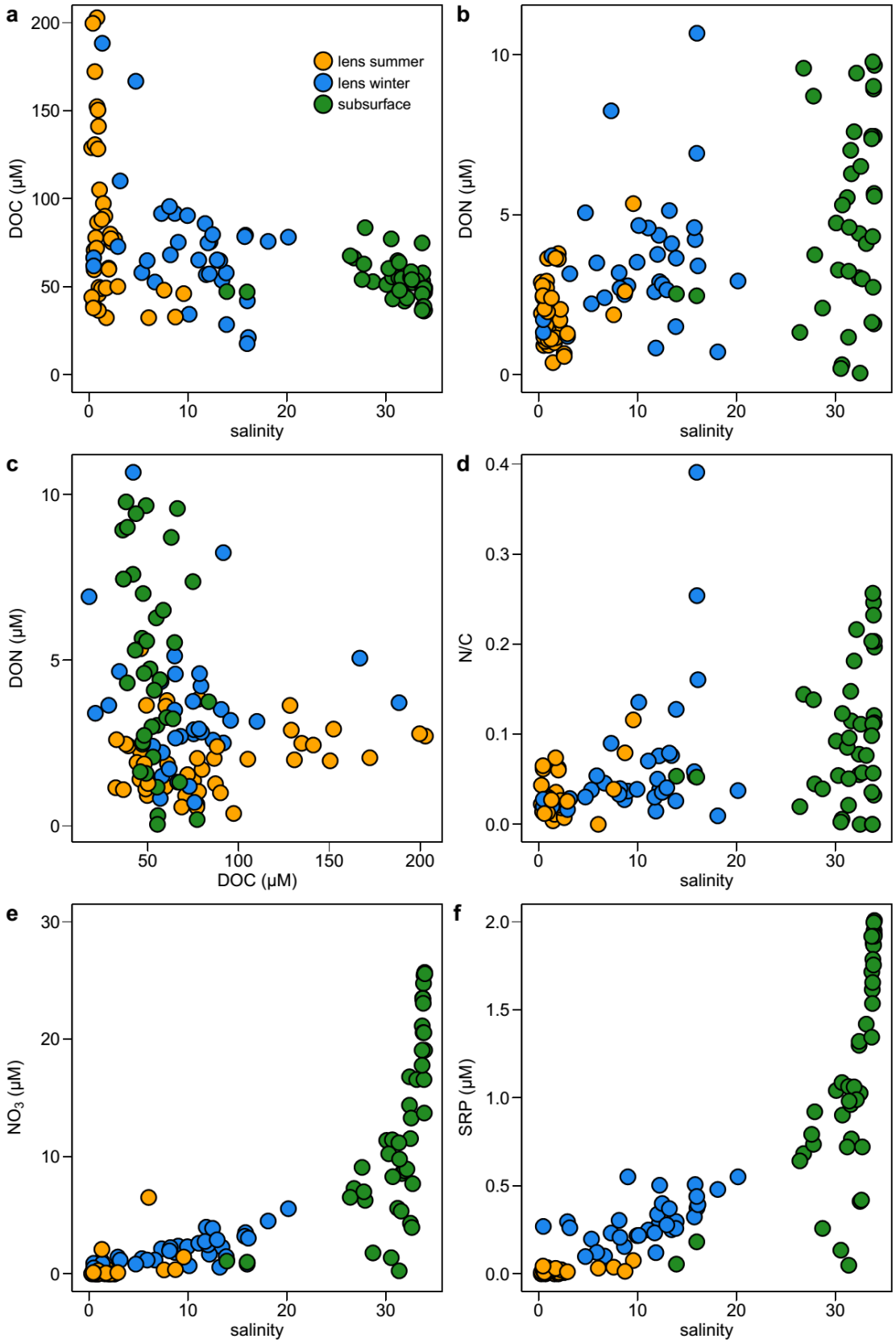

Figure 5.2. Trends in DOM composition and nutrient concentrations across the Baker-Martinez Fjord: (a) DOC and (b) DON versus salinity; (c) DON versus DOC; (d) molar N/C of DOM versus salinity; (e) NO_3 and (f) SRP versus salinity.

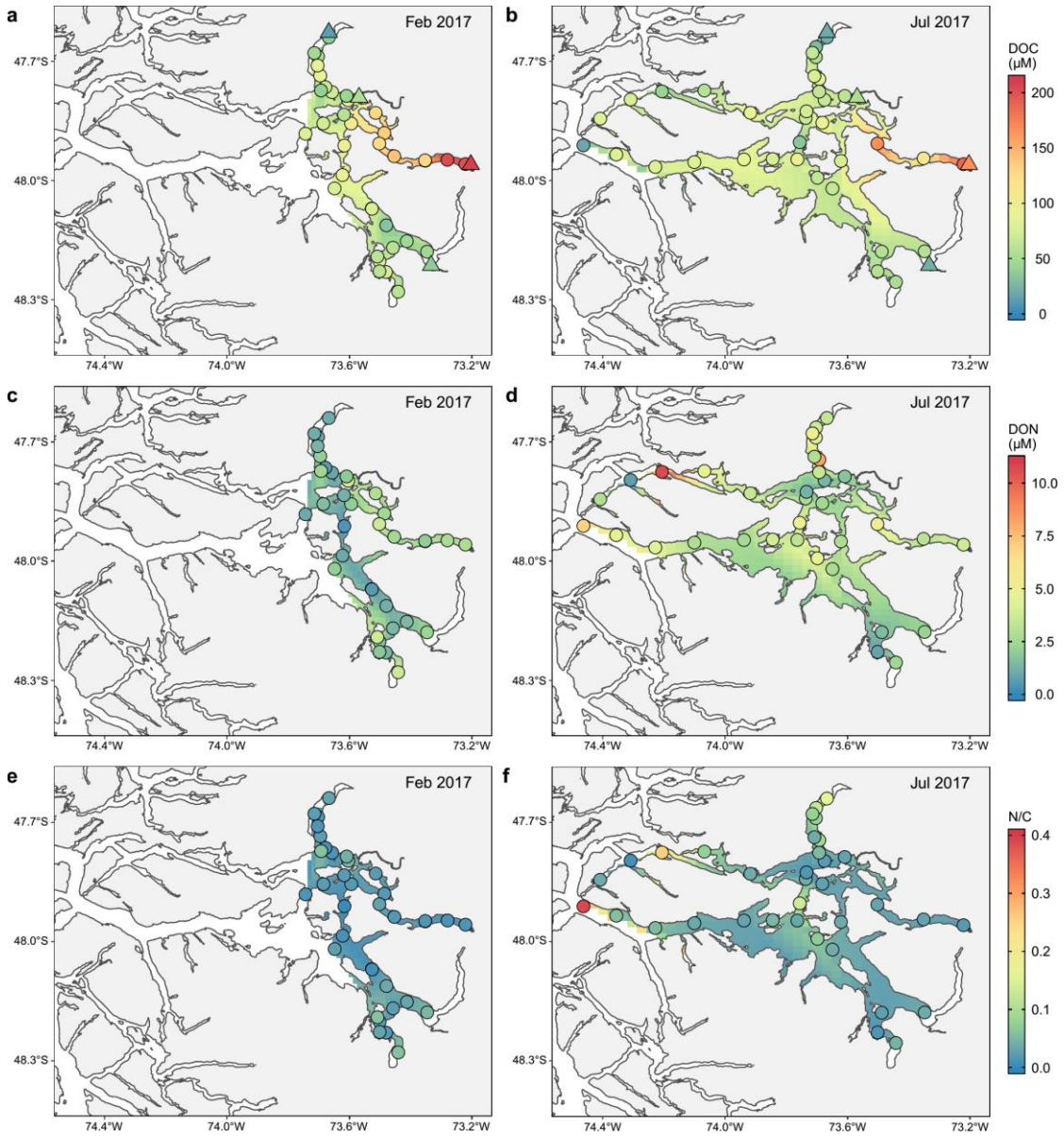

Figure 5.3. Spatial and seasonal patterns in DOC and DON concentrations and N/C ratios across the Baker-Martinez Fjord. Colour scales apply to both left and right plots on each row.

controlled by differences in river composition (Figure 5.5). Generally, differences between the rivers and fjord surface layer are not statistically significant, except for protein/tryptophan-like component C_{354} in summer (Mann Whitney, p=0.019) which is linked with DOM bioavailability in northern Patagonian catchments (Chapter 4) and is present in all BMF rivers but completely absent at many fjord stations. Moderate summertime C_{354} loadings (~10%) in rivers show a marked decrease (to ~0%) at stations immediately downstream of the river mouths (Figure 5.5e). Seasonal comparisons show that protein-like DOM is significantly lower in winter in both the rivers and fjord surface (Mann Whitney, p<0.05), except for C_{354} in the fjord which is largely absent in

both seasons (Figure 5.4 and Figure 5.6). However, large isolated spikes in C_{354} intensity in Jorge Montt Fjord and the Baker Channel in winter suggest additional sources for this fluorophore (Figure 5.5e–f). Overall, protein-like fluorescence varies independently of DOC concentrations and is either not correlated (C_{304}) or negatively correlated (C_{328}, C_{354}; Spearman, $p<0.001$) with N/C (Figure 5.6). In contrast, humic-like fluorescence is positively correlated with DOC and displays a negative association with N/C (Figure 5.6). Humic-like loadings in the fjord in winter are less variable than in rivers but both display a significant increase in C_{498} compared to summer (Figure 5.4). In addition, C_{446} and C_{390} in the winter fjord are significantly elevated with respect to river inputs (Mann Whitney; $p<0.001$) and summer conditions (Mann Whitney; $p<0.05$). This suggests a stronger association with marine conditions for these components.

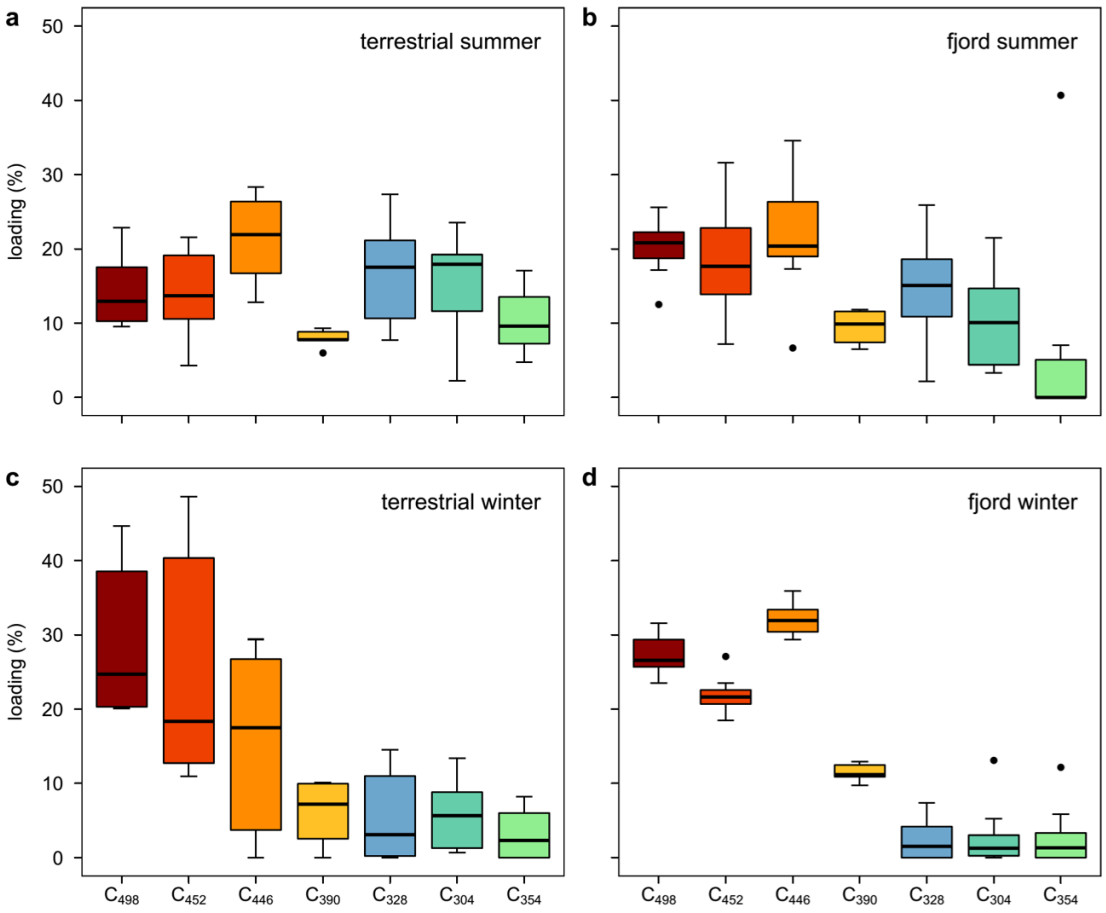

Figure 5.4. Seasonal patterns in PARAFAC component loadings for riverine inputs (left column) and fjord stations at 1 m depth (right column). Humic-like and protein-like components are in warm and cool colours respectively.

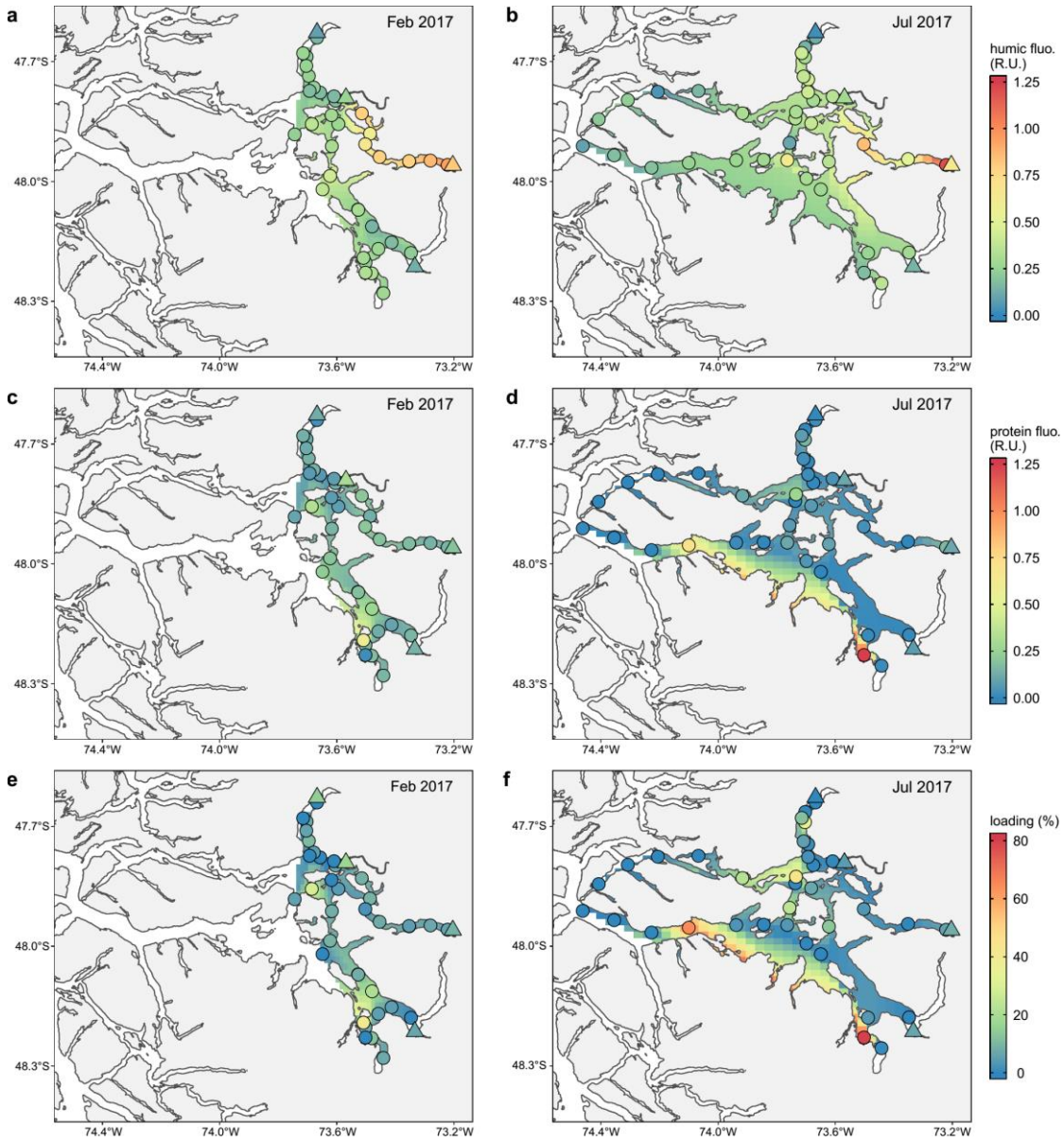

Figure 5.5. Seasonal and spatial patterns in DOM fluorescence across the Baker-Martinez Fjord shown as (a-b) summed humic-like and (c-d) summed protein-like intensities in Raman Units (R.U.) and as (e-f) loadings for protein-like C_{354} component. Filled circles are fjord stations or underway sample locations on which the interpolated surface is based. Filled triangles are riverine end-members positioned at the river mouths.

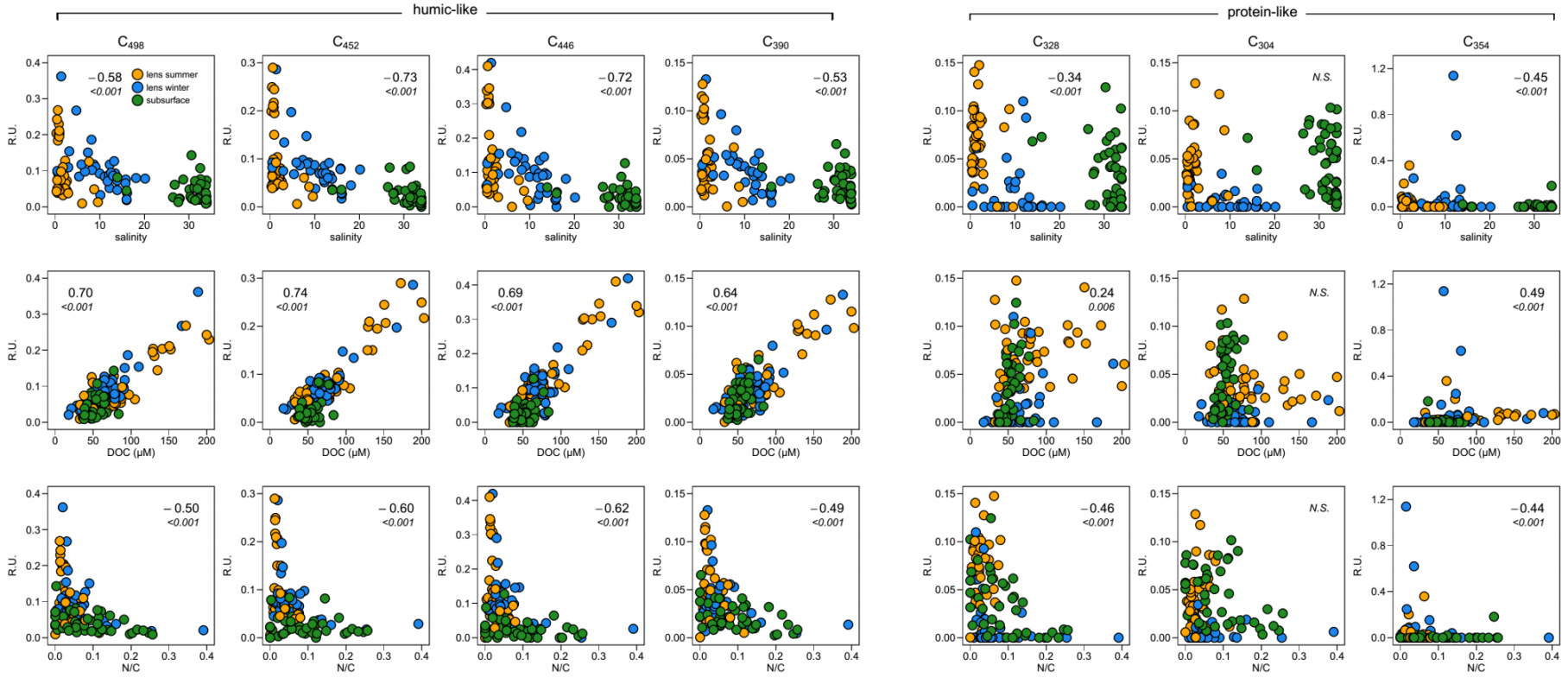

Figure 5.6. PARAFAC model component intensities versus salinity (top row), DOC concentrations (middle row) and molar N/C ratios (bottom row) for all fjord samples. Note different vertical scales for each fluorophore. Key in upper left-hand plot applies to all plots. Each plot is annotated with Spearman's rho correlation coefficient (and *p*-value in italics), or *N.S.* in the case of no significant correlation.

5.4.4.2. Molecular level data

A total of 18,383 individual molecular formulae in the mass range of 175–1000 Da were identified across 26 fjord and 8 river samples of SPE-DOM. Of these, 5321 (28.9%) were common to all fjord samples and 2870 (15.6%) were exclusive to the fjord. Only 976 formulae (5.3%) were found exclusively in river samples and these were mostly aliphatic or HUPs. HUPs comprise the bulk of all formulae (72.1 ± 3.1%) and relative intensity (83.7 ± 5.5%) in each sample, including many very low intensity peaks.

5.4.4.3. Multivariate analyses and environmental correlations

PCA results show that samples from different depths and seasons have distinct molecular compositions and fluorescence characteristics (Figure 5.7). The first 3 axes of the PCA explain 82.7% of the variance in the dataset. PC1 scores distinguish surface layer and subsurface fjord samples, with the former typically enriched in aromatic compounds and the latter in O-rich HUPs, O-rich aliphatics and peptides (Figure 5.7a). Subsurface samples are also associated with greater C_{304} (protein-like) and C_{390} (marine humic-like) fluorescence loadings. PC2 scores are linked to a seasonal shift in DOM composition in the fjord lens (Figure 5.7a). Positive PC2 values reflect summer conditions with more protein-like fluorescence, peptides and O-rich aliphatics. Negative PC2 scores show dominance of humic-like fluorescence, O-poor HUPs and O-poor aliphatics in winter. The relationship between PC2 and PC3 scores suggests convergence in DOM composition across much of the fjord lens in winter, characterised by higher C_{390} fluorescence, O-poor HUPs and O-poor aliphatics (Figure 5.7b). In contrast, high protein-like fluorescence, O-rich aliphatics and peptides are stronger in Jorge Montt Fjord and the Baker/Pascua River plumes in summer. The summer lens in Steffen and Mitchell Fjords is linked with greater contributions from O-rich HUPs (Figure 5.7b).

Significant correlations between PCA scores and environmental variables show that subsurface samples are strongly linked to higher salinities and dissolved nutrient concentrations, including DON (Figure 5.7a). The surface layer is linked with higher DOC but there is no seasonal trend (Figure 5.7a). In contrast, summer DOM in the surface layer is associated with warmer temperatures and higher turbidity whilst winter DOM is strongly linked to higher chlorophyll levels (Figure 5.7a). The characteristics

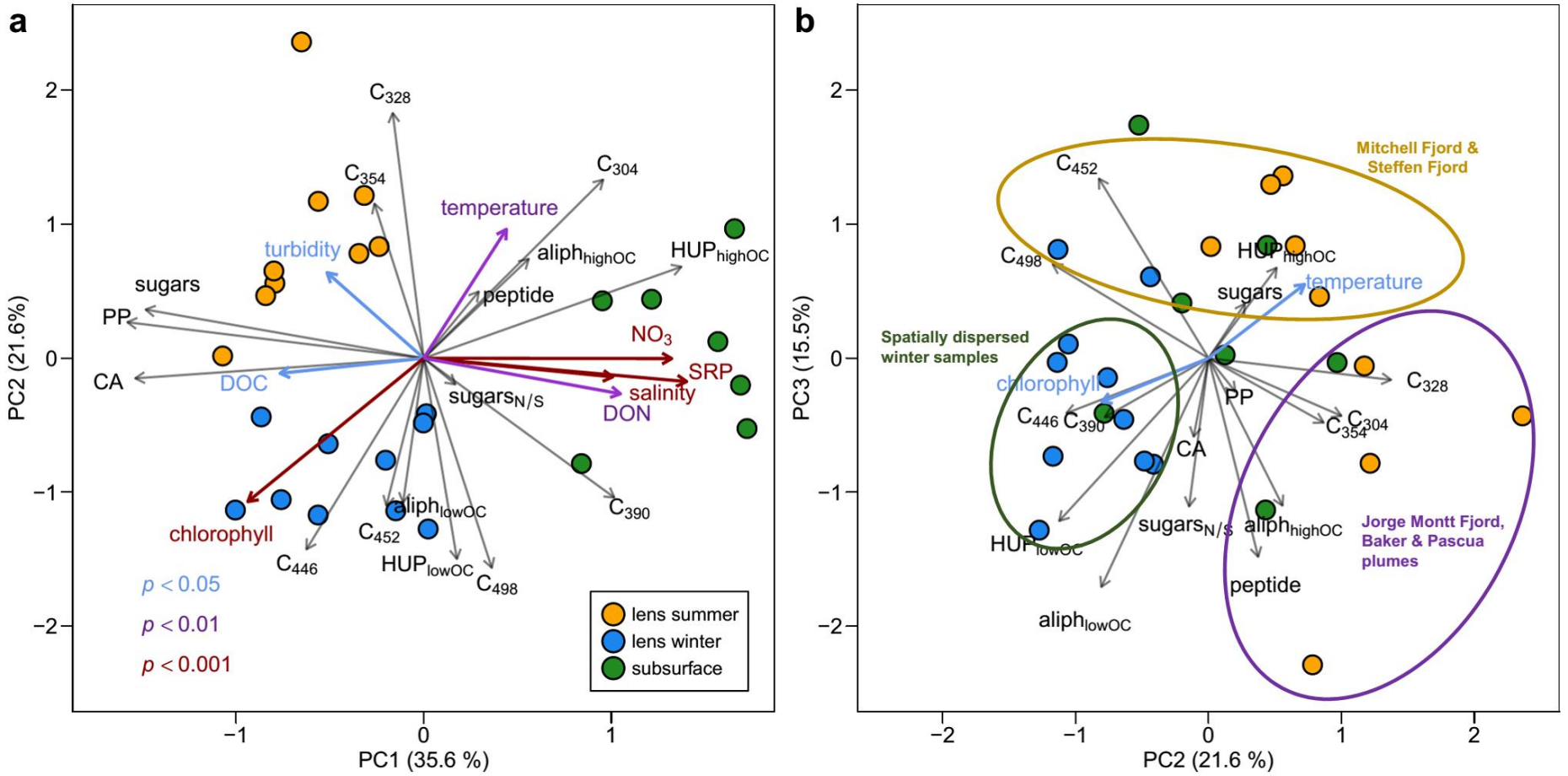

Figure 5.7. Multivariate principal components analysis (PCA) of DOM composition in Baker-Martinez Fjord based on PARAFAC fluorescence loadings and FT-ICR MS molecular data with environmental correlations determined by permutation. Results presented with respect to the (a) first and second; and (b) second and third principal components, respectively (percentages show the amount of variability explained by each axis). Grey arrows relate to variables used in PCA and coloured arrows relate to environmental correlations differentiated by significance level (see key on subplot a).

of molecular formulae that are correlated (positively and negatively) with season, salinity, chlorophyll and turbidity (four key factors linked to the separation of samples in the PCA) are summarised in Table 5.3. Surface layer DOM is typically more aromatic in summer and the dominant HUPs group sees a shift from more O-rich formulae to O-poor and N-containing formulae in winter. Formulae with N are positively correlated with salinity and the winter season but negatively correlated with chlorophyll and turbidity (Table 5.3). These relationships are primarily driven by changes in the dominant HUPs compound category. Strong positive correlations between DON concentrations and the relative intensities of all N-containing formulae, and specifically N-containing HUPs (both give Pearson's r=0.89; p<0.001; excluding one outlier sample), validate formulae assignments with an independent measure of DOM composition. Peptide-like formulae, as a minor constituent of total DOM, show a weaker correlation with DON (Pearson's r=0.55; p<0.01). They are positively associated with both turbid conditions in the summer lens and higher salinities, suggesting separate links with meltwaters and fjord waters, and negatively correlated with chlorophyll levels (Table 5.3).

Table 5.3. Characteristics of molecular formulae in fjord DOM that are positively and negatively correlated (Spearman, p<0.05) with season, salinity, chlorophyll and turbidity and those formulae that are not correlated with any environmental variable.

		season						salinity						chlorophyll						turbidity						no correlation		
		summer			*winter*			*pos*			*neg*			*pos*			*neg*			*pos*			*neg*					
Counts	No. formulae	1770	±	27	2075	±	45	2942	±	196	4334	±	118	4075	±	105	2453	±	185	3624	±	89	2445	±	169	782	±	26
Weighted averages	mass	476.6	±	2.3	464.4	±	1.0	451.0	±	0.6	498.9	±	2.7	521.1	±	2.1	446.6	±	0.7	492.4	±	3.0	448.4	±	0.6	492.4	±	2.0
	C	20.8	±	0.1	22.8	±	0.1	20.9	±	0.0	22.4	±	0.1	24.9	±	0.1	19.9	±	0.0	22.0	±	0.1	20.7	±	0.0	22.8	±	0.10
	H	20.1	±	0.1	28.3	±	0.1	26.0	±	0.0	20.3	±	0.1	25.1	±	0.3	24.9	±	0.0	19.8	±	0.1	25.8	±	0.0	28.7	±	0.15
	O	13.0	±	0.1	10.0	±	0.0	10.6	±	0.0	13.1	±	0.1	12.3	±	0.1	11.1	±	0.0	13.0	±	0.1	10.6	±	0.0	11.5	±	0.06
	N	0.03	±	0.00	0.12	±	0.01	0.21	±	0.01	0.05	±	0.00	0.05	±	0.00	0.25	±	0.02	0.05	±	0.00	0.23	±	0.02	0.15	±	0.01
	S	0.01	±	0.00	0.06	±	0.00	0.08	±	0.00	0.01	±	0.00	0.02	±	0.00	0.08	±	0.00	0.02	±	0.00	0.08	±	0.00	0.15	±	0.01
	HC	0.97	±	0.01	1.24	±	0.00	1.25	±	0.00	0.91	±	0.01	0.99	±	0.01	1.25	±	0.00	0.91	±	0.01	1.25	±	0.00	1.26	±	0.01
	OC	0.63	±	0.00	0.44	±	0.00	0.51	±	0.00	0.59	±	0.00	0.50	±	0.01	0.56	±	0.00	0.60	±	0.00	0.51	±	0.00	0.51	±	0.00
	NC	0.00	±	0.00	0.01	±	0.00	0.01	±	0.00	0.00	±	0.00	0.00	±	0.00	0.01	±	0.00	0.00	±	0.00	0.01	±	0.00	0.01	±	0.00
	AImod	0.36	±	0.00	0.26	±	0.00	0.22	±	0.00	0.42	±	0.00	0.40	±	0.01	0.20	±	0.00	0.42	±	0.00	0.22	±	0.00	0.22	±	0.00
Relative intensities (%)	Aliph. O-rich	0.22	±	0.02	0.00	±	0.00	0.65	±	0.04	0.13	±	0.01	0.00	±	0.00	0.83	±	0.04	0.15	±	0.01	0.39	±	0.03	0.08	±	0.00
	Aliph. O-poor	0.16	±	0.02	0.19	±	0.01	0.30	±	0.01	0.80	±	0.05	1.17	±	0.06	0.23	±	0.01	0.65	±	0.05	0.19	±	0.01	0.48	±	0.02
	Peptide	0.06	±	0.01	0.01	±	0.00	0.10	±	0.02	0.00	±	0.00	0.00	±	0.00	0.15	±	0.02	0.00	±	0.00	0.09	±	0.02	0.06	±	0.02
	HUP O-rich	20.33	±	1.14	10.53	±	0.72	24.43	±	1.66	22.43	±	1.47	8.40	±	0.68	23.86	±	1.59	21.39	±	1.44	21.96	±	1.59	1.72	±	0.04
	HUP O-poor	0.53	±	0.03	22.95	±	0.85	16.21	±	0.94	3.92	±	0.19	12.34	±	0.57	4.90	±	0.47	2.96	±	0.14	13.58	±	0.88	0.75	±	0.02
	HUP with N	0.02	±	0.00	1.20	±	0.17	2.44	±	0.38	0.14	±	0.01	0.12	±	0.00	2.16	±	0.36	0.11	±	0.01	2.37	±	0.37	0.07	±	0.00
	PP O-rich	3.20	±	0.26	0.00	±	0.00	0.00	±	0.00	7.28	±	0.61	5.07	±	0.45	0.00	±	0.00	7.02	±	0.59	0.00	±	0.00	0.04	±	0.00
	PP O-poor	0.76	±	0.05	0.02	±	0.00	0.04	±	0.01	2.16	±	0.15	1.73	±	0.12	0.02	±	0.00	2.07	±	0.14	0.03	±	0.00	0.04	±	0.00
	PP with N	0.01	±	0.00	0.01	±	0.00	0.02	±	0.00	0.07	±	0.00	0.06	±	0.00	0.01	±	0.00	0.07	±	0.00	0.01	±	0.00	0.03	±	0.00
	CA O-rich	0.27	±	0.03	0.01	±	0.00	0.00	±	0.00	2.27	±	0.19	2.18	±	0.19	0.00	±	0.00	1.62	±	0.13	0.00	±	0.00	0.01	±	0.00
	CA O-poor	0.01	±	0.00	0.00	±	0.00	0.00	±	0.00	0.11	±	0.01	0.10	±	0.01	0.00	±	0.00	0.07	±	0.00	0.00	±	0.00	0.02	±	0.00
	CA with N	0.00	±	0.00	0.00	±	0.00	0.00	±	0.00	0.00	±	0.00	0.00	±	0.00	0.00	±	0.00	0.00	±	0.00	0.00	±	0.00	0.01	±	0.00
	Sugars	0.02	±	0.00	0.00	±	0.00	0.04	±	0.01	0.17	±	0.02	0.14	±	0.02	0.04	±	0.01	0.16	±	0.02	0.01	±	0.00	0.03	±	0.00

Reported values are either (as labelled) formulae counts, intensity-weighted averages of summary molecular properties, or the mean relative intensities for all formulae subdivided into compound categories; all ± 1 standard error (SE).
Aliph. = aliphatics; HUP = highly unsaturated and phenolic; PP = polyphenolic; CA = condensed aromatics.

5.5. Discussion

Since carbon is the bulk constituent of organic matter by mass, DOC and POC estimates are considered representative of DOM and POM in the following discussion.

5.5.1. Rivers as a major source of DOM

The magnitudes of terrestrial organic matter fluxes to the BMF are largely unknown and our flux calculations are a significant step towards quantifying and characterising the inputs to this fjord from its four principal tributary rivers. Despite the low number of samples and averaged concentrations used in our calculations, this study provides useful first order flux estimates for rivers for which there are limited biogeochemical data. We acknowledge the potential for our calculations to overestimate annual POC fluxes due to the use of summertime concentrations, which are likely to be higher due to elevated turbidity levels in the rivers. For example, a published time series for 2007–2009 shows that summertime SSCs (163 mg L^{-1}) may be almost double the wintertime concentrations (89 mg L^{-1}) in the Baker River (Quiroga *et al.*, 2012). However, it is not clear how representative these data are of the 2017 field season given the acceleration of glacial melting (Chen *et al.*, 2007; Willis *et al.*, 2012a; Dussaillant *et al.*, 2019). It is also unclear how the percentage organic content of these suspended sediments might vary over the year and there no comparable data from other similarly glaciated regions which could provide insight, as, in most cases, studies have focused on individual seasons rather than generating annual time series. We recognise that unconstrained seasonal variations in POC are a limitation of our study but consider our flux estimates to be useful baselines which could be refined by future studies.

In the absence of more reliable data, we judge the reliability of our flux calculations by the similarity of our concentration and discharge data to other studies. For example, our POC concentrations are in line with those reported for the Baker River (100 µg C L^{-1}) and the Baker/Pascua plumes (87.4 ± 47.8 µg C L^{-1}) in the fjord (Vargas *et al.*, 2011). No published data are available to verify our river DOC measurements but our results are generally consistent with a dominance of DOM over POM in the Baker River plume (González *et al.*, 2013). Our annual discharge estimates for the largest rivers, Baker and Pascua, are consistent with independent analyses of annual records (Pantoja *et al.*, 2011; Dussaillant *et al.*, 2012). Whilst the lack of previous discharge measurements for the

Huemules or Bravo precludes comparison, these rivers represent a small proportion of total freshwater flux and, in the Bravo River, OC fluxes are driven primarily by DOC concentrations rather than discharge.

The major rivers emptying into BMF deliver significant quantities of DOM over the course of a year (Table 5.1). The largest rivers, Baker and Pascua, dominate total supply which is largely driven by discharge. The relative importance of riverine DOM therefore increases with respect to autochthonous sources during peak summer discharge conditions, especially in the vicinity of major river plumes. This is consistent with dominant terrestrial signatures determined from stable isotopes in POM at the fjord heads (Vargas *et al.*, 2011). Based on estimates of annual primary production, we calculate that the four major rivers supply a substantial proportion (up to 57%) of the annual inputs of organic matter to the BMF (Table 5.4). The exact proportion is dependent on which measured rates of primary production are used, which available data suggests is likely to be highly spatially variable (Table 5.4). It is difficult to constrain our estimates further due to limited data on primary production rates for this fjord. All available primary production data were obtained during spring blooms which likely reflect maximum productivity and overestimate total carbon fixation when extrapolated over the year (Aracena *et al.*, 2011; González *et al.*, 2013; Jacob *et al.*, 2014). Also, it is not clear how much of the total carbon annually fixed into biomass is transferred into the fjord DOM pool. Thus, our estimates of riverine DOM contributions are likely to be conservative.

Although additional inputs from other allochthonous sources (Jorge Montt Glacier, smaller streams, overland runoff, groundwater discharge and atmospheric deposition) are unconstrained, these do not affect the relative balance between primary production and the major river inputs. Moreover, direct anthropogenic inputs of organic matter are deemed negligible given the minimal human population and agricultural activities in the tributary basins (Tateishi *et al.*, 2011, 2014) and the complete absence of an aquaculture industry in the BMF (Quiroga *et al.*, 2013; Quiñones *et al.*, 2019). Our calculations therefore demonstrate that rivers may provide a critical subsidy of non-anthropogenic, terrestrial organic matter to the BMF, especially where productivity is low in the near-shore turbid zones (González *et al.*, 2013).

Table 5.4. Balance of annual autochthonous production and allochthonous inputs by rivers of organic matter in Baker-Martinez Fjord. A range of estimates of autochthonous production are based on different reported primary production rates in milligrams of carbon fixed per square metre per day extrapolated over a year for the entire fjord region, measured as 1355 km^2. Total OC inputs reflect the sum of annual carbon fixation by primary production and riverine delivery. The percentage balances of primary production, river DOC and river POC are with respect to the total OC input.

Location	Measured rate of primary production (mg C m^{-2} d^{-1})	Ref	Annual primary production (Gg C a^{-1})	Total OC input (Gg C a^{-1})	Balance of inputs (% total)		
					Primary production	River DOC	River POC
Tortel	91	(Aracena *et al.*, 2011)	45.0	87.6	51	41	8
Steffen Fjord	345	(Aracena *et al.*, 2011)	170.6	213.3	80	17	3
Steffen Fjord	49	(González *et al.*, 2011)	24.2	66.8	36	53	10
Baker Fjord	360	(González *et al.*, 2011)	178.0	220.7	81	16	3
Martinez Channel	422 ± 255	(González *et al.*, 2011)	82.6–334.8	208.7–377.5	40–89	9–57	2–3
Steffen Fjord 1	120	(Jacob *et al.*, 2014)	59.3	102.0	58	35	7
Steffen Fjord 2	840	(Jacob *et al.*, 2014)	415.4	458.1	91	8	1
Steffen Fjord 3	576	(Jacob *et al.*, 2014)	284.9	327.5	87	11	2
Steffen Fjord mouth	512 ± 364	(Jacob *et al.*, 2014)	73.2–433.2	115.8–475.9	63–91	8–30	1–6

Table 5.5. DOC:POC ratios for major input rivers of the Baker-Martinez Fjord compared to published data for water masses in other fjords and channels in Chilean Patagonia and the Arctic.

Location and sample	Sample type	DOC (mg L^{-1})	POC (mg L^{-1})	DOC:POC	Study
CHILEAN PATAGONIA					
Baker-Martinez Fjord					
Baker River[a]	river	0.644	0.114	5.6	*This study*
Pascua River[a]	river	0.364	0.136	2.7	*This study*
Huemules River[a]	river	0.153	0.079	1.9	*This study*
Bravo River[a]	river	2.518	0.045	56.0	*This study*
Martinez Channel[b]	surface fjord	1.320	0.140	9.4	1
Inner Sea of Chiloé					
Mean for inner sea area[b]	surface marine	0.910	0.256	3.6	2
Reloncavi Fjord[c]	surface fjord	0.740	0.425	1.7	2
Magellan Strait					
Magellan Strait[b]	surface marine	1.720	0.392	4.4	3
Beagle Magellan Water	subsurface marine	0.815	0.234	3.5	4
Sub-Antarctic Shelf Water	subsurface marine	0.700	0.129	5.4	4
Sub-Antarctic Water	subsurface marine	0.640	0.077	8.3	4
ARCTIC					
Young Sound, Greenland[d]	surface fjord	1.285	0.024	53.5	5
	subsurface fjord	1.261	0.026	48.5	5
	shelf water	1.068	0.025	42.7	5
	river	0.504	0.056	9.0	5
Kongsfjorden, Svalbard					
October	surface fjord	1.158	0.189	6.1	6
April	surface fjord	0.713	0.283	2.5	6
August	surface fjord	1.091	0.276	4.0	7
August	subsurface fjord	1.309	0.068	19.3	7
August	river	0.877	0.673	1.3	7
Norway					
Ballsfjord	surface fjord	1.500	0.748	2.0	8
Ullsfjord	surface fjord	1.370	0.325	4.2	8

Table notes

a. Annual mean concentrations reported in Table 5.1.
b. DOC:POC calculated from concentrations converted from depth-integrated concentrations reported in study.
c. As b. but concentrations read off from graph in study and expressed as mean for all stations within Reloncavi Fjord.
d. Mean concentrations for summer (July) study period; molar DOC concentrations converted into mg L^{-1}.

Refs

1. (González *et al*., 2013); 2. (González *et al.*, 2019); 3. (González *et al.*, 2013); 4. (Barrera *et al.*, 2017); 5. (Paulsen *et al.*, 2017); 6. (Brogi *et al*., 2019); 7. (Zhu *et al.*, 2016); 8. (Gašparović *et al.*, 2005).

Despite glacially dominated discharge regimes, the bulk composition of total organic matter export from the Baker, Pascua and Huemules is atypical of glacial runoff. In other glacial regions, high sediment loadings in meltwaters drive large POM fluxes

which comprise up to ~90% of total organic matter export (Bhatia *et al.*, 2013; Lawson *et al.*, 2014b; Hood *et al.*, 2015). In our study region, POM loadings are small due to low SSCs compared to other glacial rivers (Knudsen *et al.*, 2007; Lawson *et al.*, 2014a; Srivastava *et al.*, 2014), and low sedimentary organic content. Long water residence times in proglacial and freshwater lakes in these catchments (Table 5.1) may lead to the settling out of particulates and the consumption of labile POM from river waters before they reach the fjord (Meyers *et al.*, 1984; Meyers and Ishiwatari, 1993; Chifflard *et al.*, 2019). Nevertheless, the estimated ratios of DOC:POC in our study rivers fall within the range observed across other water masses in fjords and inlets across Chilean Patagonia and the Arctic (Table 5.5). However, it should be noted that very few studies report paired DOC and POC concentrations for glaciated fjords and the exact role of terrestrial POM in carbon cycling processes within these settings is not well understood (Hopwood *et al.*, 2019). Studies which highlight a role for terrestrial POM as a food source in BMF (Vargas *et al.*, 2011; González *et al.*, 2013; Meerhoff *et al.*, 2019) may underestimate the true significance of terrestrial organic matter since riverine DOM is a greater and potentially more labile flux.

5.5.2. Seasonal impact of rivers on fjord DOM

The seasonal shift in the composition of fjord surface DOM is affected by changing river fluxes, and specifically glacial meltwater contributions, in three main ways.

First, seasonal changes in catchment hydrology and DOM sources affect the composition of the riverine inputs that are transferred into the fjord lens. Higher summertime protein-like fluorescence in the fjord lens (Figure 5.4) is consistent with high glacier melt inputs during peak discharge conditions (Barker *et al.*, 2006; Hodson *et al.*, 2008; Hood *et al.*, 2009; Dubnick *et al.*, 2010; Fellman *et al.*, 2010a; Stubbins *et al.*, 2012). These signals are strongest downstream of the largest glacially-fed rivers, Baker and Pascua, and Jorge Montt Glacier (Figure 5.7), although we are unable to constrain the composition of direct melt inputs from the latter. Stronger humic-like fluorescence in the winter lens reflects greater freshwater contributions of terrestrial DOM from non-glacial, vegetated or wetland sectors of the river catchments (Fellman *et al.*, 2008, 2014). Whilst the year-round presence of condensed aromatics and polyphenolics in the surface lens (Figure 5.7) attests to continual riverine inputs of

vascular plant- and soil-derived material (Koch *et al.*, 2005; Ohno *et al.*, 2010), positive correlation of these compounds with the summer season shows the stronger influence of terrestrial DOM during high discharge conditions (Table 5.3). The lack of correlation between humic-like fluorescence and bulk polyphenolic/condensed aromatic content (Figure 5.7) suggests that fluorescence signatures may covary with only a subset of these compounds and comprise an overall minor fraction (<1%) of total DOM (Cory *et al.*, 2011).

Second, the magnitude of the freshwater flux controls the degree of mixing between terrestrial and marine end-members. Reduced glacier melting in winter leads to lower river discharge and an overall thinning of the freshwater lens (Table 5.2), and a likely shoreward migration of the pycnocline in winter (Rebolledo *et al.*, 2019). The increased influence of marine waters is apparent in higher surface salinities and dissolved nutrient concentrations, including DON (Figure 5.7; Table 5.2). On a molecular level, this is manifest as an increase in the intensity of N-containing HUPs as the dominant constituent of DON in the fjord (Table 5.3). DOM with a higher heteroatom content reflects material ultimately derived from marine rather than terrestrial sources (Kujawinski *et al.*, 2004; Sleighter and Hatcher, 2008). However, negative correlations between these formulae and chlorophyll (Table 5.3) suggests that they are sourced from a subsurface pool of more recalcitrant DOM rather than recent production. Thus protein- and peptide-like substances, as indicators of fresh production or recently re-worked material (Aluwihare *et al.*, 2005; Aluwihare and Meador, 2008), display little association with N-content (Figure 5.6; Table 5.3), countering classical assumptions that these compounds are a significant organic N component in coastal waters (Aluwihare and Meador, 2008; Fellman *et al.*, 2010a). Rather, fjord DON may be largely unreactive and its presence reflects a greater degree of marine water influence by conservative mixing. This is corroborated by the positive relationship between formulae belonging to the "island of stability" group — a relatively recalcitrant pool of marine DOM (Lechtenfeld *et al.*, 2014) — and salinity (Figure 5.8). Elevated loadings of marine humic-like fluorescence (C_{390}) with respect to river inputs in winter also support this mechanism (Figure 5.4).

Third, lower turbidity levels associated with reduced glacial meltwater inputs facilitate higher primary production rates and stronger signals of autochthonous DOM in winter.

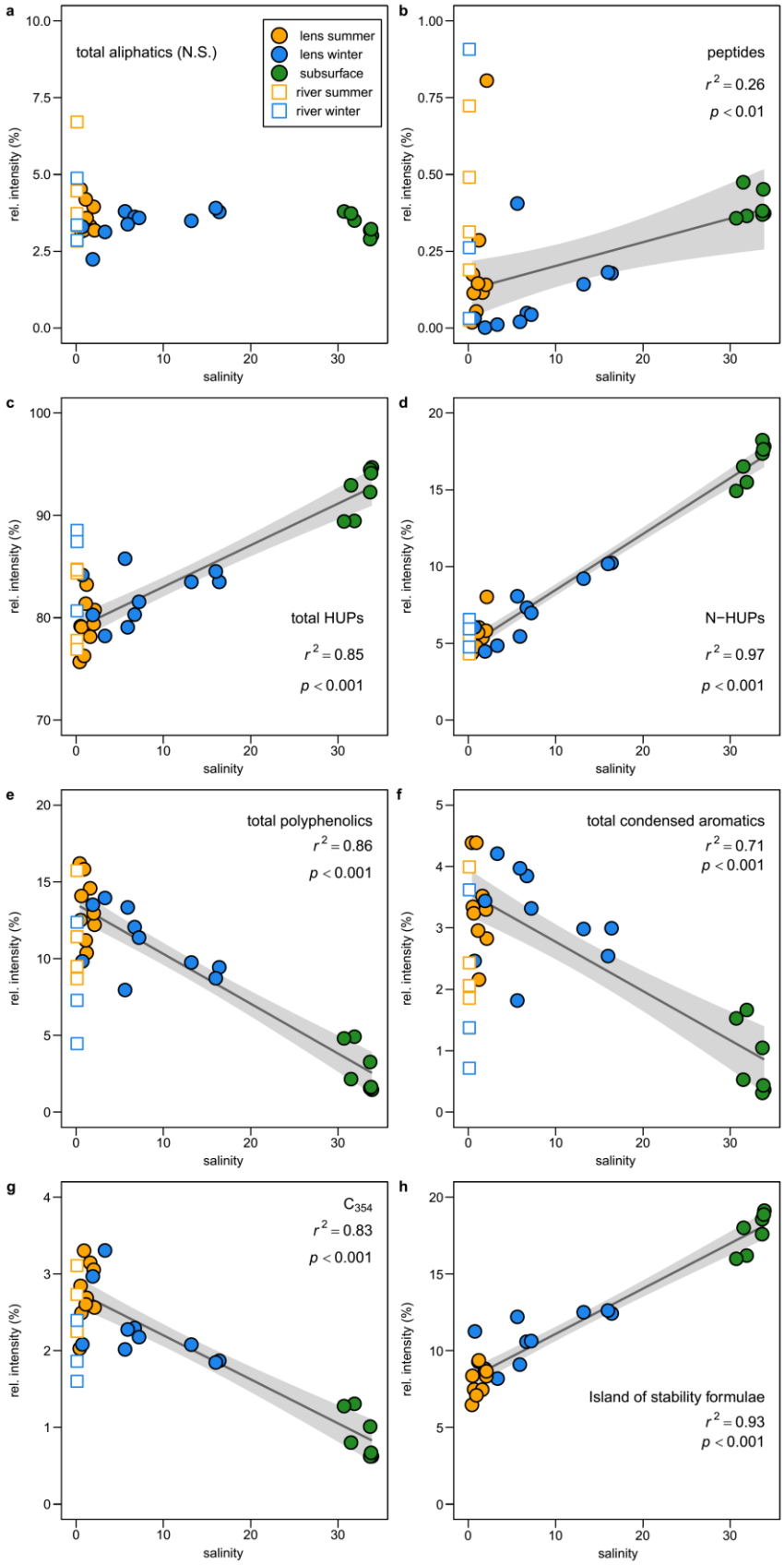

Figure 5.8. Changes in FT-ICR MS compound category relative intensities with salinity variations across summer and winter surface lens samples and subsurface samples from Baker-Martinez Fjord. Significant regression lines with shaded 95% confidence intervals shown alongside quoted r^2 and *p*-values. Input river samples plotted for reference. Key in subplot a applies to all subplots.

Increased intensities of O-poor HUPs and O-poor aliphatics in the winter surface layer, and their positive association with chlorophyll (Figure 5.7; Table 5.3), is consistent with the characteristics of DOM derived from marine phytoplankton and algae (Sleighter and Hatcher, 2008; Kujawinski *et al.*, 2009; Landa *et al.*, 2014). We cannot discount groundwater as a possible source for these compounds, especially when the relative importance of groundwater contributions may increase with lower river discharge. However, in the absence of data to constrain groundwater inputs we suggest that the stronger intensities of these compounds in the surface layer (Figure 5.7; Table 5.3) points towards an autochthonous source. Moreover, the convergence in DOM composition across the fjord lens in winter (Figure 5.7b) suggests an overriding process or dominant source that is distinct from summertime conditions. We attribute this to higher primary production across the fjord which superimposes autochthonous signatures onto terrestrial aromatic/humic DOM and increased marine water influences by conservative mixing. Stronger allochthonous signatures including O-rich aliphatics and O-rich HUPs in summer show how rivers reassert a dominant influence over bulk DOM composition with increasing discharge.

Overall, the primary source of labile DOM for marine heterotrophs will vary seasonally with river discharge. Increased glacier melt inputs may suppress the production of fresh organic matter in summer, favouring a heterotrophic community better adapted to utilising terrestrial/glacial DOM (Gutiérrez *et al.*, 2015; Paulsen *et al.*, 2018), despite observations of an apparent preference for marine DOM substrates in other glacial fjords (Holding *et al.*, 2017). Previous work on BMF has highlighted a similar sensitivity of the pelagic food web to increased glacier melt inputs, with changes in zooplankton community structure during glacial lake outburst floods (GLOFs) attributed to an increased availability of terrestrial POM as a food source (Meerhoff *et al.*, 2019); although it is not clear much of the terrestrial material is exclusively glacial in origin.

5.5.3. Changes in DOM composition along the salinity gradient

We used a correlative approach to track changes in DOM composition with salinity, similar to other coastal studies (Osterholz *et al.*, 2016; Seidel *et al.*, 2017). However, our samples were spatially dispersed and capture complex mixing processes between

multiple river end-members and marine waters which complicate the interpretation of conventional mixing diagrams (Asmala *et al.*, 2016). For example, increased DOC concentrations and humic-like signals along Steffen Fjord and downstream of the Pascua River illustrate the influence of more concentrated terrestrial inputs from more distant rivers, streams or surface runoff (Figure 5.3 and Figure 5.5). This effect has been observed in Young Sound, Greenland, where material from distant Arctic river inputs mixes with local inputs from more dilute glacial waters (Paulsen *et al.*, 2018). Moreover, at our most distant site (S21), salinities never reach fully marine conditions due to a considerable freshwater input even in winter. Instead we interpret a salinity gradient that cuts across spatial, seasonal and depth variations in the fjord to reflect the overall impact of a shifting balance of different water sources on DOM composition.

Relative enrichment in the fjord lens with more aromatic substances, such as polyphenolics (Figure 5.8), with respect to most river inputs is at first counterintuitive given their known association with vascular plants and soils (Ohno *et al.*, 2010). We speculate that although the range of observations in the fjord lens is encapsulated by variability in the input rivers, unconstrained inputs via smaller streams and surface runoff contributes additional aromatic DOM from the surrounding vegetated slopes. Differences between riverine end-members and surface lens samples might also reflect an internal composition adjustment, with increased relative intensities of aromatic compounds balanced by decreases in HUPs. Photodegradation is a removal mechanism for HUPs, PPs and CAs (Tremblay *et al.*, 2007; Stubbins *et al.*, 2010) but would be limited in turbid conditions (Osterholz *et al.*, 2016). Bacterial conversion of reactive humic-like material to more recalcitrant forms (Nelson *et al.*, 2004; Shimotori *et al.*, 2010; Romera-Castillo *et al.*, 2011), which might explain higher in-fjord loadings of C_{446}, would also likely remove a range of phenolic and aromatic compounds (Stubbins *et al.*, 2010; Mostovaya *et al.*, 2017). Negative correlations between humic-like fluorescence and salinity confirm the removal of aromatic DOM from surface waters (Spencer *et al.*, 2009; Stubbins *et al.*, 2010; Timko *et al.*, 2015). Overall, the variations with respect to salinity show a typical estuarine transition from aromatic-rich terrestrial DOM to more unsaturated compounds with higher heteroatom content in marine waters (Medeiros *et al.*, 2015; Osterholz *et al.*, 2016; Seidel *et al.*, 2017). This is consistent with selective removal of high O/C material by bacterial degradation and contributions

of phytoplankton-derived compounds with lower O/C (Medeiros *et al.*, 2015) and higher heteroatom content (Osterholz *et al.*, 2016; Wünsch *et al.*, 2016).

Protein-like fluorescence displays a more complex pattern with salinity across sample types (Figure 5.6) and may provide a sensitive indicator of both biologically produced and bioavailable DOM (Paulsen *et al.*, 2018). Elevated signals in the subsurface and summer lens contrast with a general absence in the winter lens, except for a few isolated spikes in C_{328} and C_{354}. This is consistent with independent sources of protein-like material in glacially-fed rivers and marine waters (Murphy *et al.*, 2008; Barker *et al.*, 2009; Dubnick *et al.*, 2010; Lønborg *et al.*, 2015). In-fjord contributions of protein-like DOM might include sloppy feeding by grazers and bacterial degradation of faecal pellets which could contain terrestrial organic matter (Poulet *et al.*, 1991; Møller *et al.*, 2003; Urban-Rich *et al.*, 2004; Møller, 2007). Reduction of protein signals in winter reflects decreased glacier melt inputs since a more productive fjord ecosystem would likely increase the supply of autochthonous proteins, unless it were rapidly degraded (Determann *et al.*, 1998; Stedmon *et al.*, 2003; Yamashita *et al.*, 2008). High spikes in tryptophan fluorescence (C_{354}) suggest excess production in Baker Channel and Jorge Montt Fjord, although presence in the latter might reflect continuous contributions via subglacial discharge or sub-marine melting (Moffat *et al.*, 2018). Other subsurface sources of C_{354} are discounted due to a near complete absence below the freshwater lens (Figure 5.6).

5.5.4. Compositional influence on DOM reactivity and cycling

In oligotrophic fjord systems with low productivity, in-washed terrestrial organic matter may offer a valuable source of nutrients to pelagic communities (Vargas *et al.*, 2011). However, DOM in BMF has a low overall nitrogen content that is unlikely to satisfy biological nutrient requirements of the Redfield ratio alone (Figure 5.2). Low inorganic nitrogen concentrations may further compound nutrient scarcity. Bioavailability may be further limited by the dominance of HUPs, which are relatively unreactive (Mostovaya *et al.*, 2017) and comprise the bulk of all nitrogen containing compounds. Nevertheless, separate components of N-rich DOM may provide labile substrates within a larger recalcitrant pool. Here we review evidence for consumption of proteins and processes affecting peptides, as examples of labile compounds linked to sources of

labile nitrogen (Aluwihare *et al.*, 2005; Mulholland and Lee, 2009; Lønborg *et al.*, 2015).

A significant reduction in C_{354} fluorescence in the summer lens with respect to riverine inputs (Figure 5.4) is most apparent immediately downstream of the river mouths (Figure 5.5). This is consistent with bio-incubation results which suggest that tryptophan-like material is a bioavailable component of DOM in Patagonian rivers (Chapter 4). However, data from the fjord do not suggest consumption of the N-containing polyphenolic formulae significantly correlated with C_{354} in terrestrial systems (Figure 5.8). Moreover, protein-like fluorescence is not positively correlated with the N-content of DOM (Figure 5.6), countering prevailing assumptions that it serves as a proxy for labile organic nitrogen in estuarine and marine systems (Fellman *et al.*, 2010a; Lønborg *et al.*, 2015; Yamashita *et al.*, 2015). Generally, additional C_{354} sources in the fjord render it unsuitable as a tracer for terrestrial DOM reactivity in marine waters.

Peptides and nitrogen containing HUPs (N-HUPs) show different positive associations in summer and winter (Figure 5.9). The surface lens in summer is relatively more enriched in peptides with respect to N-HUPs, whilst the trend is reversed in winter. This likely reflects two distinct modes of seasonal mixing. Stronger freshwater inputs in summer suppress the influence of marine waters as a major source of N-HUPs (and DON) in the fjord and higher peptide intensities reflect increased riverine contributions from glaciers and lakes (Spencer *et al.*, 2014b). The relationship in the summer lens is therefore in line with the range of conditions in input rivers (Figure 5.9). In winter, greater influence from marine N-HUPs explains the general trajectory of surface lens samples towards subsurface conditions (Figure 5.9). This is supported by a trend towards lower mass peptides with higher S-content in the winter lens, which are more characteristic of marine signals (Table 5.6). An outlier to this trend is the S4 sample (Figure 5.9), which could be under greater influence from the Baker River plume even in winter. Moreover, elevated peptide signals downstream of Jorge Montt Glacier in summer (Figure 5.7) could indicate direct inputs from glacier melt or autochthonous production; either mechanism could also explain elevated protein-like fluorescence. The presence of O-rich aliphatics and aromatics supports a strong input from terrestrial sources (Figure 5.9).

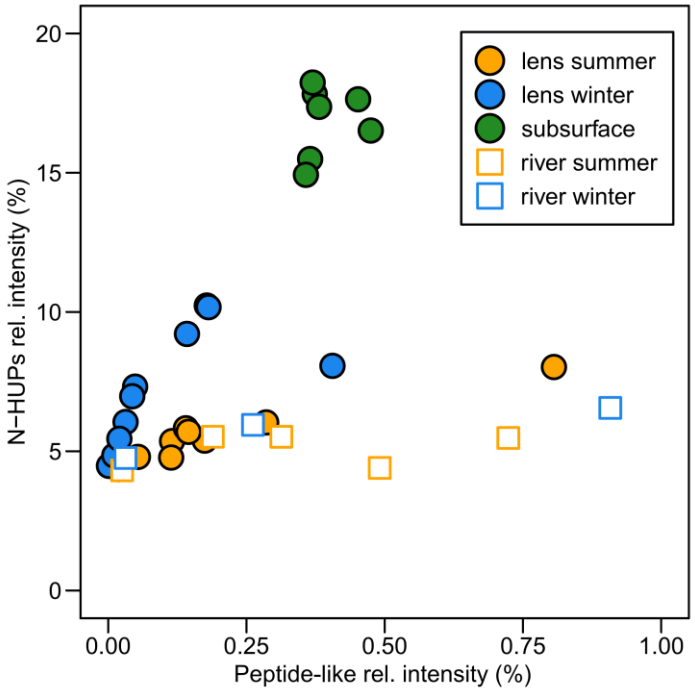

Figure 5.9. FT-ICR MS relative intensities of nitrogen-containing highly unsaturated and phenolic compounds (N-HUPs) versus peptide-like formulae in surface layer, subsurface and river samples from Baker-Martinez Fjord.

A significant multivariate analysis of variance (MANOVA; $p<0.001$) reveals distinct peptide characteristics in river, fjord lens and subsurface samples (Table 5.6). They are differentiated by mass, intensity, aromaticity, O/C and S-content. Subsequent ANOVAs show significant differences between rivers and subsurface peptides ($p<0.001$), suggesting distinct terrestrial and marine end-members. Increased mixing of marine waters likely causes a similar significant difference in the winter lens with respect to river inputs ($p<0.001$) and summer conditions ($p<0.001$). The river peptides are not significantly different between the seasons except for higher S-content in summer ($p<0.001$), which is the reverse of the pattern in the fjord lens. In summer, peptides in the fjord lens only differ from rivers in intensity ($p<0.001$) and suggest a dominant control by freshwater DOM. The differences in source and composition may have implications for their reactivity and overall organic matter cycling in the fjord.

Whilst mixing largely drives the seasonal differences in peptides there is tentative evidence of biodegradation in the fjord lens. Peptides may be consumed by phytoplankton or bacteria (Mulholland and Lee, 2009) and such processes could

account for the reduced number and intensity of peptide formulae in the surface lens with respect to the rivers (Table 5.6). This pattern is most apparent in winter when overall productivity is higher but the variable compositions of multiple river inputs complicate this trend. Whilst autochthonous production could increase peptide abundance, tightly coupled production and consumption processes might maintain low overall abundance and account for increased N-HUPs if they reflect a pool of degradation products. Selective removal of the most N-rich peptides could explain why the residual peptides in the winter lens exhibit a lower N-content than either the rivers or subsurface samples (Table 5.6), which is not explained by mixing alone. However, differences in N-content are not significant in the MANOVA test. We can only speculate on the consumption of peptides in the fjord lens, but the results are consistent with the view that they can provide a labile source of dissolved N from a larger more refractory pool (Aluwihare *et al.*, 2005; Aluwihare and Meador, 2008).

Table 5.6. Characteristics of peptide-like formulae present in river, surface layer and subsurface fjord samples. Values are means ± SE across all samples of that type. Highlighted rows indicate properties that are significantly different between sample type, identified through a multivariate analysis of variance test (MANOVA, p<0.001).*

	rivers		lens		
	summer	winter	summer	winter	subsurface
No. formulae	140 ± 33	159 ± 79	118 ± 27	76 ± 25	314 ± 20
rel intens (%)	0.32 ± 0.11	0.38 ± 0.24	0.21 ± 0.08	0.11 ± 0.04	0.40 ± 0.02
mass	467.1 ± 11.3	461.2 ± 12.0	450.6 ± 4.2	449.0 ± 5.2	438.3 ± 1.1
C	19.5 ± 0.3	19.6 ± 0.2	19.4 ± 0.2	20.15 ± 0.29	18.71 ± 0.10
H	30.4 ± 0.6	30.4 ± 0.7	30.2 ± 0.3	30.70 ± 0.37	28.96 ± 0.12
O	11.5 ± 0.5	11.2 ± 0.5	10.7 ± 0.2	9.67 ± 0.23	9.82 ± 0.03
N	1.3 ± 0.2	1.2 ± 0.1	1.1 ± 0.0	1.0 ± 0.0	1.2 ± 0.0
S	0.02 ± 0.02	0.00 ± 0.00	0.04 ± 0.02	0.25 ± 0.06	0.37 ± 0.02
H/C	1.57 ± 0.01	1.55 ± 0.02	1.55 ± 0.01	1.52 ± 0.01	1.55 ± 0.00
O/C	0.61 ± 0.02	0.58 ± 0.02	0.57 ± 0.01	0.49 ± 0.01	0.53 ± 0.00
N/C	0.07 ± 0.01	0.06 ± 0.01	0.06 ± 0.00	0.05 ± 0.00	0.07 ± 0.00
AI_{mod}	0.01 ± 0.00	0.02 ± 0.00	0.02 ± 0.00	0.03 ± 0.00	0.02 ± 0.00
DBE	5.91 ± 0.09	6.01 ± 0.09	5.90 ± 0.08	6.32 ± 0.11	5.82 ± 0.04

* A one-way MANOVA was conducted to test whether sample type (as an independent factor variable) affects the characteristics of peptide-like formulae (as dependent continuous variables). A significant multivariate main effect of sample type was found for the highlighted rows (variables: relative intensity, mass, S, O/C and AI_{mod}). The number of formulae for each sample type was excluded from the test as an invalid variable type. Test statistics include Pillai's trace = 0.17; F-test statistic = 75.9; $p < 2.2 \times 10^{-16}$. The null hypothesis of no effect was rejected.

5.5.5. Biogeochemical impacts of changing glacier melt inputs

We have applied, for the first time, spectrofluorescence and ultrahigh resolution mass spectrometry techniques to study seasonal changes in DOM composition in a glaciated fjord. Our data suggest an overall transition from aromatic and humic-rich signatures to increasingly aliphatic and heteroatom-rich DOM along a declining salinity gradient, akin to patterns in temperate and tropical estuaries (Medeiros *et al.*, 2015; Osterholz *et al.*, 2016; Seidel *et al.*, 2017). However, we note unique influences from glaciers which provide direct contributions of DOM, control conservative mixing patterns and regulate primary production of autochthonous DOM. From these results we infer the following biogeochemical impacts of enhanced glacier melting on the BMF, which may highlight potential sensitivities in other glaciated fjords.

1. **Reduced efficiency of the fjord as a carbon sink.** The summertime reduction in autochthonous DOM is consistent with the suppression of primary productivity by glacier melt inputs. These may become increasingly influential in Patagonian fjords if meltwater fluxes comprise an increasing fraction of total freshwater discharge to the ocean. Such conditions are facilitated by enhanced melting of the icefields (Foresta *et al.*, 2018) and a regional decline in rainfall, which has been linked to shifting wind patterns and climate change (Garreaud *et al.*, 2013; Garreaud, 2018; Aguayo *et al.*, 2019). The overall effects of increased light and nutrient limitation will lead to lower rates of carbon fixation and smaller standing stocks of carbon in the pelagic foodweb. Although we make no assessment of how efficiently new biomass is exported to sediments in the BMF, the total flux will likely decline along with standing stocks (Aracena *et al.*, 2011). As a result, fjord sediments will become increasingly dominated by older terrestrial carbon rather than fresh biological sources and glaciated fjords in Patagonia (and elsewhere) may play a reduced role in carbon sequestration (Rebolledo *et al.*, 2019). The severity of these effects and impact on regional carbon budgets will depend on the strength and duration of the melt season and the influence of lakes. Earlier onset and more intense melting would allow conditions less favourable to primary productivity to persist for longer and increasingly offset carbon fixation over the remainder of the year. Newly formed and expanding freshwater lakes in deglaciating valleys may act as sediment traps (Carrivick and Tweed, 2013; Wilson *et al.*, 2018) and buffer the downstream impact of glacial meltwaters. Fjords are recognised as globally important carbon sinks

(Smith *et al.*, 2015; Cui *et al.*, 2016), but those in glaciated regions may sensitive to increased runoff from land-terminating glaciers (Aracena *et al.*, 2011).

2. **Carbon cycling will be increasingly influenced by allochthonous DOM.** As stronger meltwater discharge suppresses primary productivity and reduces marine water influence by conservative mixing, in-washed allochthonous DOM may become an increasingly important resource for marine heterotrophs (González *et al.*, 2013). The overall reactivity of this material will relate to its bulk composition and any upstream degradation processes. The competitive advantage of glacial biota in the fjord at times of high melt input might favour the continued removal of any labile components in glacially-derived DOM (Gutiérrez *et al.*, 2015; Paulsen *et al.*, 2018). However, higher river flows or meltwaters draining through soils and wetlands may access more non-glacial sources of aromatic and humic DOM (Young, 2014), which may become a relatively important substrate for heterotrophs in the absence of more labile components (Mostovaya *et al.*, 2017). Future studies should assess changes in the lability of DOM in both the fjord and surrounding rivers over an annual cycle to identify the impact of changing melt inputs on carbon cycling processes.

3. **Changes in organic nitrogen substrates available to fjord communities.** The availability and composition of reactive organic nitrogen compounds, such as peptides, appears linked to changes in glacier melt inputs which affect primary production and the mixing balance of marine and riverine waters. Nitrogen cycling may therefore be sensitive to changes in peptide supply, if different peptides favour specific species, and to changes in planktonic community structure linked to water mass, if different species preferentially utilise different components of DOM (Liu *et al.*, 2017). Future investigations should attempt to isolate the lability of different peptide sources and directly address their role in nitrogen cycling in the fjord. This could be critical for other glaciated fjords or high Arctic seas, where nitrogen-limitation is often observed (Rysgaard *et al.*, 1999).

4. **An intensification of the above processes during GLOFs.** The failure of ice-dammed lakes along the margins of the NPI are occurring with increasing frequency and may create more temporary disturbances to ecosystem function and organic matter cycling in the BMF (Dussaillant *et al.*, 2012; Anacona *et al.*, 2015; Meerhoff

et al., 2019). The exact composition of GLOF waters and their variation is unclear, but it is reasonable to assume a similar character to average summer discharge except with higher POM loadings due to the rapid mobilisation of sediments during these events. Overall, a stronger, more turbid freshwater pulse is likely to reinforce summertime conditions in the fjord. These disturbances might also trigger a shift in zooplankton community structure, favouring those species able to utilise the increased abundance of terrestrial POM as a food source (Quiroga *et al.*, 2016; Meerhoff *et al.*, 2019). Moreover, the typical timing of GLOFs either side of the main melt season, when primary production might otherwise be less light limited, could interrupt the seasonal progression of the fjord ecosystem at potentially critical stages in species' life cycles (González *et al.*, 2013; Aniya, 2014, 2017).

5. **Expansion of the above conditions to fjords with marine-terminating glaciers on the western side of the SPI.** Taking the Jorge Montt Fjord as an example, ultimate glacier retreat onto land (Rivera *et al.*, 2012) will lead to a reduced primary productivity in that particular sub-fjord. Conditions here may therefore converge with those in Steffen Fjord or the Baker and Pascua River plumes, where turbid river discharge exerts an overriding control on biogeochemical processes. In particular, the enhanced peptide and protein-like signals in the surface lens of Jorge Montt Fjord will be sensitive to glacier retreat, regardless of whether they indicate a present-day state of enhanced local production (Meire *et al.*, 2017; Hopwood *et al.*, 2018), upwelling of subglacial meltwaters (Dubnick *et al.*, 2010) or sub-marine melting (Moffat *et al.*, 2018).

5.6. Conclusions

Rivers supply a major source of organic matter to the BMF and may dominate the supply of labile material during peak discharge. Unlike other glacially dominated landscapes, organic matter export is driven by dissolved phases which could have a more profound impact on biogeochemical processes via the microbial loop. The significance of terrestrial subsidies may be reinforced by the suppression of autochthonous DOM production under more turbid conditions. Seasonal changes in fjord DOM composition show the increase in protein-like signatures linked to enhanced glacier melt in summer and a shift towards aliphatic and unsaturated compounds

characteristic of enhanced phytoplankton activity in winter. The overall transition along the salinity gradient is consistent with typical estuarine patterns, showing the removal of terrestrial aromatics and humic-rich material in surface waters and the increasing influence of unsaturated and heteroatom-rich marine DOM. We note that the impact of labile protein-like material in summer river fluxes may be limited to food webs at the fjord heads. Despite probable in-fjord production, protein-like signals are not linked with nitrogen-rich organic matter. Instead DON concentrations may be driven by marine compounds which offer limited lability to heterotrophs in the surface layer. A seasonal shift from terrestrially sourced peptide-like formulae in summer to more marine compounds in winter may have a strong influence over the dynamic uptake of this more reactive sub-pool of nitrogen-containing DOM. However, the exact lability of fjord DOM over the annual cycle has not been explicitly tested and should be a focus of future research to evaluate the impact of glacier melt on organic matter cycling. A stronger and more widespread control on fjord biogeochemistry by glacial and riverine DOM is expected as climate change leads to more intense and prolonged glacier melt seasons and the ongoing retreat of the Patagonian icefields.

6. Thesis conclusions

The overarching aim of this thesis was to provide the first regional scale assessment of the potential impact of changing glacier melt inputs on organic matter in aquatic systems in Chilean Patagonia. This helps contribute towards a global assessment of how glacier retreat affects downstream biogeochemistry. The following sections summarise the main findings of each analytical chapter.

6.1. Summary of main findings

6.1.1. Deglaciation-induced landscape change affects the composition and export of organic matter in Chilean Patagonian rivers (Chapter 3)

This study used quantitative and high-resolution composition data to assess how freshwater fluxes of organic matter are influenced by landscape factors in contiguous river catchments across Chilean Patagonia (42–48°S). The principles of space-for-time substitution were used to infer how landscape change arising from deglaciation might alter organic carbon cycling and freshwater biogeochemistry.

Main findings:

- Glaciers in Chilean Patagonia drive higher catchment yields of POC and export DOM that is relatively enriched in protein-like and aliphatic signatures when compared to non-glacial rivers, consistent with observations from glaciated regions in the northern hemisphere. However, the overall strength of these signals is relatively muted in Chilean Patagonia due to the modulating effects of organic matter sinks and sources in the downstream landscape.
- From the available data and analytical approach taken, it is not possible to verify whether the glaciers of Chilean Patagonia are a source of anthropogenic carbon to downstream ecosystems, as has been suggested for glaciers in the northern hemisphere and downwind of industry.
- Freshwater lakes are important sinks for organic carbon and may become increasingly influential as they expand in response to glacier retreat. Proglacial lakes may be particularly effective in trapping sediments and POM and enabling

other landscape covers (e.g. vegetation, wetlands) to become the dominant drivers of DOM composition in downstream rivers.

- In the long term, a shift in the hydrological regimes of catchments undergoing significant deglaciation would mean that organic matter export becomes less influenced by seasonal meltwater cycles. Correspondingly, freshwater biota may be increasingly subject to stochastic delivery of organic matter from non-glacial sources (e.g. vegetation, wetlands, soils), driven by weather events.

This chapter presented the first regional scale assessment of riverine organic matter fluxes and their composition in Chilean Patagonia, and hypothesised the biogeochemical implications of ongoing deglaciation.

6.1.2. Potential vegetation controls on the bioavailability of dissolved organic matter in deglaciating catchments of Chilean Patagonia (Chapter 4)

This study used incubation experiments to test the bioavailability of DOC in catchments with relatively low levels of glacier cover (a sub-region of the study area used in Chapter 3). The results from these incubations were combined with insights from regional scale trends in DOM composition to identify the character and potential sources of bioavailable material. This allowed assessment of factors which may exert an increasing control over aquatic organic matter cycling following extensive glacier retreat.

Main findings:

- BDOC is proportionately lower in Chilean Patagonian rivers (7–23%) than in glaciated regions of the northern hemisphere (31–69%), and even for catchments from those regions with comparable glacier cover (<40%).
- Low BDOC in Chilean Patagonia may be due to intrinsic compositional factors (such as low nitrogen content, higher molecular mass and aromaticity), which could result from preferential removal of labile components due to significant processing of DOM in lakes prior to downstream export.
- All sampled rivers display a consistent pattern of bioavailability which relates DOC consumption to a sub-pool of DOM associated with tryptophan-like fluorescence and nitrogen-rich polyphenolic formulae. These compounds suggest a source of DOM from decaying leaf litter (potentially related to broadleaf

evergreen forest cover), which may exert an increasing control over DOM bioavailability in catchments with diminished glacier cover.

This chapter presented the first estimates of DOM bioavailability derived from incubation studies in Chilean Patagonian rivers. The results contrasted with those from other glaciated regions insofar as no systematic relationship between DOM bioavailability and catchment glacier cover could be determined. This study highlighted the potential role for vegetation influences to override other controls on organic matter cycling in Chilean Patagonia.

6.1.3. Organic matter composition in a Patagonian fjord linked to changing glacier melt inputs (Chapter 5)

This study explored the impact of changing glacier melt inputs on organic matter cycling in a glacially influenced fjord through the analysis of seasonal changes in DOM composition. Spatiotemporal patterns in DOM composition helped to distinguish contributions of material from glacial, other terrestrial and marine sources. This complemented findings from the other chapters which inferred the impacts of glacial meltwaters on downstream biogeochemistry from terrestrial perspectives.

Main findings:

- Riverine inputs of DOM comprise a significant fraction (possibly up to 57%) of the total organic matter pool in the Baker-Martinez Fjord and may be an important resource for microbial ecosystems, especially where turbid glacial meltwaters suppress fresh organic matter production.
- Peak river discharge, linked to summertime glacier melting, is associated with:
    i. increased inputs of terrestrial DOM (including contributions of protein-rich DOM from glaciers) to the surface layer of the fjord
    ii. reduced vertical mixing of marine DOM from depth
    iii. the suppression of fresh autochthonous DOM production.
- Conditions in the Jorge Montt Fjord reflect year-round influences from melting of the marine-terminating glacier.
- The Baker-Martinez Fjord exhibits variations in DOM composition along a salinity gradient that are consistent with those observed in temperate estuaries. These show a transition from aromatic and humic-rich DOM, derived from

terrestrial sources, to more aliphatic and heteroatom rich DOM, from marine sources.

- Seasonal variations in the composition of peptides in the fjord surface lens may be linked to changes in meltwater inputs and vertical mixing, and suggest a role for these compounds (which represent a small sub-pool of nitrogen containing DOM) in organic nitrogen cycling.

This chapter presented the first molecular level data to describe seasonal variations in DOM composition for a glacially influenced fjord. The findings suggest that strong glacial meltwater inputs may hamper autochthonous DOM production and exert a strong control on conservative mixing with marine water sources. The results are consistent with the hypothesis that land- and marine-terminating glaciers exert different controls on fjord biogeochemistry.

6.2. Wider implications of findings

This thesis has provided the first regional scale assessment of the potential impact of changing glacier melt inputs on organic matter in aquatic systems in Chilean Patagonia. The wider implications of its findings are summarised below.

6.2.1. Glacial organic matter

In order to make meaningful claims about the contributions of glaciers to aquatic biogeochemistry it is necessary to understand those contributions within a regional context. This thesis has offered a landscape-level perspective on the sources and cycling of organic matter in an understudied glaciated region. The character of the proglacial environment modulates the downstream transfer of glacial organic matter and imposes a significant influence on riverine biogeochemistry.

The landscape-level approach taken in this thesis has confirmed certain findings obtained in other studies via more direct glacial sampling. For example, data from Chilean Patagonia confirm the ubiquity of microbial influences on glacial DOM (Dubnick *et al.*, 2010). However, although studies in the northern hemisphere have posited a link between anthropogenic carbon and glacial meltwater (Stubbins *et al.*, 2012), this cannot be confirmed by available evidence from Chilean Patagonia. If there

is such a relationship in this region, it may be more difficult to detect in samples subject to more varied sources of richer organic matter, which could overwhelm glacial influences in Chilean Patagonia. Similarly, the bioavailability of organic matter should be understood within a regional context. Bioavailability is a relative concept and so the lability of glacial organic matter may only be properly evaluated in comparison to other potential sources within a study region.

Having established the significance of regional landscape on organic matter in aquatic systems, it follows that changes to the landscape will impact upon those systems. Such impacts have been identified in other studies of non-glacial regions (Aufdenkampe *et al.*, 2011; Asmala *et al.*, 2016). The space-for-time methodology offered in this thesis illustrates a complex array of controls on riverine organic matter fluxes through the emergence of new sources and sinks linked to deglaciation. This thesis may therefore serve as a foundation for investigations into the effect of future landscape change on organic matter cycling in Chilean Patagonia.

6.2.2. Freshwater lakes

Lakes are growing in number and size as glaciers retreat in Chilean Patagonia (Wilson *et al.*, 2018). The evidence presented in this thesis is consistent with the established position that freshwater lakes act as effective carbon sinks and that this function scales with lake size and residence time (Tranvik *et al.*, 2009; Catalán *et al.*, 2016; Evans *et al.*, 2017). However, the data here suggest that this role of lakes is more pronounced in glacial than non-glacial catchments. This informs how the biogeochemical function of lakes evolves in response to changing connectivity with glaciers (Carrivick and Tweed, 2013; Sommaruga, 2014). Since this thesis has established a significant role for freshwater lakes in regulating organic matter export in glacial catchments, an understanding of carbon cycling in Chilean Patagonia should rest upon a comprehensive assessment of freshwater ecology and biogeochemistry across the different lakes of this region.

6.2.3. Carbon cycling in glaciated fjords

Data presented here are consistent with the view emerging from carbon production and burial studies in Patagonian fjords, that glaciers may exert a negative control on primary

production (Aracena *et al.*, 2011; Rebolledo *et al.*, 2019). The extent to which the findings from Chilean Patagonia are regionally specific or representative of other glaciated fjords is uncertain and necessitates further investigation. In other glaciated regions (e.g. Gulf of Alaska) glaciers are thought to supply highly reactive organic matter and stimulate carbon cycling by marine bacteria, although most studies infer these effects from terrestrial samples (Hood *et al.*, 2009; Fellman *et al.*, 2014). In contrast, fjord-based studies in Greenland suggest that autochthonous DOM could provide a more significant resource to marine bacteria (Paulsen *et al.*, 2018). Data from Baker-Martinez Fjord highlight variations in DOM composition corresponding to influences from marine- and land-terminating glaciers. These variations suggest that organic carbon cycling in fjords may depend on the degree of connectivity with glaciers. This engages with mounting evidence that marine-terminating glaciers sustain more productive fjord ecosystems, subject to other factors, such as fjord geometry (Meire *et al.*, 2017; Hopwood *et al.*, 2018, 2019).

6.2.4. Organic nitrogen cycling

Incubation results identified a potential link between DOM bioavailability and nitrogen-containing polyphenolic compounds (likely derived from vascular plants) in several northern (42–45°S) catchments. Whether these provide a reactive substrate to bacteria or control the accessibility of tryptophan-like substances through binding is uncertain. The rapid removal of tryptophan-like fluorescence from river waters entering the Baker-Martinez Fjord suggests that similar controls on DOM bioavailability may also operate in this more southerly region (48°S). In this same fjord, seasonal variations in peptide composition may suggest that a relatively minor constituent of the total organic nitrogen pool plays a disproportionate role in biogeochemical processes. The available evidence highlights a potential role for organic matter in nitrogen cycling across the aquatic continuum in Chilean Patagonia, which may be representative of other nitrogen-limited systems (Brookshire *et al.*, 2005, 2007).

6.3. Opportunities for further study

The limitations pertaining to the methodologies and analyses deployed in this thesis are outlined in the relevant chapters. The principal factor limiting the scope of research, which is common to all chapters, relates to the availability of appropriate samples from

Chilean Patagonia. This section will identify potential opportunities for further study which could address the issues raised by this principal limitation.

- **Direct sampling of glacial snow, ice and runoff.** Direct sampling would enable better characterisation of glacial signatures, which could then be traced through the hydrological network. This would complement the landscape-level perspectives provided in Chapters 3 and 4 and overcome the limitations associated with samples collected far downstream of glaciers. For example, it would also help to confirm if Chilean Patagonian glaciers are a source of stored anthropogenic pollutants, which could have important implications for freshwater ecology and water quality in glacial rivers.

- **Higher resolution sampling.** More frequent sampling from a single site would enable more reliable characterisation of conditions. This would help to overcome the limitations associated with samples collected from a single moment in time, which may be less representative due to random variabilities (e.g. rain events). For example, extended monitoring periods across multiple seasons would capture seasonal changes and provide data to estimate annual catchment fluxes more reliably. Moreover, year-round sampling within the Baker-Martinez Fjord would encompass the spring bloom period, which may be the most significant period of primary production in this system (Meerhoff *et al.*, 2014), and how it is affected by the onset of glacier melting. Furthermore, collecting samples from a wider range of sites within a single river catchment could provide insight into changes in organic matter composition between sites. This would provide higher resolution spatial data to test the findings from the regional-scale assessment of landscape level controls provided in Chapters 3 and 4.

- **Extend scope of BDOC incubations.** Taking larger volume samples offers greater analytical potential to directly monitor changes in composition (e.g. at the molecular level) over incubation experiments. This would test the findings of Chapter 4, which inferred compositional changes indirectly from regional data. Extending incubation studies to more locations across the region would provide better insight into carbon cycling processes across the aquatic continuum. For example, incubating samples

from catchments with higher glacier cover would enhance the findings from Chapter 4, allowing more robust assessment of glacial influences in Chilean Patagonia. Also, incubation of fjord waters would complement the study of terrestrial systems in Chapter 4 and allow direct measurement of fjord DOM bioavailability which is inferred from compositional data in Chapter 5.

- **Better POM characterisation.** Larger volume particulate samples would allow more comprehensive analysis (elemental, isotopic, biomarker extraction) to characterise its sources and processing in Chilean Patagonia. For example, this would improve understanding of how particulate material contributes to carbon cycling and burial processes in the lakes and fjords of Patagonia (Rebolledo *et al.*, 2019). Such investigations would balance the dominant focus on DOM in this thesis.

- **Direct sampling of proglacial and other freshwater lakes.** Focused study of organic matter composition and processing in freshwater lakes, enabling a comparison between glacial and non-glacial lakes, would help to test the suggestion in Chapter 3 that they may have different biogeochemical influences. Moreover, it would enable a better understanding of DOM transformation processes in lakes, which was highlighted in Chapter 4 as a potential factor controlling bioavailability.

- **Application of FT-ICR MS to other glaciated fjords.** Conducting FT-ICR MS analysis on samples from other glaciated fjords would test how far the findings of Chapter 5 are representative of similar landscapes within and beyond Chilean Patagonia.

- **Application of radiocarbon analyses to investigation of organic matter.** Radiocarbon analysis of DOC has revealed potentially unique carbon cycling processes in glaciated regions of the northern hemisphere (Hood *et al.*, 2009; Spencer *et al.*, 2014b). Whilst this thesis has begun to assess the role of glaciers on organic carbon cycling in Chilean Patagonia, understanding could be greatly advanced through radiocarbon analyses. The results of such analyses could then be directly compared with data from other glaciated regions.

7. References

Abarzúa, A. M., Villagrán, C. and Moreno, P. I. (2004) Deglacial and postglacial climate history in east-central Isla Grande de Chiloé, southern Chile (43°S), *Quaternary Research*. doi: 10.1016/j.yqres.2004.04.005.

Aguayo, R., León-Muñoz, J., Vargas-Baecheler, J., Montecinos, A., Garreaud, R., Urbina, M., Soto, D. and Iriarte, J. L. (2019) The glass half-empty: climate change drives lower freshwater input in the coastal system of the Chilean Northern Patagonia, *Climatic Change*. doi: 10.1007/s10584-019-02495-6.

Aiken, C. M. (2012) Seasonal thermal structure and exchange in Baker Channel, Chile, *Dynamics of Atmospheres and Oceans*, 58, p. 1–19. doi: 10.1016/J.DYNATMOCE.2012.07.001.

Aiken, G. (2014) Fluorescence and Dissolved Organic Matter, in Baker, A. et al. (eds) *Aquatic Organic Matter Fluorescence*. Cambridge: Cambridge University Press (Cambridge Environmental Chemistry Series), p. 35–74. doi: 10.1017/CBO9781139045452.005.

Aluwihare, L. I., Repeta, D. J., Pantoja, S. and Johnson, C. G. (2005) Two chemically distinct pools of organic nitrogen accumulate in the ocean, *Science*. doi: 10.1126/science.1108925.

Aluwihare, L. I. and Meador, T. (2008) Chemical Composition of Marine Dissolved Organic Nitrogen, in *Nitrogen in the Marine Environment*. doi: 10.1016/B978-0-12-372522-6.00003-7.

Amaral, V., Graeber, D., Calliari, D. and Alonso, C. (2016) Strong linkages between DOM optical properties and main clades of aquatic bacteria, *Limnology and Oceanography*, 61(3), p. 906–918. doi: 10.1002/lno.10258.

Anacona, P. I., Mackintosh, A. and Norton, K. P. (2015) Hazardous processes and events from glacier and permafrost areas: Lessons from the Chilean and Argentinean Andes, *Earth Surface Processes and Landforms*, 40(1), p. 2–21. doi: 10.1002/esp.3524.

Andersen, C. M. and Bro, R. (2003) Practical aspects of PARAFAC modeling of fluorescence excitation-emission data, *Journal of Chemometrics*. doi: 10.1002/cem.790.

Andersson, A. and Rudehall, A. (1993) Proportion of plankton biomass in particulate organic carbon in the northern Baltic Sea, *Marine Ecology Progress Series*. doi: 10.3354/meps095133.

Anesio, A. M. A. M., Hodson, A. J., FRITZ, A., Psenner, R. and Sattler, B. (2009) High microbial activity on glaciers: Importance to the global carbon cycle, *Global Change Biology*, 15(4), p. 955–960. doi: 10.1111/j.1365-2486.2008.01758.x.

Anesio, A. M., Lutz, S., Chrismas, N. A. M. and Benning, L. G. (2017) The microbiome of glaciers and ice sheets, *npj Biofilms and Microbiomes*, 3(1), p. 10. doi: 10.1038/s41522-017-0019-0.

Anesio, A. M. and Laybourn-Parry, J. (2012) Glaciers and ice sheets as a biome, *Trends in Ecology & Evolution*, 27(4), p. 219–225. doi: 10.1016/j.tree.2011.09.012.

Anesio, A. M., Sattler, B., Foreman, C., Telling, J., Hodson, A., Tranter, M. and Psenner, R. (2010) Carbon fluxes through bacterial communities on glacier surfaces, *Annals of Glaciology*. doi: 10.3189/172756411795932092.

Aniya, M. (2014) GLOF of a side-lake, Laguna de los Tempanos, of Glaciar Steffen, Hielo Patagonico Norte, South America, *Summaries of JSSI and JSSE Joint Conference on Snow and Ice Research*, 2014, p. 7. doi: 10.14851/jcsir.2014.0_7.

Aniya, M. (2017) Glacier variations of Hielo Patagónico Norte, Chile, over 70 years from 1945 to 2015, *Bulletin of Glaciological Research*. doi: 10.5331/bgr.17R01.

Antony, R., Grannas, A. M., Willoughby, A. S., Sleighter, R. L., Thamban, M. and Hatcher, P. G. (2014) Origin and Sources of Dissolved Organic Matter in Snow on the East Antarctic Ice Sheet, *Environmental Science & Technology*, 48(11), p. 6151–6159. doi: 10.1021/es405246a.

Antony, R., Willoughby, A. S., Grannas, A. M., Catanzano, V., Sleighter, R. L., Thamban, M., Hatcher, P. G. and Nair, S. (2017) Molecular Insights on Dissolved Organic Matter Transformation by Supraglacial Microbial Communities, *Environmental Science and Technology*. doi: 10.1021/acs.est.6b05780.

Aracena, C., Lange, C. B., Rebolledo, L., Iriarte, J. L., Rebolledo, L. and Pantoja, S. (2011) Latitudinal patterns of export production recorded in surface sediments of the Chilean Patagonian fjords (41–55°S) as a response to water column productivity, *Continental Shelf Research*, 31(3–4), p. 340–355. doi: 10.1016/j.csr.2010.08.008.

Arienzo, M. M., McConnell, J. R., Murphy, L. N., Chellman, N., Das, S., Kipfstuhl, S. and Mulvaney, R. (2017) Holocene black carbon in Antarctica paralleled Southern Hemisphere climate, *Journal of Geophysical Research*. doi: 10.1002/2017JD026599.

Arimitsu, M. L., Hobson, K. A., Webber, D. N., Piatt, J. F., Hood, E. W. and Fellman, J. B. (2018) Tracing biogeochemical subsidies from glacier runoff into Alaska's coastal marine food webs, *Global Change Biology*. doi: 10.1111/gcb.13875.

Arimitsu, M. L., Piatt, J. F. and Mueter, F. (2016) Influence of glacier runoff on ecosystem structure in Gulf of Alaska fjords, *Marine Ecology Progress Series*. doi: 10.3354/meps11888.

Armbruster, D. A. and Pry, T. (2008) Limit of blank, limit of detection and limit of quantitation, *The Clinical Biochemist Reviews*, 29 (Suppl 1), p. S49–S52.

Armesto, J. J., Casassa, I. and Dollenz, O. (1992) Age structure and dynamics of Patagonian beech forests in Torres del Paine National Park, Chile, *Vegetatio*. doi: 10.1007/BF00031633.

Arora-Williams, K., Olesen, S. W., Scandella, B. P., Delwiche, K., Spencer, S. J., Myers, E. M., Abraham, S., Sooklal, A. and Preheim, S. P. (2018) Dynamics of microbial populations mediating biogeochemical cycling in a freshwater lake, *Microbiome*. doi: 10.1186/s40168-018-0556-7.

Artifon, V., Zanardi-Lamardo, E. and Fillmann, G. (2019) Aquatic organic matter: Classification and interaction with organic microcontaminants, *Science of the Total Environment*. doi: 10.1016/j.scitotenv.2018.08.385.

Asmala, E., Kaartokallio, H., Carstensen, J. and Thomas, D. N. (2016) Variation in riverine inputs affect dissolved organic matter characteristics throughout the estuarine gradient, *Frontiers in Marine Science*. doi: 10.3389/fmars.2015.00125.

Aufdenkampe, A. K., Hedges, J. I., Richey, J. E., Krusche, A. V. and Llerena, C. A. (2001) Sorptive fractionation of dissolved organic nitrogen and amino acids onto fine sediments within the Amazon Basin, *Limnology and Oceanography*. doi: 10.4319/lo.2001.46.8.1921.

Aufdenkampe, A. K., Mayorga, E., Raymond, P. A., Melack, J. M., Doney, S. C., Alin, S. R., Aalto, R. E. and Yoo, K. (2011) Riverine coupling of biogeochemical cycles between land, oceans, and atmosphere, in *Frontiers in Ecology and the Environment*. doi: 10.1890/100014.

Azam, F., Smith, D. C., Steward, G. F. and Hagström, Å. (1994) Bacteria-organic matter coupling and its significance for oceanic carbon cycling, *Microbial Ecology*. doi: 10.1007/BF00166806.

Badr, E.-S. A., Tappin, A. D. and Achterberg, E. P. (2008) Distributions and seasonal variability of dissolved organic nitrogen in two estuaries in SW England, *Marine Chemistry*, 110(3–4), p. 153–164. doi: 10.1016/J.MARCHEM.2008.04.007.

Bai, L., Cao, C., Wang, C., Xu, H., Zhang, H., Slaveykova, V. I. and Jiang, H. (2017) Toward Quantitative Understanding of the Bioavailability of Dissolved Organic Matter in Freshwater Lake during Cyanobacteria Blooming, *Environmental Science and Technology*. doi: 10.1021/acs.est.7b00826.

Barker, J. D., Dubnick, A., Lyons, W. B. and Chin, Y. P. (2013) Changes in Dissolved Organic Matter (DOM) Fluorescence in Proglacial Antarctic Streams, *Arctic, Antarctic, and Alpine Research*, 45(3), p. 305–317. doi: 10.1657/1938-4246-45.3.305.

Barker, J. D., Sharp, M. J. and Turner, R. J. (2009) Using synchronous fluorescence spectroscopy and principal components analysis to monitor dissolved organic matter dynamics in a glacier system,

Hydrological Processes, 23(10), p. 1487–1500. doi: 10.1002/hyp.7274.

Barker, J. D., Sharp, M. J., Fitzsimons, S. J. and Turner, R. J. (2006) Abundance and Dynamics of Dissolved Organic Carbon in Glacier Systems, *Arctic, Antarctic, and Alpine Research*, 38(2), p. 163–172. doi: 10.1657/1523-0430(2006)38[163:AADODO]2.0.CO;2.

Barrera, F., Lara, R. J., Krock, B., Garzón-Cardona, J. E., Fabro, E. and Koch, B. P. (2017) Factors influencing the characteristics and distribution or surface organic matter in the Pacific-Atlantic connection, *Journal of Marine Systems*. doi: 10.1016/j.jmarsys.2017.07.004.

Bartholomew, I., Nienow, P., Sole, A., Mair, D., Cowton, T., Palmer, S. and Wadham, J. (2011) Supraglacial forcing of subglacial drainage in the ablation zone of the Greenland ice sheet, *Geophysical Research Letters*. doi: 10.1029/2011GL047063.

Battin, T. J., Besemer, K., Bengtsson, M. M., Romani, A. M. and Packmann, A. I. (2016) The ecology and biogeochemistry of stream biofilms, *Nature Reviews Microbiology*. doi: 10.1038/nrmicro.2016.15.

Battin, T. J., Kaplan, L. A., Findlay, S., Hopkinson, C. S., Marti, E., Packman, A. I., Newbold, J. D. and Sabater, F. (2008) Biophysical controls on organic carbon fluxes in fluvial networks, *Nature Geoscience*, 1(2), p. 95–100. doi: 10.1038/ngeo101.

Battin, T. J., Luyssaert, S., Kaplan, L. A., Aufdenkampe, A. K., Richter, A. and Tranvik, L. J. (2009) The boundless carbon cycle, *Nature Geoscience*. doi: 10.1038/ngeo618.

Bauer, J. E. and Bianchi, T. S. (2012) Dissolved Organic Carbon Cycling and Transformation, in *Treatise on Estuarine and Coastal Science*. doi: 10.1016/B978-0-12-374711-2.00502-7.

Benjamini, Y. and Hochberg, Y. (1995) Controlling the False Discovery Rate: A Practical and Powerful Approach to Multiple Testing, *Journal of the Royal Statistical Society: Series B (Methodological)*, 57(1), p. 289–300. doi: 10.1111/j.2517-6161.1995.tb02031.x.

Benner, R. and Kaiser, K. (2011) Biological and photochemical transformations of amino acids and lignin phenols in riverine dissolved organic matter, *Biogeochemistry*. doi: 10.1007/s10533-010-9435-4.

Bhatia, M. P., Das, S. B., Longnecker, K., Charette, M. A. and Kujawinski, E. B. (2010) Molecular characterization of dissolved organic matter associated with the Greenland ice sheet, *Geochimica et Cosmochimica Acta*, 74(13), p. 3768–3784. doi: 10.1016/j.gca.2010.03.035.

Bhatia, M. P. M. P., Das, S. B. S. B., Xu, L., Charette, M. A. M. A., Wadham, J. L. J. L. and Kujawinski, E. B. E. B. (2013) Organic carbon export from the Greenland ice sheet, *Geochimica et Cosmochimica Acta*, 109, p. 329–344. doi: 10.1016/j.gca.2013.02.006.

Bittar, T. B., Berger, S. A., Birsa, L. M., Walters, T. L., Thompson, M. E., Spencer, R. G. M., Mann, E. L., Stubbins, A., Frischer, M. E. and Brandes, J. A. (2016) Seasonal dynamics of dissolved, particulate and microbial components of a tidal saltmarsh-dominated estuary under contrasting levels of freshwater discharge, *Estuarine, Coastal and Shelf Science*. doi: 10.1016/j.ecss.2016.08.046.

Bogdal, C., Scheringer, M., Abad, E., Abalos, M., Van Bavel, B., Hagberg, J. and Fiedler, H. (2013) Worldwide distribution of persistent organic pollutants in air, including results of air monitoring by passive air sampling in five continents, *TrAC - Trends in Analytical Chemistry*. doi: 10.1016/j.trac.2012.05.011.

Bolan, N. S., Baskaran, S. and Thiagarajan, S. (1996) An evaluation of the methods of measurement of dissolved organic carbon in soils, manures, sludges, and stream water, *Communications in Soil Science and Plant Analysis*. doi: 10.1080/00103629609369735.

Boyd, E. S., Skidmore, M., Mitchell, A. C., Bakermans, C. and Peters, J. W. (2010) Methanogenesis in subglacial sediments, *Environmental Microbiology Reports*, 2(5), p. 685–692. doi: 10.1111/j.1758-2229.2010.00162.x.

Boyd, E. S., Hamilton, T. L., Havig, J. R., Skidmore, M. L. and Shock, E. L. (2014) Chemolithotrophic primary production in a subglacial ecosystem, *Applied and Environmental Microbiology*. doi:

10.1128/AEM.01956-14.

Boyd, E. S., Lange, R. K., Mitchell, A. C., Havig, J. R., Hamilton, T. L., Lafrenière, M. J., Shock, E. L., Peters, J. W. and Skidmore, M. (2011) Diversity, abundance, and potential activity of nitrifying and nitrate-reducing microbial assemblages in a subglacial ecosystem, *Applied and Environmental Microbiology*, 77(14), p. 4778–4787. doi: 10.1128/AEM.00376-11.

Breault, R. F., Colman, J. A., Aiken, G. R. and Mcknight, D. (1996) Copper speciation and binding by organic matter in copper-contaminated streamwater, *Environmental Science and Technology*. doi: 10.1021/es9601301.

Brett, M. T., Bunn, S. E., Chandra, S., Galloway, A. W. E., Guo, F., Kainz, M. J., Kankaala, P., Lau, D. C. P., Moulton, T. P., Power, M. E., Rasmussen, J. B., Taipale, S. J., Thorp, J. H. and Wehr, J. D. (2017) How important are terrestrial organic carbon inputs for secondary production in freshwater ecosystems?, *Freshwater Biology*, 62(5), p. 833–853. doi: 10.1111/fwb.12909.

Bro, R. and Kiers, H. A. L. (2003) A new efficient method for determining the number of components in PARAFAC models, *Journal of Chemometrics*. doi: 10.1002/cem.801.

Brogi, S. R., Jung, J. Y., Ha, S. Y. and Hur, J. (2019) Seasonal differences in dissolved organic matter properties and sources in an Arctic fjord: Implications for future conditions, *Science of the Total Environment*. doi: 10.1016/j.scitotenv.2019.133740.

Brookshire, E. N. J., Valett, H. M., Thomas, S. A. and Webster, J. R. (2005) Coupled cycling of dissolved organic nitrogen and carbon in a forest stream, *Ecology*, 86(9), p. 2487–2496. doi: 10.1890/04-1184.

Brookshire, E. N. J., Valett, H. M., Thomas, S. A. and Webster, J. R. (2007) Atmospheric N deposition increases organic N loss from temperate forests, *Ecosystems*. doi: 10.1007/s10021-007-9019-x.

Brown, L. E., Hannah, D. M. and Milner, A. M. (2007) Vulnerability of alpine stream biodiversity to shrinking glaciers and snowpacks, *Global Change Biology*. doi: 10.1111/j.1365-2486.2007.01341.x.

Brym, A., Paerl, H. W., Montgomery, M. T., Handsel, L. T., Ziervogel, K. and Osburn, C. L. (2014) Optical and chemical characterization of base-extracted particulate organic matter in coastal marine environments, *Marine Chemistry*, 162, p. 96–113. doi: 10.1016/J.MARCHEM.2014.03.006.

Burd, A. B., Frey, S., Cabre, A., Ito, T., Levine, N. M., Lønborg, C., Long, M., Mauritz, M., Thomas, R. Q., Stephens, B. M., Vanwalleghem, T. and Zeng, N. (2016) Terrestrial and marine perspectives on modeling organic matter degradation pathways, *Global Change Biology*. doi: 10.1111/gcb.12987.

Bustamante, M. S. (2009) The southern Chilean fjord region: oceanographic aspects, *Marine benthic fauna of chilean patagonia*.

Calleja, M. L., Kerhervé, P., Bourgeois, S., Kędra, M., Leynaert, A., Devred, E., Babin, M. and Morata, N. (2017) Effects of increase glacier discharge on phytoplankton bloom dynamics and pelagic geochemistry in a high Arctic fjord, *Progress in Oceanography*, 159, p. 195–210. doi: 10.1016/J.POCEAN.2017.07.005.

Calvete, C. and Sobarzo, M. (2011) Quantification of the surface brackish water layer and frontal zones in southern Chilean fjords between Boca del Guafo (43°30′S) and Estero Elefantes (46°30′S), *Continental Shelf Research*, 31(3–4), p. 162–171. doi: 10.1016/J.CSR.2010.09.013.

Cammack, W. K. L., Kalff, J., Prairie, Y. T. and Smith, E. M. (2004) Fluorescent dissolved organic matter in lakes: Relationships with heterotrophic metabolism, *Limnology and Oceanography*, 49(6), p. 2034–2045. doi: 10.4319/lo.2004.49.6.2034.

Cannone, N., Diolaiuti, G., Guglielmin, M. and Smiraglia, C. (2008) Accelerating climate change impacts on alpine glacier forefield ecosystems in the European Alps, *Ecological Applications*. doi: 10.1890/07-1188.1.

Cárdenas, C. S., Gerea, M., Garcia, P. E., Pérez, G. L., Diéguez, M. C., Rapacioli, R., Reissig, M. and Queimaliños, C. (2017) Interplay between climate and hydrogeomorphic features and their effect on the seasonal variation of dissolved organic matter in shallow temperate lakes of the Southern Andes

(Patagonia, Argentina): a field study based on optical properties, *Ecohydrology*. doi: 10.1002/eco.1872.

Carlson, C. A., Bates, N. R., Hansell, D. A. and Steinberg, D. K. (2001) Carbon Cycle, *Encyclopedia of Ocean Sciences*. Academic Press, p. 477–486. doi: 10.1016/B978-012374473-9.00272-1.

Carrivick, J. L., Davies, B. J., James, W. H. M., Quincey, D. J. and Glasser, N. F. (2016) Distributed ice thickness and glacier volume in southern South America, *Global and Planetary Change*, 146, p. 122–132. doi: 10.1016/j.gloplacha.2016.09.010.

Carrivick, J. L. and Tweed, F. S. (2013) Proglacial Lakes: Character, behaviour and geological importance, *Quaternary Science Reviews*. doi: 10.1016/j.quascirev.2013.07.028.

Carrivick, J. L. and Tweed, F. S. (2016) A global assessment of the societal impacts of glacier outburst floods, *Global and Planetary Change*, 144, p. 1–16. doi: 10.1016/J.GLOPLACHA.2016.07.001.

Catalá, T. S., Reche, I., Fuentes-Lema, A., Romera-Castillo, C., Nieto-Cid, M., Ortega-Retuerta, E., Calvo, E., Álvarez, M., Marrasé, C., Stedmon, C. A. and Álvarez-Salgado, X. A. (2015) Turnover time of fluorescent dissolved organic matter in the dark global ocean, *Nature Communications*, 6, p. 5986. doi: 10.1038/ncomms6986.

Catalán, N., Marcé, R., Kothawala, D. N. and Tranvik, L. J. (2016) Organic carbon decomposition rates controlled by water retention time across inland waters, *Nature Geoscience*, 9(7), p. 501–504. doi: 10.1038/ngeo2720.

Cawley, K. M., Butler, K. D., Aiken, G. R., Larsen, L. G., Huntington, T. G. and McKnight, D. M. (2012) Identifying fluorescent pulp mill effluent in the Gulf of Maine and its watershed, *Marine Pollution Bulletin*, 64(8), p. 1678–1687.

Chen, H., Abdulla, H. A. N., Sanders, R. L., Myneni, S. C. B., Mopper, K. and Hatcher, P. G. (2014) Production of Black Carbon-like and Aliphatic Molecules from Terrestrial Dissolved Organic Matter in the Presence of Sunlight and Iron, *Environmental Science and Technology Letters*. doi: 10.1021/ez5002598.

Chen, J. L., Wilson, C. R., Tapley, B. D., Blankenship, D. D. and Ivins, E. R. (2007) Patagonia Icefield melting observed by Gravity Recovery and Climate Experiment (GRACE), *Geophysical Research Letters*. doi: 10.1029/2007GL031871.

Chifflard, P., Fasching, C., Reiss, M., Ditzel, L. and Boodoo, K. S. (2019) Dissolved and particulate organic carbon in icelandic proglacial streams: A first estimate, *Water (Switzerland)*. doi: 10.3390/w11040748.

Chimner, R. A., Bonvissuto, G. L., Victoria Cremona, M., Gaitan, J. J. and López, C. R. (2011) Ecohydrological conditions of wetlands along a precipitation gradient in Patagonia, Argentina, *Ecologia Austral*.

Chin, Y. P., Traina, S. J., Swank, C. R. and Backhus, D. (1998) Abundance and properties of dissolved organic matter in pore waters of a freshwater wetland, *Limnology and Oceanography*. doi: 10.4319/lo.1998.43.6.1287.

Christner, B. C., Priscu, J. C., Achberger, A. M., Barbante, C., Carter, S. P., Christianson, K., … Tulaczyk, S. (2014) A microbial ecosystem beneath the West Antarctic ice sheet, *Nature*, 512(7514), p. 310–313. doi: 10.1038/nature13667.

Chu, V. W. (2014) Greenland ice sheet hydrology: A review, *Progress in Physical Geography*, 38(1), p. 19–54. doi: 10.1177/0309133313507075.

Clausen, J. C., Ortega, I. M., Glaude, C. M., Relyea, R. A., Garay, G. and Guineo, O. (2006) Classification of wetlands in a patagonian National Park, Chile, *Wetlands*. doi: 10.1672/0277-5212(2006)26[217:COWIAP]2.0.CO;2.

Coble, A. A., Koenig, L. E., Potter, J. D., Parham, L. M. and McDowell, W. H. (2019) Homogenization of dissolved organic matter within a river network occurs in the smallest headwaters, *Biogeochemistry*, 143(1), p. 85–104. doi: 10.1007/s10533-019-00551-y.

Coffin, R. B. (1989) Bacterial uptake of dissolved free and combined amino acids in estuarine waters, *Limnology and Oceanography*. doi: 10.4319/lo.1989.34.3.0531.

Cook, J., Edwards, A., Takeuchi, N. and Irvine-Fynn, T. (2016) Cryoconite: The dark biological secret of the cryosphere, *Progress in Physical Geography*. doi: 10.1177/0309133315616574.

Cook, J. M., Hodson, A. J., Anesio, A. M., Hanna, E., Yallop, M., Stibal, M., Telling, J. and Huybrechts, P. (2012) An improved estimate of microbially mediated carbon fluxes from the Greenland ice sheet, *Journal of Glaciology*, 58(212), p. 1098–1108. doi: 10.3189/2012JoG12J001.

Cory, R. M., Boyer, E. W. and McKnight, D. M. (2011) Spectral Methods to Advance Understanding of Dissolved Organic Carbon Dynamics in Forested Catchments, in. doi: 10.1007/978-94-007-1363-5_6.

Cory, R. M. and Kaplan, L. A. (2012) Biological lability of streamwater fluorescent dissolved organic matter, *Limnology and Oceanography*. doi: 10.4319/lo.2012.57.5.1347.

Cui, X., Bianchi, T. S. and Savage, C. (2017) Erosion of modern terrestrial organic matter as a major component of sediments in fjords, *Geophysical Research Letters*, 44(3), p. 1457–1465. doi: 10.1002/2016GL072260.

Cui, X., Bianchi, T. S., Savage, C. and Smith, R. W. (2016) Organic carbon burial in fjords: Terrestrial versus marine inputs, *Earth and Planetary Science Letters*, 451, p. 41–50. doi: 10.1016/J.EPSL.2016.07.003.

Cuss, C. W. and Guéguen, C. (2015) Relationships between molecular weight and fluorescence properties for size-fractionated dissolved organic matter from fresh and aged sources, *Water Research*. doi: 10.1016/j.watres.2014.10.013.

D'Andrilli, J., Junker, J. R., Smith, H. J., Scholl, E. A. and Foreman, C. M. (2019) DOM composition alters ecosystem function during microbial processing of isolated sources, *Biogeochemistry*. doi: 10.1007/s10533-018-00534-5.

D'Andrilli, J., Foreman, C. M., Sigl, M., Priscu, J. C. and McConnell, J. R. (2017) A 21000-year record of fluorescent organic matter markers in the WAIS Divide ice core, *Climate of the Past*, 13(5), p. 533–544. doi: 10.5194/cp-13-533-2017.

Dai, M., Yin, Z., Meng, F., Liu, Q. and Cai, W. J. (2012) Spatial distribution of riverine DOC inputs to the ocean: An updated global synthesis, *Current Opinion in Environmental Sustainability*. doi: 10.1016/j.cosust.2012.03.003.

Dainard, P. G., Guéguen, C., McDonald, N. and Williams, W. J. (2015) Photobleaching of fluorescent dissolved organic matter in Beaufort Sea and North Atlantic Subtropical Gyre, *Marine Chemistry*, 177, p. 630–637. doi: 10.1016/J.MARCHEM.2015.10.004.

Davies, B. J. J. and Glasser, N. F. F. (2012) Accelerating shrinkage of Patagonian glaciers from the Little Ice Age (∼AD 1870) to 2011, *Journal of Glaciology*. Cambridge University Press, 58(212), p. 1063–1084. doi: 10.3189/2012JoG12J026.

Dávila, P. M., Figueroa, D. and Müller, E. (2002) Freshwater input into the coastal ocean and its relation with the salinity distribution off austral Chile (35-55°s), *Continental Shelf Research*, 22(3), p. 521–534. doi: 10.1016/S0278-4343(01)00072-3.

Delgado, L. E., Sepúlveda, M. B. and Marín, V. H. (2013) Provision of ecosystem services by the Aysén watershed, Chilean Patagonia, to rural households, *Ecosystem Services*. doi: 10.1016/j.ecoser.2013.04.008.

Denis, M., Jeanneau, L., Pierson-Wickman, A. C., Humbert, G., Petitjean, P., Jaffrézic, A. and Gruau, G. (2017a) A comparative study on the pore-size and filter type effect on the molecular composition of soil and stream dissolved organic matter, *Organic Geochemistry*. doi: 10.1016/j.orggeochem.2017.05.002.

Denis, M., Jeanneau, L., Petitjean, P., Murzeau, A., Liotaud, M., Yonnet, L. and Gruau, G. (2017b) New molecular evidence for surface and sub-surface soil erosion controls on the composition of stream DOM during storm events, *Biogeosciences*. doi: 10.5194/bg-14-5039-2017.

Derrien, M., Brogi, S. R. and Gonçalves-Araujo, R. (2019) Characterization of aquatic organic matter: Assessment, perspectives and research priorities, *Water Research*. doi: 10.1016/j.watres.2019.114908.

Determann, S., Lobbes, J. örg M., Reuter, R. and Rullkötter, J. ürgen (1998) Ultraviolet fluorescence excitation and emission spectroscopy of marine algae and bacteria, *Marine Chemistry*, 62(1–2), p. 137–156. doi: 10.1016/S0304-4203(98)00026-7.

Dieser, M., Broemsen, E. L. J. E., Cameron, K. A., King, G. M., Achberger, A., Choquette, K., Hagedorn, B., Sletten, R., Junge, K. and Christner, B. C. (2014) Molecular and biogeochemical evidence for methane cycling beneath the western margin of the Greenland Ice Sheet., *The ISME journal*, 8(11), p. 2305–16. doi: 10.1038/ismej.2014.59.

Dirección General de Aguas (2019) *Hydrometeorological service: DGA stations statistics*. Available at: http://www.dga.cl/servicioshidrometeorologicos/Paginas/default.aspx.

Dittmar, T., Koch, B., Hertkorn, N. and Kattner, G. (2008) A simple and efficient method for the solid-phase extraction of dissolved organic matter (SPE-DOM) from seawater, *Limnology and Oceanography: Methods*, 6(6), p. 230–235. doi: 10.4319/lom.2008.6.230.

Dubnick, A., Barker, J., Sharp, M., Wadham, J., Lis, G., Telling, J., Fitzsimons, S. and Jackson, M. (2010) Characterization of dissolved organic matter (DOM) from glacial environments using total fluorescence spectroscopy and parallel factor analysis, *Annals of Glaciology*, 51(56), p. 111–122.

Dussaillant, A. J., Buytaert, W., Meier, C. and Espinoza, F. (2012) Hydrological regime of remote catchments with extreme gradients under accelerated change: the Baker basin in Patagonia, *Hydrological Sciences Journal*. doi: 10.1080/02626667.2012.726993.

Dussaillant, I., Berthier, E. and Brun, F. (2018) Geodetic mass balance of the northern patagonian icefield from 2000 to 2012 using two independent methods, *Frontiers in Earth Science*. doi: 10.3389/feart.2018.00008.

Dussaillant, I., Berthier, E., Brun, F., Masiokas, M., Hugonnet, R., Favier, V., Rabatel, A., Pitte, P. and Ruiz, L. (2019) Two decades of glacier mass loss along the Andes, *Nature Geoscience*. doi: 10.1038/s41561-019-0432-5.

Eisma, D. (1986) Flocculation and de-flocculation of suspended matter in estuaries, *Netherlands Journal of Sea Research*. doi: 10.1016/0077-7579(86)90041-4.

Evans, C. D., Futter, M. N., Moldan, F., Valinia, S., Frogbrook, Z. and Kothawala, D. N. (2017) Variability in organic carbon reactivity across lake residence time and trophic gradients, *Nature Geoscience*. doi: 10.1038/NGEO3051.

Farr, T. G., Rosen, P. A., Caro, E., Crippen, R., Duren, R., Hensley, S., Kobrick, M., Paller, M., Rodriguez, E., Roth, L., Seal, D., Shaffer, S., Shimada, J., Umland, J., Werner, M., Oskin, M., Burbank, D. and Alsdorf, D. E. (2007) The shuttle radar topography mission, *Reviews of Geophysics*. doi: 10.1029/2005RG000183.

Fellman, J. B., Hood, E., Raymond, P. A., Hudson, J., Bozeman, M. and Arimitsu, M. (2015a) Evidence for the assimilation of ancient glacier organic carbon in a proglacial stream food web, *Limnology and Oceanography*, 60(4), p. 1118–1128. doi: 10.1002/lno.10088.

Fellman, J. B., D'Amore, D. V., Hood, E. and Boone, R. D. (2008) Fluorescence characteristics and biodegradability of dissolved organic matter in forest and wetland soils from coastal temperate watersheds in southeast Alaska, *Biogeochemistry*, 88(2), p. 169–184. doi: 10.1007/s10533-008-9203-x.

Fellman, J. B., Spencer, R. G. M., Hernes, P. J., Edwards, R. T., D'Amore, D. V. and Hood, E. (2010a) The impact of glacier runoff on the biodegradability and biochemical composition of terrigenous dissolved organic matter in near-shore marine ecosystems, *Marine Chemistry*, 121(1–4), p. 112–122. doi: 10.1016/j.marchem.2010.03.009.

Fellman, J. B., Hood, E. and Spencer, R. G. M. (2010b) Fluorescence spectroscopy opens new windows into dissolved organic matter dynamics in freshwater ecosystems: A review, *Limnology and Oceanography*, 55(6), p. 2452–2462. doi: 10.4319/lo.2010.55.6.2452.

Fellman, J. B., Hood, E., Spencer, R. G. M., Stubbins, A. and Raymond, P. A. (2014) Watershed Glacier Coverage Influences Dissolved Organic Matter Biogeochemistry in Coastal Watersheds of Southeast Alaska, *Ecosystems*, 17(6), p. 1014–1025. doi: 10.1007/s10021-014-9777-1.

Fellman, J. B., Hood, E., Raymond, P. A., Stubbins, A. and Spencer, R. G. M. (2015b) Spatial Variation in the Origin of Dissolved Organic Carbon in Snow on the Juneau Icefield, Southeast Alaska, *Environmental Science and Technology*. doi: 10.1021/acs.est.5b02685.

Fellman, J. B., Hood, E., D'Amore, D. V, Edwards, R. T. and White, D. (2009) Seasonal changes in the chemical quality and biodegradability of dissolved organic matter exported from soils to streams in coastal temperate rainforest watersheds, *Biogeochemistry*, 95(2), p. 277–293. doi: 10.1007/s10533-009-9336-6.

Fettweis, X., Tedesco, M., Van Den Broeke, M. and Ettema, J. (2011) Melting trends over the Greenland ice sheet (1958-2009) from spaceborne microwave data and regional climate models, *Cryosphere*. doi: 10.5194/tc-5-359-2011.

Foresta, L., Gourmelen, N., Weissgerber, F., Nienow, P., Williams, J. J., Shepherd, A., Drinkwater, M. R. and Plummer, S. (2018) Heterogeneous and rapid ice loss over the Patagonian Ice Fields revealed by CryoSat-2 swath radar altimetry, *Remote Sensing of Environment*, 211, p. 441–455. doi: 10.1016/J.RSE.2018.03.041.

Gabrieli, J., Vallelonga, P., Cozzi, G., Gabrielli, P., Gambaro, A., Sigl, M., Decet, F., Schwikowski, M., Gäggeler, H., Boutron, C., Cescon, P. and Barbante, C. (2010) Post 17th-century changes of european pah emissions recorded in high-altitude alpine snow and ice, *Environmental Science and Technology*. doi: 10.1021/es903365s.

Galloway, J. N., Dentener, F. J., Capone, D. G., Boyer, E. W., Howarth, R. W., Seitzinger, S. P., Asner, G. P., Cleveland, C. C., Green, P. A., Holland, E. A., Karl, D. M., Michaels, A. F., Porter, J. H., Townsend, A. R. and Vörösmarty, C. J. (2004) Nitrogen cycles: Past, present, and future, *Biogeochemistry*. doi: 10.1007/s10533-004-0370-0.

Galy, V., Peucker-Ehrenbrink, B. and Eglinton, T. (2015) Global carbon export from the terrestrial biosphere controlled by erosion, *Nature*. doi: 10.1038/nature14400.

Garcia, R. D., Reissig, M., Queimaliños, C. P., Garcia, P. E. and Dieguez, M. C. (2015) Climate-driven terrestrial inputs in ultraoligotrophic mountain streams of Andean Patagonia revealed through chromophoric and fluorescent dissolved organic matter, *Science of The Total Environment*, 521–522, p. 280–292. doi: 10.1016/J.SCITOTENV.2015.03.102.

Gardner, A. S., Moholdt, G., Cogley, J. G., Wouters, B., Arendt, A. A., Wahr, J., Berthier, E., Hock, R., Pfeffer, W. T., Kaser, G., Ligtenberg, S. R. M., Bolch, T., Sharp, M. J., Hagen, J. O., van den Broeke, M. R. and Paul, F. (2013) A Reconciled Estimate of Glacier Contributions to Sea Level Rise: 2003 to 2009, *Science*, 340(6134), p. 852–857.

Garreaud, R. D. (2018) Record-breaking climate anomalies lead to severe drought and environmental disruption in western Patagonia in 2016, *Climate Research*. doi: 10.3354/cr01505.

Garreaud, R., Lopez, P., Minvielle, M. and Rojas, M. (2013) Large-scale control on the Patagonian climate, *Journal of Climate*. doi: 10.1175/JCLI-D-12-00001.1.

Gašparović, B., Plavšić, M., Ćosović, B. and Reigstad, M. (2005) Organic matter characterization and fate in the sub-arctic Norwegian fjords during the late spring/summer period, *Estuarine, Coastal and Shelf Science*. doi: 10.1016/j.ecss.2004.08.008.

Glasser, N. F., Harrison, S., Jansson, K. N., Anderson, K. and Cowley, A. (2011) Global sea-level contribution from the Patagonian Icefields since the Little Ice Age maximum, *Nature Geoscience*, 4(5), p. 303–307. doi: 10.1038/ngeo1122.

Glasser, N. F., Holt, T. O., Evans, Z. D., Davies, B. J., Pelto, M. and Harrison, S. (2016) Recent spatial and temporal variations in debris cover on Patagonian glaciers, *Geomorphology*, 273, p. 202–216. doi: 10.1016/J.GEOMORPH.2016.07.036.

Gonçalves-Araujo, R., Granskog, M. A., Bracher, A., Azetsu-Scott, K., Dodd, P. A. and Stedmon, C. A. (2016) Using fluorescent dissolved organic matter to trace and distinguish the origin of Arctic

surface waters, *Scientific Reports*, 6, p. 33978. doi: 10.1038/srep33978.

González, H. E., Castro, L., Daneri, G., Iriarte, J. L., Silva, N., Vargas, C. A., Giesecke, R. and Sánchez, N. (2011) Seasonal plankton variability in Chilean Patagonia fjords: Carbon flow through the pelagic food web of Aysen Fjord and plankton dynamics in the Moraleda Channel basin, *Continental Shelf Research*, 31(3–4), p. 225–243. doi: 10.1016/J.CSR.2010.08.010.

González, H. E., Nimptsch, J., Giesecke, R. and Silva, N. (2019) Organic matter distribution, composition and its possible fate in the Chilean North-Patagonian estuarine system, *Science of the Total Environment*. doi: 10.1016/j.scitotenv.2018.11.445.

González, H. E., Castro, L. R., Daneri, G., Iriarte, J. L., Silva, N., Tapia, F., Teca, E. and Vargas, C. A. (2013) Land–ocean gradient in haline stratification and its effects on plankton dynamics and trophic carbon fluxes in Chilean Patagonian fjords (47–50°S), *Progress in Oceanography*, 119, p. 32–47. doi: 10.1016/J.POCEAN.2013.06.003.

Graeber, D., Gelbrecht, J., Pusch, M. T., Anlanger, C. and von Schiller, D. (2012) Agriculture has changed the amount and composition of dissolved organic matter in Central European headwater streams, *Science of The Total Environment*, 438, p. 435–446. doi: 10.1016/J.SCITOTENV.2012.08.087.

Graeber, D., Boëchat, I. G., Encina-Montoya, F., Esse, C., Gelbrecht, J., Goyenola, G., Gücker, B., Heinz, M., Kronvang, B., Meerhoff, M., Nimptsch, J., Pusch, M. T., Silva, R. C. S., Von Schiller, D. and Zwirnmann, E. (2015) Global effects of agriculture on fluvial dissolved organic matter, *Scientific Reports*. doi: 10.1038/srep16328.

Graly, J. A., Humphrey, N. F., Landowski, C. M. and Harper, J. T. (2014) Chemical weathering under the Greenland ice sheet, *Geology*. doi: 10.1130/G35370.1.

Grannas, A. M., Hockaday, W. C., Hatcher, P. G., Thompson, L. G. and Mosley-Thompson, E. (2006) New revelations on the nature of organic matter in ice cores, *Journal of Geophysical Research Atmospheres*. doi: 10.1029/2005JD006251.

Granskog, M. A., Nomura, D., Müller, S., Krell, A., Toyota, T. and Hattorl, H. (2015) Evidence for significant protein-like dissolved organic matter accumulation in Sea of Okhotsk sea ice, *Annals of Glaciology*. doi: 10.3189/2015AoG69A002.

Grant, D. (1977) Chemical structure of humic substances, *Nature*. doi: 10.1038/270709a0.

Grasshoff, Klaus; Kremling, Klaus; Ehrhardt, M. (1999) Methods of Seawater Analysis - Chapter 10 - Nutrients, in *Methods of Seawater Analysis*. doi: 10.1002/9783527613984.

Grossart, H. P. and Simon, M. (1998) Significance of limnetic organic aggregates (lake snow) for the sinking flux of particulate organic matter in a large lake, *Aquatic Microbial Ecology*. doi: 10.3354/ame015115.

Guéguen, C., Cuss, C. W., Cassels, C. J. and Carmack, E. C. (2014) Absorption and fluorescence of dissolved organic matter in the waters of the Canadian Arctic Archipelago, Baffin Bay, and the Labrador Sea, *Journal of Geophysical Research: Oceans*, 119(3), p. 2034–2047. doi: 10.1002/2013JC009173.

Gumbricht, T., Román-Cuesta, R. M., Verchot, L. V, Herold, M., Wittmann, F., Householder, E., Herold, N. and Murdiyarso, D. (2019) Tropical and Subtropical Wetlands Distribution version 2. Center for International Forestry Research (CIFOR). doi: 10.17528/CIFOR/DATA.00058.

Gutiérrez, M. H., Galand, P. E., Moffat, C. and Pantoja, S. (2015) Melting glacier impacts community structure of Bacteria, Archaea and Fungi in a Chilean Patagonia fjord, *Environmental Microbiology*, 17(10), p. 3882–3897. doi: 10.1111/1462-2920.12872.

Halbach, L., Vihtakari, M., Duarte, P., Everett, A., Granskog, M. A., Hop, H., Kauko, H. M., Kristiansen, S., Myhre, P. I., Pavlov, A. K., Pramanik, A., Tatarek, A., Torsvik, T., Wiktor, J. M., Wold, A., Wulff, A., Steen, H. and Assmy, P. (2019) Tidewater glaciers and bedrock characteristics control the phytoplankton growth environment in a fjord in the arctic, *Frontiers in Marine Science*. doi: 10.3389/fmars.2019.254.

Hallet, B., Hunter, L. and Bogen, J. (1996) Rates of erosion and sediment evacuation by glaciers: A review of field data and their implications, *Global and Planetary Change*. doi: 10.1016/0921-8181(95)00021-6.

Hartmann, J. and Moosdorf, N. (2012) The new global lithological map database GLiM: A representation of rock properties at the Earth surface, *Geochemistry, Geophysics, Geosystems*. doi: 10.1029/2012GC004370.

Hawkes, J. A., Patriarca, C., Sjöberg, P. J. R., Tranvik, L. J. and Bergquist, J. (2018) Extreme isomeric complexity of dissolved organic matter found across aquatic environments, *Limnology and Oceanography Letters*, 3(2), p. 21–30. doi: 10.1002/lol2.10064.

Hawkings, J., Wadham, J., Tranter, M., Telling, J., Bagshaw, E., Beaton, A., Simmons, S. L., Chandler, D., Tedstone, A. and Nienow, P. (2016) The Greenland Ice Sheet as a hot spot of phosphorus weathering and export in the Arctic, *Global Biogeochemical Cycles*, 30(2), p. 191–210. doi: 10.1002/2015GB005237.

Hawkings, J. R., Wadham, J. L., Tranter, M., Raiswell, R., Benning, L. G., Statham, P. J., Tedstone, A., Nienow, P., Lee, K. and Telling, J. (2014) Ice sheets as a significant source of highly reactive nanoparticulate iron to the oceans, *Nature Communications*, 5, p. 3929. doi: 10.1038/ncomms4929.

Hawkings, J. R., Wadham, J. L., Tranter, M., Lawson, E., Sole, A., Cowton, T., Tedstone, A. J., Bartholomew, I., Nienow, P., Chandler, D. and Telling, J. (2015) The effect of warming climate on nutrient and solute export from the Greenland Ice Sheet, *Geochemical Perspectives Letters*, 1, p. 94–104. doi: 10.7185/geochemlet.1510.

Hawkings, J. R., Hatton, J. E., Hendry, K. R., de Souza, G. F., Wadham, J. L., Ivanovic, R., Kohler, T. J., Stibal, M., Beaton, A., Lamarche-Gagnon, G., Tedstone, A., Hain, M. P., Bagshaw, E., Pike, J. and Tranter, M. (2018) The silicon cycle impacted by past ice sheets, *Nature Communications*, 9(1), p. 3210. doi: 10.1038/s41467-018-05689-1.

Hedges, J. I. and Stern, J. H. (1984) Carbon and nitrogen determinations of carbonate-containing solids, *Limnology and Oceanography*. doi: 10.4319/lo.1984.29.3.0657.

Hemingway, J. D., Spencer, R. G. M., Podgorski, D. C., Zito, P., Sen, I. S. and Galy, V. V. (2019) Glacier meltwater and monsoon precipitation drive Upper Ganges Basin dissolved organic matter composition, *Geochimica et Cosmochimica Acta*, 244, p. 216–228. doi: 10.1016/J.GCA.2018.10.012.

Hernes, P. J. and Benner, R. (2003) Photochemical and microbial degradation of dissolved lignin phenols: Implications for the fate of terrigenous dissolved organic matter in marine environments, *Journal of Geophysical Research C: Oceans*.

Hernes, P. J., Bergamaschi, B. A., Eckard, R. S. and Spencer, R. G. M. (2009) Fluorescence-based proxies for lignin in freshwater dissolved organic matter, *Journal of Geophysical Research: Biogeosciences*. doi: 10.1029/2009JG000938.

Herzsprung, P., Von Tümpling, W., Hertkorn, N., Harir, M., Büttner, O., Bravidor, J., Friese, K. and Schmitt-Kopplin, P. (2012) Variations of DOM quality in inflows of a drinking water reservoir: Linking of van krevelen diagrams with EEMF spectra by rank correlation, *Environmental Science and Technology*. doi: 10.1021/es300345c.

Hilton, R. G. (2017) Climate regulates the erosional carbon export from the terrestrial biosphere, *Geomorphology*. doi: 10.1016/j.geomorph.2016.03.028.

Hilton, R. G., Gaillardet, J. Ô., Calmels, D. and Birck, J. L. (2014) Geological respiration of a mountain belt revealed by the trace element rhenium, *Earth and Planetary Science Letters*. doi: 10.1016/j.epsl.2014.06.021.

Hodson, A. J. (2014) Understanding the dynamics of black carbon and associated contaminants in glacial systems, *Wiley Interdisciplinary Reviews: Water*. doi: 10.1002/wat2.1016.

Hodson, A., Anesio, A. M., Tranter, M., Fountain, A., Osborn, M., Priscu, J., Laybourn-Parry, J. and Sattler, B. (2008) Glacial ecosystems, *Ecological Monographs*, p. 41–67. doi: 10.1890/07-0187.1.

Holding, J. M., Duarte, C. M., Delgado-Huertas, A., Soetaert, K., Vonk, J. E., Agustí, S., Wassmann, P. and Middelburg, J. J. (2017) Autochthonous and allochthonous contributions of organic carbon to microbial food webs in Svalbard fjords, *Limnology and Oceanography*, 62(3), p. 1307–1323. doi: 10.1002/lno.10526.

Holmes, R. M., McClelland, J. W., Peterson, B. J., Tank, S. E., Bulygina, E., Eglinton, T. I., Gordeev, V. V., Gurtovaya, T. Y., Raymond, P. A., Repeta, D. J., Staples, R., Striegl, R. G., Zhulidov, A. V. and Zimov, S. A. (2012) Seasonal and Annual Fluxes of Nutrients and Organic Matter from Large Rivers to the Arctic Ocean and Surrounding Seas, *Estuaries and Coasts*. doi: 10.1007/s12237-011-9386-6.

Hood, E. and Berner, L. (2009) Effects of changing glacial coverage on the physical and biogeochemical properties of coastal streams in southeastern Alaska, *Journal of Geophysical Research: Biogeosciences*, 114(3). doi: 10.1029/2009JG000971.

Hood, E. and Scott, D. (2008) Riverine organic matter and nutrients in southeast Alaska affected by glacial coverage, *Nature Geoscience*, 1(9), p. 583–587. doi: 10.1038/ngeo280.

Hood, E., Fellman, J., Spencer, R. G. M., Hernes, P. J., Edwards, R., D'Amore, D., Scott, D., D'Amore, D. and Scott, D. (2009) Glaciers as a source of ancient and labile organic matter to the marine environment, *Nature*, 462(7276), p. 1044–7. doi: 10.1038/nature08580.

Hood, E., Battin, T. J., Fellman, J., Neel, S. O., Spencer, R. G. M., O'Neel, S., Spencer, R. G. M., O'Neel, S. and Spencer, R. G. M. (2015) Storage and release of organic carbon from glaciers and ice sheets, *Nature*, 8(2), p. 91–96. doi: 10.1038/ngeo2331.

Hoostal, M. J. and Bouzat, J. L. (2008) The modulating role of dissolved organic matter on spatial patterns of microbial metabolism in Lake Erie sediments, *Microbial Ecology*. doi: 10.1007/s00248-007-9281-7.

Hopkinson, C. S., Buffam, I., Hobbie, J., Vallino, J., Perdue, M., Eversmeyer, B., Prahl, F., Covert, J., Hudson, R., Moran, M. A., Smith, E., Baross, J., Crump, B., Findlay, S. and Foreman, K. (1998) Terrestrial inputs of organic matter to coastal ecosystems: An intercomparison of chemical characteristics and bioavailability, *Biogeochemistry*. doi: 10.1023/A:1006016030299.

Hopwood, M. J., Carroll, D., Browning, T. J., Meire, L., Mortensen, J., Krisch, S. and Achterberg, E. P. (2018) Non-linear response of summertime marine productivity to increased meltwater discharge around Greenland, *Nature Communications*. doi: 10.1038/s41467-018-05488-8.

Hopwood, M. J., Carroll, D., Dunse, T., Hodson, A., Holding, J. M., Iriarte, J. L., Ribeiro, S., Achterberg, E. P., Cantoni, C., Carlson, D. F., Chierici, M., Clarke, J. S., Cozzi, S., Fransson, A., Juul-Pedersen, T., Winding, M. S. and Meire, L. (2019) Review Article: How does glacier discharge affect marine biogeochemistry and primary production in the Arctic?, *The Cryosphere Discussions*. doi: 10.5194/tc-2019-136.

Huss, M. and Hock, R. (2018) Global-scale hydrological response to future glacier mass loss, *Nature Climate Change*. doi: 10.1038/s41558-017-0049-x.

Huybrechts, P., Letreguilly, A. and Reeh, N. (1991) The Greenland ice sheet and greenhouse warming, *Global and Planetary Change*. doi: 10.1016/0921-8181(91)90119-H.

Iriarte, J. L., Pantoja, S. and Daneri, G. (2014) Oceanographic Processes in Chilean Fjords of Patagonia: From small to large-scale studies, *Progress in Oceanography*, p. 1–7. doi: 10.1016/j.pocean.2014.10.004.

Iturraspe, R. (2018) Patagonian Peatlands (Argentina and Chile), in *The Wetland Book II: Distribution, Description, and Conservation*. doi: 10.1007/978-94-007-4001-3_230.

Ivins, E. R., Watkins, M. M., Yuan, D. N., Dietrich, R., Casassa, G. and Rülke, A. (2011) On-land ice loss and glacial isostatic adjustment at the Drake Passage: 2003-2009, *Journal of Geophysical Research: Solid Earth*. doi: 10.1029/2010JB007607.

Jaber, W. A. (2016) Derivation of mass balance and surface velocity of Glaciers by means of high resolution synthetic aperture radar: Application to the Patagonian icefields and Antarctica, *DLR Deutsches Zentrum fur Luft- und Raumfahrt e.V. - Forschungsberichte*.

Jacob, B. G., Tapia, F. J., Daneri, G., Iriarte, J. L., Montero, P., Sobarzo, M. and Quiñones, R. A. (2014) Springtime size-fractionated primary production across hydrographic and PAR-light gradients in Chilean Patagonia (41-50°S), *Progress in Oceanography*. doi: 10.1016/j.pocean.2014.08.003.

Jacob, T., Wahr, J., Pfeffer, W. T. and Swenson, S. (2012) Recent contributions of glaciers and ice caps to sea level rise, *Nature*, 482, p. 514. doi: 10.1038/nature10847.

Jacobsen, D., Milner, A. M., Brown, L. E. and Dangles, O. (2012) Biodiversity under threat in glacier-fed river systems, *Nature Climate Change*. doi: 10.1038/nclimate1435.

Jacobsen, D. and Dangles, O. (2012) Environmental harshness and global richness patterns in glacier-fed streams, *Global Ecology and Biogeography*. doi: 10.1111/j.1466-8238.2011.00699.x.

Jeanneau, L., Denis, M., Pierson-Wickmann, A. C., Gruau, G., Lambert, T. and Petitjean, P. (2015) Sources of dissolved organic matter during storm and inter-storm conditions in a lowland headwater catchment: Constraints from high-frequency molecular data, *Biogeosciences*. doi: 10.5194/bg-12-4333-2015.

Jones, T. G., Evans, C. D., Jones, D. L., Hill, P. W. and Freeman, C. (2016) Transformations in DOC along a source to sea continuum; impacts of photo-degradation, biological processes and mixing, *Aquatic Sciences*. doi: 10.1007/s00027-015-0461-0.

Jørgensen, L., Stedmon, C. A., Kragh, T., Markager, S., Middelboe, M. and Søndergaard, M. (2011) Global trends in the fluorescence characteristics and distribution of marine dissolved organic matter, *Marine Chemistry*, 126(1–4), p. 139–148. doi: 10.1016/J.MARCHEM.2011.05.002.

Judd, K. E., Crump, B. C. and Kling, G. W. (2006) Variation in dissolved organic matter controls bacterial production and community composition, *Ecology*. doi: 10.1890/0012-9658(2006)87[2068:VIDOMC]2.0.CO;2.

Junk, W. J. (2013) Current state of knowledge regarding South America wetlands and their future under global climate change, *Aquatic Sciences*. doi: 10.1007/s00027-012-0253-8.

Kamjunke, N., Nimptsch, J., Harir, M., Herzsprung, P., Schmitt-Kopplin, P., Neu, T. R., Graeber, D., Osorio, S., Valenzuela, J., Carlos Reyes, J., Woelfl, S. and Hertkorn, N. (2017) Land-based salmon aquacultures change the quality and bacterial degradation of riverine dissolved organic matter, *Scientific Reports*. doi: 10.1038/srep43739.

Keil, R. G., Montluçon, D. B., Prahl, F. G. and Hedges, J. I. (1994) Sorptive preservation of labile organic matter in marine sediments, *Nature*. doi: 10.1038/370549a0.

Kellerman, A. M., Guillemette, F., Podgorski, D. C., Aiken, G. R., Butler, K. D. and Spencer, R. G. M. (2018) Unifying Concepts Linking Dissolved Organic Matter Composition to Persistence in Aquatic Ecosystems, *Environmental Science and Technology*. doi: 10.1021/acs.est.7b05513.

Kellerman, A. M., Hawkings, J. R., Wadham, J. L., Kohler, T. J., Stibal, M., Grater, E., Marshall, M., Hatton, J. E., Beaton, A. and Spencer, R. G. M. (2020) Glacier outflow dissolved organic matter as a window into seasonally changing carbon 1 sources: Leverett Glacier, Greenland, *Journal of Geophysical Research: Biogeosciences*, 125, doi: 10.1029/2019JG005161

Kellerman, A. M., Dittmar, T., Kothawala, D. N. and Tranvik, L. J. (2014) Chemodiversity of dissolved organic matter in lakes driven by climate and hydrology, *Nature Communications*. doi: 10.1038/ncomms4804.

Kellerman, A. M., Kothawala, D. N., Dittmar, T. and Tranvik, L. J. (2015) Persistence of dissolved organic matter in lakes related to its molecular characteristics, *Nature Geoscience*, 8(6), p. 454–457. doi: 10.1038/ngeo2440.

Kerner, M. and Spitzy, A. (2001) Nitrate Regeneration Coupled to Degradation of Different Size Fractions of DON by the Picoplankton in the Elbe Estuary, *Microbial Ecology*, 41(1), p. 69–81. doi: 10.1007/s002480000031.

Kerr, A. and Sugden, D. (1994) The sensitivity of the south chilean snowline to climatic change, *Climatic Change*. doi: 10.1007/BF01104136.

Kilian, R. and Lamy, F. (2012) A review of Glacial and Holocene paleoclimate records from southernmost Patagonia (49-55°S), *Quaternary Science Reviews*. doi: 10.1016/j.quascirev.2012.07.017.

Knudsen-Leerbeck, H., Mantikci, M., Bentzon-Tilia, M., Traving, S. J., Riemann, L., Hansen, J. L. S. and Markager, S. (2017) Seasonal dynamics and bioavailability of dissolved organic matter in two contrasting temperate estuaries, *Biogeochemistry*. doi: 10.1007/s10533-017-0357-2.

Knudsen, N. T., Yde, J. C. and Gasser, G. (2007) Suspended sediment transport in glacial meltwater during the initial quiescent phase after a major surge event at Kuannersuit Glacier, Greenland, *Geografisk Tidsskrift*. doi: 10.1080/00167223.2007.10801370.

Koch, B. P. and Dittmar, T. (2006) From mass to structure: An aromaticity index for high-resolution mass data of natural organic matter, *Rapid Communications in Mass Spectrometry*, 20(5), p. 926–932. doi: 10.1002/rcm.2386.

Koch, B. P., Witt, M., Engbrodt, R., Dittmar, T. and Kattner, G. (2005) Molecular formulae of marine and terrigenous dissolved organic matter detected by electrospray ionization Fourier transform ion cyclotron resonance mass spectrometry, *Geochimica et Cosmochimica Acta*, 69(13), p. 3299–3308. doi: 10.1016/j.gca.2005.02.027.

Kohler, T. J., Žárský, J. D., Yde, J. C., Lamarche-Gagnon, G., Hawkings, J. R., Tedstone, A. J., Wadham, J. L., Box, J. E., Beaton, A. D. and Stibal, M. (2017) Carbon dating reveals a seasonal progression in the source of particulate organic carbon exported from the Greenland Ice Sheet, *Geophysical Research Letters*. doi: 10.1002/2017GL073219.

Kothawala, D. N., von Wachenfeldt, E., Koehler, B. and Tranvik, L. J. (2012) Selective loss and preservation of lake water dissolved organic matter fluorescence during long-term dark incubations, *Science of The Total Environment*, 433, p. 238–246. doi: 10.1016/J.SCITOTENV.2012.06.029.

Kothawala, D. N., Stedmon, C. A., Müller, R. A., Weyhenmeyer, G. A., Köhler, S. J. and Tranvik, L. J. (2013) Controls of dissolved organic matter quality: evidence from a large-scale boreal lake survey, *Global Change Biology*, 20(4), p. 1101–1114. doi: 10.1111/gcb.12488.

Kowalczuk, P., Durako, M. J., Young, H., Kahn, A. E., Cooper, W. J. and Gonsior, M. (2009) Characterization of dissolved organic matter fluorescence in the South Atlantic Bight with use of PARAFAC model: Interannual variability, *Marine Chemistry*, 113(3–4), p. 182–196. doi: 10.1016/J.MARCHEM.2009.01.015.

Kujawinski, E. B., Longnecker, K., Blough, N. V, Vecchio, R. Del, Finlay, L., Kitner, J. B. and Giovannoni, S. J. (2009) Identification of possible source markers in marine dissolved organic matter using ultrahigh resolution mass spectrometry, *Geochimica et Cosmochimica Acta*, 73(15), p. 4384–4399. doi: 10.1016/j.gca.2009.04.033.

Kujawinski, E. B., Del Vecchio, R., Blough, N. V., Klein, G. C. and Marshall, A. G. (2004) Probing molecular-level transformations of dissolved organic matter: Insights on photochemical degradation and protozoan modification of DOM from electrospray ionization Fourier transform ion cyclotron resonance mass spectrometry, in *Marine Chemistry*. doi: 10.1016/j.marchem.2004.06.038.

Kuliński, K., Kedra, M., Legezyńska, J., Gluchowska, M., Zaborska, A., Kędra, M., Legeżyńska, J., Gluchowska, M. and Zaborska, A. (2014) Particulate organic matter sinks and sources in high Arctic fjord, *Journal of Marine Systems*, 139, p. 27–37. doi: 10.1016/j.jmarsys.2014.04.018.

Kumar, V., Tiwari, M., Nagoji, S. and Tripathi, S. (2016) Evidence of Anomalously Low δ 13 C of Marine Organic Matter in an Arctic Fjord, *Scientific Reports*. doi: 10.1038/srep36192.

Labieniec, M. and Gabryelak, T. (2006) Interactions of tannic acid and its derivatives (ellagic and gallic acid) with calf thymus DNA and bovine serum albumin using spectroscopic method, *Journal of Photochemistry and Photobiology B: Biology*, 82(1), p. 72–78. doi: 10.1016/J.JPHOTOBIOL.2005.09.005.

Lafrenière, M. J. and Sharp, M. J. (2006) The Concentration and Fluorescence of Dissolved Organic Carbon (DOC) in Glacial and Nonglacial Catchments: Interpreting Hydrological Flow Routing and DOC Sources, *Arctic, Antarctic, and Alpine Research*. doi: 10.1657/1523-

0430(2004)036[0156:tcafod]2.0.co;2.

Lamarche-Gagnon, G., Wadham, J. L., Sherwood Lollar, B., Arndt, S., Fietzek, P., Beaton, A. D., Tedstone, A. J., Telling, J., Bagshaw, E. A., Hawkings, J. R., Kohler, T. J., Zarsky, J. D., Mowlem, M. C., Anesio, A. M. and Stibal, M. (2019) Greenland melt drives continuous export of methane from the ice-sheet bed, *Nature*. doi: 10.1038/s41586-018-0800-0.

Lambert, T., Bouillon, S., Darchambeau, F., Massicotte, P. and Borges, A. V. (2016) Shift in the chemical composition of dissolved organic matter in the Congo River network, *Biogeosciences*, 13(18), p. 5405–5420. doi: 10.5194/bg-13-5405-2016.

Lambert, T., Bouillon, S., Darchambeau, F., Morana, C., Roland, F. A. E., Descy, J. P. and Borges, A. V. (2017) Effects of human land use on the terrestrial and aquatic sources of fluvial organic matter in a temperate river basin (The Meuse River, Belgium), *Biogeochemistry*. doi: 10.1007/s10533-017-0387-9.

Landa, M., Cottrell, M. T., Kirchman, D. L., Kaiser, K., Medeiros, P. M., Tremblay, L., Batailler, N., Caparros, J., Catala, P., Escoubeyrou, K., Oriol, L., Blain, S. and Obernosterer, I. (2014) Phylogenetic and structural response of heterotrophic bacteria to dissolved organic matter of different chemical composition in a continuous culture study, *Environmental Microbiology*, 16(6), p. 1668–1681. doi: 10.1111/1462-2920.12242.

Landaeta, M. F., López, G., Suárez-Donoso, N., Bustos, C. A. and Balbontín, F. (2012) Larval fish distribution, growth and feeding in Patagonian fjords: Potential effects of freshwater discharge, *Environmental Biology of Fishes*. doi: 10.1007/s10641-011-9891-2.

Lawson, E. C., Wadham, J. L., Tranter, M., Stibal, M., Lis, G. P., Butler, C. E. H., Laybourn-Parry, J., Nienow, P., Chandler, D. and Dewsbury, P. (2014a) Greenland ice sheet exports labile organic carbon to the arctic oceans, *Biogeosciences*, 11(14), p. 4015–4028. doi: 10.5194/bg-11-4015-2014.

Lawson, E. C., Bhatia, M. P., Wadham, J. L. and Kujawinski, E. B. (2014b) Continuous summer export of nitrogen-rich organic matter from the greenland ice sheet inferred by ultrahigh resolution mass spectrometry, *Environmental Science and Technology*, 48(24), p. 14248–14257. doi: 10.1021/es501732h.

Lechtenfeld, O. J., Kattner, G., Flerus, R., McCallister, S. L., Schmitt-Kopplin, P. and Koch, B. P. (2014) Molecular transformation and degradation of refractory dissolved organic matter in the Atlantic and Southern Ocean, *Geochimica et Cosmochimica Acta*. doi: 10.1016/j.gca.2013.11.009.

Legrand, M., Preunkert, S., Schock, M., Cerqueira, M., Kasper-Giebl, A., Afonso, J., Pio, C. A., Gelencsér, A. and Dombrowski-Etchevers, I. (2007) Major 20th century changes of carbonaceous aerosol components (EC, WinOC, DOC, HULIS, carboxylic acids, and cellulose) derived from Alpine ice cores, *Journal of Geophysical Research Atmospheres*. doi: 10.1029/2006JD008080.

Lenaerts, J. T. M., Van Den Broeke, M. R., Van Wessem, J. M., Van De Berg, W. J., Van Meijgaard, E., Van Ulft, L. H. and Schaefer, M. (2014) Extreme precipitation and climate gradients in patagonia revealed by high-resolution regional atmospheric climate modeling, *Journal of Climate*. doi: 10.1175/JCLI-D-13-00579.1.

León-Muñoz, J., Tecklin, D., Farías, A. and Díaz, S. (2007) Salmonicultura en los Lagos del Sur de Chile - Ecorregión Valdiviana Salmon Farming in the Lakes of Southern Chile - Valdivian Ecoregion History, tendencies and environmental impacts, *WWF*.

León-Muñoz, J., Echeverría, C., Marcé, R., Riss, W., Sherman, B. and Iriarte, J. L. (2013) The combined impact of land use change and aquaculture on sediment and water quality in oligotrophic Lake Rupanco (North Patagonia, Chile, 40.8°S), *Journal of Environmental Management*. doi: 10.1016/j.jenvman.2013.05.008.

Li, C., Bosch, C., Kang, S., Andersson, A., Chen, P., Zhang, Q., Cong, Z., Chen, B., Qin, D. and Gustafsson, Ö. (2016) Sources of black carbon to the Himalayan-Tibetan Plateau glaciers, *Nature Communications*. doi: 10.1038/ncomms12574.

Li, P., Chen, L., Zhang, W. and Huang, Q. (2015) Spatiotemporal Distribution, Sources, and Photobleaching Imprint of Dissolved Organic Matter in the Yangtze Estuary and Its Adjacent Sea

Using Fluorescence and Parallel Factor Analysis, *PLOS ONE*, 10(6), p. e0130852. doi: 10.1371/journal.pone.0130852.

Liermann, S., Beylich, A. A. and van Welden, A. (2012) Contemporary suspended sediment transfer and accumulation processes in the small proglacial Sætrevatnet sub-catchment, Bødalen, western Norway, *Geomorphology*. doi: 10.1016/j.geomorph.2012.03.035.

Lindsay, J. B. (2016) Whitebox GAT: A case study in geomorphometric analysis, *Computers and Geosciences*. doi: 10.1016/j.cageo.2016.07.003.

Liu, S., Wawrik, B. and Liu, Z. (2017) Different bacterial communities involved in peptide decomposition between normoxic and hypoxic coastal waters, *Frontiers in Microbiology*. doi: 10.3389/fmicb.2017.00353.

Liu, W., Wang, Y., Russell, A. and Edgerton, E. S. (2005) Atmospheric aerosol over two urban-rural pairs in the southeastern United States: Chemical composition and possible sources, *Atmospheric Environment*. doi: 10.1016/j.atmosenv.2005.03.048.

Lønborg, C., Yokokawa, T., Herndl, G. J. and Antón Álvarez-Salgado, X. (2015) Production and degradation of fluorescent dissolved organic matter in surface waters of the eastern north Atlantic ocean, *Deep-Sea Research Part I: Oceanographic Research Papers*. doi: 10.1016/j.dsr.2014.11.001.

Lopez, P., Chevallier, P., Favier, V., Pouyaud, B., Ordenes, F. and Oerlemans, J. (2010) A regional view of fluctuations in glacier length in southern South America, *Global and Planetary Change*. doi: 10.1016/j.gloplacha.2009.12.009.

Loriaux, T. and Casassa, G. (2013) Evolution of glacial lakes from the Northern Patagonia Icefield and terrestrial water storage in a sea-level rise context, *Global and Planetary Change*. doi: 10.1016/j.gloplacha.2012.12.012.

Lu, Y., Lu, Y. C., Hu, H. Q., Xie, F. J., Wei, X. Y. and Fan, X. (2017) Structural characterization of lignin and its degradation products with spectroscopic methods, *Journal of Spectroscopy*. doi: 10.1155/2017/8951658.

Macdonald, M. L., Wadham, J. L., Telling, J. and Skidmore, M. L. (2018) Glacial Erosion Liberates Lithologic Energy Sources for Microbes and Acidity for Chemical Weathering Beneath Glaciers and Ice Sheets, *Frontiers in Earth Science*. doi: 10.3389/feart.2018.00212.

Mader, H. M., Pettitt, M. E., Wadham, J. L., Wolff, E. W. and Parkes, R. J. (2006) Subsurface ice as a microbial habitat, *Geology*, 34(3), p. 169–172. doi: 10.1130/G22096.1.

Maie, N., Parish, K. J., Watanabe, A., Knicker, H., Benner, R., Abe, T., Kaiser, K. and Jaffé, R. (2006) Chemical characteristics of dissolved organic nitrogen in an oligotrophic subtropical coastal ecosystem, *Geochimica et Cosmochimica Acta*, 70(17), p. 4491–4506. doi: 10.1016/j.gca.2006.06.1554.

Maie, N., Scully, N. M., Pisani, O. and Jaffé, R. (2007) Composition of a protein-like fluorophore of dissolved organic matter in coastal wetland and estuarine ecosystems, *Water Research*. doi: 10.1016/j.watres.2006.11.006.

Mann, P. J., Davydova, A., Zimov, N., Spencer, R. G. M., Davydov, S., Bulygina, E., Zimov, S. and Holmes, R. M. (2012) Controls on the composition and lability of dissolved organic matter in Siberia's Kolyma River basin, *Journal of Geophysical Research: Biogeosciences*. doi: 10.1029/2011JG001798.

Marshall, A. G., Hendrickson, C. L. and Jackson, G. S. (1998) Fourier Transform Ion Cyclotron Resonance Mass Spectromeyry: A Primer, *Mass Spectrometry Reviews*. doi: 10.1002/(SICI)1098-2787(1998)17:1<1::AID-MAS1>3.0.CO;2-K.

Mayr, C., Rebolledo, L., Schulte, K., Schuster, A., Zolitschka, B., Försterra, G. and Häussermann, V. (2014) Responses of nitrogen and carbon deposition rates in Comau Fjord (42°S, southern Chile) to natural and anthropogenic impacts during the last century, *Continental Shelf Research*, 78, p. 29–38. doi: 10.1016/J.CSR.2014.02.004.

McClelland, J. W., Holmes, R. M., Peterson, B. J., Raymond, P. A., Striegl, R. G., Zhulidov, A. V.,

Zimov, S. A., Zimov, N., Tank, S. E., Spencer, R. G. M., Staples, R., Gurtovaya, T. Y. and Griffin, C. G. (2016) Particulate organic carbon and nitrogen export from major Arctic rivers, *Global Biogeochemical Cycles*. doi: 10.1002/2015GB005351.

McConnell, J. R., Edwards, R., Kok, G. L., Flanner, M. G., Zender, C. S., Saltzman, E. S., Banta, J. R., Pasteris, D. R., Carter, M. M. and Kahl, J. D. W. (2007) 20th-Century industrial black carbon emissions altered arctic climate forcing, *Science*. doi: 10.1126/science.1144856.

McKnight, D., Thurman, E. M., Wershaw, R. L. and Hemond, H. (1985) Biogeochemistry of aquatic humic substances in Thoreau's Bog, Concord, Massachusetts., *Ecology*. doi: 10.2307/1939187.

McKnight, D. M., Boyer, E. W., Westerhoff, P. K., Doran, P. T., Kulbe, T. and Andersen, D. T. (2001) Spectrofluorometric characterization of dissolved organic matter for indication of precursor organic material and aromaticity, *Limnology and Oceanography*. doi: 10.4319/lo.2001.46.1.0038.

McKnight, D. M., Wershaw, R. L., Bencala, K. E., Zellweger, G. W. and Feder, G. L. (1992) Humic substances and trace metals associated with Fe and Al oxides deposited in an acidic mountain stream, *Science of the Total Environment, The*. doi: 10.1016/0048-9697(92)90113-7.

McKnight, D. M. and Tate, C. M. (1997) Canada Stream: A Glacial Meltwater Stream in Taylor Valley, South Victoria Land, Antarctica, *Journal of the North American Benthological Society*. doi: 10.2307/1468224.

Medeiros, P. M., Seidel, M., Ward, N. D., Carpenter, E. J., Gomes, H. R., Niggemann, J., Krusche, A. V, Richey, J. E., Yager, P. L. and Dittmar, T. (2015) Fate of the Amazon River dissolved organic matter in the tropical Atlantic Ocean, *Global Biogeochemical Cycles*, 29(5), p. 677–690. doi: 10.1002/2015GB005115.

Meerhoff, E., Castro, L. R., Tapia, F. J. and Pérez-Santos, I. (2019) Hydrographic and Biological Impacts of a Glacial Lake Outburst Flood (GLOF) in a Patagonian Fjord, *Estuaries and Coasts*, 42(1), p. 132–143. doi: 10.1007/s12237-018-0449-9.

Meerhoff, E., Tapia, F. J. and Castro, L. R. (2014) Spatial structure of the meroplankton community along a Patagonian fjord – The role of changing freshwater inputs, *Progress in Oceanography*, 129, p. 125–135. doi: 10.1016/J.POCEAN.2014.05.015.

Meire, L., Mortensen, J., Meire, P., Juul-Pedersen, T., Sejr, M. K., Rysgaard, S., Nygaard, R., Huybrechts, P. and Meysman, F. J. R. (2017) Marine-terminating glaciers sustain high productivity in Greenland fjords, *Global Change Biology*. doi: 10.1111/gcb.13801.

Messager, M. L., Lehner, B., Grill, G., Nedeva, I. and Schmitt, O. (2016) Estimating the volume and age of water stored in global lakes using a geo-statistical approach, *Nature Communications*. doi: 10.1038/ncomms13603.

Meyers, P. A. and Ishiwatari, R. (1993) Lacustrine organic geochemistry-an overview of indicators of organic matter sources and diagenesis in lake sediments, *Organic Geochemistry*. doi: 10.1016/0146-6380(93)90100-P.

Meyers, P. A., Leenheer, M. J., Eaoie, B. J. and Maule, S. J. (1984) Organic geochemistry of suspended and settling particulate matter in Lake Michigan, *Geochimica et Cosmochimica Acta*. doi: 10.1016/0016-7037(84)90273-4.

Mikucki, J. A., Lee, P. A., Ghosh, D., Purcell, A. M., Mitchell, A. C., Mankoff, K. D., … Team, W. S. (2016) Subglacial Lake Whillans microbial biogeochemistry: A synthesis of current knowledge, *Philosophical Transactions of the Royal Society A: Mathematical, Physical and Engineering Sciences*, 374(2059), p. 20140290. doi: 10.1098/rsta.2014.0290.

Millan, R., Rignot, E., Rivera, A., Martineau, V., Mouginot, J., Zamora, R., Uribe, J., Lenzano, G., De Fleurian, B., Li, X., Gim, Y. and Kirchner, D. (2019) Ice Thickness and Bed Elevation of the Northern and Southern Patagonian Icefields, *Geophysical Research Letters*. doi: 10.1029/2019GL082485.

Milner, A. M., Khamis, K., Battin, T. J., Brittain, J. E., Barrand, N. E., Füreder, L., Cauvy-Fraunié, S., Gíslason, G. M., Jacobsen, D., Hannah, D. M., Hodson, A. J., Hood, E., Lencioni, V., Ólafsson, J. S., Robinson, C. T., Tranter, M. and Brown, L. E. (2017) Glacier shrinkage driving global changes

in downstream systems, *Proceedings of the National Academy of Sciences of the United States of America*. doi: 10.1073/pnas.1619807114.

Min, J., Meng-Xia, X., Dong, Z., Yuan, L., Xiao-Yu, L. and Xing, C. (2004) Spectroscopic studies on the interaction of cinnamic acid and its hydroxyl derivatives with human serum albumin, *Journal of Molecular Structure*, 692(1–3), p. 71–80. doi: 10.1016/J.MOLSTRUC.2004.01.003.

Mishra, B., Barik, A., Priyadarsini, K. I. and Mohan, H. (2005) Fluorescence spectroscopic studies on binding of a flavonoid antioxidant quercetin to serum albumins, *Journal of Chemical Sciences*, 117(6), p. 641–647. doi: 10.1007/BF02708293.

Mladenov, N., Alados-Arboledas, L., Olmo, F. J., Lyamani, H., Delgado, A., Molina, A. and Reche, I. (2011) Applications of optical spectroscopy and stable isotope analyses to organic aerosol source discrimination in an urban area, *Atmospheric Environment*. doi: 10.1016/j.atmosenv.2011.01.029.

Moffat, C. (2014) Wind-driven modulation of warm water supply to a proglacial fjord, Jorge Montt Glacier, Patagonia, *Geophysical Research Letters*, 41(11), p. 3943–3950. doi: 10.1002/2014GL060071.

Moffat, C., Tapia, F. J., Nittrouer, C. A., Hallet, B., Bown, F., Boldt Love, K. and Iturra, C. (2018) Seasonal Evolution of Ocean Heat Supply and Freshwater Discharge From a Rapidly Retreating Tidewater Glacier: Jorge Montt, Patagonia, *Journal of Geophysical Research: Oceans*. doi: 10.1002/2017JC013069.

Molina, L. T., Gallardo, L., Andrade, M., Baumgardner, D., Borbor-Cõrdova, M., Bõrquez, R., Casassa, G., Cereceda-Balic, F., Dawidowski, L., Garreaud, R., Huneeus, N., Lambert, F., McCarty, J. L., Mc Phee, J., Mena-Carrasco, M., Raga, G. B., Schmitt, C. and Schwarz, J. P. (2015) Pollution and its Impacts on the South American Cryosphere, *Earth's Future*. doi: 10.1002/2015EF000311.

Møller, E. F. (2007) Production of dissolved organic carbon by sloppy feeding in the copepods Acartia tonsa, Centropages typicus, and Temora longicornis, *Limnology and Oceanography*. doi: 10.4319/lo.2007.52.1.0079.

Møller, E. F., Thor, P. and Nielsen, T. G. (2003) Production of DOC by Calanus finmarchicus, C. glacialis and C. hyperboreus through sloppy feeding and leakage from fecal pellets, *Marine Ecology Progress Series*. doi: 10.3354/meps262185.

Mopper, K. and Schultz, C. A. (1993) Fluorescence as a possible tool for studying the nature and water column distribution of DOC components, *Marine Chemistry*. doi: 10.1016/0304-4203(93)90124-7.

Mostovaya, A., Hawkes, J. A., Dittmar, T. and Tranvik, L. J. (2017) Molecular Determinants of Dissolved Organic Matter Reactivity in Lake Water, *Frontiers in Earth Science*, p. 106. doi: 10.3389/feart.2017.00106.

Mulholland, M. R. and Lee, C. (2009) Peptide hydrolysis and the uptake of dipeptides by phytoplankton, *Limnology and Oceanography*. doi: 10.4319/lo.2009.54.3.0856.

Murphy, K. R., Stedmon, C. A., Graeber, D. and Bro, R. (2013) Fluorescence spectroscopy and multi-way techniques. PARAFAC, *Analytical Methods*, 5(23), p. 6557. doi: 10.1039/c3ay41160e.

Murphy, K. R., Stedmon, C. A., Wenig, P. and Bro, R. (2014a) OpenFluor– an online spectral library of auto-fluorescence by organic compounds in the environment, *Anal. Methods*, 6(3), p. 658–661. doi: 10.1039/C3AY41935E.

Murphy, K. R., Bro, R. and Stedmon, C. A. (2014b) Chemometric Analysis of Organic Matter Fluorescence, in Coble, P. et al. (eds) *Aquatic Organic Matter Fluorescence*. Cambridge: Cambridge University Press, p. 339–375. doi: 10.1017/CBO9781139045452.016.

Murphy, K. R., Hambly, A., Singh, S., Henderson, R. K., Baker, A., Stuetz, R. and Khan, S. J. (2011) Organic Matter Fluorescence in Municipal Water Recycling Schemes: Toward a Unified PARAFAC Model, *Environmental Science & Technology*, 45(7), p. 2909–2916. doi: 10.1021/es103015e.

Murphy, K. R., Stedmon, C. A., Waite, T. D. and Ruiz, G. M. (2008) Distinguishing between terrestrial and autochthonous organic matter sources in marine environments using fluorescence spectroscopy,

Marine Chemistry, 108(1–2), p. 40–58.

Murphy, K. R., Ruiz, G. M., Dunsmuir, W. T. M. and Waite, T. D. (2006) Optimized Parameters for Fluorescence-Based Verification of Ballast Water Exchange by Ships, *Environmental Science & Technology*, 40(7), p. 2357–2362. doi: 10.1021/es0519381.

Musilova, M., Tranter, M., Wadham, J., Telling, J., Tedstone, A. and Anesio, A. M. (2017) Microbially driven export of labile organic carbon from the Greenland ice sheet, *Nature Geoscience*, 10(5), p. 360–365. doi: 10.1038/ngeo2920.

Nebbioso, A. and Piccolo, A. (2013) Molecular characterization of dissolved organic matter (DOM): A critical review, *Analytical and Bioanalytical Chemistry*, p. 109–124. doi: 10.1007/s00216-012-6363-2.

Nelson, N. B., Carlson, C. A. and Steinberg, D. K. (2004) Production of chromophoric dissolved organic matter by Sargasso Sea microbes, in *Marine Chemistry*. doi: 10.1016/j.marchem.2004.02.017.

New, M., Lister, D., Hulme, M. and Makin, I. (2002) A high-resolution data set of surface climate over global land areas, *Climate Research*. doi: 10.3354/cr021001.

Nicholes, M. J., Williamson, C. J., Tranter, M., Holland, A., Poniecka, E., Yallop, M. L., … Stibal, M. (2019) Bacterial dynamics in supraglacial habitats of the Greenland ice sheet, *Frontiers in Microbiology*. doi: 10.3389/fmicb.2019.01366.

Niklitschek, E. J., Soto, D., Lafon, A., Molinet, C. and Toledo, P. (2013) Southward expansion of the Chilean salmon industry in the Patagonian Fjords: Main environmental challenges, *Reviews in Aquaculture*. doi: 10.1111/raq.12012.

Nimptsch, J., Woelfl, S., Osorio, S., Valenzuela, J., Ebersbach, P., von Tuempling, W., Palma, R., Encina, F., Figueroa, D., Kamjunke, N. and Graeber, D. (2015) Tracing dissolved organic matter (DOM) from land-based aquaculture systems in North Patagonian streams, *Science of the Total Environment*. doi: 10.1016/j.scitotenv.2015.07.160.

Nollet, L. (2013) Characterization of Humic Matter, in *Handbook of Water Analysis, Third Edition*. doi: 10.1201/b15314-32.

O'Donnell, E. C., Wadham, J. L., Lis, G. P., Tranter, M., Pickard, A. E., Stibal, M., Dewsbury, P. and Fitzsimons, S. (2016) Identification and analysis of low molecular weight dissolved organic carbon in subglacial basal ice ecosystems by ion chromatography, *Biogeosciences*, 13, p. 3833–3846. doi: 10.5194/bgd-12-14139-2015.

Ohno, T. and Bro, R. (2006) Dissolved Organic Matter Characterization Using Multiway Spectral Decomposition of Fluorescence Landscapes, *Soil Science Society of America Journal*. doi: 10.2136/sssaj2006.0005.

Ohno, T., He, Z., Sleighter, R. L., Honeycutt, C. W. and Hatcher, P. G. (2010) Ultrahigh resolution mass spectrometry and indicator species analysis to identify marker components of soil- and plant biomass-derived organic matter fractions, *Environmental Science and Technology*. doi: 10.1021/es101089t.

Oksanen, J., Blanchet, F. G., Kindt, R., Legendre, P., Minchin, P. R., O'Hara, R. B., Simpson, G. L., Solymos, P., Stevens, M. H. H. and Wagner, H. (2016) Vegan: community ecology package. R package version 2.2–1. 2015.

Osburn, C. L., Boyd, T. J., Montgomery, M. T., Bianchi, T. S., Coffin, R. B. and Paerl, H. W. (2016) Optical Proxies for Terrestrial Dissolved Organic Matter in Estuaries and Coastal Waters, *Frontiers in Marine Science*. doi: 10.3389/fmars.2015.00127.

Osburn, C. L., Wigdahl, C. R., Fritz, S. C. and Saros, J. E. (2011) Dissolved organic matter composition and photoreactivity in prairie lakes of the U.S. Great Plains, *Limnology and Oceanography*, 56(6), p. 2371–2390. doi: 10.4319/lo.2011.56.6.2371.

Osburn, C. L., Anderson, N. J., Stedmon, C. A., Giles, M. E., Whiteford, E. J., McGenity, T. J., Dumbrell, A. J. and Underwood, G. J. C. (2017) Shifts in the Source and Composition of Dissolved

Organic Matter in Southwest Greenland Lakes Along a Regional Hydro-climatic Gradient, *Journal of Geophysical Research: Biogeosciences*. doi: 10.1002/2017JG003999.

Osterholz, H., Kirchman, D. L., Niggemann, J. and Dittmar, T. (2016) Environmental Drivers of Dissolved Organic Matter Molecular Composition in the Delaware Estuary, *Frontiers in Earth Science*, p. 95. doi: 10.3389/feart.2016.00095.

Osterholz, H., Dittmar, T. and Niggemann, J. (2014) Molecular evidence for rapid dissolved organic matter turnover in Arctic fjords, *Marine Chemistry*. doi: 10.1016/j.marchem.2014.01.002.

Pace, M. L., Cole, J. J., Carpenter, S. R., Kitchell, J. F., Hodgson, J. R., Van De Bogert, M. C., Bade, D. L., Kritzberg, E. S. and Bastviken, D. (2004) Whole-lake carbon-13 additions reveal terrestrial support of aquatic food webs, *Nature*. doi: 10.1038/nature02227.

Pankhurst, R. J., Weaver, S. D., Hervé, F. and Larrondo, P. (1999) Mesozoic-Cenozoic evolution of the North Patagonian Batholith in Aysen, southern Chile, *Journal of the Geological Society*. doi: 10.1144/gsjgs.156.4.0673.

Pantoja, S., Luis Iriarte, J. and Daneri, G. (2011) Oceanography of the Chilean Patagonia, *Continental Shelf Research*, 31(3–4), p. 149–153. doi: 10.1016/j.csr.2010.10.013.

Paulsen, M. L., Nielsen, S. E. B., Müller, O., Møller, E. F., Stedmon, C. A., Juul-Pedersen, T., Markager, S., Sejr, M. K., Delgado Huertas, A., Larsen, A. and Middelboe, M. (2017) Carbon Bioavailability in a High Arctic Fjord Influenced by Glacial Meltwater, NE Greenland, *Frontiers in Marine Science*. doi: 10.3389/fmars.2017.00176.

Paulsen, M. L., Müller, O., Larsen, A., Møller, E. F., Middelboe, M., Sejr, M. K. and Stedmon, C. (2018) Biological transformation of Arctic dissolved organic matter in a NE Greenland fjord, *Limnology and Oceanography*. doi: 10.1002/lno.11091.

Peleato, N. M., McKie, M., Taylor-Edmonds, L., Andrews, S. A., Legge, R. L. and Andrews, R. C. (2016) Fluorescence spectroscopy for monitoring reduction of natural organic matter and halogenated furanone precursors by biofiltration, *Chemosphere*, 153, p. 155–161. doi: 10.1016/J.CHEMOSPHERE.2016.03.018.

Perakis, S. S. and Hedin, L. O. (2002) Nitrogen loss from unpolluted South American forests mainly via dissolved organic compounds, *Nature*. doi: 10.1038/415416a.

Pérez, C. A., Armesto, J. J., Torrealba, C. and Carmona, M. R. (2003) Litterfall dynamics and nitrogen use efficiency in two evergreen temperate rainforests of southern Chile, *Austral Ecology*. doi: 10.1046/j.1442-9993.2003.01315.x.

Pérez, T., Mattar, C. and Fuster, R. (2018) Decrease in snow cover over the Aysén river catchment in Patagonia, Chile, *Water (Switzerland)*. doi: 10.3390/w10050619.

Petsch, S. T., Edwards, K. J. and Eglinton, T. I. (2005) Microbial transformations of organic matter in black shales and implications for global biogeochemical cycles, *Palaeogeography, Palaeoclimatology, Palaeoecology*, p. 157–170. doi: 10.1016/j.palaeo.2004.10.019.

Pfeffer, W. T., Arendt, A. A., Bliss, A., Bolch, T., Cogley, J. G., Gardner, A. S., … Wyatt, F. R. (2014) The randolph glacier inventory: A globally complete inventory of glaciers, *Journal of Glaciology*. doi: 10.3189/2014JoG13J176.

Pickard, G. L. (2011) Some Physical Oceanographic Features of Inlets of Chile, *Journal of the Fisheries Research Board of Canada*. doi: 10.1139/f71-163.

Polk, M. H., Young, K. R., Baraer, M., Mark, B. G., McKenzie, J. M., Bury, J. and Carey, M. (2017) Exploring hydrologic connections between tropical mountain wetlands and glacier recession in Peru's Cordillera Blanca, *Applied Geography*. doi: 10.1016/j.apgeog.2016.11.004.

Van De Poll, W. H., Kulk, G., Rozema, P. D., Brussaard, C. P. D., Visser, R. J. W. and Buma, A. G. J. (2018) Contrasting glacial meltwater effects on post-bloom phytoplankton on temporal and spatial scales in Kongsfjorden, Spitsbergen, *Elementa*. doi: 10.1525/elementa.307.

Porter, L. J. (1992) Structure and Chemical Properties of the Condensed Tannins, in *Plant Polyphenols*.

doi: 10.1007/978-1-4615-3476-1_14.

Poulet, S. A., Williams, R., Conway, D. V. P. and Videau, C. (1991) Co-occurrence of copepods and dissolved free amino acids in shelf sea waters, *Marine Biology*. doi: 10.1007/BF01313646.

Pozo, K., Harner, T., Shoeib, M., Urrutia, R., Barra, R., Parra, O. and Focardi, S. (2004) Passive-sampler derived air concentrations of persistent organic pollutants on a north-south transect in Chile, *Environmental Science and Technology*. doi: 10.1021/es049065i.

Di Prinzio, C. Y. and Pascual, M. A. (2008) The establishment of exotic Chinook salmon (Oncorhynchus tshawytscha) in Pacific rivers of Chubut, Patagonia, Argentina, *Annales de Limnologie*. doi: 10.1051/limn:2008020.

QGIS Development Team (2019) QGIS Geographic Information System, *Open Source Geospatial Foundation Project*. Available at: http://qgis.osgeo.org/.

Quiñones, R. A., Fuentes, M., Montes, R. M., Soto, D. and León-Muñoz, J. (2019) Environmental issues in Chilean salmon farming: a review, in *Reviews in Aquaculture*. doi: 10.1111/raq.12337.

Quiroga, E., Ortiz, P., Reid, B. and Gerdes, D. (2013) Classification of the ecological quality of the Aysen and Baker Fjords (Patagonia, Chile) using biotic indices, *Marine Pollution Bulletin*. doi: 10.1016/j.marpolbul.2012.11.041.

Quiroga, E., Ortiz, P., González-Saldías, R., Reid, B., Tapia, F. J., Pérez-Santos, I., Rebolledo, L., Mansilla, R., Pineda, C., Cari, I., Salinas, N., Montiel, A. and Gerdes, D. (2016) Seasonal benthic patterns in a glacial Patagonian fford: The role of suspended sediment and terrestrial organic matter, *Marine Ecology Progress Series*. doi: 10.3354/meps11903.

Quiroga, E., Ortiz, P., Gerdes, D., Reid, B., Villagran, S. and Quiñones, R. (2012) Organic enrichment and structure of macrobenthic communities in the glacial Baker Fjord, Northern Patagonia, Chile, *Journal of the Marine Biological Association of the United Kingdom*. doi: 10.1017/S0025315411000385.

R Core Team (2015) R: A language and environment for statistical computing., *R Foundation for Statistical Computing: Vienna, Austria*. Available at: http://www.r-project.org/.

Rabassa, J. and Clapperton, C. M. (1990) Quaternary glaciations of the southern Andes, *Quaternary Science Reviews*. doi: 10.1016/0277-3791(90)90016-4.

Raeke, J., Lechtenfeld, O. J., Wagner, M., Herzsprung, P. and Reemtsma, T. (2016) Selectivity of solid phase extraction of freshwater dissolved organic matter and its effect on ultrahigh resolution mass spectra, *Environmental Science: Processes and Impacts*. doi: 10.1039/c6em00200e.

Raffl, C., Mallaun, M., Mayer, R. and Erschbamer, B. (2006) Vegetation succession pattern and diversity changes in a Glacier Valley, Central Alps, Austria, *Arctic, Antarctic, and Alpine Research*. doi: 10.1657/1523-0430(2006)38[421:VSPADC]2.0.CO;2.

Raymond, P. A. and Bauer, J. E. (2001) Riverine export of aged terrestrial organic matter to the North Atlantic Ocean., *Nature*, 409(6819), p. 497–500. doi: 10.1038/35054034.

Rebolledo, L., Bertrand, S., Lange, C. B., Tapia, F. J., Quiroga, E., Troch, M., Silva, N., Cárdenas, P. and Pantoja, S. (2019) Compositional and biogeochemical variations of sediments across the terrestrial-marine continuum of the Baker-Martínez fjord system (Chile, 48°S), *Progress in Oceanography*, 174, p. 89–104. doi: 10.1016/J.POCEAN.2018.12.004.

Rebolledo, L., González, H. E., Muñoz, P., Iriarte, J. L., Lange, C. B., Salamanca, M., Pantoja, S. and Salamanca, M. (2011) Siliceous productivity changes in Gulf of Ancud sediments (42°S, 72°W), southern Chile, over the last ~150 years, *Continental Shelf Research*, 31(3–4), p. 356–365. doi: 10.1016/j.csr.2010.06.015.

RGI Consortium (2017) Randolph Glacier Inventory – A Dataset of Global Glacier Outlines: Version 6.0: Technical Report, Global Land Ice Measurements from Space, Colorado, USA. doi: 10.7265/N5-RGI-60.

Riedel, T., Zark, M., Vähätalo, A. V, Niggemann, J., Spencer, R. G. M., Hernes, P. J. and Dittmar, T.

(2016) Molecular Signatures of Biogeochemical Transformations in Dissolved Organic Matter from Ten World Rivers, *Frontiers in Earth Science*, p. 85. doi: 10.3389/feart.2016.00085.

Rignot, E., Rivera, A. and Casassa, G. (2003) Contribution of the Patagonia Icefields of South America to Sea Level Rise, *Science*, 302(5644), p. 434–437. doi: 10.1126/science.1087393.

Rivera, A., Corripio, J., Bravo, C. and Cisternas, S. (2012) Glaciar Jorge Montt (Chilean Patagonia) dynamics derived from photos obtained by fixed cameras and satellite image feature tracking, *Annals of Glaciology*. Cambridge University Press, 53(60), p. 147–155. doi: 10.3189/2012AoG60A152.

Rivera, A., Benham, T., Casassa, G., Bamber, J. and Dowdeswell, J. A. (2007) Ice elevation and areal changes of glaciers from the Northern Patagonia Icefield, Chile, *Global and Planetary Change*, 59(1–4), p. 126–137. doi: 10.1016/j.gloplacha.2006.11.037.

Rogers, R. D. and Schumm, S. A. (1991) The effect of sparse vegetative cover on erosion and sediment yield, *Journal of Hydrology*. doi: 10.1016/0022-1694(91)90065-P.

Romera-Castillo, C., Sarmento, H., Alvarez-Salgado, X. A. Á., Gasol, J. M. and Marrasé, C. (2011) Net production and consumption of fluorescent colored dissolved organic matter by natural bacterial assemblages growing on marine phytoplankton exudates, *Applied and Environmental Microbiology*. doi: 10.1128/AEM.00200-11.

Ross, L., Pérez-Santos, I., Valle-Levinson, A. and Schneider, W. (2014) Semidiurnal internal tides in a Patagonian fjord, *Progress in Oceanography*, 129, p. 19–34. doi: 10.1016/j.pocean.2014.03.006.

Ross, L., Valle-Levinson, A., Pérez-Santos, I., Tapia, F. J. and Schneider, W. (2015) Baroclinic annular variability of internal motions in a Patagonian fjord, *Journal of Geophysical Research: Oceans*. doi: 10.1002/2014JC010669.

Rowe, P. M., Cordero, R. R., Warren, S. G., Stewart, E., Doherty, S. J., Pankow, A., Schrempf, M., Casassa, G., Carrasco, J., Pizarro, J., MacDonell, S., Damiani, A., Lambert, F., Rondanelli, R., Huneeus, N., Fernandoy, F. and Neshyba, S. (2019) Black carbon and other light-absorbing impurities in snow in the Chilean Andes, *Scientific Reports*. doi: 10.1038/s41598-019-39312-0.

Rysgaard, S., Nielsen, T. G. and Hansen, B. W. (1999) Seasonal variation in nutrients, pelagic primary production and grazing in a high-Arctic coastal marine ecosystem, Young Sound, Northeast Greenland, *Marine Ecology Progress Series*, 179, p. 13–25. doi: 10.3354/meps179013.

Sagredo, E. A. and Lowell, T. V. (2012) Climatology of Andean glaciers: A framework to understand glacier response to climate change, *Global and Planetary Change*. doi: 10.1016/j.gloplacha.2012.02.010.

Saidy, A. R., Smernik, R. J., Baldock, J. A., Kaiser, K. and Sanderman, J. (2013) The sorption of organic carbon onto differing clay minerals in the presence and absence of hydrous iron oxide, *Geoderma*. doi: 10.1016/j.geoderma.2013.05.026.

Schaefer, M., Machguth, H., Falvey, M. and Casassa, G. (2013) Modeling past and future surface mass balance of the Northern Patagonia Icefield, *Journal of Geophysical Research: Earth Surface*. doi: 10.1002/jgrf.20038.

Schillawski, S. and Petsch, S. (2008) Release of biodegradable dissolved organic matter from ancient sedimentary rocks, *Global Biogeochemical Cycles*, 22(3). doi: 10.1029/2007GB002980.

Schneider, W., Pérez-Santos, I., Ross, L., Bravo, L., Seguel, R. and Hernández, F. (2014) On the hydrography of Puyuhuapi Channel, Chilean Patagonia, *Progress in Oceanography*, 129, p. 8–18. doi: 10.1016/j.pocean.2014.03.007.

Schuur, E. A. G., Bockheim, J., Canadell, J. G., Euskirchen, E., Field, C. B., Goryachkin, S. V., … Zimov, S. A. (2008) Vulnerability of Permafrost Carbon to Climate Change: Implications for the Global Carbon Cycle, *BioScience*, 58(8), p. 701. doi: 10.1641/B580807.

Scipioni, C., Villanueva, F., Pozo, K. and Mabilia, R. (2012) Preliminary characterization of polycyclic aromatic hydrocarbons, nitrated polycyclic aromatic hydrocarbons and polychlorinated dibenzo-p-dioxins and furans in atmospheric PM10 of an urban and a remote area of Chile, *Environmental*

Technology (United Kingdom). doi: 10.1080/09593330.2011.597433.

Seguel, M., Tocornal, M. A. and Sfeir, A. (2005) Floraciones algales nocivas en los canales y fiordos del sur de Chile, *Ciencia y Tecnología del Mar*.

Seidel, M., Manecki, M., Herlemann, D. P. R., Deutsch, B., Schulz-Bull, D., Jürgens, K. and Dittmar, T. (2017) Composition and Transformation of Dissolved Organic Matter in the Baltic Sea, *Frontiers in Earth Science*, p. 31. doi: 10.3389/feart.2017.00031.

Shank, L. M., Howell, S., Clarke, A. D., Freitag, S., Brekhovskikh, V., Kapustin, V., McNaughton, C., Campos, T. and Wood, R. (2012) Organic matter and non-refractory aerosol over the remote Southeast Pacific: Oceanic and combustion sources, *Atmospheric Chemistry and Physics*. doi: 10.5194/acp-12-557-2012.

Sharp, M., Parkes, J., Cragg, B., Fairchild, I. J., Lamb, H. and Tranter, M. (1999) Widespread bacterial populations at glacier beds and their relationship to rock weathering and carbon cycling, *Geology*, 27(2), p. 107–110. doi: 10.1130/0091-7613(1999)027<0107:WBPAGB>2.3.CO.

Shimotori, K., Omori, Y. and Hama, T. (2010) Bacterial production of marine humic-like fluorescent dissolved organic matter and its biogeochemical importance, *Aquatic Microbial Ecology*. doi: 10.3354/ame01350.

Sholkovitz, E. R. (1976) Flocculation of dissolved organic and inorganic matter during the mixing of river water and seawater, *Geochimica et Cosmochimica Acta*. doi: 10.1016/0016-7037(76)90035-1.

Shutova, Y., Baker, A., Bridgeman, J. and Henderson, R. K. (2014) Spectroscopic characterisation of dissolved organic matter changes in drinking water treatment: From PARAFAC analysis to online monitoring wavelengths, *Water Research*, 54, p. 159–169. doi: 10.1016/J.WATRES.2014.01.053.

Silva, N., Vargas, C. A. and Prego, R. (2011) Land–ocean distribution of allochthonous organic matter in surface sediments of the Chiloé and Aysén interior seas (Chilean Northern Patagonia), *Continental Shelf Research*, 31(3–4), p. 330–339. doi: 10.1016/J.CSR.2010.09.009.

Singer, G. a., Fasching, C., Wilhelm, L., Niggemann, J., Steier, P., Dittmar, T. and Battin, T. J. (2012) Biogeochemically diverse organic matter in Alpine glaciers and its downstream fate, *Nature Geoscience*, 5(10), p. 710–714. doi: 10.1038/ngeo1581.

Sleighter, R. L. and Hatcher, P. G. (2008) Molecular characterization of dissolved organic matter (DOM) along a river to ocean transect of the lower Chesapeake Bay by ultrahigh resolution electrospray ionization Fourier transform ion cyclotron resonance mass spectrometry, *Marine Chemistry*. doi: 10.1016/j.marchem.2008.04.008.

Smith, D. F., Podgorski, D. C., Rodgers, R. P., Blakney, G. T. and Hendrickson, C. L. (2018a) 21 Tesla FT-ICR Mass Spectrometer for Ultrahigh-Resolution Analysis of Complex Organic Mixtures, *Analytical Chemistry*. doi: 10.1021/acs.analchem.7b04159.

Smith, H. J., Foster, R. A., McKnight, D. M., Lisle, J. T., Littmann, S., Kuypers, M. M. M. and Foreman, C. M. (2017) Microbial formation of labile organic carbon in Antarctic glacial environments, *Nature Geoscience*. doi: 10.1038/ngeo2925.

Smith, H. J., Dieser, M., McKnight, D. M., SanClements, M. D. and Foreman, C. M. (2018b) Relationship between dissolved organic matter quality and microbial community composition across polar glacial environments, *FEMS Microbiology Ecology*. doi: 10.1093/femsec/fiy090.

Smith, R. W., Bianchi, T. S., Allison, M., Savage, C. and Galy, V. (2015) High rates of organic carbon burial in fjord sediments globally, *Nature Geoscience*, 8(6), p. 450–453. doi: 10.1038/ngeo2421.

Sommaruga, R. (2014) When glaciers and ice sheets melt: Consequences for planktonic organisms, *Journal of Plankton Research*. doi: 10.1093/plankt/fbv027.

Sommaruga, R. and Kandolf, G. (2014) Negative consequences of glacial turbidity for the survival of freshwater planktonic heterotrophic flagellates, *Scientific Reports*. doi: 10.1038/srep04113.

Søndergaard, M., Stedmon, C. A. and Borch, N. H. (2003) Fate of terrigenous dissolved organic matter (DOM) in estuaries: Aggregation and bioavailability, *Ophelia*. Taylor & Francis, 57(3), p. 161–176.

doi: 10.1080/00785236.2003.10409512.

Spencer, R. G. M., Vermilyea, A., Fellman, J., Raymond, P., Stubbins, A., Scott, D. and Hood, E. (2014a) Seasonal variability of organic matter composition in an Alaskan glacier outflow: insights into glacier carbon sources, *Environmental Research Letters*, 9(5), p. 055005. doi: 10.1088/1748-9326/9/5/055005.

Spencer, R. G. M. M., Guo, W., Raymond, P. A., Dittmar, T., Hood, E., Fellman, J. and Stubbins, A. (2014b) Source and biolability of ancient dissolved organic matter in glacier and lake ecosystems on the tibetan plateau, *Geochimica et Cosmochimica Acta*, 142, p. 64–74. doi: 10.1016/j.gca.2014.08.006.

Spencer, R. G. M. M., Mann, P. J., Dittmar, T., Eglinton, T. I., McIntyre, C., Holmes, R. M., Zimov, N. and Stubbins, A. (2015) Detecting the signature of permafrost thaw in Arctic rivers, *Geophysical Research Letters*, 42(8), p. 2830–2835. doi: 10.1002/2015GL063498.

Spencer, R. G. M., Stubbins, A., Hernes, P. J., Baker, A., Mopper, K., Aufdenkampe, A. K., Dyda, R. Y., Mwamba, V. L., Mangangu, A. M., Wabakanghanzi, J. N. and Six, J. (2009) Photochemical degradation of dissolved organic matter and dissolved lignin phenols from the Congo River, *Journal of Geophysical Research: Biogeosciences*, 114(G3), p. G03010. doi: 10.1029/2009JG000968.

Srivastava, D., Kumar, A., Verma, A. and Swaroop, S. (2014) Characterization of suspended sediment in Meltwater from Glaciers of Garhwal Himalaya, *Hydrological Processes*. doi: 10.1002/hyp.9631.

Srur, A. M., Villalba, R., Rodríguez-Catón, M., Amoroso, M. M. and Marcotti, E. (2018) Climate and Nothofagus pumilio establishment at upper treelines in the patagonian andes, *Frontiers in Earth Science*. doi: 10.3389/feart.2018.00057.

Stedmon, C. A. and Bro, R. (2008) Characterizing dissolved organic matter fluorescence with parallel factor analysis: A tutorial, *Limnology and Oceanography: Methods*. doi: 10.4319/lom.2008.6.572.

Stedmon, C. A., Thomas, D. N., Papadimitriou, S., Granskog, M. A. and Dieckmann, G. S. (2011) Using fluorescence to characterize dissolved organic matter in Antarctic sea ice brines, *Journal of Geophysical Research: Biogeosciences*, 116(G3). doi: 10.1029/2011JG001716.

Stedmon, C. A., Thomas, D. N., Granskog, M., Kaartokallio, H., Papadimitriou, S. and Kuosa, H. (2007a) Characteristics of Dissolved Organic Matter in Baltic Coastal Sea Ice: Allochthonous or Autochthonous Origins?, *Environmental Science & Technology*, 41(21), p. 7273–7279. doi: 10.1021/es071210f.

Stedmon, C. A. and Markager, S. (2005a) Resolving the variability in dissolved organic matter fluorescence in a temperate estuary and its catchment using PARAFAC analysis, *Limnology and Oceanography*. doi: 10.4319/lo.2005.50.2.0686.

Stedmon, C. A. and Markager, S. (2005b) Tracing the production and degradation of autochthonous fractions of dissolved organic matter by fluorescence analysis, *Limnology and Oceanography*. doi: 10.4319/lo.2005.50.5.1415.

Stedmon, C. A., Markager, S. and Bro, R. (2003) Tracing dissolved organic matter in aquatic environments using a new approach to fluorescence spectroscopy, *Marine Chemistry*, 82(3–4), p. 239–254. doi: 10.1016/S0304-4203(03)00072-0.

Stedmon, C. A., Markager, S., Tranvik, L., Kronberg, L., Slätis, T. and Martinsen, W. (2007b) Photochemical production of ammonium and transformation of dissolved organic matter in the Baltic Sea, *Marine Chemistry*, 104(3–4), p. 227–240. doi: 10.1016/j.marchem.2006.11.005.

Stibal, M., Wadham, J. L., Lis, G. P., Telling, J., Pancost, R. D., Dubnick, A., Sharp, M. J., Lawson, E. C., Butler, C. E. H., Hasan, F., Tranter, M. and Anesio, A. M. (2012a) Methanogenic potential of Arctic and Antarctic subglacial environments with contrasting organic carbon sources, *Global Change Biology*, 18(11), p. 3332–3345. doi: 10.1111/j.1365-2486.2012.02763.x.

Stibal, M., Hasan, F., Wadham, J. L., Sharp, M. J. and Anesio, A. M. (2012b) Prokaryotic diversity in sediments beneath two polar glaciers with contrasting organic carbon substrates, *Extremophiles*, 16(2), p. 255–265. doi: 10.1007/s00792-011-0426-8.

Stibal, M., Tranter, M., Benning, L. G. and Rehak, J. (2008) Microbial primary production on an Arctic glacier is insignificant in comparison with allochthonous organic carbon input, *Environmental Microbiology*, 10(8), p. 2172–2178. doi: 10.1111/j.1462-2920.2008.01620.x.

Stibal, M., Šabacká, M. and Žárský, J. (2012c) Biological processes on glacier and ice sheet surfaces, *Nature Geoscience*, 5(11), p. 771–774. doi: 10.1038/NGEO1611.

Stubbins, A., Spencer, R. G. M., Mann, P. J., Holmes, R. M., McClelland, J. W., Niggemann, J. and Dittmar, T. (2015) Utilizing colored dissolved organic matter to derive dissolved black carbon export by arctic rivers, *Frontiers in Earth Science*. doi: 10.3389/feart.2015.00063.

Stubbins, A., Lapierre, J. F., Berggren, M., Prairie, Y. T., Dittmar, T. and Del Giorgio, P. A. (2014) What's in an EEM? Molecular signatures associated with dissolved organic fluorescence in boreal Canada, *Environmental Science and Technology*. doi: 10.1021/es502086e.

Stubbins, A., Spencer, R. G. M., Chen, H., Hatcher, P. G., Mopper, K., Hernes, P. J., Mwamba, V. L., Mangangu, A. M., Wabakanghanzi, J. N. and Six, J. (2010) Illuminated darkness: Molecular signatures of Congo River dissolved organic matter and its photochemical alteration as revealed by ultrahigh precision mass spectrometry, *Limnology and Oceanography*. doi: 10.4319/lo.2010.55.4.1467.

Stubbins, A., Hood, E., Raymond, P. A., Aiken, G. R., Sleighter, R. L., Hernes, P. J., Butman, D., Hatcher, P. G., Striegl, R. G., Schuster, P., Abdulla, H. a. N., Vermilyea, A. W., Scott, D. T. and Spencer, R. G. M. (2012) Anthropogenic aerosols as a source of ancient dissolved organic matter in glaciers, *Nature Geoscience*, 5(3), p. 198–201. doi: 10.1038/ngeo1403.

Sulzberger, B. and Durisch-Kaiser, E. (2009) Chemical characterization of dissolved organic matter (DOM): A prerequisite for understanding UV-induced changes of DOM absorption properties and bioavailability, *Aquatic Sciences*, 71(2), p. 104–126. doi: 10.1007/s00027-008-8082-5.

Sun, L., Perdue, E. M., Meyer, J. L. and Weis, J. (1997) Use of elemental composition to predict bioavailability of dissolved organic matter in a Georgia river, *Limnology and Oceanography*. doi: 10.4319/lo.1997.42.4.0714.

Tan, Z., Leung, L. R., Li, H., Tesfa, T., Vanmaercke, M., Poesen, J., Zhang, X., Lu, H. and Hartmann, J. (2017) A Global Data Analysis for Representing Sediment and Particulate Organic Carbon Yield in Earth System Models, *Water Resources Research*. doi: 10.1002/2017WR020806.

Tanaka, K., Kuma, K., Hamasaki, K. and Yamashita, Y. (2014) Accumulation of humic-like fluorescent dissolved organic matter in the Japan Sea, *Scientific Reports*, 4, p. 5292. doi: 10.1038/srep05292.

Tateishi, R., Hoan, N. T., Kobayashi, T., Alsaaideh, B., Tana, G. and Phong, D. X. (2014) Production of Global Land Cover Data – GLCNMO2008, *Journal of Geography and Geology*. doi: 10.5539/jgg.v6n3p99.

Tateishi, R., Uriyangqai, B., Al-Bilbisi, H., Ghar, M. A., Tsend-Ayush, J., Kobayashi, T., Kasimu, A., Hoan, N. T., Shalaby, A., Alsaaideh, B., Enkhzaya, T., Gegentana and Sato, H. P. (2011) Production of global land cover data – GLCNMO, *International Journal of Digital Earth*. Taylor & Francis, 4(1), p. 22–49. doi: 10.1080/17538941003777521.

Telling, J., Anesio, A. M., Tranter, M., Irvine-Fynn, T., Hodson, A., Butler, C. and Wadham, J. (2011) Nitrogen fixation on Arctic glaciers, Svalbard, *Journal of Geophysical Research*, 116(G3), p. G03039. doi: 10.1029/2010JG001632.

Telling, J., Anesio, A. M., Tranter, M., Stibal, M., Hawkings, J., Irvine-Fynn, T., Hodson, A., Butler, C., Yallop, M. and Wadham, J. (2012) Controls on the autochthonous production and respiration of organic matter in cryoconite holes on high Arctic glaciers, *Journal of Geophysical Research: Biogeosciences*, 117(1). doi: 10.1029/2011JG001828.

Tello, A., Corner, R. A. and Telfer, T. C. (2010) How do land-based salmonid farms affect stream ecology? *Environmental Pollution*. doi: 10.1016/j.envpol.2009.11.029.

Thurman, E. M. (1985) *Organic Geochemistry of Natural Waters*, *Organic Geochemistry of Natural Waters*. doi: 10.1007/978-94-009-5095-5.

Timko, S. A., Maydanov, A., Pittelli, S. L., Conte, M. H., Cooper, W. J., Koch, B. P., Schmitt-Kopplin, P. and Gonsior, M. (2015) Depth-dependent photodegradation of marine dissolved organic matter, *Frontiers in Marine Science*. doi: 10.3389/fmars.2015.00066.

Tranter, M. (2014) Biogeochemistry: Microbes eat rock under ice, *Nature*, 512(7514), p. 256–257. doi: 10.1038/512256a.

Tranter, M. (2015) Grand challenge for low temperature and pressure geochemistry—Sparks in the dark, on Earth, Mars, and throughout the Galaxy, *Frontiers in Earth Science*. doi: 10.3389/feart.2015.00069.

Tranter, M., Skidmore, M. and Wadham, J. (2005) Hydrological controls on microbial communities in subglacial environments, *Hydrological Processes*, p. 995–998. doi: 10.1002/hyp.5854.

Tranter, M., Sharp, M. J., Lamb, H. R., Brown, G. H., Hubbard, B. P. and Willis, I. C. (2002) Geochemical weathering at the bed of Haut glacier d'Arolla, Switzerland - A new model, *Hydrological Processes*, 16(5), p. 959–993. doi: 10.1002/hyp.309.

Tranvik, L. J., Downing, J. A., Cotner, J. B., Loiselle, S. A., Striegl, R. G., Ballatore, T. J., … Weyhenmeyer, G. A. (2009) Lakes and reservoirs as regulators of carbon cycling and climate, *Limnology and Oceanography*. doi: 10.4319/lo.2009.54.6_part_2.2298.

Tremblay, L. B., Dittmar, T., Marshall, A. G., Cooper, W. J. and Cooper, W. T. (2007) Molecular characterization of dissolved organic matter in a North Brazilian mangrove porewater and mangrove-fringed estuaries by ultrahigh resolution Fourier Transform-Ion Cyclotron Resonance mass spectrometry and excitation/emission spectroscopy, *Marine Chemistry*. doi: 10.1016/j.marchem.2006.12.015.

Tscherko, D., Rustemeier, J., Richter, A., Wanek, W. and Kandeler, E. (2003) Functional diversity of the soil microflora in primary succession across two glacier forelands in the Central Alps, *European Journal of Soil Science*. doi: 10.1046/j.1351-0754.2003.0570.x.

Urban-Rich, J., McCarty, J. T. and Shailer, M. (2004) Effects of food concentration and diet on chromophoric dissolved organic matter accumulation and fluorescent composition during grazing experiments with the copepod Calanus finmarchicus, in *ICES Journal of Marine Science*. doi: 10.1016/j.icesjms.2004.03.024.

Valdés-Pineda, R., Pizarro, R., García-Chevesich, P., Valdés, J. B., Olivares, C., Vera, M., Balocchi, F., Pérez, F., Vallejos, C., Fuentes, R., Abarza, A. and Helwig, B. (2014) Water governance in Chile: Availability, management and climate change, *Journal of Hydrology*. doi: 10.1016/j.jhydrol.2014.04.016.

Vandekerkhove, E., Bertrand, S., Reid, B., Bartels, A. and Charlier, B. (2016) Sources of dissolved silica to the fjords of northern Patagonia (44-48°S): The importance of volcanic ash soil distribution and weathering, *Earth Surface Processes and Landforms*. doi: 10.1002/esp.3840.

Vargas, C. A., Martinez, R. A., San Martin, V., Aguayo, M., Silva, N. and Torres, R. (2011) Allochthonous subsidies of organic matter across a lake–river–fjord landscape in the Chilean Patagonia: Implications for marine zooplankton in inner fjord areas, *Continental Shelf Research*, 31(3–4), p. 187–201. doi: 10.1016/J.CSR.2010.06.016.

Wadham, J. L., Arndt, S., Tulaczyk, S., Stibal, M., Tranter, M., Telling, J., Lis, G. P., Lawson, E., Ridgwell, A., Dubnick, A., Sharp, M. J., Anesio, A. M. and Butler, C. E. H. (2012) Potential methane reservoirs beneath Antarctica, *Nature*, 488(7413), p. 633–637. doi: 10.1038/nature11374.

Wadham, J. L., Hodson, A. J., Tranter, M. and Dowdeswell, J. A. (1997) The rate of chemical weathering beneath a quiescent, surge-type, polythermal-based glacier, southern Spitsbergen, Svalbard, *Annals of Glaciology*, 24, p. 27–31.

Wadham, J. L., Hawkings, J. R., Tarasov, L., Gregoire, L. J., Spencer, R. G. M., Gutjahr, M., Ridgwell, A. and Kohfeld, K. E. (2019) Ice sheets matter for the global carbon cycle, *Nature Communications*, 10(1), p. 3567. doi: 10.1038/s41467-019-11394-4.

Wadham, J. L., Hawkings, J., Telling, J., Chandler, D., Alcock, J., O'Donnell, E., Kaur, P., Bagshaw, E., Tranter, M., Tedstone, A. and Nienow, P. (2016) Sources, cycling and export of nitrogen on the

Greenland Ice Sheet, *Biogeosciences*. doi: 10.5194/bg-13-6339-2016.

Wadham, J. L., Tranter, M., Hodson, A. J., Hodgkins, R., Bottrell, S., Cooper, R. and Raiswell, R. (2010) Hydro-biogeochemical coupling beneath a large polythermal Arctic glacier: Implications for subice sheet biogeochemistry, *Journal of Geophysical Research: Earth Surface*, 115(4). doi: 10.1029/2009JF001602.

Wadham, J. L., Tranter, M., Tulaczyk, S. and Sharp, M. (2008) Subglacial methanogenesis: A potential climatic amplifier? *Global Biogeochemical Cycles*, 22(2). doi: 10.1029/2007GB002951.

Waggoner, D. C., Chen, H., Willoughby, A. S. and Hatcher, P. G. (2015) Formation of black carbon-like and alicyclic aliphatic compounds by hydroxyl radical initiated degradation of lignin, *Organic Geochemistry*, 82, p. 69–76. doi: 10.1016/j.orggeochem.2015.02.007.

Wagner, S. and Jaffé, R. (2015) Effect of photodegradation on molecular size distribution and quality of dissolved black carbon, *Organic Geochemistry*, 86, p. 1–4. doi: 10.1016/j.orggeochem.2015.05.005.

Wagner, S., Jaffé, R. and Stubbins, A. (2018) Dissolved black carbon in aquatic ecosystems, *Limnology and Oceanography Letters*, 3(3), p. 168–185. doi: 10.1002/lol2.10076.

Wagner, S., Jaffé, R., Cawley, K., Dittmar, T. and Stubbins, A. (2015) Associations Between the Molecular and Optical Properties of Dissolved Organic Matter in the Florida Everglades, a Model Coastal Wetland System, *Frontiers in Chemistry*, 3. doi: 10.3389/fchem.2015.00066.

Walker, J. D. and Colwell, R. R. (1974) Microbial petroleum degradation: use of mixed hydrocarbon substrates, *Applied Microbiology*, 27(6), 1053–1060.

Walker, S. A., Amon, R. M. W., Stedmon, C., Duan, S. and Louchouarn, P. (2009) The use of PARAFAC modeling to trace terrestrial dissolved organic matter and fingerprint water masses in coastal Canadian Arctic surface waters, *Journal of Geophysical Research: Biogeosciences*. doi: 10.1029/2009JG000990.

Wang, X. ping, Xu, B. qing, Kang, S. chang, Cong, Z. yuan and Yao, T. dong (2008) The historical residue trends of DDT, hexachlorocyclohexanes and polycyclic aromatic hydrocarbons in an ice core from Mt. Everest, central Himalayas, China, *Atmospheric Environment*. doi: 10.1016/j.atmosenv.2008.04.035.

Ward, N. D., Bianchi, T. S., Medeiros, P. M., Seidel, M., Richey, J. E., Keil, R. G. and Sawakuchi, H. O. (2017) Where Carbon Goes When Water Flows: Carbon Cycling across the Aquatic Continuum, *Frontiers in Marine Science*, p. 7. doi: 10.3389/fmars.2017.00007.

Weathers, K. C. and Likens, G. E. (1997) Clouds in southern Chile: An important source of nitrogen to nitrogen- limited ecosystems?, *Environmental Science and Technology*. doi: 10.1021/es9603416.

Weiss, J. (1943) Fluorescence of organic molecules, *Nature*. doi: 10.1038/152176a0.

Weller, D., Miranda, C. G., Moreno, P. I., Villa-Martínez, R. and Stern, C. R. (2014) The large late-glacial Ho eruption of the Hudson volcano, southern Chile, *Bulletin of Volcanology*. doi: 10.1007/s00445-014-0831-9.

Welti, N., Striebel, M., Ulseth, A. J., Cross, W. F., DeVilbiss, S., Glibert, P. M., Guo, L., Hirst, A. G., Hood, J., Kominoski, J. S., MacNeill, K. L., Mehring, A. S., Welter, J. R. and Hillebrand, H. (2017) Bridging food webs, ecosystem metabolism, and biogeochemistry using ecological stoichiometry theory, *Frontiers in Microbiology*. doi: 10.3389/fmicb.2017.01298.

Wickland, K. P., Neff, J. C. and Aiken, G. R. (2007) Dissolved organic carbon in Alaskan boreal forest: Sources, chemical characteristics, and biodegradability, *Ecosystems*. doi: 10.1007/s10021-007-9101-4.

Wilhelm, L., Singer, G. A., Fasching, C., Battin, T. J. and Besemer, K. (2013) Microbial biodiversity in glacier-fed streams, *The ISME Journal*, 7(8), p. 1651–1660. doi: 10.1038/ismej.2013.44.

Williams, C. J., Frost, P. C. and Xenopoulos, M. A. (2013) Beyond best management practices: pelagic biogeochemical dynamics in urban stormwater ponds, *Ecological Applications*, 23(6), p. 1384–

1395. doi: 10.1890/12-0825.1.

Williams, C. J., Yamashita, Y., Wilson, H. F., Jaffé, R. and Xenopoulos, M. A. (2010) Unraveling the role of land use and microbial activity in shaping dissolved organic matter characteristics in stream ecosystems, *Limnology and Oceanography*, 55(3), p. 1159–1171. doi: 10.4319/lo.2010.55.3.1159.

Willis, M. J., Melkonian, A. K., Pritchard, M. E. and Ramage, J. M. (2012a) Ice loss rates at the Northern Patagonian Icefield derived using a decade of satellite remote sensing, *Remote Sensing of Environment*. doi: 10.1016/j.rse.2011.09.017.

Willis, M. J., Melkonian, A. K., Pritchard, M. E. and Rivera, A. (2012b) Ice loss from the Southern Patagonian Ice Field, South America, between 2000 and 2012, *Geophysical Research Letters*. doi: 10.1029/2012GL053136.

Wilson, R., Glasser, N. F., Reynolds, J. M., Harrison, S., Anacona, P. I., Schaefer, M. and Shannon, S. (2018) Glacial lakes of the Central and Patagonian Andes, *Global and Planetary Change*, 162, p. 275–291. doi: 10.1016/J.GLOPLACHA.2018.01.004.

Wozniak, A. S., Bauer, J. E. T., Sleighter, R. L., Dickhut, R. M. and Hatcher, P. G. (2008) Technical Note: Molecular characterization of aerosol-derived water soluble organic carbon using ultrahigh resolution electrospray ionization Fourier transform ion cyclotron resonance mass spectrometry, *Atmospheric Chemistry and Physics*. doi: 10.5194/acp-8-5099-2008.

Wünsch, U. J., Murphy, K. R. and Stedmon, C. A. (2015) Fluorescence Quantum Yields of Natural Organic Matter and Organic Compounds: Implications for the Fluorescence-based Interpretation of Organic Matter Composition, *Frontiers in Marine Science*. doi: 10.3389/fmars.2015.00098.

Wünsch, U. J., Koch, B. P., Witt, M. and Needoba, J. A. (2016) Seasonal variability of dissolved organic matter in the Columbia River: In situ sensors elucidate biogeochemical and molecular analyses, *Biogeosciences Discussions*. doi: 10.5194/bg-2016-263.

Wünsch, U. J., Geuer, J. K., Lechtenfeld, O. J., Koch, B. P., Murphy, K. R. and Stedmon, C. A. (2018) Quantifying the impact of solid-phase extraction on chromophoric dissolved organic matter composition, *Marine Chemistry*. doi: 10.1016/J.MARCHEM.2018.08.010.

Wymore, A. S., Rodríguez-Cardona, B. and McDowell, W. H. (2016) Understanding dissolved organic matter biogeochemistry through in situ nutrient manipulations in stream ecosystems, *Journal of Visualized Experiments*. doi: 10.3791/54704.

Wynn, P. M., Hodson, A. J., Heaton, T. H. E. and Chenery, S. R. (2007) Nitrate production beneath a High Arctic glacier, Svalbard, *Chemical Geology*, 244(1–2), p. 88–102. doi: 10.1016/j.chemgeo.2007.06.008.

Yamashita, Y., Fichot, C. G., Shen, Y., Jaffé, R. and Benner, R. (2015) Linkages among fluorescent dissolved organic matter, dissolved amino acids and lignin-derived phenols in a river-influenced ocean margin, *Frontiers in Marine Science*. doi: 10.3389/fmars.2015.00092.

Yamashita, Y., Scinto, L. J., Maie, N. and Jaffé, R. (2010) Dissolved Organic Matter Characteristics Across a Subtropical Wetland's Landscape: Application of Optical Properties in the Assessment of Environmental Dynamics, *Ecosystems*, 13(7), p. 1006–1019. doi: 10.1007/s10021-010-9370-1.

Yamashita, Y., Jaffé, R., Maie, N. and Tanoue, E. (2008) Assessing the dynamics of dissolved organic matter (DOM) in coastal environments by excitation emission matrix fluorescence and parallel factor analysis (EEM-PARAFAC), *Limnology and Oceanography*. doi: 10.4319/lo.2008.53.5.1900.

Yasuhara, A. and Fuwa, K. (1982) Determination of fatty acids in airborne particulate matter, dust and soot by mass chromatography, *Journal of Chromatography A*. doi: 10.1016/S0021-9673(00)99616-X.

Young, K. R. (2014) Ecology of land cover change in glaciated tropical mountains, *Revista Peruana de Biologia*. doi: 10.15381/rpb.v21i3.10900.

Zemp, M., Huss, M., Thibert, E., Eckert, N., McNabb, R., Huber, J., Barandun, M., Machguth, H., Nussbaumer, S. U., Gärtner-Roer, I., Thomson, L., Paul, F., Maussion, F., Kutuzov, S. and Cogley, J. G. (2019) Global glacier mass changes and their contributions to sea-level rise from 1961 to 2016,

Nature. doi: 10.1038/s41586-019-1071-0.

Zemp, M., Frey, H., Gärtner-Roer, I., Nussbaumer, S. U., Hoelzle, M., Paul, F., … Vincent, C. (2015) Historically unprecedented global glacier decline in the early 21st century, *Journal of Glaciology*. doi: 10.3189/2015JoG15J017.

Zhu, Z. Y., Wu, Y., Liu, S. M., Wenger, F., Hu, J., Zhang, J. and Zhang, R. F. (2016) Organic carbon flux and particulate organic matter composition in Arctic valley glaciers: Examples from the Bayelva River and adjacent Kongsfjorden, *Biogeosciences*. doi: 10.5194/bg-13-975-2016.

Zhuang, W.-E. and Yang, L. (2018) Impacts of global changes on the biogeochemistry and environmental effects of dissolved organic matter at the land-ocean interface: a review, *Environmental Science and Pollution Research*, 25(5), p. 4165–4173. doi: 10.1007/s11356-017-1027-6.